Packetised Wireless Communication Systems in Interference Limited Environments

A thesis submitted to the
University of Auckland, New Zealand
for the degree of
Doctor of Philosophy in Electrical and Electronic Engineering

Matthew D. Orange

March 1998

Abstract

There is a strong likelihood that future wireless communication systems will employ packetised transmission techniques. Such an approach would provide a number of benefits, including the ability to integrate with emerging wired systems based on Asynchronous Transfer Mode (ATM). In addition, packet-based wireless networks would allow for diverse traffic types and in particular, speech and data traffic, to be integrated more readily.

This thesis presents theoretical models and performance studies for various interference limited, packet-based, speech and data wireless communication systems. Two packetised random access protocols are considered for investigation, namely Slotted ALOHA (S-ALOHA) and Packet Reservation Multiple Access (PRMA). The S-ALOHA protocol is designed specifically for data traffic, whereas the PRMA protocol is optimised for speech traffic, with the ability to also cater for data traffic.

Previously published research into S-ALOHA and PRMA has generally focused on the performance of these protocols in idealised single cell systems, free from cochannel interference. Previous studies have normally only considered simple signal propagation models that give little or no consideration to signal variability. A common assumption made in previous studies assumes that all packets involved in collisions with other packets are lost, while those packets received in the absence of other packets are received successfully.

In this thesis, the performance of S-ALOHA and PRMA in more realistic multiple cell configurations, namely the outdoor cellular and in-building pico-cellular environments, has been considered. The fluctuations in received signal strengths have been modeled in this thesis using narrowband statistical propagation models. In addition, the assumption relating to packet collisions has been reconsidered in this thesis because practical receivers are often capable of locking onto one packet in the presence of other intra-cell and inter-cell interfering packets, due to the receiver capture effect. A capture probability model has been developed in this thesis, which defines the probability of a desired packet capturing the central cell base station in the presence of both intra-cell and inter-cell interfering packets. Accompanying Markov analysis theory has been developed to analyse the performance of multiple cell S-ALOHA and PRMA systems.

Having developed the necessary framework, it has been possible to successfully analyse various multiple cell S-ALOHA and PRMA systems. These include a multiple cell data-only S-ALOHA system, multiple cell speech-only PRMA systems with and without selection diversity and speech packet retransmission and an integrated speech-data multiple cell PRMA system with selection diversity and speech packet retransmission.

Acknowledgements

I would like to express my gratitude to the following who have provided assistance and encouragement during my time as a Ph.D student:

My supervisor, Dr Kevin Sowerby, for his devoted guidance and support. He has encouraged me to explore my own ideas, while ensuring that I remain objective in my approach. I am grateful for the many hours we spent discussing my research.

Dr Alan Coulson for his assistance and for the thought provoking discussions we had on a regular basis. He has always challenged me to approach problems from a fresh perspective.

My colleagues in the Radio Systems Group and in particular Keith Butterworth, Phillip Marshall and Dr Michael Neve who have assisted me in various ways.

The University Grants Committee, Industrial Research Ltd. (IRL), and the Telecommunications Users Association of New Zealand (TUANZ) for their financial support. This funding has been extremely beneficial in helping me to complete my research.

I would like to thank my family and friends for their constant encouragement and support. I would especially like to thank my grandfather, Pa Orange, for first suggesting the idea of a Ph.D.

Finally, I would like to thank my wife, Jasjit, for her undivided love and patience. She has always been there for me when I have needed her.

Table of Contents

CHAPTER 7
MULTIPLE CELL PRMA SPEECH SYSTEMS WITH PACKET RETRANSMISSION AND SELECTION DIVERSITY 149

CHAPTER 8
MULTIPLE CELL PRMA SPEECH-DATA SYSTEMS 179

Chapter 1

Introduction

In the 21st century, it is envisaged that individuals will have the ability to transmit voice, data and video to virtually any other person in the world, regardless of their location using wireless based communication. Instead of disparate wireless systems and technologies being required for each type of information, it is possible that a single integrated system that caters for the unique requirements of each information source could be employed. Such a system would not only be capable of delivering a wide range of services, but it would provide these services to a large number of users in an efficient, accurate, and timely manner.

1.1 Evolution of Systems and Services

The realisation of a truly integrated approach to wireless communications is yet to be fully realised, with existing wireless systems still somewhat disparate in their inter-working and provision of services. Technologies and systems currently providing wireless communications services can be grouped into six distinct groups [1,2], including cellular mobile radio systems, cordless telephony, high speed wireless local-area networks (WLANs), wide-area mobile data systems, paging/messaging systems, and satellite-based mobile systems. Despite the wide variety of these developments, the wireless evolution has proceeded along two main paths, as illustrated in Fig. 1.1, namely voice-orientated and data-orientated wireless systems[1].

This pattern of separation between voice and data wireless systems has already been observed in the development of wired networks, where the existing infrastructure is still very fragmented. At present, there are wired PBXs for local voice communications within office complexes, the public switched telephone network (PSTN) for wide-area voice communications, wired LAN for high speed local data communications, packet-switched networks and voice-band modems for low-speed, wide-area data communications and a separate cable network for wide-area video distribution. This separation has arisen because each individual network was designed to meet the individual requirements of the particular information type being transported. The same pattern of separation exists in the wireless information industry. The new-generation wireless information networks are evolving around either voice-driven applications such as digital cellular, cordless telephone and wireless PBX or around data-driven networks such as wireless LANs and mobile data networks. While it is true that all the major standards initiatives are addressing the integration of services, there is still a separation of the industrial communities that participate in the various standards bodies. That is, the GSM, North American Digital Cellular, DECT and other groups are supported primarily by representatives of the voice-communications industry, whereas IEEE 802.11, WINForum and HIPERLAN are supported primarily by those with an interest in data communications.

[1] Or alternatively, circuit-switched isochronous transmission versus packet-switched asynchronous transmission.

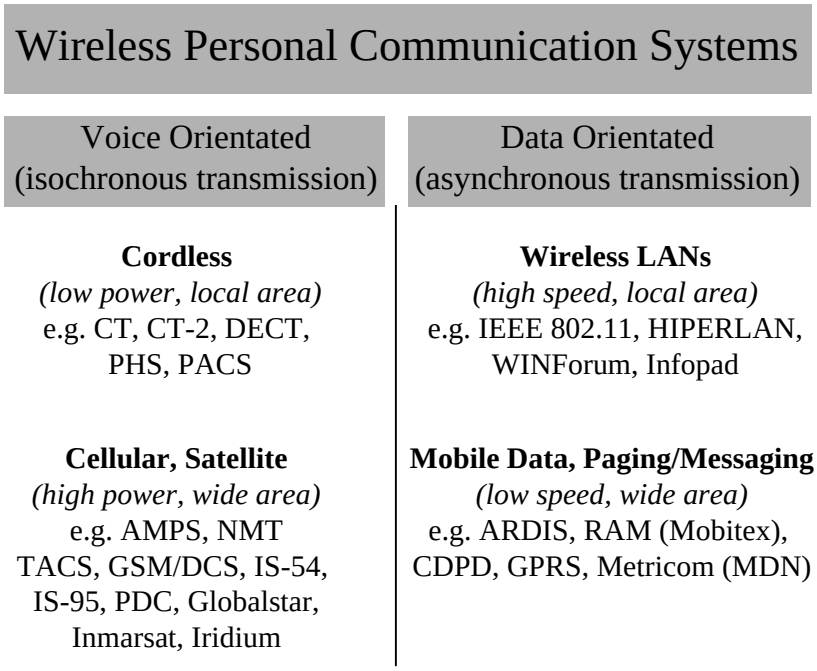

Figure 1.1: *Categories of current wireless personal communication systems.*

1.2 A Perspective on Third Generation Wireless Networks

Standards organisations have begun tackling the integration issue in wireless networks. In Europe, a third-generation mobile system, the Universal Mobile Telecommunications System (UMTS) is under research [3]. UMTS is being standardised by the European Telecommunication Standards Institute (ETSI). Work in ETSI is supported by research in the RACE[2] II and ACTS[3] programs, funded by the European Union. The International Telecommunications Union (ITU) is working on a third-generation system with similar goals, namely the Future Public Land Mobile Telecommunication Systems (FPLMTS). FPLMTS has recently been renamed to International Mobile Telecommunication System 2000 (IMT-2000). A key element in both UMTS and IMT-2000 is the provision of new wideband services such as wireless multimedia, including real-time video and high speed data. These are in addition to more conventional services already offered by second-generation mobile systems. The aim is to provide a single integrated system capable of supporting all services, including voice, data and video in various forms and combinations.

Third generation systems will also be required to integrate with the wired network infrastructure, the target being the asynchronous transfer mode (ATM) based broadband integrated services digital network (B-ISDN). ATM employs packet-switched transmission and is gaining momentum in the wired industry as the preferred common backbone technology for supporting a wide variety of services. Intuitively it would seem that the preferred transmission technology of future wireless systems should also be based on packet switching [4].

[2] Research and Development in Advanced Communication Technologies in Europe.
[3] Advanced Communications Technologies and Services.

The benefits of a packetised wireless communication system include [5]:

- accommodation of mixed information types;
- simplification of information routing in a network subject to continual reorganisation and;
- harmonisation with the anticipated evolution of fixed networks.

Information packets in such a system would be transferred from spatially dispersed terminals to base stations over a shared multiple access communications channel. A key element for ensuring that all terminals gain fair and equitable access to the channel is the inclusion of an appropriate multiple access protocol. Unlike circuit-switched wireless systems, which normally employ frequency division, time division, or code division multiple access (FDMA, TDMA or CDMA) protocols, packet-switched wireless systems normally employ random multiple access (RMA) protocols[4]. Random access has historically been used for transferring bursty data traffic.

Random access protocols often allow terminals to transmit information to the base station with little, or no regard for other terminals who are also transmitting. This can result in a number of terminals all transmitting packets at the same time. Because the base station is generally capable of receiving only one packet at a time, unsuccessful packets are retransmitted after random time delays. This process of " contention" is inherent in all random access protocols.

The earliest random access protocols are the ALOHA [6] and slotted ALOHA (S-ALOHA) [7] protocols. S-ALOHA is one of the simplest random access protocols in existence and more importantly, forms the basis for a large number of other random access protocols. The development and analysis of random access protocols that allow terminals to efficiently transmit both packetised speech and data information in a wireless environment was motivated by Goodman in [8], when he proposed the Packet Reservation Multiple Access (PRMA) scheme. PRMA is a combination of S-ALOHA and TDMA techniques. Since PRMA was first proposed, there has been a significant research effort devoted to the development and analysis of random access protocols, which are capable of transmitting both speech and data information.

From a European perspective, two basic access techniques are now being proposed for the future generation of wireless systems: a CDMA orientated one [9] and a PRMA orientated one [4,10-14], although it is not yet clear which technique will prevail. In reality, the hyper-debated comparison between these access techniques cannot be solved in absolute terms. Rather, the comparison results strictly depend on the reference environment. In particular, consideration must be given with regard to the types of services required, the capacity and performance requirements and the technological status at the time of system implementation. A reasonable compromise could be the coexistence of the two techniques in the third generation framework, each one being implemented in the environments where it offers better performance.

Nevertheless, in Europe, PRMA has the advantage over CDMA of being considered the natural evolution of the successful pan-European GSM system [15]. European manufacturers are more inclined towards PRMA since it offers the possibility of partially reusing the already developed equipment as well as exploiting the already consolidated know-how.

[4] Normally referred to as random access (RA) techniques.

1.3 The Contributions of This Thesis

It appears increasingly likely that future wireless systems and standards will employ a packetised approach to provide flexibility in the integrated transmission of speech, data and video information. With this vision in mind, a number of individuals and organisations have, over the last decade, focused on the development and analysis of random access protocols that can meet the requirements of a future system. In this thesis, the PRMA and S-ALOHA protocols have been chosen for investigation. While a large body of published research has already been devoted to the analysis of these protocols, it has focused chiefly on the performance of these protocols in somewhat idealised circumstances. In particular, the analyses have often been performed in isolated conditions in which interference from cochannel cells is not explicitly considered. With future systems set to employ small frequency reuse distances to maximise their capacity, the exclusion of cochannel interference from such analyses appears to be untenable.

The key contribution of this thesis is the performance analysis of S-ALOHA and PRMA in interference limited multiple cell systems. Such an analysis involves combining knowledge of both interference limited conventional multiple cell (e.g., FDMA/TDMA) systems, with knowledge of single cell S-ALOHA and PRMA systems. In a conventional multiple cell system, as illustrated in Fig. 1.2(a), a desired signal experiences interference from users operating in cochannel cells. In a single cell S-ALOHA or PRMA system, as illustrated in Fig. 1.2(b), a desired signal receives interference from other contenders within the same cell. In this thesis, the combined effect of same-cell and cochannel cell interference on the performance and stability of S-ALOHA and PRMA is determined (Fig. 1.2(c)).

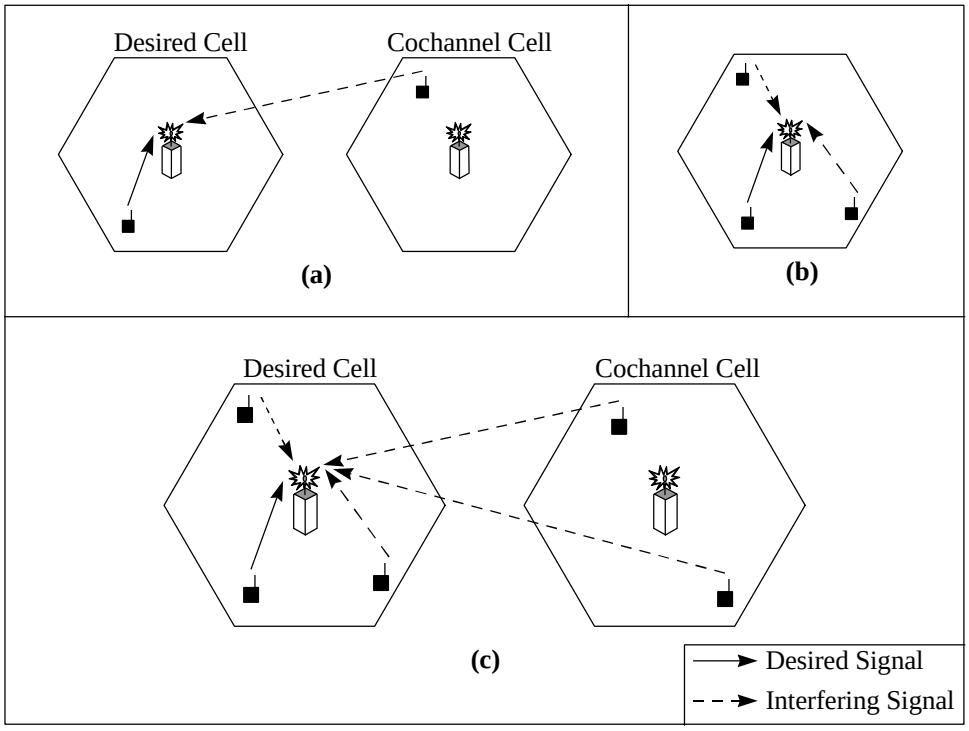

Figure 1.2: *Interference in* **(a)** *a conventional (e.g., FDMA/TDMA) multiple cell system,* **(b)** *a single cell S-ALOHA or PRMA system and* **(c)** *a multiple cell S-ALOHA or PRMA system.*

In order to study the performance of these protocols in multiple cell, variable channel environments, it is necessary to determine the probability of a desired signal being received correctly at a base station in the presence of unwanted signals from the same cell and from cochannel cells. In this thesis, this probability is referred to as the *capture probability*. The complement of the capture probability is the *outage probability*. A body of research has previously been developed for calculating outage probabilities in conventional multiple cell systems suffering only cochannel interference [16], while other research has considered the capture probability in single cell random access systems affected by only interfering (contending) signals from the same cell [17]. Capture probability expressions are developed in this thesis, which allow both same-cell and cochannel cell interference to be considered. These expressions can be applied to the analysis of many multiple cell random access systems. With respect to S-ALOHA and PRMA, these capture probability expressions are used in this thesis to consider the:

- Development of techniques for estimating cochannel interference;
- Performance in more realistic geographical and propagation environments;
- Effect of propagation and system parameters;
- Optimum choice of cluster size;
- Cell averaged performance versus location dependent performance;
- Optimum approach for handling cochannel interference;
- Effect of base station antenna diversity on system performance;
- Integrated speech-data systems versus separate speech and data systems.

Techniques for Estimating Cochannel Interference : With a multiple cell random access system, the performance of each cell is dependent on the operation of surrounding cochannel cells. The cochannel interference received by a cell is a combination of new and retransmitted packets produced by terminals in cochannel cells. The number of packets being retransmitted in cochannel cells depends fundamentally on the level of congestion in these cells as well as the level of cochannel interference that these cells receive. For example, it is conceivable that excessive retransmissions in one cell may cause additional retransmissions to occur in nearby cochannel cells, which in turn may cause the performance of the original cell to deteriorate further. This inter-dependency between cells leads to difficulties in estimating the level of cochannel interference received by any individual cell. In this thesis, a number of techniques for estimating the level of cochannel interference in multiple cell S-ALOHA and PRMA systems are developed and their respective merits are evaluated.

Realistic Geographical and Propagation Environments : Unlike previous research into S-ALOHA and PRMA, this thesis considers more realistic geographical and propagation environments. In particular, the performance of both outdoor cellular and in-building pico-cellular S-ALOHA and PRMA systems are evaluated. The investigation of in-building systems is of particular interest, as this is where such systems could conceivably find their greatest application. The performance of S-ALOHA and PRMA is determined using a number of outdoor and indoor propagation models. In addition, the effect of the receiver capture ratio[5], the level of shadowing variability and pathloss exponent on the performance of the various systems is determined.

Optimum Choice of Cluster Size : The single cell assumption made in previous research of PRMA and S-ALOHA needs to be reconsidered because future wireless systems employing random

[5] Also referred to as the protection ratio, or minimum required signal to interference ratio.

access would most certainly exist in a multiple cell configuration, governed by an appropriate frequency reuse plan. The study, by previous researchers, of only single cell systems is due to either: a desire to concentrate on details of the random access protocol else; an assumption of a large frequency reuse distance in which case cochannel interference becomes negligible. However, large frequency reuse distances in future wireless networks are unlikely to be realised because more than ever, these networks will strive for high spectral efficiency through the use of small cluster sizes. In this thesis, a number of frequency reuse plans are considered and the optimum arrangement is determined for each system considered.

Cell Averaged Versus Location Dependent Performance : Previous research into random access systems has normally focused on the "cell-averaged" performance of a system. This is not always the best performance measure to use, however, as significant variations in a terminals performance may exist, depending on the terminals location. In this thesis, the location dependent performance of terminals in multiple cell S-ALOHA and PRMA systems is determined.

Approaches for Handling Cochannel Interference : The question of whether or not speech terminals in a PRMA system should retransmit packets corrupted by cochannel interference, is investigated in this thesis. A tradeoff exists between the performance improvement of the retransmitting speech terminal and the performance degradation of other terminals, who would receive an increased level of interference. It may be better in some circumstances to discard the corrupted information and continue to transmit newer information. This has the benefit of reducing the level of interference experienced by other users in the network, as packets are not continually being retransmitted.

Effect of Base Station Antenna Diversity : Over recent years, a number of sophisticated techniques for reducing and avoiding cochannel interference in cellular radio systems have been proposed [18]. In this thesis, a relatively simple base station selection diversity technique is investigated for it's ability to reduce inter-cell interference in various multiple cell PRMA systems. In particular, an ideal SIR (signal to interference ratio) selection diversity scheme is considered during transmission of reserved PRMA speech packets.

Integrated Versus Separate Systems : The effect of mixing speech and data traffic in a multiple cell random access system is also determined in this thesis. In particular, this thesis resolves whether or not the integration of speech and data into a unified system provides improved performance over disparate speech and data systems.

1.4 Publications

A number of publications have been produced from the author's research, including national conference papers [19,20], technical reports [21], an international journal paper [22] and international conference papers [23-25]. These publications reflect a progression of research ideas and system complexities, culminating in the work presented in this thesis. The various publications, together with their standing in the overall research, are discussed in this section.

In [19] an overview of the field of study was presented, together with an initial outline of the proposed research. It was stated in [19] that the overall aim of the research was to investigate the integration of speech and data traffic over a shared wireless communication channel using

PRMA. The transmission quality of this channel was assumed to be severely limited by the surrounding physical environment.

In order to determine the performance of such a complex system, it was necessary to first start with a relatively simple system and then progressively incorporate more complexity and detail into the analysis. The Markov analysis of a single cell, speech only PRMA system without receiver capture was presented in [20]. Monte Carlo simulation results for the same system with capture were also presented in [20]. In [21], the performance of a single cell PRMA system with and without capture was determined using both Markov analysis and Monte Carlo simulation. The work presented in [21] sought to provide a sound analytical foundation for PRMA upon which later work could be based.

In [22], a generalised multiple cell packet speech system was considered. Analytical expressions for the capture probability in such a system were derived. Unlike previous studies, this analysis considered a packet-based system in which interference originated from both “same cell” and cochannel cell users.

The work presented in [22] laid the groundwork required for the consideration of particular packet-based wireless systems, such as PRMA and S-ALOHA, in a multiple cell context. For example, in [23] the performance of an interference limited outdoor cellular speech-only PRMA system with selection diversity was determined. Performance results were obtained from both Markov analysis and computer simulation techniques.

In [24], the performance of an interference limited outdoor cellular S-ALOHA system was determined using Markov analysis. A novel technique for estimating the level of inter-cell interference in packet-based communication systems, such as S-ALOHA, was presented in [24].

In [25], the performance of an in-building picocellular speech-data PRMA was determined via Monte Carlo computer simulation. Systems with and without speech packet retransmission were considered. Propagation measurements made in the building in which the PRMA system was assumed to operate, were incorporated in the analysis.

1.5 The Structure of this Thesis

The overall structure of this thesis is presented in Fig. 1.3. Chapters 2 and 3 summarise the two fundamental areas of communication theory which this thesis seeks to merge, namely random access and radiowave propagation. In particular, Chapter 2 presents an overview of packet based random access wireless communications systems. The unique nature and individual requirements of speech and data traffic are outlined. The S-ALOHA and PRMA protocols are introduced with respect to single cell, simple channel systems and the appropriate performance measures for such systems are presented. Chapter 2 also contains a literature review of S-ALOHA and PRMA.

Chapter 3 presents background material relating to signal propagation in multiple cell systems. This material is fundamentally concerned with the presentation of relevant statistical propagation models. In particular, propagation models are presented for outdoor cellular and in-building pico-cellular environments.

In Chapter 4, a framework for analysing S-ALOHA and PRMA in multiple cell, variable channel systems is developed. In particular, the layout of terminals in multiple cell random access systems is presented. Working assumptions relating to the allocation of bandwidth between cells in such systems are outlined. Chapter 4 also considers the probability of a desired signal in such a system, successfully capturing the base station, given the presence of same-cell and cochannel cell interfering signals. This capture probability theory is used extensively throughout the remainder of the thesis. Operation in multiple cell systems necessitates the consideration of cochannel interference and in particular, its effect on protocol operation. The areas of protocol operation affected by interference are identified and a number of additional performance measures are presented.

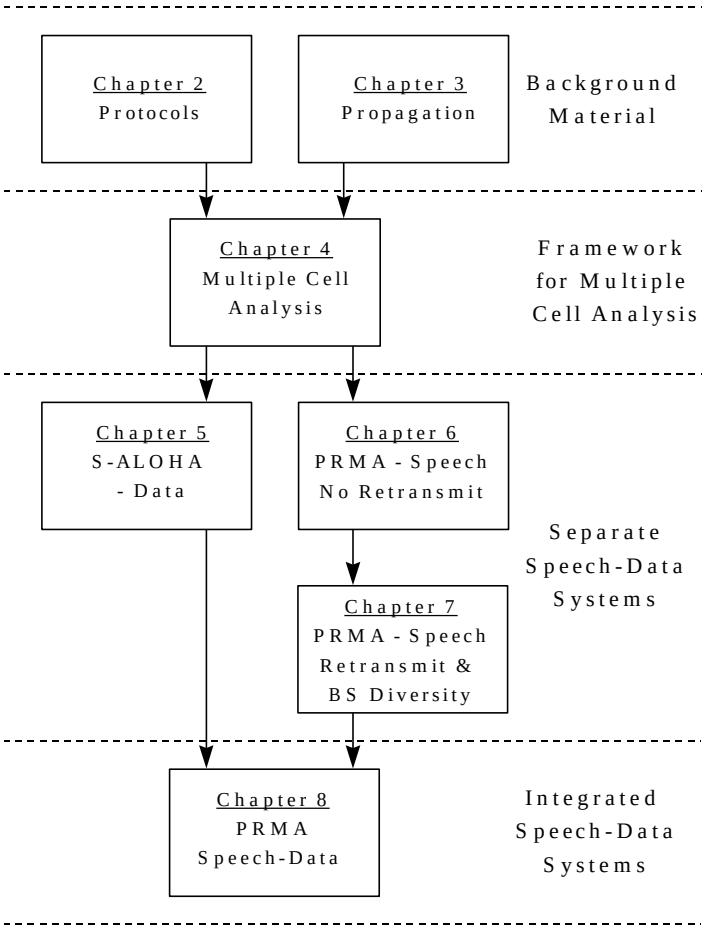

Figure 1.3: *The structure of this thesis.*

Chapters 5, 6, and 7 present performance analyses for multiple-cell data-only S-ALOHA systems and multiple-cell speech-only PRMA systems (without and with speech packet retransmission and selection diversity), respectively. In particular, the performance of outdoor cellular and in-building pico-cellular S-ALOHA and PRMA systems are determined. The key issues that were presented in Section §1.3 are investigated with respect to each of these three systems. The performance results of Chapters 5-7 are obtained from both detailed Markov analyses and Monte Carlo simulations. These analyses and simulations become progressively more complicated as

the systems being considered become more complicated. The Markov analysis is, however, capable of providing more computationally efficient results than those obtained from Monte Carlo simulations. With respect to this thesis, simulation results are used primarily as a validation tool, with which to compare the Markov analysis results.

The Markov analysis considered in each of these three chapters (Chapters 5-7) does not attempt to incorporate the actual operation of cochannel cells, as it is mathematically difficult, if not impossible, to include such operation within such an analysis. Instead, the problem is constrained so that only the central cell of any particular system is modeled. This approach requires that the expected level of cochannel interference received at the central cell base station be determined. A number of methods for estimating this quantity in both multiple cell S-ALOHA and PRMA systems are developed throughout Chapters 5-7.

In Chapter 8, the performance of an integrated speech-data PRMA system is evaluated in an outdoor cellular setting. It is assumed that the bandwidth of this system is the composite of the individual data and speech systems considered previously in Chapters 5-7. Comparisons are made between the integrated and separate approaches. The relevant Markov analysis theory that has been developed for the integrated situation, is presented in Chapter 8. However, the performance results of Chapter 8 are obtained solely from Monte Carlo simulations, as computation via Markov analysis is prohibitively difficult.

This thesis concludes in Chapter 9, with a summary of the research reported in the previous chapters.

1.6 Summary

The demand for wireless personal communication systems continues to increase, with future systems likely to support a host of new services in addition to those already offered by second generation systems. It is increasingly likely that these future systems will adopt an integrated approach to allow for seamless transmission of diverse traffic sources. With this in mind, several packet-based random access protocols are investigated for their ability to operate in high capacity interference limited wireless systems.

References

[1] D. C. Cox, “Wireless network access for personal communications,” *IEEE Commun. Mag.*, vol. 30, no. 12, Dec. 1992, pp. 96 - 115.

[2] J. E. Padgett, C. G. Gunther, T. Hattori, “Overview of wireless personal communications,” *IEEE Commun. Mag.*, vol. 33, no. 1, Jan. 1995, pp. 28 - 41.

[3] T. Magedanz, “Integration and evolution of existing mobile telecommunications systems toward UMTS,” *IEEE Commun. Mag.*, vol. 34, no. 9, Sep. 1996, pp. 90 - 96.

[4] G. Brasche, B. Walke, “Concepts, services and protocols of the new GSM phase 2+ general packet radio service,” *IEEE Commun. Mag.*, vol. 35, no. 8, Aug. 1997, pp. 94 - 104.

[5] D. J. Goodman, “Cellular packet communications,” *IEEE Trans. Commun.*, vol. 38, no. 8, Aug. 1990, pp. 1272 - 1280.

[6] N. Abramson, “The ALOHA system - another alternative for computer communications,” *Proc. 1970 Fall Joint Comput. Conf. AFIPS Press*, vol. 37, 1970, pp. 281 - 285.

[7] L. G. Roberts, “ALOHA packet systems with and without slots and capture,” *Comput. Commun. Rev*., vol. 5, no. 2, Apr. 1975, pp. 28 - 42.

[8] D. J. Goodman, R. A. Valenzuela, K. T. Gayliard, B. Ramamurthi, "Packet reservation multiple access for local wireless communications," *IEEE Trans. Commun*., vol. 37, no.8, 1989, pp.885-890.

[9] T. Stefansson, M. Allkins, “Real-time testbed for assessing a CDMA-based system,” *IEEE Personal Commun. Mag.*, vol. 2, no. 5, Oct. 1995, pp. 75 - 80.

[10] J. M. Devile, “A reservation based multiple access scheme for a future universal mobile telecommunications system,” *in Proc. 7th IEE European Conf. on Mobile and Personal Communications*, no. 387, Brighton, United Kingdom, Dec. 1993, pp. 210 - 215.

[11] J. Dunlop, P. Cosimini, D. Robertson, “Optimisation of packet access mechanisms for advanced time division multiple access (ATDMA),” *in Proc. 7th IEE European Conf. on Mobile and Personal Communications*, no. 387, Brighton, United Kingdom, Dec. 1993, pp. 237 - 242.

[12] J. Dunlop, D. Robertson, P.Cosimini, J. De Vile, “Development and optimisation of a statistical multiplexing mechanism for ATDMA,” *in Proc. 44th IEEE Veh. Technol. Conf.*, Stockholm, Sweden, May 1994, pp. 1040 - 1044.

[13] R. Beraldi, A. Iera, S. Marano, P. Salerno, “A new dynamic reservation multiple access protocol for supporting multimedia traffic in third generation cellular system,” *in Proc. 1994 IEEE International Conf. on Communication Systems, ICCS'94*, Singapore, Nov. 1994, pp. 314 - 319.

[14] D. Cygan, F. David, H. J. Eul, J. Hofmann, N. Metzner, W. Mohr, “RACE-II advanced TDMA mobile access project - an approach for UMTS,” *in Proc. 1994 International Zurich Seminar on Digital Communications*, Zurich, Switzerland, Mar. 1994, pp. 428 - 439.

[15] P. Taaghol, R. Tafazolli, B. G. Evans, “Burst reservation multiple access techniques for the GSM/DCS and DECT systems,” *in Proc. 7th IEEE International Symposium on Personal, Indoor and Mobile Radio Communications, PIMRC'96*, Taipei, Taiwan, Oct. 1996, pp. 412 - 416.

[16] K. W. Sowerby, *Outage probability in mobile radio systems*. Ph.D Thesis, Department of Electrical & Electronic Engineering, The University of Auckland, New Zealand, Feb. 1989.

[17] J. P. M. G. Linnartz, *Narrowband land-mobile radio networks*. Massachusetts: Artech House, 1993.

[18] G. J. Pottie, "System design choices in personal communications," *IEEE Personal Commun. Mag.*, vol. 2, no. 5, Oct. 1995, pp. 50 - 67.

[19] M. D. Orange, "Integration of voice and data traffic in future wireless networks under fading channel conditions," *in Proc. 1994 New Zealand Postgraduate Conf. for Engineering and Technology Students*, Palmerston North, New Zealand, Aug. 1994, pp. 326 - 327.

[20] M. D. Orange, "The effect of Rayleigh fading on packet reservation multiple access," *in Proc. 1995 New Zealand Postgraduate Conf. for Engineering and Technology Students*, Auckland, New Zealand, Aug. 1995, pp. 240 - 245.

[21] M. D. Orange, "Performance of microcellular PRMA in a fading channel environment," *in School of Engineering Report No. 557*, The University of Auckland, New Zealand, Dec. 1995.

[22] M. D. Orange, K. W. Sowerby, "Capture effect in a Rayleigh faded cellular packet speech system," *Electronics Letters*, vol. 32, no. 4, Feb. 15th 1996, pp. 298 - 299.

[23] M. D. Orange, K. W. Sowerby, "The effect of receiver capture and cochannel interference on PRMA," *in Proc. 46th IEEE Veh. Technol. Conf.*, Atlanta, Georgia, Apr. 1996, pp. 1741 - 1745.

[24] M. D. Orange, K. W. Sowerby, A. J. Coulson, "Markov analysis of an outdoor S-ALOHA system with frequency reuse," *in Proc. 7th Virginia Tech/MPRG Symposium on Wireless Personal Communications*, Blacksburg, Virginia, Jun. 1997, pp. 13-1 - 13-12.

[25] M. D. Orange, K. W. Sowerby, A. J. Coulson, K. S. Butterworth, "Performance of a speech-data PRMA system in an in-building environment," *in Proc. 47th IEEE Veh. Technol. Conf.*, Phoenix, Arizona, May 1997, pp. 1518 - 1522.

Chapter 2

Random Access Protocols for Wireless Personal Communications

2.1 Introduction

This thesis is concerned with the ability of packet based random access protocols to operate in high capacity, interference-limited wireless systems. In this chapter the concept of random access is described, with special regard given to the slotted ALOHA (S-ALOHA) and Packet Reservation Multiple Access (PRMA) protocols. The descriptions presented in this chapter assume a single cell, simple channel system in which cochannel interference is not considered. Such an operating environment has commonly been considered in previous analyses of these protocols. By a 'simple' channel it is assumed that packets are only received correctly by the base station when received in the absence of other competing packets.

Random access techniques rely on packetisation whereby the information is segmented into discrete length blocks. Appropriate models that represent the generation of speech and data packets are presented in §2.2. Section §2.2 also presents the unique characteristics and requirements of speech and data traffic. The appropriate performance measures by which a random access transmission technique can be evaluated are outlined. These measures include the throughput, data packet delay, speech packet dropping probability and system stability.

In §2.3 and §2.4 an overview of the S-ALOHA and PRMA random access protocols are presented, respectively. These descriptions relate to their operation in a single cell, simple channel system. The S-ALOHA protocol is designed specifically for data traffic, whereas the PRMA protocol is optimised for speech traffic. However, the PRMA protocol can also cater for the integrated transmission of speech and data traffic, by allowing the data users to communicate with the base station using a S-ALOHA approach. Section §2.5 presents a detailed literature review of data-only S-ALOHA, speech-only PRMA and speech-data PRMA research. This review considers both single cell and multiple cell systems.

2.2 Transmission of Packetised Speech and Data Information

In a random access wireless communication system, the information transmitted by the terminals is first segmented into discrete length packets. Information packets transmitted from terminals to base stations consist of both a payload (actual information) and a header as illustrated in Fig. 2.1. The header contains the terminal ID, which identifies which terminal the packet originated from, as well as the information type and priority level. It also contains the base station ID which identifies which base station the packet is being sent to. It is assumed that fixed size packets are employed by both speech and data terminals in all the systems considered in this thesis. In particular, it is assumed that each speech or data packet contains an H bit header and an I bit

information field[1]. The random access protocols considered in this thesis are organised according to a Time Division Multiplex (TDM) structure, whereby the uplink channel timescale is partitioned into *frames*, with each frame containing *N timeslots*. Fig. 2.2 presents this structure.

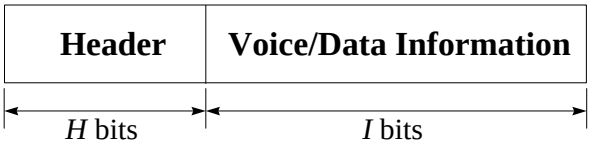

Figure 2.1: *Packet structure for speech and data information.*

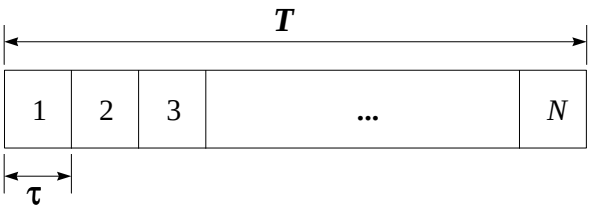

Figure 2.2: *Frame and timeslot organisation.*

The duration, t , of one timeslot is given by

$$t = \frac{T}{N}, \tag{2.1}$$

where T is the duration of a single frame. All the terminals are synchronised such that their packets are transmitted on the leading edge of a timeslot. During a given timeslot no more than one packet can be transmitted from a particular speech or data terminal to its base station. The nature of speech and data packet generation is described in §2.2.1 and §2.2.2, respectively.

2.2.1 Speech Traffic

Speech traffic is inherently bursty, with a typical conversation consisting of a series of *talkspurts* and *gaps*. There are principal spurts and gaps (related to the talking, pausing and listening patterns of a conversation). There are also *mini-spurts* and *mini-gaps* (due to the short silent intervals that punctuate continuous speech). Fig. 2.3 illustrates a recorded speech signal and the corresponding speech activity detection as classified by the speech activity detector presented in [1]. Two models that have been proposed to model the process of speech generation are:

- The “slow” speech activity model which responds only to the principal talkspurts and gaps. It is based on the original Time Assignment Speech Interpolation (TASI) system devised to improve the efficiency of undersea transmissions [2].

[1] The efficiency of random access protocols in fading environments is known to be dependent on packet size, and as such, the size of the packets represents an important design consideration. In this thesis, however, only a fixed packet of size H=576 and I=64 has been considered.

- The more sensitive "fast" speech activity model which also responds to the mini-spurts and mini-gaps. It is based on the behaviour of the speech detector used in an experimental wide-band packet communications system [3].

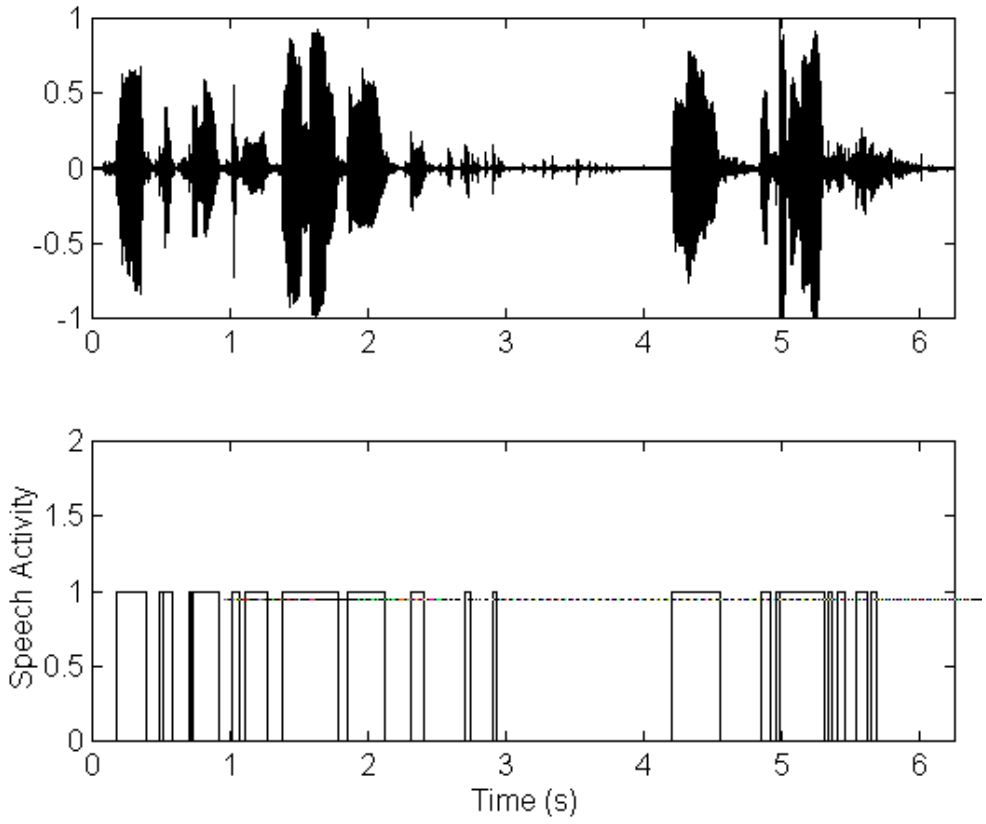

Figure 2.3: *The classification of a recorded speech signal according to an " on-off" process (1 corresponds to speech and 0 corresponds to silence).*

Only the slow speech activity model is used in this thesis. This model, illustrated in Fig. 2.4, consists of a two-state discrete Markov process with exponentially distributed sojourn times. The probability that a silent gap of mean duration t_2 seconds, ends during a t second timeslot is [4]

$$l_s = 1 - \exp(-t / t_2). \qquad \textbf{(2.2)}$$

This is the probability of a transition from the silent state, *SIL* to the talking state, *TLK*. Correspondingly, the probability that a principal talkspurt with mean duration t_1 seconds ends in a timeslot of duration t seconds is [4]

$$g = 1 - \exp(-t / t_1). \qquad \textbf{(2.3)}$$

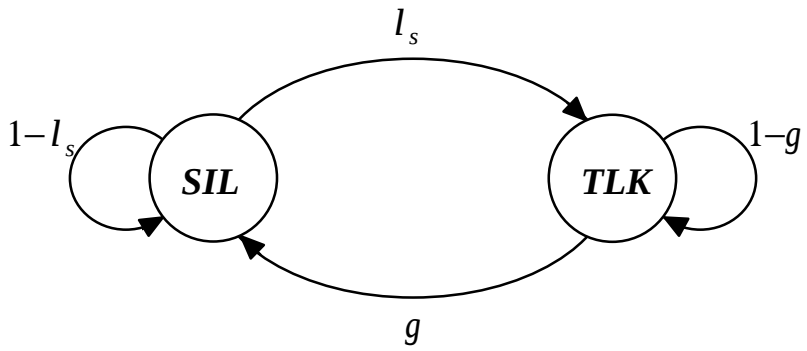

Figure 2.4: *Slow speech activity model.*

Mean values of talkspurt and silent gap durations, as reported in [4], are given in Table 2.1. The corresponding mean speech activity factor (*SAF*), which is the percentage of time that a single speech source is active, is given by

$$SAF = \frac{t_1}{t_1 + t_2} = 0.426 . \qquad \textbf{(2.4)}$$

Condition	Value (s)
Principal Talkspurt, t_1	1.000
Principal Gap, t_2	1.350

Table 2.1: *Parameters for slow speech activity model.*

From Fig. 2.4, it is possible to visualise a speech signal as being composed of a series of talkspurts and silences. A speech terminal operating in a packet-based system will generate a burst of packets corresponding to each talkspurt. In this sense, speech can be considered a source of ‘ long’ information. No packets are generated during the silent periods of speech.

2.2.2 Data Traffic

The characterisation of data traffic is, in many ways, more difficult than the characterisation of speech traffic. This is because the size of a data communication session can vary from a short electronic mail message, carrying only a few bytes of information, up to a long file transfer such as the text of a book, which may be several megabytes long. On the average, the volume of information involved in a data communication session is much smaller than that of a digitised-speech communication session [5, p.2].

Because of this difficulty in uniquely characterising the generation of data traffic, the data traffic model considered in this thesis is relatively simple and is similar to that used in previous analyses of S-ALOHA and PRMA type systems. This tri-state Markov model, illustrated in Fig. 2.5, assumes that the data traffic is a source of ‘short’ information, whereby data messages are

contained within single packets (e.g., email messages). New packets are generated in the origination state (*O*). In the transmission state (*T*), the terminal is busy either transmitting a new packet or re-transmitting a previously unsuccessful packet. The data terminal returns to the *O*-state if it successfully transmits a packet to the base station; otherwise, it enters the retransmission or backlogged state (*RT*). From the latter state, retransmission (i.e., transition into the *T*-state) occurs. A backlogged terminal is blocked in the sense that no new messages can arrive when the terminal is in state *RT*. This implies the absence of a buffer for more than one packet in a data terminal. The specific transition probabilities between the three states depends on the particular system under consideration. Terminal transition probabilities for both S-ALOHA and PRMA data terminals will be presented in later sections of this chapter.

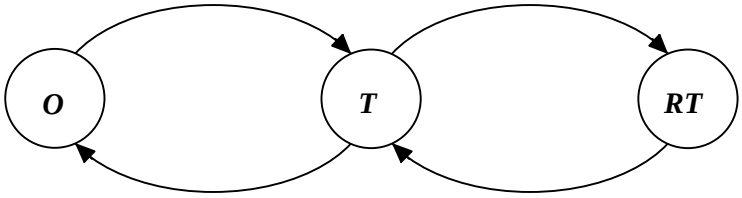

Figure 2.5: *Data terminal model with finite buffer.*

2.2.3 Performance Requirements

In a packetised communication network, speech and data services have different and sometimes contradictory requirements, as summarised in Table 2.2. For example, because of the speech user's expectation of telephone quality speech in the public wired network, packetised speech services must be designed with careful attention to minimising time delays. Inter-packet delays in excess of 30 ms will be noticeable and annoying to the listener[2].

Service	Design Constraint	Performance Targets
Speech	Delay < 30 ms	MOS[3] > 4.0 Decoded BER < 10^{-3} Frame Error Rate < 2%
Low Delay Data	Delay < 30 ms	BER < 10^{-6} Errored Sec. < 10 s/h
High Delay Data	Delay < 300 ms	BER < 10^{-6} Errored Sec. < 10 s/h
Unconstrained Delay Data	Packet Loss < 10^{-6}	Av. Delay < 50 ms 90% Delay < 100 ms

Table 2.2: *Service quality objectives for speech and data services [6].*

[2] In this thesis a packet delay limit of 36 ms is considered in order to accommodate other system parameters and to make the analysis more tractable.
[3] Mean Opinion Score.

In contrast, delay in a data network, while not desirable, is generally acceptable to the data user. Packetised speech can tolerate packet loss rates in the order of 10^{-2}, or bit error rates in the order of 10^{-3} without a noticeable degradation in service quality. An error rate of 10^{-6} is normally accepted for data, but any loss of data packets is totally unacceptable.

2.2.4 Performance Measures

The performance of random access protocols that cater for speech or data traffic can be measured using a number of performance measures. These measures generally relate to the efficiency, delay, accuracy and stability of the system involved. The following performance measures are commonly employed in the analysis of single cell, simple channel S-ALOHA and PRMA systems:

Channel Throughput, h : The channel throughput is defined as the average number of successful packet transmissions per packet transmission time. This measure is used to study the overall efficiency of a random access technique.

Data Packet Delay, W : The data packet delay is the average delay, in slots, that a data packet is held in a terminal's buffer before being successfully transmitted[4]. The delay involved in successful transmission of a data packet depends on how many times it needs to be retransmitted and how long the terminal must wait between retransmissions. Data packets must be retransmitted because loss of data information is normally unacceptable. In S-ALOHA and PRMA, the delay increases significantly when there are a large number of terminals seeking access to the channel.

Speech Packet Dropping Probability, P_{drop} : The speech packet dropping probability is the probability that a speech packet is dropped at a speech terminal due to excessive delay in successfully accessing the base station. Speech packets are dropped to accommodate the delay sensitive nature of speech information. Packets held beyond a certain delay limit are dropped in favour of more recent packets. The probability of packet dropping increases when there are a large number of terminals seeking access to the channel.

Expected Drift, Δ : The expected drift is a measure of the systems dynamic behaviour. With S-ALOHA and PRMA, as with all contention-based random access protocols, there are important issues relating to the stability of the system. The expected drift can be defined as the difference between the expected input traffic and the expected output traffic in a particular system state [7]. The system is expected to operate in a state where the expected drift is equal to zero. These points are referred to as *equilibrium points*.

In Chapter 4 (§4.6.3), additional performance measures are introduced to account for the effect of cochannel interference in multiple cell S-ALOHA and PRMA systems. In particular, the *system utilisation* and *speech packet interference probability* are presented. A further examination of the performance measures, together with analytical expressions are given in Chapters 5-8 of this thesis.

[4] Propagation delays are neglected in this thesis.

2.3 The S-ALOHA Protocol

The S-ALOHA [8] protocol has developed from the original ALOHA[5] protocol. ALOHA derives its name from the ALOHA system, a communications network developed by Abramson and his colleagues at the University of Hawaii and first put into operation in 1971 [9]. The initial system used ground-based UHF radios to connect computers on several of the island campuses with the university's main computer centre at Oahu, by use of a random access protocol which has since been known as the ALOHA protocol.

The concept of S-ALOHA is very simple: users generate information according to a random process, with a terminal generating a new packet in a given timeslot with probability l_d (probability of transition between *O* and *T* states in Fig. 2.5). Once a user has generated a packet, it will attempt to transmit it in the next timeslot. Of course, because multiple users may transmit packets during the same timeslot, there is the possibility of collisions occurring between packets. Thus, after sending a packet, the user waits a length of time equal to the round-trip delay for an acknowledgment from the receiver. If no acknowledgment is received, the packet is assumed lost in a collision and is transmitted again with a randomly selected delay to hopefully avoid repeated collisions. The probability of a data packet being retransmitted in a given timeslot is denoted by p_d (probability of transition between *RT* and *T* states in Fig. 2.5). This procedure continues until the packet is successfully received by the base station. The S-ALOHA process is illustrated in the form of a flow diagram in Fig. 2.6. When a S-ALOHA terminal is attempting to retransmit an unsuccessful packet, no new packets may be generated.

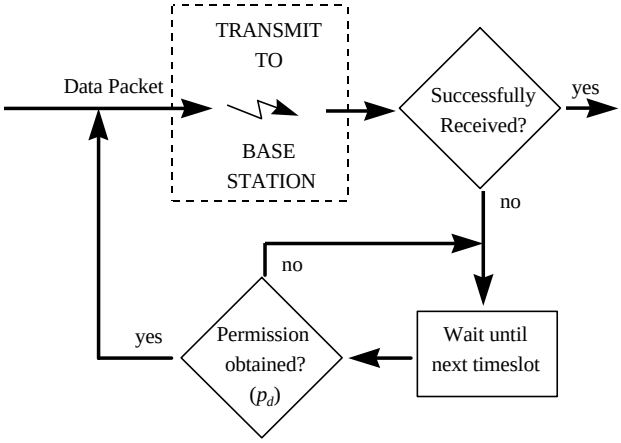

Figure 2.6: *Flow diagram of S-ALOHA operation.*

Fig. 2.7 illustrates a situation where packets are transmitted by three individual terminals. When a collision occurs between terminals 2 and 3 in timeslot 2 (TS2), the individual terminals wait a random time before attempting to retransmit their packets in subsequent timeslots. It is well known that in a single cell simple channel system, the maximum throughput, h, for ALOHA is about 18% (1/*e*) and about 36% (1/2*e*) for S-ALOHA [5, p.466]. This is illustrated in Fig. 2.8.

[5] Also referred to as pure-ALOHA.

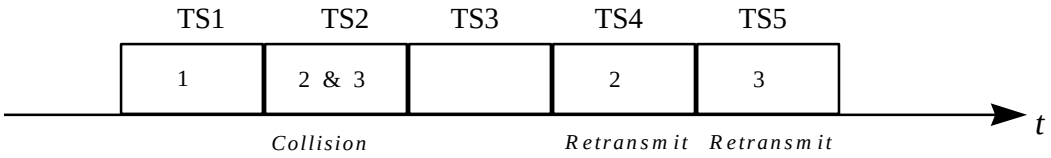

Figure 2.7: *Collision Mechanisms in S-ALOHA.*

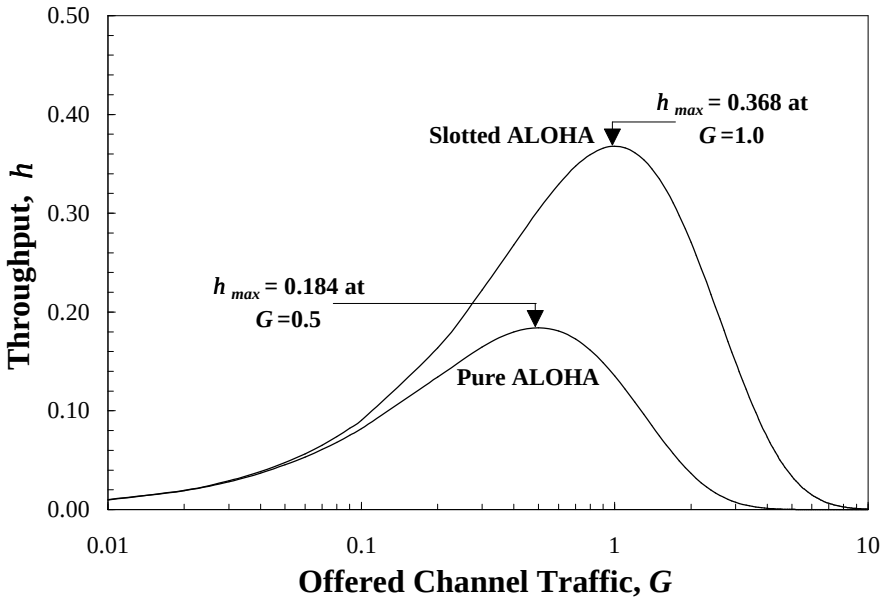

Figure 2.8: *Throughput versus traffic load for Pure and Slotted ALOHA in single cell simple channel systems (from [5]).*

2.4 The PRMA Protocol

The development and analysis of protocols that allow terminals to efficiently transmit packetised speech and data information in a wireless environment was motivated by Goodman in [10], when he proposed the Packet Reservation Multiple Access (PRMA) scheme. PRMA merges characteristics of the S-ALOHA and TDMA protocols. PRMA employs a Time Division Multiplex (TDM) based structure as presented in Fig. 2.2. For a speech terminal source rate of R_s bits/sec, channel rate per cell R_{cell} bits/sec, header size H bits/packet and frame duration T seconds, the number of slots in each frame is given by [11]

$$N = \text{int}\left[\frac{R_{cell}T}{R_sT + H}\right], \qquad \textbf{(2.5)}$$

where int[x] is the largest integer $\leq x$. The frame structure is designed so that speech sources generate exactly one packet per frame. Speech terminals generate bursts of packets corresponding to talkspurts whereas data terminals generate packets randomly. Speech and data terminals recognise timeslots as being either available or reserved. Speech and data terminals with new

packets contend for access during available timeslots. Permission to transmit during an available timeslot is granted if the output of the terminal's uniform random number generator is less than or equal to the permission probability, where the speech permission probability p_s, is normally greater than the data permission probability p_d. Permission to transmit at each terminal is independent of permissions at other terminals.

When a speech terminal contends successfully, it obtains a reservation for exclusive use of that timeslot in subsequent frames until it has no more packets to transmit. In this way, the speech terminals with reservations share the channel as in TDMA. Data terminals on the other hand, must contend each time that they have a packet to transmit. If a contending speech or data packet is unsuccessful in capturing the base station, the terminal involved may retransmit the packet in a future available timeslot. Speech packets, however, cannot be held at a speech terminal indefinitely due to the delay requirements of speech. Therefore, in PRMA any speech packet held beyond a certain number of slots is dropped by its terminal. Data packets, on the other hand, are retransmitted until successful, due to their stringent error requirements which do not allow them to be dropped. Flow diagrams that illustrate the process by which speech and data packets are transmitted in a PRMA system are presented in Figs. 2.9 and 2.10, respectively.

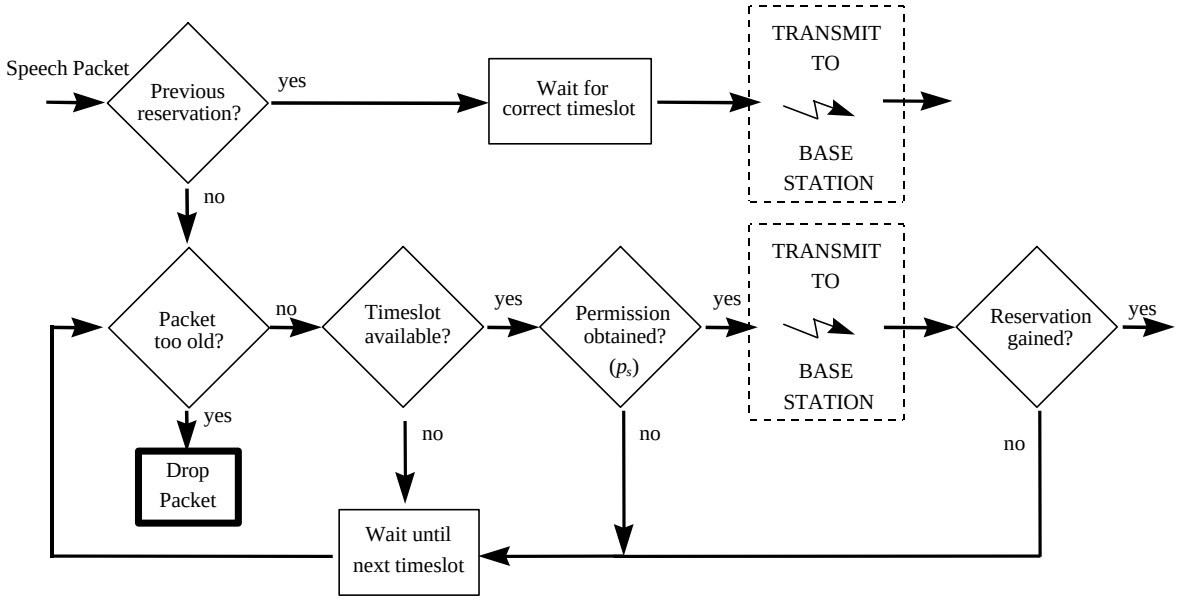

Figure 2.9: *Flow diagram of PRMA operation (speech users).*

A speech terminal contains a first-in-first-out (FIFO) buffer to store packets awaiting transmission. The capacity of the speech buffer is B_s packets. If the buffer is full when a new packet arrives, the terminal drops the oldest packet and stores the new packet. With the packet dropping mechanism, the speech buffer size required is

$$B_s = [D_{max} / T], \qquad \textbf{(2.6)}$$

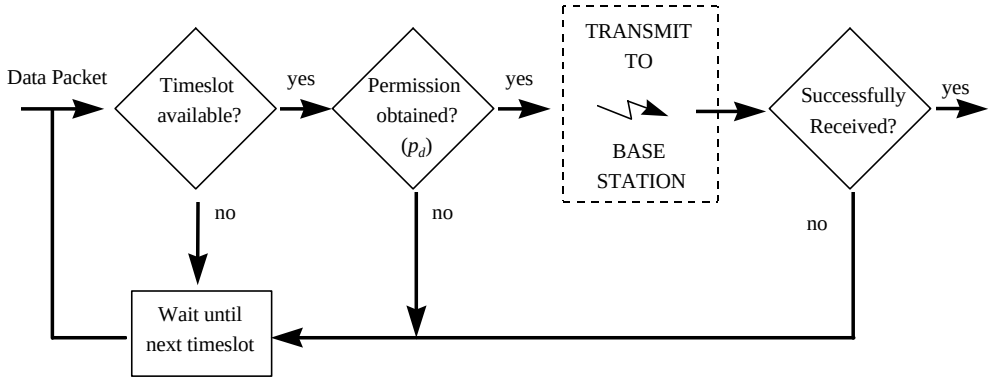

Figure 2.10: *Flow diagram of PRMA operation (data users).*

with $[x]$ denoting the smallest integer $\geq x$. T is the frame duration and D_{max} is the maximum transmission delay for speech. For short speech packets (for example, 16 ms of speech information) packet dropping probabilities, P_{drop}, up to 0.01 are acceptable [12]. Using speech interpolation techniques [13,14], even higher packet dropping rates may be tolerated. In this thesis packet dropping probabilities of either 1% and 5% are considered.

Fig. 2.11 illustrates the operation of a single cell speech-only PRMA system. In this example, there are eight time slots per frame and the base station feedback packets for frame K-1 have established that, in frame K, six slots are already reserved and two slots are available.

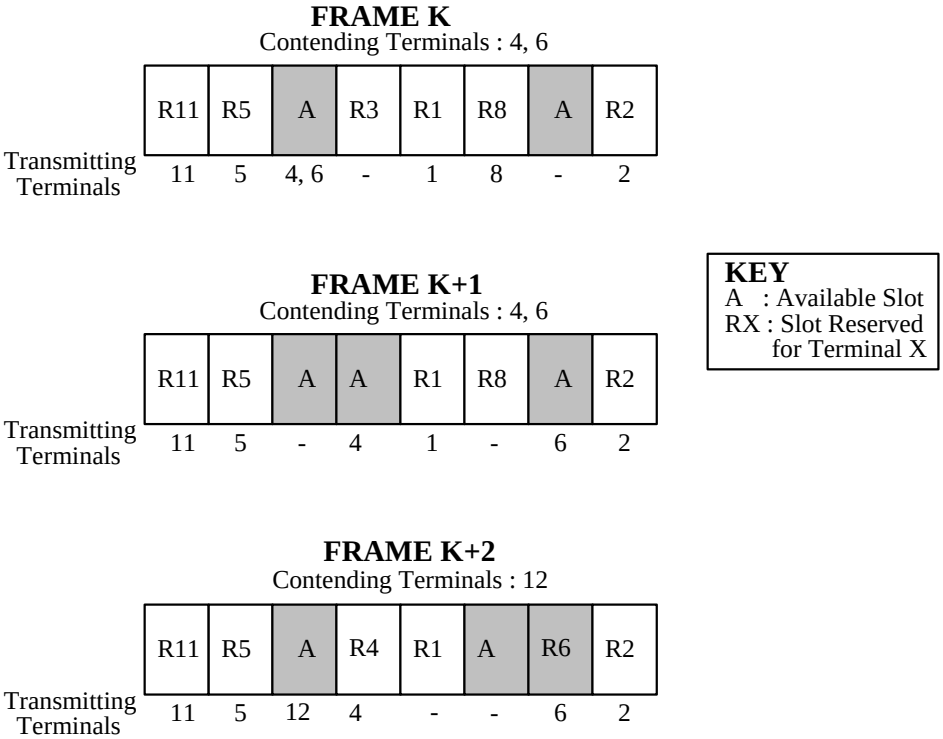

Figure 2.11: *PRMA protocol operation example*

At the beginning of frame K, terminals 4 and 6 are contending for access to the channel. Both of these terminals obtain permission to transmit in slot 3 and, because their packets collide, neither obtain a reservation. In slot 7, both terminals fail to obtain permission to transmit and, thus, remain in the contending state at the beginning of frame K+1. Meanwhile in frame K-1, terminal 3 transmitted the final packet in its talkspurt. Therefore in frame K (slot 4) it does not use its reservation. The base station feedback packet for slot 4 of frame K indicates that slot 4 is available in frame K+1.

In frame K+1, neither terminal 6 nor terminal 4 has permission to transmit in slot 3. In slot 4, terminal 4 has permission but terminal 6 does not. Thus, terminal 4 gains a reservation for slot 4. Terminal 6 obtains permission to transmit in slot 7 and reserves that slot in frame K+2. In frame K+1, terminal 8 gives up its reservation of slot 6, and a talkspurt begins at terminal 12 which enters the contending state. In frame K+2, terminal 12 gains a reservation (slot 3) and terminal 1 releases its reservation (slot 5).

Fig. 2.12 presents the speech packet dropping probability for a speech-only, single cell, simple channel PRMA system. In this particular example the single cell PRMA system is capable of supporting 37 speech terminals at $P_{drop} = 0.01$ and 44 speech terminals at $P_{drop} = 0.05$. This particular system is based on the parameters of [15], in which N=20 timeslots per frame was assumed. This result illustrates the ability of PRMA to support significantly more users compared to the number of timeslots.

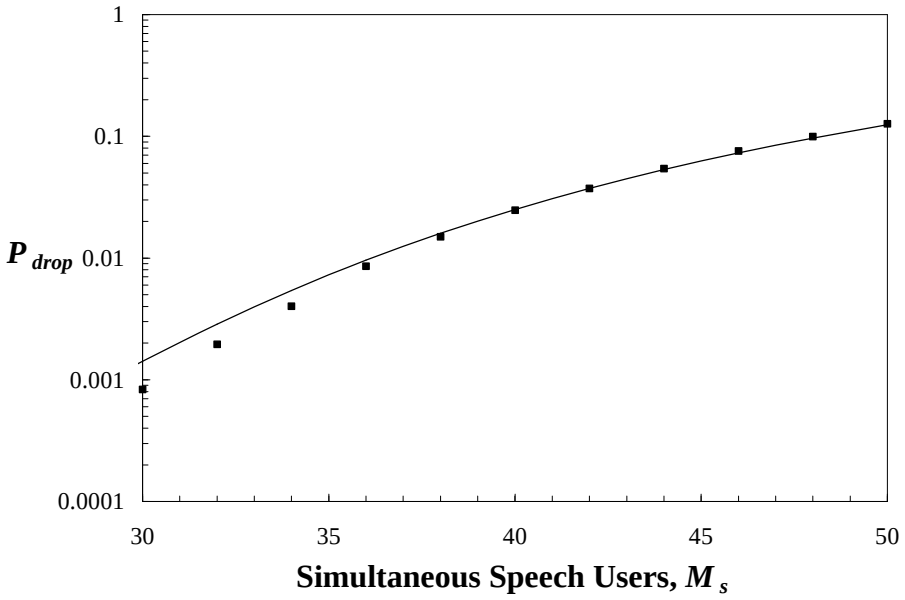

Figure 2.12: *Speech packet dropping probability in a speech-only, single cell, simple channel PRMA system. The parameters assumed are the same as those in [15]. Both Markov analysis results (lines) and simulation results (single points) are presented.*

This is achieved by the statistical multiplexing nature of PRMA, whereby individual speech signals are multiplexed at the talkspurt level as opposed to the call level, as in TDMA. In an equivalent TDMA system without any overheads[6], it would be possible to support only 22.5 speech terminals [15].

2.5 Literature Review

Considerable research has already been undertaken into S-ALOHA and PRMA. A summary of the key research, as it relates to the work examined in this thesis, is presented in this section. This literature review considers research relating to S-ALOHA and PRMA in single cell, simple channel systems. This is then extended to research that has considered single cell S-ALOHA and PRMA systems with variable channels. Finally, multiple cell S-ALOHA and PRMA systems are examined. Unlike the simple channel model described in §2.1, realistic radio channels allow for situations in which a packet may be received successfully by the base station in the presence of other competing packets. This phenomenon is due to the variable nature of the propagation channel, which results in the received powers of individual packets being different. In such a situation, a dominant packet (i.e., a packet with a high power level) may be capable of *capturing*[7] the base station receiver.

2.5.1 S-ALOHA Systems

Single Cell S-ALOHA Systems with Simple Channel

In [7] Carleial and Hellman used Markov analysis [16,17] to study a single cell, simple channel S-ALOHA system. Expressions were developed to describe the throughput, delay and drift for such a system. The bistable nature of S-ALOHA was studied in detail. Bi-stability refers to the situation where the system can, in some circumstances, possess two statistically stable equilibrium points, one in a desirable low-delay region, and the other in an un-desirable high delay region, with the system oscillating between the two equilibrium points. In [18] it was shown that S-ALOHA can possess either one stable equilibrium point or three equilibrium points, with the first and third points stable and the second one unstable. Similar findings were presented by Kleinrock and Lam in [19], also via Markov analysis.

Markov analysis involves formulating a Markovian model of the system and obtaining the state probability distribution of the Markov chain from the state transition probabilities. While Markov analysis is a more involved technique, it provides information regarding the dynamic behaviour and throughput-delay characteristics of the system, which other techniques such as the *infinite population model*[8] and *equilibrium point analysis* (EPA) are unable to provide. The infinite population analysis was devised by Abramson in [9] to evaluate the performance of the ALOHA system. This technique assumes that the system stays in equilibrium and that the traffic source consists of an infinite number of users, who collectively form an independent Poisson source. It can be readily applied to the analysis of complex contention-based systems (e.g. [20]). However, the infinite population model cannot reveal the dynamic behaviour of the system; that is, this technique cannot give any solution to the stability problem which is present in all contention-

[6] i.e., without packet headers.
[7] The concept of receiver capture will be discussed in detail in Chapter 4.
[8] Also referred to as S-G (throughput-delay) analysis, or Poisson analysis.

based systems. EPA analysis represents a simplification of the more complex Markov analysis. EPA assumes that the system is always at an equilibrium point. Under this assumption it is not necessary to calculate the state transition probabilities of the Markov chain. The importance of the equilibrium point in contention-based systems was first noticed by Carleial and Hellman [7] and Kleinrock and Lam [19]. Fukuda introduced an analytical technique based on this result in [21-23].

Single Cell S-ALOHA Systems with Variable Channel

Over more recent years, S-ALOHA has been analysed in single cell systems with more realistic channels. In [24] Namislo carried out a Markov analysis of a single cell S-ALOHA system with receiver capture, although no specific channel or capture model was considered. In [25] Goodman and Saleh considered a channel model based on distance-dependent pathloss, while in [26] Arnbak and Blitterswijk considered a Rayleigh fading channel. The performance of S-ALOHA in a single cell system with Rayleigh fading, shadowing and near-far effect was analysed by van der Plas and Linnartz [27] and Sheikh, Yao and Wu [28]. It was found in both [24] and [27] that receiver capture, aided by a highly variable propagation channel, reduced the bi-stability of S-ALOHA substantially, compared to the case where a simple channel was considered. The central finding of [24-28] was that a variable channel enhanced the overall performance of single cell S-ALOHA systems. Other research into single cell variable channel S-ALOHA systems has been presented in [29-33].

Multiple Cell S-ALOHA Systems

Most recently, several researchers have considered the operation of S-ALOHA in multiple cell systems. In [34] Linnartz investigated the performance of S-ALOHA in a cellular environment using an infinite population model. It was found that frequency reuse distances in packet switched systems, such as S-ALOHA, can be smaller than in circuit switched systems. In this situation, S-ALOHA overcomes the effect of cochannel interference through random retransmission of information. This is as opposed to the spatial isolation of cochannel cells, as is usual in FDMA/TDMA systems. In [35] Zorzi and Pupolin proposed S-ALOHA as a multiple access scheme for voice cellular communications. An analysis of a system with complete frequency reuse was performed using an infinite population model. Other research into multiple cell S-ALOHA systems has been presented in [36-38].

2.5.2 PRMA Systems

Single Cell PRMA Systems with Simple Channel

Initial studies of both speech and joint speech-data PRMA systems focused primarily on the performance in an interference-free, single cell architecture. These studies assume that all packets involved in collisions with other packets at the base station receiver are destroyed; likewise all packets not in collision are received correctly. In [11], Goodman presented an overview of the cellular packet switch and packet reservation multiple access concepts. In [15] Goodman and Wei investigated the performance of PRMA via computer simulation and found the protocol to be capable of supporting 1.64 speech conversations per channel at a packet dropping probability of 1%. The effect of frame duration, speech activity detector and speech permission probability, p_s, on the speech packet dropping probability were determined.

Nanda, Goodman and Timor used equilibrium point analysis (EPA) in [39] to study a speech-only PRMA system. Expressions for the speech packet dropping probability, P_{drop}, and throughput, h, were derived, and the necessary conditions for system stability and efficiency were established. In [40] and [41] the performance of an integrated speech-data PRMA system was determined by Nanda using equilibrium point analysis. It was found that PRMA gracefully accepted low-rate data terminals with moderate data packet delays. The EPA used in this paper required a judicious change of variables to reduce the analysis to a univariate problem of the same form as the speech-only system of [39]. In the analysis of [39], the probability distribution functions were derived when there was a single equilibrium point. It was assumed that the equilibrium value of the state variable was equal to the mean. This method underestimates the system performance since it assumes that the system is always at a stable equilibrium point. In practice, the system state moves to a state space according to some state distribution. The error between analysis and computer simulation results in [39] is too large in some cases to satisfy designer's requirements.

In [42] a modification to the original integrated speech-data PRMA system of [40] and [41] was proposed by Wong and Goodman, whereby data terminals could reserve multiple slots across a frame. From the computer simulation results, this modification was shown to improve slot utilisation without compromising speech transmission performance. In [43], Eastwood, Hanzo and Cheung investigated the ability of PRMA to transport a mixture of speech, data and video information. This investigation was performed using computer simulations. In [44] Wu, Mukumoto and Fukuda determined the performance of a speech-data PRMA system using the theory of Markov analysis. This analysis method appears to be more accurate than methods proposed in earlier papers [39-41], which use an EPA technique. However, [44] did not present any results regarding the speech packet dropping probability. In addition, the analysis of [44] assumed that terminal departures from the various states only occurred at the end of frames, when in practice, they occur at the end of timeslots.

Qi and Wyrwas presented a Markov analysis of a speech-only PRMA system in [45]. Results relating to the speech packet dropping probability, throughput and first exit time (FET) [19] were presented. The agreement between analytical and simulation results was better than the agreement shown in [39], where EPA was employed. Unlike [44], the Markov analysis of [45] assumed terminal departures from the various states occurred at the end of timeslots. The analysis presented in [45] forms the basis for the mathematical analysis of PRMA presented in this thesis. While Markov analysis is more complicated than EPA, it is able to reveal more information about the system's performance and stability than EPA. Other research into single cell, simple channel PRMA systems has been presented in [46-53].

Single Cell PRMA Systems with Variable Channel

In [54], the performance of a speech-only PRMA system in the presence of random packet transmission impairments was investigated using computer simulation. It was assumed that speech terminals that lose reservations early due to transmission errors have to recontend for a new reservation and hence, risk dropping old packets while waiting. In [55], a modified PRMA protocol was proposed to minimise premature loss of reservations when the protocol operates in the presence of random packet transmission impairments. This modification was also suggested as part of the research presented in [56].

In [57] a speech-only PRMA system was studied via Markov analysis. The Markov analysis was an extension of that presented in [45]. A propagation channel which accounted for distance dependent pathloss, lognormal shadowing and Rayleigh fading was considered. It was found that the capture effect was capable of providing considerable improvements to PRMA performance, especially in highly variable propagation environments. In [58] the performance of a speech-only PRMA system was determined via Markov analysis. In this system, the desired terminal was assumed to transmit packets suffering from Rician fading, whereas other contending packets suffered from Rayleigh fading.

In [59] Qi and Wyrwas presented two analysis methods for a joint speech-data PRMA system suffering from random packet transmission impairments. The first was a combined EPA and Markov analysis, while the second was a Markov analysis which used an approximate marginal distribution of backlogged data terminals. Expressions were derived for the speech packet dropping probability, P_{drop}, data packet delay, W, and throughput, h, in the presence of random packet errors. The two methods were found to produce similar results, although the latter method was more complex than the former method.

In [60] the performance of a speech-only PRMA system was determined by Qiu and Li using Markov analysis. A combined Rician-Lognormal channel was considered and the capture effect was incorporated. Other research into single cell, variable channel PRMA systems has been presented in [61-64].

Multiple Cell PRMA Systems

In the simulation studies of [65-68] and [69] the performance of speech-only and speech-data cellular PRMA systems were determined, respectively. A channel model which incorporated distance dependent pathloss and lognormal shadowing was used. In [65-69], it is assumed that a powerful error correcting code protects the packet header, which prevents it from being destroyed even when cochannel interference causes corruption to the packet's information field. By making this assumption, it is implicitly assumed that a terminal's reservation is not lost prematurely due to cochannel interference. Only the packet transmitted in the presence of the cochannel interference is lost, with the following packets of the same talkspurt able to be transmitted. The findings of [69] indicated that the performance of PRMA may be severely affected by cochannel interference. It was suggested that methods should be investigated to reduce the impact of this cochannel interference.

In the simulation study of [70] the concept of Space and Time Reservation Multiple Access (STRMA) was presented. STRMA can be viewed as a dynamic cellular PRMA protocol, whereby terminals not only reserve bandwidth for a certain period of time (as in the original PRMA protocol), but also reserve the bandwidth over a certain geographical space in order to reduce interference to nearby cells. By reserving the bandwidth for a particular user part of the time in part of the network, a frequency reuse pattern is created but this pattern is no longer fixed. In the simulation study of [71], Mastroforti determined the performance of a speech-only PRMA system in a cellular environment. A channel model which incorporated distance dependent pathloss and lognormal shadowing was considered.

2.6 Summary

In this chapter, it has been shown that significant differences exist between the nature and requirements of speech and data traffic. These differences present challenges when designing transmission protocols capable of integrating speech and data traffic in an efficient and accurate manner.

The concept of transmitting speech and data information using packetised random access methods has also been presented in this chapter. In particular, the S-ALOHA and PRMA protocols have been presented in terms of their operation in single cell systems, free from cochannel interference. S-ALOHA is confined to the transmission of data traffic, whereas PRMA is capable of supporting both speech and data traffic. Appropriate performance measures, from which the performance of S-ALOHA and PRMA may be determined, have been presented. These include the throughput, data packet delay, speech packet dropping probability and drift. A detailed literature review that considers not only single cell S-ALOHA and PRMA systems but also multiple cell S-ALOHA and PRMA systems has also been presented.

This chapter has focused primarily on the theoretical considerations of the random access protocols being investigated in this thesis. The aim of this thesis is, however, the consideration of S-ALOHA and PRMA in more realistic situations, namely multiple cell variable channel systems. As a first step to completing this aim, the following chapter will present an overview of radiowave propagation in multiple cell environments.

References

[1] L. Hanzo, J. C. S. Cheung, R. Steele, W. T. Webb, “A packet reservation multiple access assisted cordless telecommunication scheme,” *IEEE Trans. Veh. Technol.*, vol. 43, no. 2, May 1994, pp. 234 - 244.

[2] P. T. Brady, “A model for generating on-off speech patterns in two-way conversation,” *Bell. Syst. Tech. J*., vol. 48, pp. 2445 - 2472, Sept. 1969.

[3] R. W. Muise, T. J. Schonfeld, G. H. Zimmerman III, “Experiments in wideband packet technology,” in *Proc. 1986 Zurich Seminar.*, pp. D4.1 - D4.5.

[4] S. Nanda, D. J. Goodman, U. Timor, “Performance of PRMA: a packet voice protocol for cellular systems,” *IEEE Trans. Veh. Technol.*, vol. 40, no. 3, Aug. 1991, pp. 584 - 598.

[5] K. Pahlavan, A. H. Levesque, *Wireless Information Networks*, John Wiley and Sons Inc., 1995.

[6] D. Grillo, N. Metzner, E. D. Murray, “Testbed for assessing the performance of a TDMA-based radio access design for UMTS,” *IEEE Personal Commun. Mag.*, vol. 2, no. 2, Apr. 1995, pp. 36 - 45.

[7] A. B. Carleial, M. E. Hellman, “Bistable behavior of ALOHA-type systems,” *IEEE Trans. Commun.*, vol. 23, no. 4, Apr. 1975, pp. 401 - 409.

[8] L. G. Roberts, “ALOHA packet systems with and without slots and capture,” *Comput. Commun. Rev*., vol. 5, no. 2, Apr. 1975, pp. 28 - 42.

[9] N. Abramson, “The ALOHA system - another alternative for computer communications,” *Proc. 1970 Fall Joint Comput. Conf.*, AFIPS Press, vol. 37, 1970, pp. 281 - 285.

[10] D. J. Goodman, R. A. Valenzuela, K. T. Gayliard, B. Ramamurthi, "Packet reservation multiple access for local wireless communications," *IEEE Trans. Commun*., vol. 37, no.8, 1989, pp.885-890.

[11] D. J. Goodman, “Cellular packet communications,” *IEEE Trans. Commun.*, vol. 38, no. 8, Aug. 1990, pp. 1272 - 1280.

[12] J. G. Gruber, L. Strawczynski, “Subjective effects of variable delay and speech clipping in dynamically managed voice systems,” *IEEE Trans. Commun.*, vol. 33, no. 8, Aug. 1985, pp. 801 - 808.

[13] N. S. Jayant, S. W. Christensen, “Effects of packet losses in waveform coded speech and improvements due to an odd-even sample interpolation procedure,” *IEEE Trans. Commun.*, vol. 29, Feb. 1981, pp. 101-109.

[14] O. J. Wasem, D. J. Goodman, C. A. Dvorak, H. G. Page, “The effect of waveform substitution on the quality of PCM packet communications,” *IEEE Trans. Commun.*, vol. 36, Mar. 1988, pp. 342-348.

[15] D. J. Goodman, S. X. Wei, “Efficiency of packet reservation multiple access,” *IEEE Trans. Veh. Technol.*, vol. 40, no. 1, Feb. 1991, pp. 170 - 176.

[16] D. L. Isaacson, R. W. Madsen, *Markov Chains: Theory and Applications.* New York, Wiley, 1976.

[17] R. B. Mattingly, C. D. Meyer, “Computing the stationary distribution vector of an irreducible Markov chain on a shared-memory multiprocessor,” *in Numerical Solution of Markov Chains*, W. J. Stewart, Ed., Dekker, 1991, pp. 491 - 510.

[18] Y. -C. Jenq, “On the stability of slotted ALOHA systems,” *IEEE Trans. Commun.*, vol. 28, no. 11, Nov. 1980, pp. 1936 - 1939.

[19] L. Kleinrock, S. S. Lam, “Packet switching in a multiaccess broadcast channel: performance evaluation,” *IEEE Trans. Commun.*, vol. 23, no. 4, Apr. 1975, pp. 410 - 422.

[20] L. Kleinrock, F. Tobagi, “Packet switching in radio channels: Part I - carrier sense multiple access modes and their throughput delay characteristics,” *IEEE Trans. Commun*., vol. 23, no. 12, Dec. 1975, pp. 1400 - 1416.

[21] A. Fukuda, “Equilibrium point analysis of ALOHA-type systems,” *Trans. IECE Japan (in Japanese)*, vol. J61-B, Nov. 1978, pp. 959 - 966.

[22] A. Fukuda, S. Tasaka, "The equilibrium point analysis - a unified analytic tool for packet broadcast networks," *in Proc. 1983 IEEE Global Telecommunications Conf.*, San Diego, California, Nov 1983, pp. 33.4.1 - 33.4.8.

[23] S. Tasaka, "Stability and performance of the R-ALOHA packet broadcast system," *IEEE Trans. Comput*., vol. 32, Aug. 1983, pp. 717 - 726.

[24] C. Namislo, "Analysis of mobile radio slotted ALOHA networks," *IEEE J. Selected Areas Commun.*, vol. 2, no. 4, Jul. 1984, pp. 583 - 588.

[25] D. J. Goodman, A. A. M. Saleh, "The near/far effect in local ALOHA radio communications," *IEEE Trans. Veh. Technol.*, vol. 36, no. 1, Feb. 1987, pp. 19 - 27.

[26] J. Arnbak, W. van Blitterswijk, "Capacity of slotted ALOHA in Rayleigh-fading channels," *IEEE J. Selected Areas Commun.*, vol. 5, no. 2, Feb. 1987, pp. 261 - 269.

[27] C. van der Plas, J. P. M. G. Linnartz, "Stability of mobile slotted ALOHA network with Rayleigh fading, shadowing, and near-far effect," *IEEE Trans. Veh. Technol.*, vol. 39, no. 4, Nov. 1990, pp. 359 - 366.

[28] A. U. H. Sheikh, Y.-D. Yao, X. Wu, "The ALOHA systems in shadowed mobile radio channels with slow or fast fading," *IEEE Trans. Veh. Technol.*, vol. 39, no. 4, Nov. 1990, pp. 289 - 298.

[29] H. H. Tan, S. V. Hung, "Performance analysis of slotted ALOHA over fading communications channels," *in Proc. 9th Annual Joint Conference of the IEEE Computer and Communications Societies, INFOCOM'90*, San Francisco, California, Jun. 1990, pp. 595 - 602.

[30] J.- P. M. G. Linnartz, R. Hekmat, R.- J. Venema, "Near-far effects in land mobile random access networks with narrow-band Rayleigh fading channels," *IEEE Trans. Veh. Technol.*, vol. 41, no. 1, Feb. 1992, pp. 77 - 89.

[31] I. Widipangestu, A. J. 'T Jong, R. Prasad, "Capture probability and throughput analysis of slotted ALOHA and unslotted np-ISMA in a Rician/Rayleigh environment," *IEEE Trans. Veh. Technol.*, vol. 43, no. 3, Aug. 1994, pp. 457 - 465.

[32] M. Zorzi, R. R. Rao, "Capture and retransmission control in mobile radio," *IEEE J. Selected Areas Commun.*, vol. 12, no. 8, Oct. 1994, pp. 1289 - 1298.

[33] M. Zorzi, "Mobile radio slotted ALOHA with capture and diversity," *Wireless Networks*, no. 1, 1995, pp. 227 - 239.

[34] J.- P. M. G. Linnartz, "Slotted ALOHA land-mobile radio networks with site diversity," *IEE Proceedings-I*, vol. 139, no. 1, Feb. 1992, pp. 58 - 70.

[35] M. Zorzi, S. Pupolin, "Slotted ALOHA for high-capacity voice cellular communications," *IEEE Trans. Veh. Technol.*, vol. 43, no. 4, Nov. 1994, pp. 1011 - 1021.

[36] K. Sakakibara, “Performance approximation of a multi-base station slotted ALOHA for wireless LAN's,” *IEEE Trans. Veh. Technol.*, vol. 41, no. 4, Nov. 1992, pp. 448 - 454.

[37] J.- P. M. G. Linnartz, “Imperfect sector antenna diversity in slotted ALOHA mobile network,” *IEEE Trans. Commun.*, vol. 44, no. 10, Oct. 1996, pp. 1322 - 1328.

[38] J. G. Lee, M. Scott Corson, “The performance of an "imbedded" ALOHA protocol in wireless networks,” *in Proc. 7th IEEE International Symposium on Personal, Indoor and Mobile Radio Communications, PIMRC'96*, Taipei, Taiwan, ROC, Oct. 1996, pp. 377 - 381.

[39] S. Nanda, D. J. Goodman, U. Timor, “Performance of PRMA: a packet voice protocol for cellular systems,” *IEEE Trans. Veh. Technol.*, vol. 40, no. 3, Aug. 1991, pp. 584 - 598.

[40] S. Nanda, “Analysis of packet reservation multiple access: voice data integration for wireless networks,” *in Proc. 1990 IEEE Global Telecommunications Conf.,* San Diego, California, Dec. 1990, pp. 1984 - 1988.

[41] S. Nanda, “Stability evaluation and design of the PRMA joint voice data system,” *IEEE Trans. Commun.*, vol. 42, no. 5, May 1994, pp. 2092 - 2104.

[42] W. C. Wong, D. J. Goodman, “A packet reservation multiple access protocol for integrated speech and data transmission,” *IEE Proceedings-I*, vol. 139, no. 6, Dec. 1992, pp. 607 - 612.

[43] M. Eastwood, L. Hanzo, J. C. S. Cheung, “Packet reservation multiple access for wireless multimedia communications,” *Electronics Letters*, vol. 29, no. 13, Jun. 24th 1993, pp. 1178 - 1180.

[44] G. Wu, K. Mukumoto, A. Fukuda, "Analysis of an integrated voice and data transmission system using packet reservation multiple access," *IEEE Trans. Veh. Technol*., vol. 43, no. 2, May 1994, pp. 289 - 297.

[45] H. Qi, R. Wyrwas, “Markov analysis for PRMA performance study,” in *Proc. 44th IEEE Veh. Technol. Conf.*, Stockholm, Sweden, May 1994, pp.1184-1188.

[46] R. Bolla, F. Davoli, M. Taffone, F. Reichert, “The PRMA-ISA protocol for multiple access of mixed voice and data traffic,” *in Proc. 44th IEEE Veh. Technol. Conf.,* Stockholm, Sweden, May 1994, pp. 1213 - 1217.

[47] P. Narasimhan, R. Yates, D. J. Goodman, “Performance analysis of frame reservation multiple access,” *in Proc.1994 3rd Annual International Conf. on Universal Personal Communications*, San Diego, California, Sep. 1994, pp. 26 - 30.

[48] S.T. Chua, K. C. Chua, K. M. Lye, “Minislotted packet reservation multiple access protocol for integrated voice-data transmission,” *in Proc. 1994 IEEE International Conf. on Communication Systems, ICCS'94*, Singapore, Nov. 1994, pp. 320 - 323.

[49] G. Bianchi, F. Borgonovo, L. Fratta, L. Musumeci, M. Zorzi, "C-PRMA: the centralised packet reservation multiple access for local wireless communications," *in GLOBECOM, 94*, San Francisco, California, Nov. 1994, pp. 1340 - 1345.

[50] J. S. Jang, B. C. Shin, "Performance evaluation of fast PRMA protocol," *Electronics Letters*, vol. 31, no. 5, Mar. 2nd 1995, pp. 347 - 349.

[51] P. Narasimhan, R. D. Yates, "A new protocol for the integration of voice and data over PRMA," *IEEE J. Selected Areas Commun.*, vol. 14, no. 4, May 1996, pp. 623 - 631.

[52] P. Taaghol, R. Tafazolli, B. G. Evans, "Burst reservation multiple access techniques for the GSM/DCS and DECT systems," *in Proc. 7th IEEE International Symposium on Personal, Indoor and Mobile Radio Communications, PIMRC'96*, Taipei, Taiwan, Oct. 1996, pp. 412 - 416.

[53] X.-F. Dong, L.-M. Li, "Spread spectrum PRMA and minimum reservation capacity spread spectrum PRMA for microcellular networks," *in Proc. 7th IEEE International Symposium on Personal, Indoor and Mobile Radio Communications, PIMRC'96*, Taipei, Taiwan, Oct. 1996, pp. 633 - 637.

[54] L. M. A. Jalloul, S. Nanda, D. J. Goodman, "Packet reservation multiple access over slow and fast fading channels," *in Proc. 40th IEEE Veh. Technol. Conf.*, Orlando, Florida, May 1990, pp. 354 - 359.

[55] K. C. Chua, W. M. Tan, "Modified packet reservation multiple access protocol," *Electronics Letters*, vol. 29, no. 8, Apr. 15th 1993, pp. 682 - 684.

[56] M. M. Khan, D. J. Goodman, "Effects of channel impairments on packet reservation multiple access," *in Proc. 44th IEEE Veh. Technol. Conf.*, Stockholm, Sweden, May 1994, pp. 1218 - 1222.

[57] H. Qi, R. Wyrwas, "Capture effects on PRMA stability and performance," *Electronics Letters*, vol. 30, no. 7, Mar. 31st 1994, pp. 539 - 540.

[58] C. van den Broek, R. Prasad, "Effect of capture on the performance of the PRMA protocol in an indoor radio environment with BPSK modulation," *in Proc. 44th IEEE Veh. Technol. Conf.*, Stockholm, Sweden, May 1994, pp. 1223 - 1227.

[59] H. Qi, R. Wyrwas, "Performance analysis of joint voice-data PRMA over random packet error channels," *IEEE Trans. Veh. Technol.*, vol. 45, no. 2, May 1996, pp. 332 - 345.

[60] X. Qiu, V. O. K. Li, "On the capacity of packet reservation multiple access with capture in personal communication systems," *IEEE Trans. Veh. Technol.*, vol. 45, no. 4, Nov. 1996, pp. 666 - 675.

[61] R. A. Ziegler, G. P. Pollini, "An experimental implementation of the PRMA protocol for wireless communication," *Proc. 43rd IEEE Veh. Technol. Conf.*, Secaucus, New Jersey, May 1993, pp. 909 - 912.

[62] L. Hanzo, J. P. Woodward, “An intelligent multimode voice communications system for indoor communications,” *IEEE Trans. Veh. Technol.*, vol. 44, no. 4, Nov. 1995, pp. 735 - 748.

[63] L. Hanzo, J. C. S. Cheung, R. Steele, W. T. Webb, “Performance of PRMA schemes via fading channels,” *in Proc. 43rd IEEE Veh. Technol. Conf.*, Secaucus, New Jersey, May 1993, pp. 913 - 916.

[64] L. Hanzo, J. C. S. Cheung, R. Steele, W. T. Webb, “A packet reservation multiple access assisted cordless telecommunication scheme,” *IEEE Trans. Veh. Technol.*, vol. 43, no. 2, May 1994, pp. 234 - 244.

[65] M. Frullone, G. Falciasecca, P. Grazioso, G. Riva, A. M. Serra, “On the performance of packet reservation multiple access with fixed and dynamic channel allocation,” *IEEE Trans. Veh. Technol.*, vol. 42, no. 1, Feb. 1993, pp. 78 - 86.

[66] M. Frullone, G. Riva, P. Grazioso, M. Missiroli, “Comparisons of multiple access schemes for personal communication systems in a mixed cellular environment,” *IEEE Trans. Veh. Technol.*, vol. 43, no. 1, Feb. 1994, pp. 99 - 109.

[67] M. Frullone, G. Riva, P. Grazioso, C. Carciofi, “Self-adaptive channel allocation strategies in cellular environments with PRMA,” *in Proc. 44th IEEE Veh. Technol. Conf.*, Stockholm, Sweden, May 1994, pp. 819 - 823.

[68] M. Frullone, G. Riva, P. Grazioso, C. Carciofi, “PRMA performance in cellular environments with self-adaptive channel allocation strategies,” *IEEE Trans. Veh. Technol.*, vol. 45, no. 4, Nov. 1996, pp. 657 - 665.

[69] D. Grillo, M. Frullone, P. Grazioso, P. Valigi, "A performance analysis of PRMA considering speech/data traffic, co-channel interference and ARQ error recovery," *in Proc. 7th IEE European Conf. on Mobile and Personal Communications*, Brighton, United Kingdom, no. 387, Dec. 1993, pp. 167-172.

[70] C. van den Broek, J.- P. M. G. Linnartz, “A simulation study of space and time reservation multiple access,” *in Proc. 6th IEEE International Symposium on Personal, Indoor and Mobile Radio Communications, PIMRC'95*, Toronto, Canada, Sep. 1995, pp. 527 - 531.

[71] M. Mastroforti, “Up-link capacity evaluation of a PRMA based system in a terrestrial radio mobile environment,” *Centro Studi e Laboratori Telecomunicazioni (CSELT) Technical Reports, Torino, Italy*, vol. 24, no. 4, Feb. 1996, pp. 113 - 130.

Chapter 3

Propagation in Outdoor Cellular and In-Building Pico-Cellular Systems

3.1 Introduction

This thesis is concerned with the analysis of wireless communication systems in which users access the shared radio resource using random access techniques. Before such systems can be analysed, an understanding of the types of environment in which they may operate is required. In this thesis, the operation of outdoor cellular and in-building pico-cellular systems are investigated. In this chapter, these particular systems are discussed in terms of their associated system layout and propagation characteristics.

In §3.2, the key elements of an outdoor cellular system are identified. Such systems are characterised by a large number of low power distributed base stations which are used to serve small geographical areas referred to as “cells”. Section §3.3 describes the nature of radiowave propagation in an outdoor cellular system. This description incorporates narrowband statistical propagation models to represent the fluctuations observed in received signal strength measurements. In particular, the variability in signal strength is modeled as the superposition of three independent phenomena, namely distance dependent pathloss, environmental shadowing and envelope fading. It should be noted that no consideration is given to wideband effects, as it is assumed that delayed signal components are mitigated through the use of equalisation.

In §3.4, the cellular concept is extended to the in-building pico-cellular architecture, where base stations may be located on each floor of a building. The analysis of in-building systems is of particular interest, as it is likely that protocols such as S-ALOHA and PRMA could find their greatest applications in such a setting. This is because of the high levels of speech and data (computer) traffic that potentially exist in such a system. Section §3.5 provides statistical descriptions of the variability of received signal strengths in the in-building pico-cellular environment. Propagation in the in-building environment is governed by the same fundamental principles which dominate in the outdoor environment, although the effect of floor losses and increased signal variability must also be accounted for. Section §3.6 presents details of a propagation study undertaken in a particular building. The results of this study will be used in this thesis to study floor-wide performance variations.

3.2 Outdoor Cellular Systems

Until the early 1980s, mobile radio system design was viewed as a broadcasting problem, in many ways similar to broadcast radio or television system design. This design philosophy embodies the use of a single, high-power transmitter situated in some prominent location providing the maximum service area coverage, as shown in Fig. 3.1(a). Although this design

strategy ensures fair-to-average coverage over a large area, it is unsatisfactory if the number of users is large. This is due to the small number of available channels per unit coverage area, which results in low system capacity. For example, the Bell system operating in New York during the 1970s could only support a maximum of twelve simultaneous conversations [1, p40].

The cellular concept represents a significant departure from this traditional technique of radio system design and offers a real solution to the capacity problem [2]. In a cellular system, a large number of relatively low-powered base stations are used, each specifically designed to serve only a small geographical area, as shown in Fig. 3.1(b). These small areas are generically referred to as cells. In an idealised situation where the terrain is flat and the morphostructure is constant and assuming the use of omnidirectional antennas, these cells would be circular. However, because it is not possible to tessellate an area with circles, the idealised circular cells are represented by hexagons. In practice, of course, the terrain surrounding a base station may not be flat and the morphostructure will not be constant, meaning that in practice cells do not have a regular shape. However, the use of the hexagonal cell structure serves to clarify the concepts involved in cellular engineering.

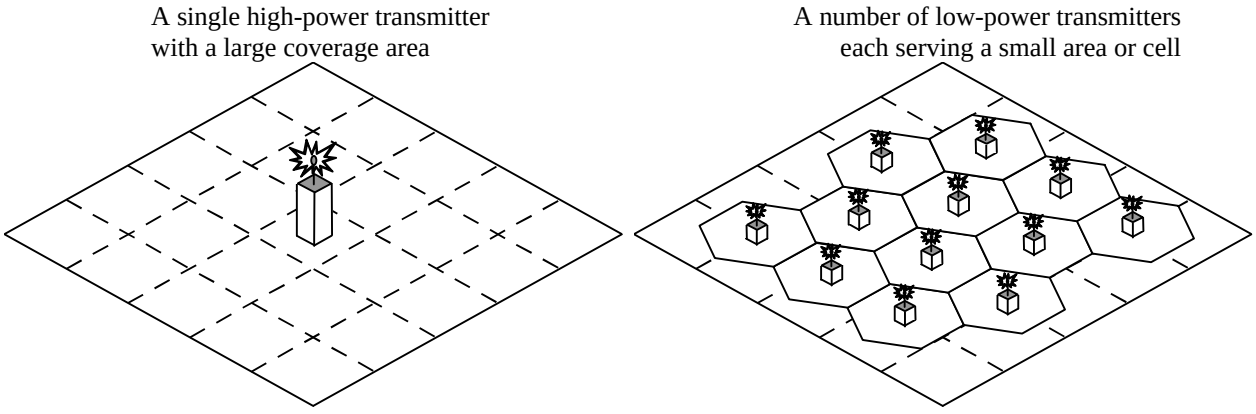

(a) *Broadcasting architecture* **(b)** *Cellular architecture*

Figure 3.1: *Conceptualised broadcasting and cellular architectures (from [3, p8]).*

The reduction in coverage area of each cell permits the reuse of the frequency allocation in cells located in different parts of the system, thereby increasing the number of channels available per unit coverage area and consequently the net system capacity. The obvious difficulty with reusing channels over relatively short distances is that cochannel interference is likely to occur. In other words, the communication between a terminal and a base station in one part of the system can interfere with the communications between other terminals and base stations operating at the same frequency, but situated in some other part of the system. Cochannel interference can seriously impair the transmission quality achievable in a wireless communication system and needs to be controlled if cellular systems are to provide a quality comparable with that of the fixed network. To ensure that the mutual interference between users remains below a harmful level, cochannel cells can be arranged so that adjacent cells use different channel groups. A typical cellular frequency reuse scheme is shown in Fig. 3.2. In this particular case, the cells are organised into seven-cell clusters, with the cells in a cluster designated as A through G. Seven

different sets of frequency channels are used in each cluster, one set in each cell. In general, a tessellating reuse cluster size of size N_c can be constructed if

$$N_c = i^2 + ij + j^2 , \qquad \textbf{(3.1)}$$

where *i* and *j* are non-negative integers, and *i*≥*j*. It follows that the allowable cluster sizes are N_c =1, 3, 4, 7, 9, 12, …Examples of 3-, 4-, and 7-cell reuse clusters are presented in Fig. 3.3.

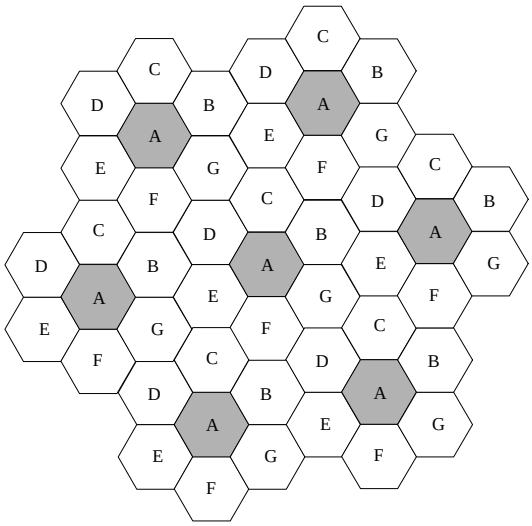

Figure 3.2: *The layout of a " seven-cell-repeat" outdoor cellular system. Every seventh cell reuses the same set of channels.*

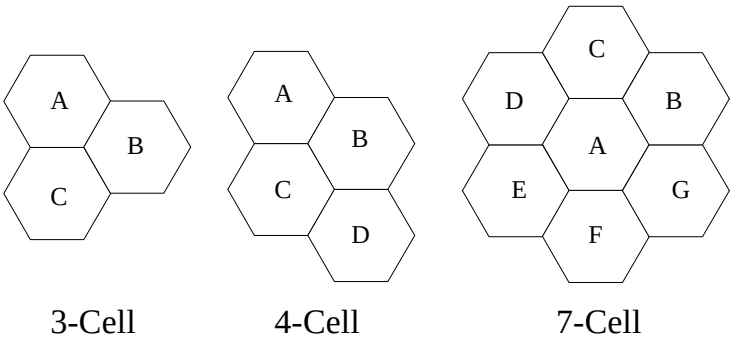

Figure 3.3: *Examples of 3-, 4-, and 7-cell reuse clusters.*

The closest distance between the centres of two cells using the same channels (in different clusters) is determined by the choice of cluster size, N_c, and cell radius[1], R_c. This distance, *D*, is called the frequency reuse distance and is given by

$$D = R_c\sqrt{3N_c} . \qquad \textbf{(3.2)}$$

[1] In this situation, the hexagonal cell is approximated by a circle.

The spectrum efficiency, *SE*, of a cellular network can be defined as the carried traffic per cell, A_c, expressed in erlangs [4], divided by the bandwidth of the total system, B_s, and divided by the area of a cell, S_U [5, p18]. The total system bandwidth, B_s, is the product of the bandwidth per cell, B_c, times the number of cells per cluster, N_c. From

$$SE = \frac{A_c}{B_s S_U} = \frac{A_c}{B_c N_c S_U}, \qquad \textbf{(3.3)}$$

it can be observed that the spectrum efficiency decreases with an increase in N_c. On the other hand, as N_c is increased the performance experienced by the user improves due to an increased separation between cochannel cells. This performance may be quantified in terms of measures such as outage probability or bit error rate. Hence, achieving high system performance and efficient use of the radio spectrum are conflicting objectives for a network designer.

3.3 Radiowave Propagation in Outdoor Cellular Systems

3.3.1 Introduction

The mechanisms which govern radio propagation in outdoor cellular systems are complex and diverse, but they can generally be attributed to three basic propagation mechanisms; reflection, diffraction and scattering [6]. Reflections arise when the plane waves are incident upon a surface with dimensions that are very large compared to the wavelength. Diffraction occurs according to Huygen's principle when there is an obstruction between the transmitter and receiver antennas, and secondary waves are generated behind the obstructing body. Scattering occurs when the plane waves are incident upon an object whose dimensions are of the order of a wavelength or less, and causes the energy to be redirected in many directions. The total signal received at the terminal receiver is therefore the phasor superposition of a number of reflected, diffracted and scattered signal components, referred to as *multipath propagation* and shown in Fig. 3.4.

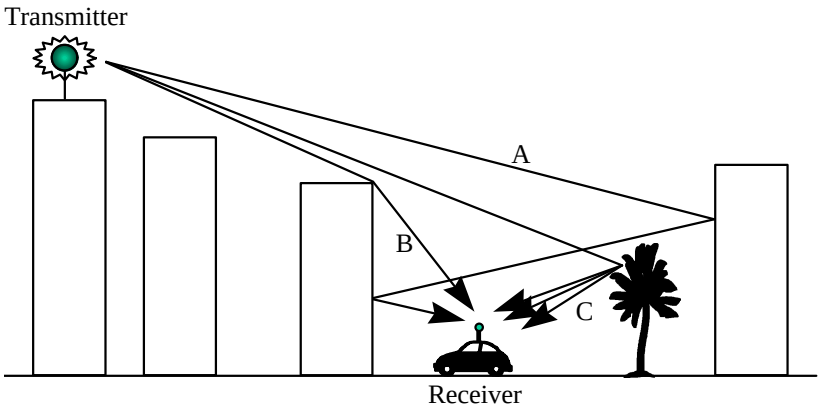

Figure 3.4: *The outdoor cellular environment: The received signal is comprised of reflected (A), diffracted (B), and scattered (C) components.*

As a result of these three propagation mechanisms, the received signal strength in a cellular system can roughly be characterised by three nearly independent phenomena; pathloss variation

with distance, slow log-normal shadowing, and fast multipath fading [7]. These phenomena are illustrated in Fig. 3.5 and discussed in detail in the following subsections. Fig. 3.5 considers the power received at a terminal from a base station as it moves through an urban environment. The base station is assumed to be transmitting an 850 MHz continuous wave RF carrier.

3.3.2 Propagation Pathloss

The difference between the level of the transmitted signal and the signal in the general area of the terminal receiver (area mean power) is referred to as the pathloss. The area mean power (blue trace, Fig. 3.5(c)), is well known to be dependent upon frequency, antenna heights, propagation path length and levels of environmental clutter [7].

Although it may seem counter-intuitive, pathloss is essential in high capacity cellular systems, the reason being that a rapid attenuation of signal strength with distance permits a small cochannel reuse distance and, therefore, a high spectral efficiency. Both theoretical and empirical models have been developed to predict the pathloss [8]. Two important theoretical formulas upon which semi-theoretical models are often based are the "free-space" transmission formula and the "plane-earth" propagation model. The free space transmission formula relates to the situation where the transmitter and the receiver are in "free-space", that is, where there are no objects in the vicinity that reflect or absorb transmitted energy. In this situation, the intensity of an electromagnetic wave is known to decay with the square of the radio path length, *r*, such that the received area mean power, $\overline{\overline{P}}$, is given by [9]

$$\overline{\overline{P}} = P_t\left(\frac{l}{4\pi r}\right)^2, \qquad \textbf{(3.4)}$$

where P_t is the transmitted power, $l = c/f$ is the wavelength of the transmitted signal, and c is the velocity of radio wave propagation in free space, which is equal to the speed of light. Hence, the free space formula suggests that the received power is inversely proportional to both the square of transmission frequency and the square of the transmission distance. The propagation pathloss, *PL* (in linear units) is given by

$$PL = \frac{P_t}{\overline{\overline{P}}} = \left(\frac{4\pi r}{l}\right)^2. \qquad \textbf{(3.5)}$$

Pathloss is often expressed in logarithmic units, so that (3.5) can be written as

$$PL[dB] = P_t[dB] - \overline{\overline{P}}[dB] = 20\log_{10}\left(\frac{4\pi r}{l}\right). \qquad \textbf{(3.6)}$$

Free space propagation does not apply in an outdoor cellular environment and the propagation pathloss depends not only on the distance and wavelength, but also on the antenna heights of the

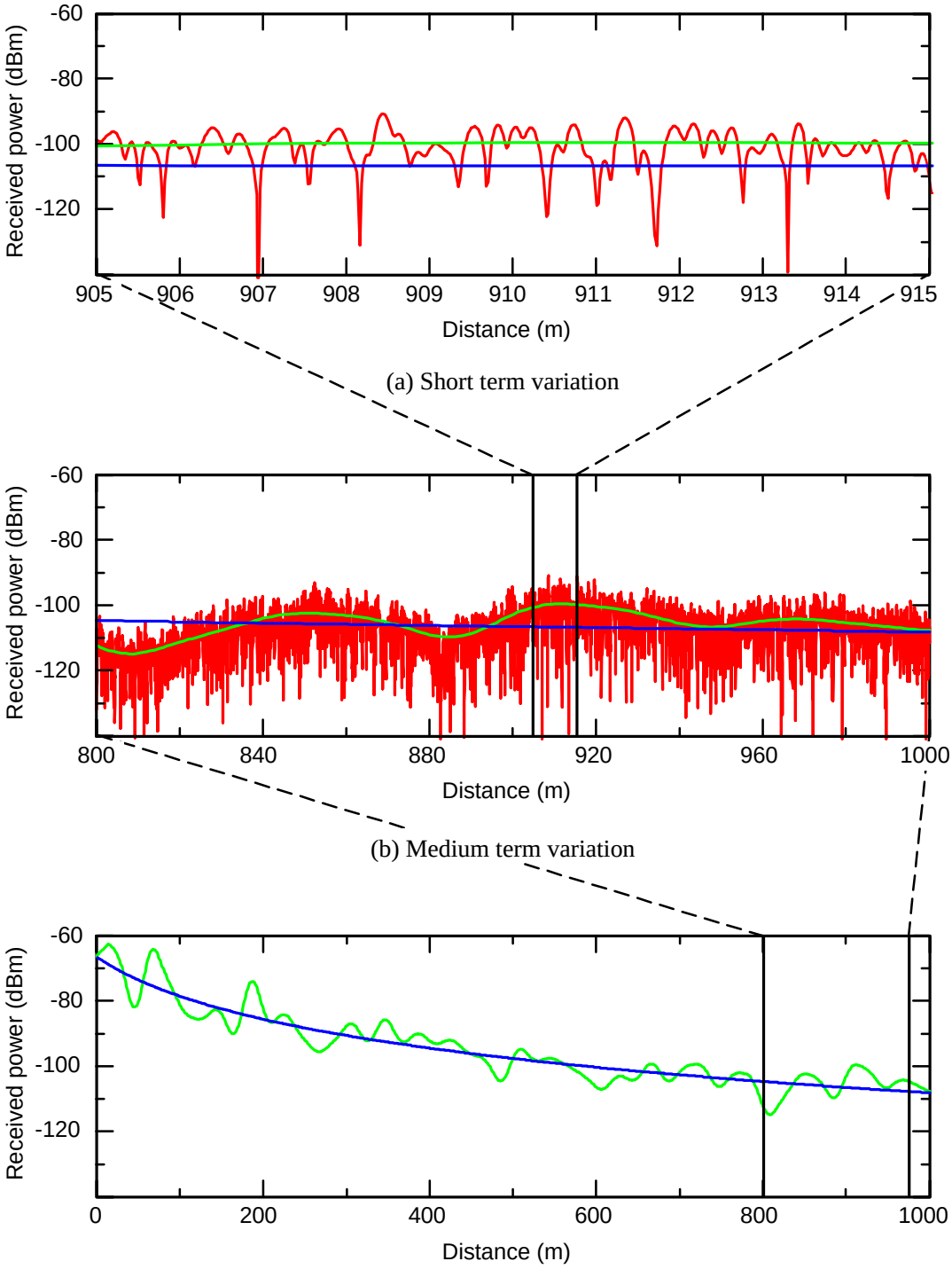

Figure 3.5: *Short, medium and long term variations of a typical outdoor cellular radio signal (from [3, p.13]).*

transmitter and receiver, and the local terrain characteristics such as buildings and hills. In this situation, the "plane-earth" propagation model may be a more appropriate basis than the "free space" model. For situations with parameters typical of outdoor cellular radio situations, except where the separation (r) between the transmitter and the receiver is small, the model predicts that over a " plane earth" the receiver power will be approximately1[0, p.65]

$$\overline{\overline{P}} = P_t\left(\frac{h_t h_r}{r^2}\right)^2, \qquad \textbf{(3.7)}$$

where h_t and h_r are the respective heights of the transmitter and receiver antennas. Unlike the free space formula, (3.7) predicts that the received signal power will be proportional to r^{-4} and independent of the transmission frequency. In fact radiowave propagation in the outdoor cellular radio environment is dependent on frequency [10, p66], and so (3.7) cannot be completely relied upon. However, the plane earth model is reasonably accurate in predicting the pathloss of 40dB/dec. The associated pathloss for the plane earth model is given by

$$PL[dB] = 40\log_{10}(r) - 20\log_{10}(h_t h_r). \qquad \textbf{(3.8)}$$

In this thesis, a normalised path loss model is adopted whereby the received area mean power is independent of antenna height or frequency, such that

$$\overline{\overline{P}} = \frac{P_t}{r^b}. \qquad \textbf{(3.9)}$$

In this situation, $\overline{\overline{P}}$ is proportional to r^{-b} where b is known as the pathloss exponent. The path loss exponent is strongly dependent on the cell size and local terrain characteristics. Table 3.1 lists typical pathloss exponents obtained in various environments [11]. The pathloss (in dB) associated with (3.9) is given by

$$PL[\text{dB}] = 10b\log_{10}(r). \qquad \textbf{(3.10)}$$

Environment	Pathloss Exponent, b
Free Space	2
Urban area cellular radio	2.7 - 3.5
Shadowed urban cellular radio	3 - 5
In-building line-of-sight	1.6 - 1.8
Obstructed in building	4 - 6
Obstructed in factories	2 - 3

Table 3.1: *Pathloss exponents for different environments [11].*

3.3.3 Lognormal Shadowing

The variability associated with large scale environmental obstacles leads to the local mean power fluctuating about a constant area mean power over medium distances (~100 m) (the green trace, Fig. 3.5(b)). This phenomenon is known as *shadowing* and arises due to obstacles in the propagation path such as buildings, hills and foliage. Experiments reported by Egli [12] indicate that this variability can be approximated by a lognormal distribution. By lognormal it is meant that the local-mean signal, $\overline{P}$, expressed in logarithmic values has a normal probability distribution function of the form

$$f_{\overline{P}[dB]}(\overline{P}[dB]) = \frac{1}{\sqrt{2p}\,s}\exp\left[\frac{-(\overline{P}[dB]-m)^2}{2s^2}\right], \qquad \textbf{(3.11)}$$

where m and s are the mean and standard deviation of the normal distribution and are measured in logarithmic units. The value of m is normally approximated by the area mean power, $\overline{\overline{P}}$, determined in §3.3.2, although strictly speaking, they are only identical when $s = 0$ dB [5, p.37]. If the local mean signal is expressed in watts, then the corresponding distribution, $f_{\overline{P}}(\overline{P})$, is a lognormal distribution of the form [13, p.23][2],

$$f_{\overline{P}}(\overline{P}) = \frac{10}{\log_e(10)\,\overline{P}\sqrt{2p}\,s}\exp\left[\frac{-(10\log_{10}(\overline{P})-m)^2}{2s^2}\right], \qquad \textbf{(3.12)}$$

where $\overline{P} = 10^{(\overline{P}[dB]/10)}$. Note that the terms m and s in (3.12) are the mean and standard deviation of the normal distribution presented in (3.11) and retain their logarithmic units. It should be appreciated that m and s are not the mean and standard deviation of the lognormal distribution. The shadowing standard deviation, s, of the normal distribution tends to be dependent on frequency and the nature of the environment in the vicinity of the terminal. In most cases, s is relatively independent of transmission path length and antenna heights [14-16]. Generally the variability of the shadowing is greater in more urbanised areas. Mogensen [17] has reported $s = 6.5$ to 8.2 dB at 900 MHz in urban areas, while Mockford *et. al.* [18] reported a value of 4.5 dB for urban areas. Values of s obtained from propagation studies undertaken at the University of Auckland are presented in Table 3.2 [14-16]. These values were obtained for three different frequencies and four different environments.

	76 MHz	465 MHz	851 MHz
Urban	4.3 dB	4.5 dB	7.2 dB
Light Urban	4.5 dB	3.9 dB	6.1 dB
Suburban	2.7 dB	2.6 dB	6.5 dB
Rural	3.1 dB	2.7 dB	3.0 dB

Table 3.2: *Values of s obtained by Rowe et. al. in Auckland at 76, 465, and 851 MHz [14-16].*

[2] If the local mean signal is expressed in volts, the corresponding distribution is also a lognormal distribution.

3.3.4 Rayleigh Fading

In addition to distance-dependent pathloss and environmental shadowing, the signal received at a terminal receiver will undergo significant envelope fading over distances of a few tens of wavelengths (the red trace, Fig. 3.5(a)). This fluctuation is attributable to multipath propagation, whereby the signal propagates by not one, but by many different paths to the receiver. The fades occur at approximately half-wavelength intervals, and at times may drop 30 dB below the local mean (represented by the green trace).

A well known model proposed by Clarke [19], considers the superposition of a number of statistically independent waves. Each of these waves are assumed to arrive from a random azimuthal direction and to have a phase which is uniformly distributed between 0 and 2π. These assumptions are reasonable given that a terminal is likely to be surrounded by many objects which will reflect the signal. Several multipath components of the transmitted signal arriving at the receiver at the same time will each have different time delays and therefore different phase shifts. These add either constructively or destructively to produce a random phase shift. This creates rapid changes in the signal strength, an effect known as *Rayleigh fading* [20-22].

It is important to realise that the Rayleigh distribution has been found to model the variability of the received signal envelope when the envelope is expressed in volts. If the signal envelope is expressed in watts, the appropriate statistical distribution is no longer the Rayleigh distribution, but rather the exponential distribution. Hence, if P is the total momentary power received, it will have an exponential probability density function of the form

$$f_P(P) = \frac{1}{\overline{P}} \exp\left[\frac{-P}{\overline{P}}\right]. \qquad \textbf{(3.13)}$$

If the momentary received power, P, is expressed in logarithmic units, then the probability distribution function is given by [23]

$$f_{P[dB]}(P[dB]) = \frac{\log_e(10)}{10\overline{P}} \exp\left[\frac{\log_e(10)\,P[dB]}{10} - \frac{10^{\frac{P[dB]}{10}}}{\overline{P}}\right], \qquad \textbf{(3.14)}$$

where the variable transformation $P[dB] = 10\log_{10}(P)$ has been used.

3.3.5 Combined Lognormal Shadowing and Rayleigh Fading

In the previous subsections, it was shown that over relatively small distances, the signal is well described by Rayleigh statistics, with the local mean over a somewhat larger area being lognormally distributed. It is of interest, therefore, to examine the overall distribution of the received signal in these larger areas.

It might be reasonable to expect the distribution to be a mixture of Rayleigh and lognormal, and investigations have indeed shown this to be the case. Parsons and Ibrahim [24] examined the Nakagami-*m* and Weibull distributions, which both contain the Rayleigh distribution as a special

case, but came to the conclusion suggested earlier by Suzuki [25] and Hansen and Meno [26], that the statistics of the radio signal can be represented by a mixture of Rayleigh and lognormal statistics in the form of a Rayleigh distribution with a lognormally varying mean. This combined distribution is normally referred to as the Suzuki distribution. The probability density function of the momentary received signal power, P, (in watts) in this case is given by

$$f_P(P) = \int_0^\infty \frac{10}{\log_e(10)\overline{P}^2\sqrt{2p}\,s} \exp\left[\frac{-(10\log_{10}(\overline{P})-m)^2}{2s^2}\right] \exp\left[\frac{-P}{\overline{P}}\right] d\overline{P}. \qquad \textbf{(3.15)}$$

Other descriptions have been used to describe the mobile radio signal. These include the Nakagami-*m* [27], the Rice [28,29], and the Weibull [30] distributions. In this thesis, however, the analysis is limited to considering only Rayleigh and Suzuki fading channels.

3.4 In-Building Pico-Cellular Systems

As the demand for wireless services increases, the number of channels assigned to a cell eventually becomes insufficient to support the required number of users. At this point advanced design techniques are needed to provide more channels per unit coverage area. In order to meet this demand, existing cellular systems are evolving into a hierarchical cellular architecture as illustrated in Fig. 3.6. With such an architecture, major travel routes and wide urban and suburban areas are covered with cells having a radius on the order of several kilometres. Streets in densely populated downtown areas are covered with micro-cells of the order of a few hundred metres and pico-cells cover in-building areas [31,32]. In this thesis, only outdoor cellular and in-building pico-cellular systems are investigated.

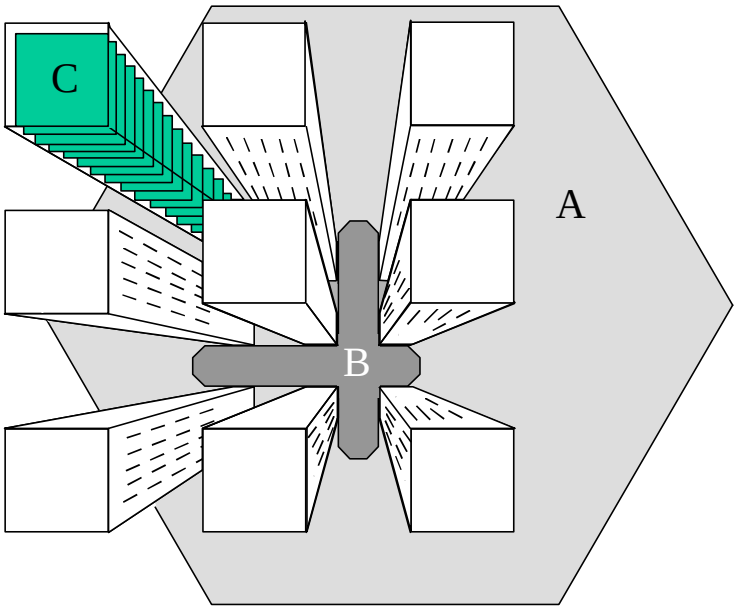

Figure 3.6: *Illustration of hierarchical cell structure: macro-cell (A) for vehicular coverage, micro-cell (B) for pedestrian coverage, and pico-cell (C) for in-building coverage. (from [33]).*

It is expected that many subscribers will want wireless coverage and mobility throughout the office in addition to that already offered by outdoor cellular systems. Such systems are becoming increasingly important for extending voice and data communication services within the work place. In-building systems allow for equipment miniaturisation, which in turn, leads to reduced costs and enables flexible deployment. Because of the increasing proliferation of speech and data traffic, it is envisaged that random access protocols such as S-ALOHA and PRMA could find their greatest application in in-building wireless systems.

With in-building systems, much lower transmitter powers are required, compared to outdoor systems. Coverage within in-building pico-cellular systems may be achieved by installing small base station units on each floor of a building, or even in individual rooms on a floor. This gives rise to three dimensional frequency reuse whereby channels used on one floor may be reused on neighbouring floors. In this thesis only single isolated buildings are analysed even though in a mature environment the interaction between nearby buildings is likely to be very important. Although analysis of a single building represents a simplification of a mature wireless environment, it is important to understand the cochannel interference issues in a single building before considering multiple buildings.

In this thesis, a multi-storey square building with sides of length a (metres) and an inter-floor spacing of b (metres) as shown in Fig. 3.7, is considered. Base stations are located on the ceilings of each floor and are shown in an arbitrary centralised arrangement[3]. The closest distance between the centres of two floors using the same channels is determined by the choice of cluster size, N_c, and inter-floor separation distance. The frequency reuse distance, D, is given by

$$D = bN_c . \tag{3.16}$$

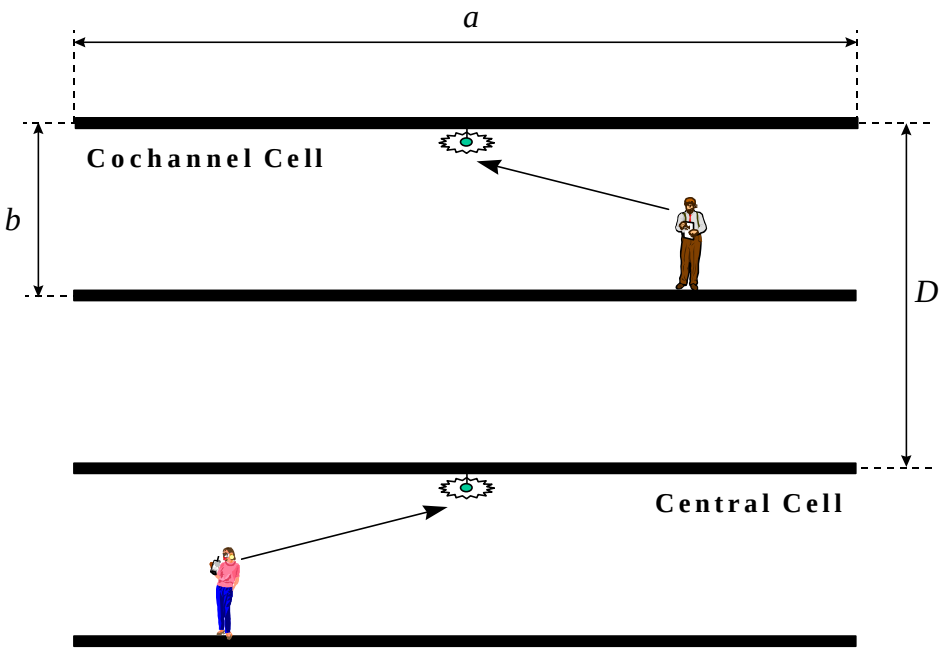

Figure 3.7: *In-building pico-cellular environment with vertical frequency reuse.*

[3] While future systems may employ multiple base stations per floor, this aspect is not considered in this thesis.

3.5 Radiowave Propagation in In-Building Pico-Cellular Systems

3.5.1 Introduction

As with outdoor environments, radio propagation in in-building environments is dominated by the mechanisms of diffraction, reflection and signal scattering and thus, can be characterised by propagation pathloss, environmental shadowing and envelope fading. However, there are differences in the propagation characteristics of in-building environments compared to outdoor environments. Some of these differences are as follows:

- Radio propagation is usually significantly more varied in in-building environments and depends on the architecture and construction of the building, the manner in which people move throughout the building and whether windows and doors are open or closed [34]. This means that the particular type of building has a direct impact on the observed propagation characteristics.

- Environmental scatterers in in-building systems are usually located much closer to the direct propagation path. Accordingly, the excess power delay in an in-building system is likely to be considerably less than in an outdoor system[4] [35].

- An in-building radio system is likely to use vertical frequency reuse. Consequently, the cochannel interferers will be significantly closer to the desired receiver than in an outdoor environment, and the received interference power will depend largely on the inter-floor propagation characteristics.

3.5.2 Propagation Pathloss

A range of distance dependent pathloss models have been proposed in the literature for multi-storey buildings[5] [36-38]. A detailed review of in-building radio propagation models is presented in [39,40]. A significant proportion of the pathloss in in-building environments can be attributed to obstacles such as walls and floors located in the propagation path. The orientation and composition of the building floors is usually more predictable than that of the building walls. Accordingly, propagation models that explicitly account for the attenuation attributable to the building floors have been proposed. Measurements presented in [36,37] by Motley and Keenan indicated that there is a linear relationship between the path-loss (when expressed in dB) and the number of floors between the transmitter and receiver, and therefore that the path-loss, PL[dB], can be expressed as,

$$PL[\text{dB}] = L[\text{dB}] + 10b\log_{10}(r) + kL_f[\text{dB}], \qquad \textbf{(3.17)}$$

[4] Note, however, that reasonably large excess delay spreads can occur in in-building systems when received signal components are reflected from external scatterers such as nearby buildings.

[5] There are also a large number of path-loss models based on ray tracing techniques. These techniques are not considered in this thesis.

where $L[\text{dB}]$ is a constant loss, measured at a reference distance (usually 1 metre), b is the propagation exponent, r is the three dimensional path length, k is the number of floors between the transmitter and receiver and $L_f\,[\text{dB}]$ is the loss associated with each floor in the building.

In [38] Seidel and Rappaport presented measurement results which indicate a non-linear relationship between the path-loss (in dB) and the number of floors between the transmitter and receiver[6]. A non-linear function defined as the *floor attenuation factor* (*FAF*) is used to represent the attenuation attributable to the floors in the propagation path. Accordingly, the mean path loss, PL[dB], over a three dimensional path length, r, is given by [38],

$$PL[\text{dB}] = L[\text{dB}] + 10b\log_{10}(r) + FAF[\text{dB}], \qquad \textbf{(3.18)}$$

where *FAF* is the cumulative floor attenuation factor expressed in dB. Both b and *FAF* depend on the number of floors separating the transmitter and receiver. In this thesis, (3.18) is used to predict pathloss in in-building environments, although the constant loss term, L[dB], is neglected[7]. This results in the area-mean power being predicted according to

$$\overline{\overline{P}} = \frac{P_t}{faf \cdot r^b}, \qquad \textbf{(3.19)}$$

where *faf* in (3.19) is the floor attenuation factor expressed in linear units. Further improvements in path-loss predictions can be achieved if the loss model includes accurate estimates of the attenuation attributable to the walls in the propagation path [36,38]. However, since the wall locations are less predictable than the floor locations, the in-building path-loss model considered in this thesis does not explicitly consider attenuation attributable to building walls. Values of b and *FAF* obtained from 1.8-1.9 GHz propagation studies in four buildings [41,42] are presented in Table 3.3. Table 3.4 gives brief descriptions of the layout and construction of these buildings as provided by the authors of [41] and [42]. Details of the propagation study undertaken in Building D, will be presented in §3.6.

3.5.3 Combined Lognormal Shadowing and Rayleigh Fading

As with outdoor environments, it is not possible to predict the exact power received at a particular location in an in-building environment from a distance dependent model, such as (3.19). Rather, there is variability about the area mean power due to environmental shadowing and envelope fading. The mathematical descriptions of these phenomena in an in-building environment are the same as those presented in §3.3.3 and §3.3.4 for an outdoor environment. Unlike with outdoor environments where lognormal shadowing standard deviations are relatively homogeneous (see Table 3.2), in-building environments exhibit increased shadowing variability.

---

[6] This indicates that the dominant received signal components do not necessarily propagate directly between the transmitter and receiver. Although the inter-floor propagation mechanisms are to a large extent unknown, it has been suggested that in many cases significant signal power may be received from components which propagate outside the building [39].

[7] This term may be neglected due to the fact that (3.18) is only used in this thesis with calculations involving power ratios, such that L[dB] always cancels out. If absolute pathloss values are required, then L[dB] should be retained.

Building	Floors, k	FAF [dB]	b	s [dB]
A [41]	0	0.00	2.6	14.1
Walnut Creek	±1	31.3	2.0	4.6
	±2	38.5	2.0	4.0
	0	0.00	3.8	12.7
B [41]	±1	35.4	2.0	6.4
San Ramon	±2	35.6	2.0	5.9
	±3	35.2	2.0	3.9
	0	0.00	3.9	16.0
	±1	26.2	2.0	10.5
C [41]	±2	33.4	2.0	9.9
SF Pacbell	±3	35.2	2.0	5.9
	±4	38.4	2.0	3.4
	±5	46.4	2.0	3.9
	0	0.00	4.8	9.6
D [42]	±1	16.0	4.8	9.8
Eng. Tower	±2	22.1	4.8	8.5
	±3	29.0	4.8	7.9

Table 3.3: *In-building propagation model parameters for 4 different buildings: floor attenuation factor, FAF, pathloss exponent, b, and lognormal shadowing standard deviation, s.*

Building	Description
A [41] Walnut Creek	New building 10 stories tall with interior still under construction. Several buildings of comparable height surround this building within a three block radius. Typical modern dry wall is mounted on metal studs on the interior of each floor. Large wall-length glass windows line the perimeter of the building. Floors are made of reinforced concrete over a steel frame.
B [41] San Ramon	This building is a modern 4 storey office building with four wings that extend in each of the four compass directions. The perimeter of the building is lined with windows that span from the floor to the ceiling along two of the four walls. The floors of the building are lightweight concrete, and non-load bearing walls are dry wall on steel studs. Interior office areas consist of areas of non-load bearing walls near the interior that are surrounded with cloth-covered metal frame plastic dividers (soft partitions) that separate individual office cubicles.
C [41] SF Pacbell	Measurements were made in this 26 storey building. This building was built on a heavily reinforced concrete frame. The floor plan consists of offices along centrally located hallways that are separated from a main corridor by solid dry wall that spans from the floor to the ceiling. The narrow slit-like windows are equally spaced in pairs along each side of the building.
D [42] Eng. Tower	This is a 12 storey building dominated by a central structural core which contains a stairwell, lifts and services. All offices are located around the outside of the central core. The outer construction consists almost entirely of windows with concrete cladding projecting out between floors. The office walls are constructed with a mix of wood and plasterboard while the central core and floors are constructed with solid reinforced concrete. For the floors above level 8 there are no buildings immediately adjacent. However, below level 8 there are buildings adjacent to three sides of the tower.

Table 3.4: *Descriptions of building layout and construction for the buildings in Table 3.3.*

In particular, the levels of lognormal shadowing measured in different buildings can be significantly different. This aspect is illustrated in Table 3.3, where values of s, measured in the four buildings of [41] and [42], are presented. This variability is attributable to the significant physical differences that exist between buildings.

Because of the inhomogeneity in in-building propagation environments, it is necessary to consider a number of buildings when studying the performance of a particular in-building system (e.g. S-ALOHA or PRMA). This allows the system designer to observe the typical variations in performance that would exist if the system were to be installed in a number of buildings. In Chapters 5-7 of this thesis, the performance of in-building S-ALOHA and PRMA systems are determined with respect to their operation in the four buildings presented in Table 3.3.

3.6 Engineering Tower Block Propagation Study

The propagation study of [42] was conducted in the 12-storey School of Engineering tower block at The University of Auckland (Building D in Tables 3.3 and 3.4). This study investigated the mean pathloss, associated variability and correlated shadowing for a large number of receiver and transmitter locations within the building. The propagation measurements were made using a 1.8 GHz channel sounder. The advantage of [42] over [41] (Buildings A-C) is that the actual raw propagation data is readily available. In particular, the mean attenuation measurements made between the various transmitter and receiver locations are included in [42]. With this information it is possible to consider Building D in considerably more detail than Buildings A-C.

The most dominant feature of Building D is a thick central concrete core which houses the stairwell and lifts. An external view and floor plan of the tower is presented in Fig. 3.8. The propagation measurements were made by placing the transmitter at the location (denoted by Txr) indicated in Fig. 3.8. The attenuation in the transmitted signal was then recorded at the individual measurement points across the floor (fifty-three in total). The transmitter was then moved to an identical location on floors above and below the original floor. The attenuation measurements were then repeated on the original floor at the same measurement points.

The parameter values for b, FAF and s presented in Table 3.3 were calculated from floor-wide averages of the propagation measurements. By applying the floor-wide model, the variability of a signal from an individual terminal is implicitly assumed to be equal to the average signal variability over the entire floor. However, this assumption is only valid if a terminal moves over a significant percentage of floor locations. In reality, terminals are likely to be confined to localised regions, for example to a single office. The results of the Engineering Tower block propagation study have confirmed that the shadowing variability over a single office is considerably less than the variability measured over the entire floor. The overestimation of shadowing results in a pessimistic system performance prediction at some locations and an optimistic prediction at others.

An alternative approach is to use the actual database of propagation measurements presented in [42]. With this database, it is possible to determine the performance of the system at various locations within the building. It is not, however, feasible to determine the performance at these locations by using mathematical analysis due to the complexity of the analysis. Instead, detailed

Monte Carlo simulations can be employed. Details of these simulations are presented in later chapters of this thesis.

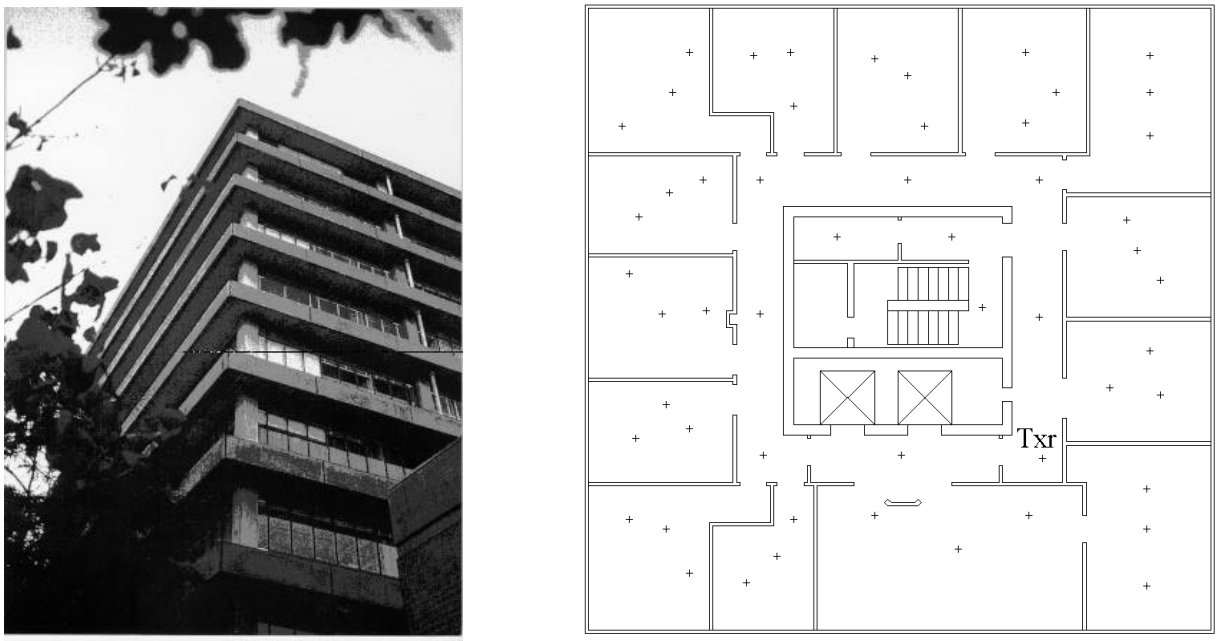

(a) **(b)**

Figure 3.8: (a) *External view and* **(b)** *typical floor plan of the School of Engineering tower block. Floor Dimensions are 18.5m´18.5m. Markers (+) indicate measurement points.*

3.7 Summary

This chapter has provided a literature review of both outdoor cellular and in-building pico-cellular systems and the associated characteristics of radiowave propagation within these environments. Empirical and statistical propagation models suitable for describing the attenuation and variability of radio propagation in these environments have been presented. These models will be used later in this thesis to assist in the performance analysis of both outdoor and in-building systems.

References

[1] G. Calhoun, *Digital Cellular Radio.* Massachusetts: Artech House, 1988.

[2] V. H. MacDonald, “The cellular concept,” *Bell Sys. Tech. J.*, vol. 58, no. 1, Jan. 1979, pp. 15 - 41.

[3] M. J. Neve, *Mobile radio propagation prediction in built-up environments using ray-methods.* Ph.D Thesis, Department of Electrical and Electronic Engineering, The University of Auckland, New Zealand, Dec. 1992.

[4] J. R. Boucher, *Voice Teletraffic Systems Engineering*. Massachusetts: Artech House, 1988.

[5] J. P. M. G. Linnartz, *Narrowband land-mobile radio networks*. Massachusetts: Artech House, 1993.

[6] J. B. Andersen, T. S. Rappaport, S. Yoshida, "Propagation measurements and models for wireless communications channels," *IEEE Commun. Mag.*, vol. 33, no. 1, Jan. 1995, pp. 42 - 49.

[7] W. C. Jakes, *Microwave Mobile Communications*. New York: John Wiley and Sons, 1974.

[8] IEEE Vehicular Technology Society Committee on Radio Propagation, "Special issue on mobile radio propagation," *IEEE Trans. Veh. Technol.*, vol. 37, no. 1, Feb. 1988, pp. 3 - 72.

[9] H. T. Friis, "A note on a simple transmission formula," *Proc. IRE*, vol. 34, May, 1946, pp. 254 - 256.

[10] W. C. Y. Lee, *Mobile communications design fundamentals*. Howard W. Sams & Co. Indiana, 1986.

[11] T. S. Rappaport, *Wireless Communications: Principles and Practice*. Prentice Hall, New Jersey, 1996.

[12] J. J. Egli, "Radio propagation above 40 MC/s over irregular terrain," *Proc. IRE*, Oct. 1957, pp. 1383 - 1391.

[13] K. W. Sowerby, *Outage probability in mobile radio systems*. Ph.D Thesis, Department of Electrical & Electronic Engineering, The University of Auckland, New Zealand, Feb. 1989.

[14] G. B. Rowe, A. G. Williamson, B. Egan, "Mobile radio propagation in Auckland at 465 MHz," *Electronics Letters*, vol. 19, no. 6, Mar. 1983, pp. 207 - 208.

[15] G. B. Rowe, A. G. Williamson, B. Egan, "Variability of mobile radio path loss in Auckland at 465 MHz," *Electronics Letters*, vol. 19, no. 15, Jul. 1983, pp. 688 - 689.

[16] G. B. Rowe, A. G. Williamson, "Mobile radio propagation in Auckland at 851 MHz," *Electronics Letters*, vol. 21, no. 22, Oct. 1986, pp. 1154 - 1155.

[17] P. E. Mogensen, P. Eggers, C. Jensen, J. B. Andersen, "Urban area radio propagation measurements at 955 and 1845 MHz for small and micro cells," *in Proc. 1991 IEEE Global Telecommunications Conf.*, Phoenix Arizona, Dec. 1991, pp. 1297 - 1302.

[18] S. Mockford, A. M. D. Turkmani, J. D. Parsons, "Local mean signal variability in rural areas at 900 MHz," *in Proc. 40th IEEE Veh. Technol. Conf.*, Orlando, Florida, May 1990, pp. 610 - 615.

[19] R. H. Clarke, "A statistical theory of mobile radio reception," *Bell Sys. Tech. J.*, vol. 47, 1968, pp. 957 - 1000.

[20] W. R. Young, Jr., "Comparison of mobile radio transmission at 150, 450, 900 and 3700 MHz," *Bell Sys. Tech. J.*, vol. 31, Nov. 1952, pp. 1068 - 1085.

[21] P. M. Trifonov, V. N. Budko, V. S. Zotov, "Structure of USW field strength spatial fluctuations in a city," *Trans. Telecomm. Radio Eng.*, vol. 9, Feb. 1964, pp. 26 - 30.

[22] H. W. Nylund, "Characteristics of small-area signal fading on mobile circuits in the 150 MHz band," *IEEE Trans. Veh. Technol.*, vol. 17, Oct. 1968, pp. 24 - 30.

[23] W. L. Shepherd, Jr. P. Milnarich, "Basic relations between a Rayleigh distributed randomly varying voltage and a decibel record of the voltage," *Proc. IEEE*, Dec. 1973, pp. 1765 - 1766.

[24] J. D. Parsons, M. F. Ibrahim, "Signal strength prediction in built-up areas, Part 2: Signal variability," *Proc. IEE Part F*, vol. 130, no. 5, 1983, pp. 385 - 391.

[25] H. Suzuki, "A statistical model for urban radio propagation," *IEEE Trans. Commun.*, vol. 25, no. 7, Jul. 1977, pp. 673 - 680.

[26] F. Hansen, F. I. Meno, "Mobile fading - Rayleigh and lognormal superimposed," *IEEE Trans. Veh. Technol.*, vol. 26, 1977, pp. 332 - 335.

[27] A. H. Wojnar, "Unknown bounds of performance in Nakagami channels," *IEEE Trans. Commun.*, vol. 34, no. 1, Jan. 1986, pp. 22 - 24.

[28] S. O. Rice, "Mathematical analysis of random noise," *Bell Sys. Tech. J.*, vol. 23, no. 3, Jul. 1944, pp. 282 - 332.

[29] S. O. Rice, "Statistical properties of a sine wave plus random noise, *Bell Sys. Tech. J.*, vol. 27, no. 1, Jan. 1948, pp. 109 - 157.

[30] J. Griffiths, J. P. McGeehan, "Inter-relationships between some statistical distributions used in radiowave propagation," *IEE Proc., Part F*, vol. 129, no. 6, Dec. 1982, pp. 411 - 417.

[31] M. Gudmundson, "Properties of cell plans for Manhattan environments," *Report No. TRITA-TTT-9115, Dept. of Telecommunication Theory, Royal Institute of Technology, ELECTRUM 207, S-164 40*, Kista, Sweden, Nov. 1991.

[32] J. Sarnecki, C. Vinodrai, A. Javed, P. O'Kelly, K. Dick, "Microcell design principles," *IEEE Commun. Mag.*, Apr. 1993, pp. 76 - 82.

[33] D. D. Falconer, F. Adachi, B. Gudmundson, "Time division multiple access methods for wireless personal communications," *IEEE Commun. Mag.*, vol. 33, no. 1, Jan. 1995, pp. 50 - 57.

[34] P. J. Marshall, *The coexistence of DS-CDMA mobile radio systems and fixed services*, Ph.D Thesis, Department of Electrical & Electronic Engineering, The University of Auckland, New Zealand, Feb. 1997.

[35] W. C. Y. Lee, *Mobile Cellular Telecommunications Systems*. McGraw-Hill, New York, 1989.

[36] J. M. Keenan, A. J. Motley, "Radio coverage in buildings," *Br. Telecom. Tech. J.*, vol. 8, no. 1, Jan. 1990, pp. 19 - 24.

[37] A. J. Motley, J. M. P. Keenan, "Personal communication radio coverage in buildings at 900 MHz and 1700 MHz," *Electronic Letters*, vol. 24, no. 12, Jun. 9th 1988, pp. 763 - 764.

[38] S. Y. Seidel, T. S. Rappaport, "Path loss prediction in multifloored buildings at 914 MHz," *Electronics Letters*, vol. 27, no. 15, Jul. 18th 1991, pp. 1384 - 1387.

[39] H. Hashemi, "The indoor radio propagation channel," *Proc. of the IEEE*, vol. 81, no. 7, Jul. 1993, pp. 943 - 968.

[40] P. M. Cartwright, *Cochannel interference in three-dimensional wireless communication systems*, Ph.D Thesis, Department of Electrical & Electronic Engineering, The University of Auckland, New Zealand, May 1997.

[41] S. Y. Seidel, T. S. Rappaport, M. J. Feuerstein, K. L. Blackard, "The impact of surrounding buildings on propagation for wireless in-building personal communications system design," *in Proc. 42nd IEEE Veh. Technol. Conf.*, Denver, Colorado, May 1992, pp. 814 - 818.

[42] K. S. Butterworth, K. W. Sowerby, A. G. Williamson, "A 1.8 GHz indoor wideband propagation study at The University of Auckland," *in School of Engineering Report No. 569, The University of Auckland*, Auckland, New Zealand, Sep. 1996.

Chapter 4

Multiple Cell System Analysis

4.1 Introduction

In Chapter 2 the S-ALOHA and PRMA protocols were introduced. The operation of these protocols was assumed to be in single cell systems, free from cochannel interference. It was assumed that all packets involved in collisions with other packets were lost, while those packets received in the absence of other packets were received successfully. In this chapter, the assumption of a single cell, simple channel system is revisited. Instead, a framework for analysing PRMA and S-ALOHA in multiple cell, variable channel systems is developed.

In §4.2, the layout of terminals in more realistic multiple cell systems, namely outdoor cellular and in-building pico-cellular systems, is presented. These particular multiple cell systems and their associated propagation characteristics were discussed in Chapter 3. The layout of base stations and terminals in these systems is presented, including the distribution of desired and interfering terminals. The working assumptions relating to the way in which the total system bandwidth is partitioned amongst the cells is also presented. It should be noted that all analysis presented in this thesis is concerned only with the uplink performance[1]. In §4.3 the assumption of a simple channel is reconsidered because practical receivers are often capable of locking onto one packet in the presence of other contending and/or interfering packets, due to the receiver *capture effect*[2]. This is made possible, in part, by the highly variable nature of the radio channel which leads to packets from a number of independent terminals having significantly different power levels. This variability, which was discussed in Chapter 3, consists of distance dependent pathloss, lognormal shadowing and Rayleigh fading. The capture probability, which is the probability of a desired packet capturing the base station in the presence of other contending and/or interfering packets, is the underlying performance measure that will be used in this thesis. The capture probability can in turn be used in the determination of system specific performance parameters, such as packet dropping probability and data packet delay.

In §4.4, capture probability expressions are derived for both Suzuki fading outdoor cellular and Suzuki fading in-building pico-cellular systems. These expressions will be used extensively throughout the remainder of this thesis. The evaluation of these expressions requires the application of numerical integration techniques. These techniques are outlined in Appendix A of this thesis. Section §4.5 presents capture probability results for both outdoor cellular and in-building pico-cellular systems. In §4.6, the effect of cochannel interference on PRMA and S-ALOHA protocol operation is discussed. The most important effect of cochannel interference is where reserved PRMA speech packets are corrupted by cochannel interference. Possible strategies for handling such events are discussed. Additional performance measures which need

[1] This approach is taken as, in general, the uplink performance represents the limiting case.
[2] This neglects the possibility of some base station diversity schemes which can capture multiple packets [

to be included in the analysis of multiple cell S-ALOHA and PRMA systems are also presented. These are in addition to the performance measures presented in § 2.2.4.

4.2 Multiple Cell Random Access Systems

The single cell assumption made in Chapter 2 needs to be reconsidered because future wireless systems employing random access would most certainly exist in multiple cell configurations, governed by appropriate frequency reuse plans. The study, by previous researchers, of only single cell systems is due to either: a desire to concentrate on details of the random access protocol else; an assumption of a large frequency reuse distance in which case cochannel interference becomes negligible. However, large frequency reuse distances in future wireless networks are unlikely to be realised because more than ever, these networks will strive for high spectral efficiency through the use of small cluster sizes. In this situation cochannel interference cannot be ignored.

The consideration of multiple cell random access systems with small to moderate frequency reuse distances means that there will not only be contending packets received at a base station, but also interfering packets from cochannel cells. In order to study the performance of multiple cell random access systems, it is necessary to consider the distribution of contending and interfering terminals throughout the environment. The notation adopted in this thesis assumes that one of the contending terminals is the "desired" terminal, while the other contenders are *intra-cell interferers*. Terminals transmitting in cochannel cells are referred to as *inter-cell interferers*[3]. The distribution of these different users throughout both the outdoor cellular and in-building pico-cellular environments is presented in the following subsections. To simplify the analysis it is assumed that base stations only accept packets from terminals in their cell: packets from cochannel cells are considered to be interference. In a more advanced implementation, it is possible that base station macro-diversity techniques [2] could also be applied, although this aspect is not considered in this thesis.

4.2.1 Outdoor Cellular Systems

The location of desired, intra-cell interfering and inter-cell interfering terminals in an outdoor cellular system is presented in Fig. 4.1. For simplicity, only one cochannel cell is illustrated in this diagram, although in practice, the central cell is surrounded by at least six nearby cochannel cells[4]. In this thesis, six cochannel cells are considered for the analysis of outdoor cellular systems, unless otherwise stated. Circular cells, of radius R_c, are considered to make the analysis more tractable. The desired terminal, denoted in this thesis using the '0' subscript, is assumed to be at a radius r_0 from the central cell base station. The lognormal shadowing experienced between the desired terminal and the central cell base station is represented by the random variable x_0, while the pathloss exponent on this link is represented by b_0. In a similar fashion the link between the *x*th intra-cell interferer and the central cell base station may be described using

[3] This convention is the same as that used in the analysis of cellular CDMA systems affected by same-cell and cochannel cell interference.

[4] If a small cluster size is employed, it may be necessary to consider the second tier of cochannel cells, in which case there would be a total of 18 cochannel cells (6 in the first tier, 12 in the second tier).

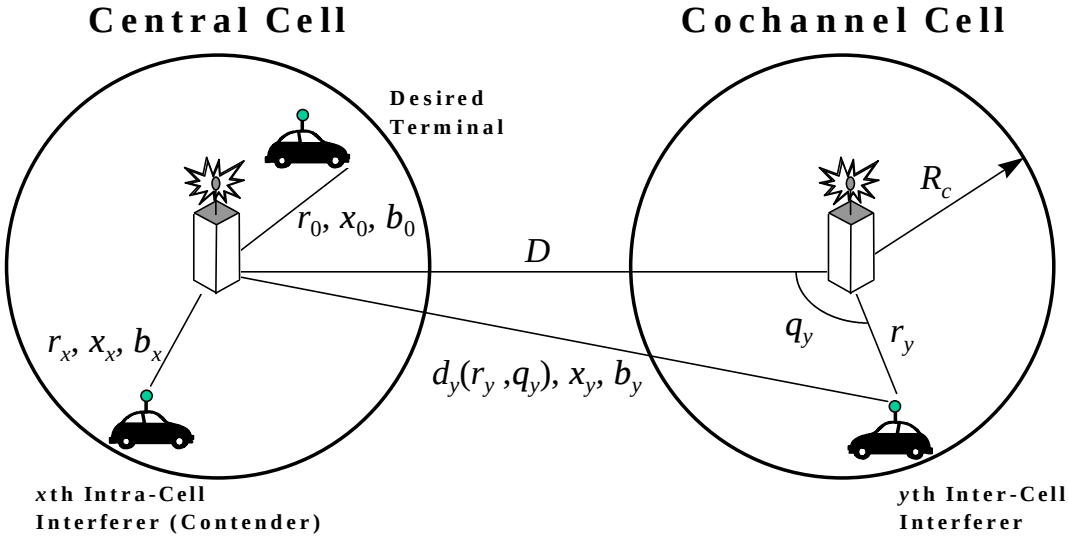

Figure 4.1: *Outdoor cellular random access system. The desired terminal must compete with both intra-cell interferers (central cell) and inter-cell interferers (cochannel cells).*

the parameters $\{r_x, x_x, b_x\}$, while the link between the *y*th inter-cell interferer and the central cell base station may be represented by $\{d_y(r_y,q_y), x_y, b_y\}$.The distance, $d_y(r_y,q_y)$, between the *y*th inter-cell interferer and the central cell base station is given by[5]

$$d_y(r_y,q_y) = \sqrt{D^2 + r_y^2 - 2Dr_y\cos(q_y)}, \qquad \textbf{(4.1)}$$

where *D* is the frequency reuse distance, r_y is the radius of the *y*th inter-cell interferer from its associated base station and q_y is the angle between the central cell base station and the *y*th inter-cell interferer. The parameters r_0, r_x, r_y, and q_y are random variables, as terminals may be located at any random distance r ($0 \le r \le R_c$) or angle q ($0 \le q \le 2\pi$) with respect to their base station. Consequently it is usual to represent these locations by a statistical distribution. Assuming uniform terminal density, the pdf, $f_r(r)$, of a terminal's radius (r) from its base station is given by

$$f_r(r) = \frac{2r}{R_c^2} \qquad 0 \le r \le R_c. \qquad \textbf{(4.2)}$$

The probability, $f_q(q)$, of a terminal being at an angle q is uniformly distributed, namely

$$f_q(q) = \frac{1}{2p} \qquad 0 \le q \le 2p. \qquad \textbf{(4.3)}$$

[5] In a simplified situation in which a moderate reuse distance is considered (such that $D>>r_y$,), the cochannel interferers can often be assumed to be located at the centre of the cochannel cells, so that $d_y(r_y, \theta_y) \approx D$. This simplifies the analysis, but can only be accurately applied to systems with larger cluster sizes.

4.2.2 In-Building Pico-Cellular Systems

The location of desired, intra-cell interfering and inter-cell interfering terminals in an in-building pico-cellular system is presented in Fig. 4.2. The building is assumed to be a square multiple storey office building with sides *a* metres long and an inter-floor vertical spacing of *b* metres. Centrally located base stations mounted on the ceilings are considered. For simplicity, only one cochannel cell is illustrated in this diagram, although in practice, there are multiple cochannel cells above and below the central cell. In this thesis, two cochannel cells are considered for the analysis of in-building pico-cellular systems, unless otherwise stated. This corresponds to the first cochannel floor above and below the central floor.

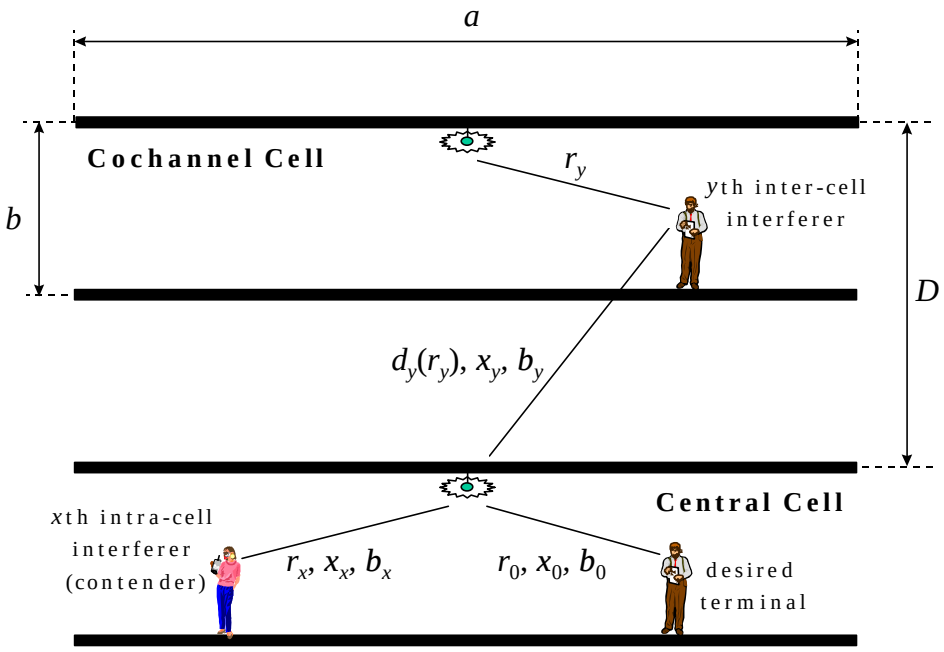

Figure 4.2: *In-building pico-cellular random access system. The desired terminal must compete with both intra-cell interferers (central cell) and inter-cell interferers (cochannel cells).*

The analysis of square in-building systems may be simplified by geometrically transforming the shape of the building from square to circular. The use of circular buildings allows the same spatial probability distributions that were presented for outdoor cellular systems, namely (4.2) and (4.3), to be considered in the analysis of in-building systems. In [3, p.267] it was shown that as long as the floor area of the equivalent circular building is the same as the floor area of the original square building, the performance results which are obtained are nearly equivalent. This transformation requires that an equivalent circular building has a floor radius of

$$R_c = \frac{a}{\sqrt{p}}, \tag{4.4}$$

given that the original square building has sides of length *a* metres. This concept is presented in Fig. 4.3. A further simplification which is made in this thesis assumes that the direct path length between a terminal and base station located on the same floor is given by the horizontal radius, *r*.

This concept is illustrated in Fig. 4.4. In reality the direct path length is the hypotenuse of the horizontal radius and the vertical height from the transmitter to the ceiling. This approximation is suitable in the case where a uniform terminal density is assumed, in which case the majority of terminals will be located further away from the base station.

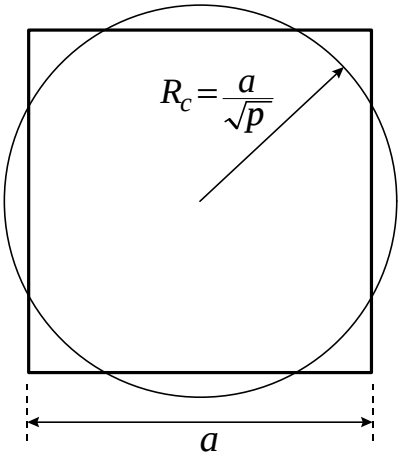

Figure 4.3: *Plan view of an a´a floor and a circular floor with equivalent area having a radius* $R_c = a/\sqrt{p}$.

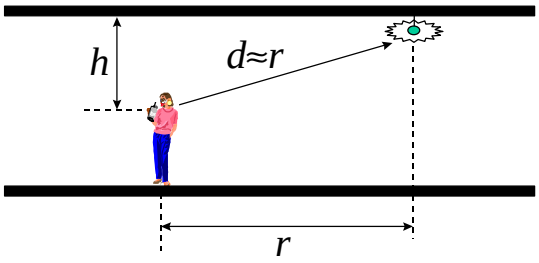

Figure 4.4: *Approximation of the terminal-base station separation distance.*

Using the same notation as for the outdoor cellular scenario, the desired terminal in the in-building system is considered to be described using the parameters $\{r_0,\ x_0,\ b_0\}$, where r_0 describes the (horizontal) separation distance between the desired terminal and central cell base station, x_0 is a random variable which describes the lognormal shadowing between the desired terminal and the central cell base station and b_0 is the pathloss exponent over this link. The parameter sets that were used in the outdoor cellular environment to describe the *x*th intra-cell and *y*th inter-cell interferer also apply in the in-building environment. The distance between the *y*th inter-cell interferer and the central cell base station, $d_y(r_y)$, can be approximated by

$$d_y(r_y) = \sqrt{r_y^2 + D^2}\ , \qquad \textbf{(4.5)}$$

The parameters r_0, r_x and r_y are all random variables, as terminals may be located at any random distance r ($0 \le r \le R_c$) with respect to their base station. It is possible to still apply the uniform terminal density assumption that was made for the outdoor environment to an in-building environment, so that the pdf, $f_r(r)$, of a terminal's radius (r) from its corresponding base station is given by (4.2).

4.2.3 Bandwidth Management

In considering multiple cell S-ALOHA and PRMA systems, certain working assumptions need to be made about the way that the available bandwidth is partitioned amongst the cells. In this thesis

it is assumed that the total system bandwidth allocated to a particular system is constant. Further, it is assumed that this bandwidth is partitioned equally amongst the N_c cells per cluster to form a particular reuse pattern. As the cluster size is reduced, the channel bitrate per cell increases, therefore resulting in shorter timeslot durations. In order to compare systems with different frequency reuse plans, the *system utilisation* performance measure is employed. This performance measure is discussed in §4.6.3.

In this thesis the performances of data-only, speech-only and speech-data systems are investigated. In order to compare the performance of separate and integrated speech and data systems (see Chapter 8), it is assumed that the total system bandwidth of the integrated system is the composite of the separate speech and data systems. The particular system parameters used in the analysis of multiple cell data-only S-ALOHA, speech-only PRMA and speech-data PRMA systems are presented in Tables 4.1-4.3. The values presented in these tables represent an arbitrary choice of system parameters. Alternative parameters could, if desired, be considered[6].

Cluster Size, N_c :	**1**	**2**	**3**	**4**
Total System Bitrate (kb/s), R_{sys}	426.66	426.66	426.66	426.66
Bitrate per Cell (kb/s), R_{cell}	426.66	213.33	142.22	106.66
Frame Duration, T (ms)	18	18	18	18
Timeslots per Frame, N	12	6	4	3
Timeslot Duration, t (ms)	1.5	3	4.5	6.0

Table 4.1: *Data-only S-ALOHA system parameters.*

Cluster Size, N_c :	**1**	**2**	**3**	**4**
Total System Bitrate (kb/s), R_{sys}	853.33	853.33	853.33	853.33
Bitrate per Cell (kb/s), R_{cell}	853.33	426.66	284.44	213.33
Frame Duration, T (ms)	18	18	18	18
Timeslots per Frame, N	24	12	8	6
Timeslot Duration, t (ms)	0.75	1.5	2.25	3.0

Table 4.2: *Speech-only PRMA system parameters.*

Cluster Size, N_c :	**1**	**2**	**3**	**4**
Total System Bitrate (kb/s), R_{sys}	1280	1280	1280	1280
Bitrate per Cell (kb/s), R_{cell}	1280	640	426.66	320
Frame Duration, T (ms)	18	18	18	18
Timeslots per Frame, N	36	18	12	9
Timeslot Duration, t (ms)	0.5	1.0	1.5	2.0

Table 4.3: *Speech-data PRMA system parameters.*

[6] Careful consideration must be given in the design of practical systems to ensure that the parameters of Tables 4.1-4.3 are compatible with other system parameters, such as the speech coding rate, R_s.

4.3 Receiver Capture in Multiple Cell Systems

Receiver capture can, in general, be defined as

> "*the phenomenon in which the decisions required from the receiver to estimate or reconstruct a potential message transmitted on the channel, are dominated by a single signal, despite the presence of interfering signals and noise*" [4, p194].

In multiple cell systems, such as those described in Section §4.2, *interfering signals* are attributable to both intra-cell and inter-cell interfering packets. In a mature random access system, the level of noise power would be negligible, compared to the interference power measured at a receiver. In this thesis, all systems are assumed to be interference limited. This means that interference is the only determinant with regard to the quality of reception.

The *capture probability*[7] is a useful performance measure, expressing the probability that a desired packet is successfully demodulated in the presence of interference power at the receiver input. Capture probability is loosely related to the quality of reception, but only to the extent that low capture probability corresponds to poor reception quality and high capture probability corresponds to good reception quality. Conditions relevant to the probability of capture are amongst other things, the received power levels, the type of modulation, the robustness of receiver synchronisation, the characteristics of the interference and the channel fading.

Exact computation of probabilities of capture is a complicated task. This is illustrated by the large number of different approximate models used to compute these probabilities [5-13]. A detailed comparison of these models is presented in [4]. In this thesis, the capture model proposed by Kuperus and Arnbak in [7], namely the *capture ratio model*, is used to compute the capture probability. This model is described and discussed in the following subsections.

4.3.1 The Capture Ratio Model

Assuming that m_{cen} packets are transmitted in the central cell and m_{coc} packets are transmitted in cochannel cells, a model is required which predicts whether one of the m_{cen} central cell packets is able to capture the central cell base station. According to the capture ratio model, a desired packet is considered to capture the base station receiver if its momentary power, P_0, exceeds the momentary composite interference power, P_I, by a specified threshold, or *capture ratio*, *z*, i.e. if,

$$\frac{P_0}{P_I} > z\,. \qquad \textbf{(4.6)}$$

In this situation, P_I is the incoherent (or power) cumulation of $m_{cen}-1$ intra-cell and m_{coc} inter-cell interfering packets, such that

[7] Normally the complement of the capture probability, namely the *outage probability* [19], is used in performance studies of wireless networks. However, in this thesis it is more convenient to deal with capture probabilities.

$$P_I = \sum_{x=1}^{m_{cen}-1} P_x + \sum_{y=m_{cen}}^{m_{cen}-1+m_{coc}} P_y \,. \qquad \textbf{(4.7)}$$

Incoherent cumulation assumes that the phases of the individual packets fluctuate significantly due to mutually independent modulation so that the composite interference power is the power sum of the individual signals. In certain situations, the assumption of incoherent interference cumulation may give pessimistic results compared to coherent cumulation, in which case the interfering signals are added on a voltage basis via phasor addition [14,15].

If $f_{P_0}(P_0)$ is the pdf of the desired packets momentary power and $f_{P_I}(P_I)$ is the pdf of the momentary composite interference power, then the probability of capture can, in general terms, be represented by

$$\Pr\left(\frac{P_0}{P_I} > z\right) = \Pr[Capture] = \int_0^{\infty} f_{P_I}(P_I) \int_{zP_I}^{\infty} f_{P_0}(P_0) dP_0 dP_I \,. \qquad \textbf{(4.8)}$$

In order to apply the capture ratio model to the analysis of the systems investigated in this thesis, the following capture probability definitions are required:

- $q(m_{cen}, m_{coc}, r_0)$ is the probability of the desired packet being received at the central base station from a distance r_0, given the presence of interference from $m_{cen}-1$ intra-cell and m_{coc} inter-cell interfering terminals averaged over all their expected positions.

- $q(m_{cen}, m_{coc})$ is the probability of the desired packet being received at the central base station, given the presence of interference from $m_{cen}-1$ intra-cell and m_{coc} inter-cell interfering terminals averaged over all expected positions of the user terminals, including the desired terminal. In other words, $q(m_{cen}, m_{coc})$ can be defined by

$$q(m_{cen}, m_{coc}) = \int_0^{R_c} q(m_{cen}, m_{coc}, r_0) f_r(r_0) dr_0 \,. \qquad \textbf{(4.9)}$$

- $U(m_{cen}, m_{coc})$ is the probability that one out of the m_{cen} simultaneously transmitted central cell packets is received correctly and is given by

$$U(m_{cen}, m_{coc}) = m_{cen} \cdot q(m_{cen}, m_{coc}) \,. \qquad \textbf{(4.10)}$$

In order to obtain these capture probabilities, information relating to the type of system, the numbers of users and the particular propagation conditions, is required. With knowledge of the capture probability, it is then possible to determine more system specific performance measures. In random access systems such as PRMA or S-ALOHA, such measures include the throughput, packet delay and packet dropping probability. This concept is represented in Fig. 4.5.

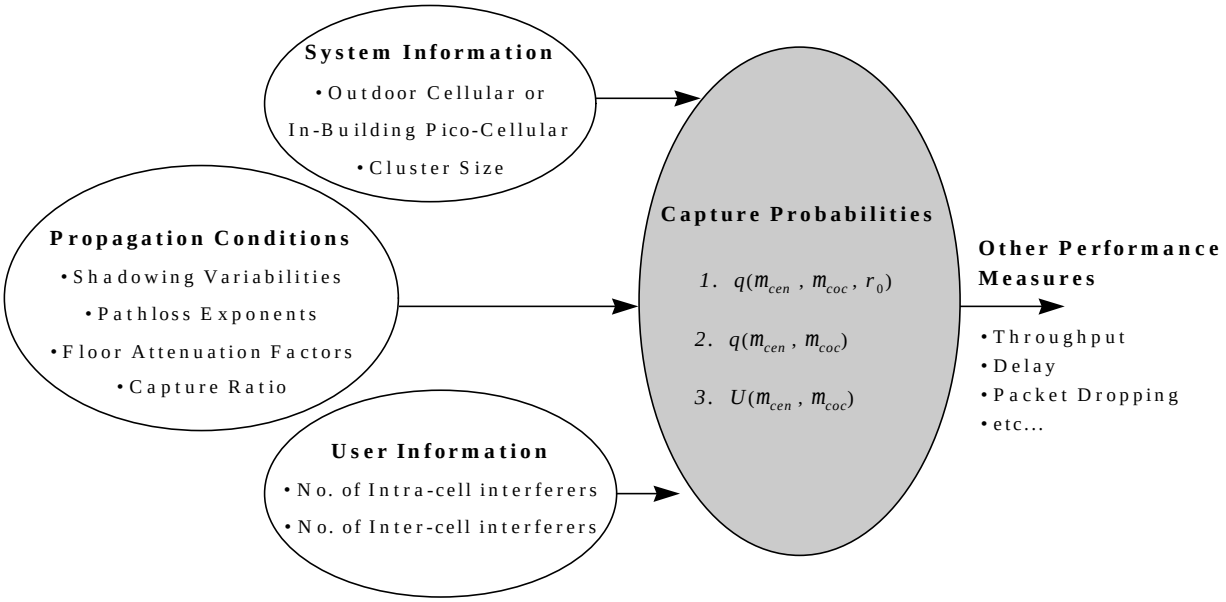

Figure 4.5: *Calculation of the capture probability requires knowledge of the system structure, propagation conditions and number of users. The capture probability can, in turn, be used in the calculation of other system specific performance measures.*

4.3.2 Choosing an Appropriate Capture Ratio

The value of *z* represents the minimum acceptable carrier to interference ratio (CIR) required for adequate packet reception. Determining a suitable value of *z* is a particularly difficult task, because of the large number of factors that influence its value. The choice of capture ratio depends on whether the 'long term', 'medium-term' or 'short term' signal level is being considered [19, p.213]. Moreover, the speed of the terminal also needs to be considered as this has an effect on the rate of fading and the subjective assessment of speech quality. In addition, the capture ratio depends on both the required output performance (i.e., at baseband) and on the type of interference.

In general, the choice of the value of *z* depends on the required quality of service and may therefore be somewhat arbitrary [4, p.78]. The outage criterion can, for instance, be a certain figure of merit subjectively determined by a representative panel of listeners or, in a digital system, an instantaneous bit error rate or digital word erasure rate [16]. Typical capture ratios for analog systems range from 3-20 dB [4, p.79], while for the digital pan-European GSM system, a capture ratio of 9.5 dB is considered to describe the performance of practical receivers [17]. In this thesis, a range of capture ratio values are adopted, including *z*=6, 10 and 14 dB.

4.3.3 The Constant Power Assumption

A central assumption of the capture ratio model is that the momentary carrier to interference ratio does not change during the timeslot. In other words, the power level of a packet is assumed to remain constant over one packet duration, i.e., the power of each bit in a packet is the same. This assumption has been used extensively in previous research and is considered to be accurate if the users are stationary or are moving very slowly.

The constant packet power assumption has been tested using a multipath channel simulator [18]. This simulator was used to reproduce the system and channel conditions that are assumed in this thesis. In particular, a Suzuki fading channel was simulated for terminal speeds of 5, 50, and 100 km/hr and a carrier frequency of 1.8 GHz. These speeds cover the range of environments considered in this thesis, namely the in-building pico-cellular and outdoor cellular environments. The power variation of a received signal was evaluated over a duration of 1 ms. This duration corresponds to the typical timeslot durations considered in this thesis. The results of the analysis are presented in Fig. 4.6.

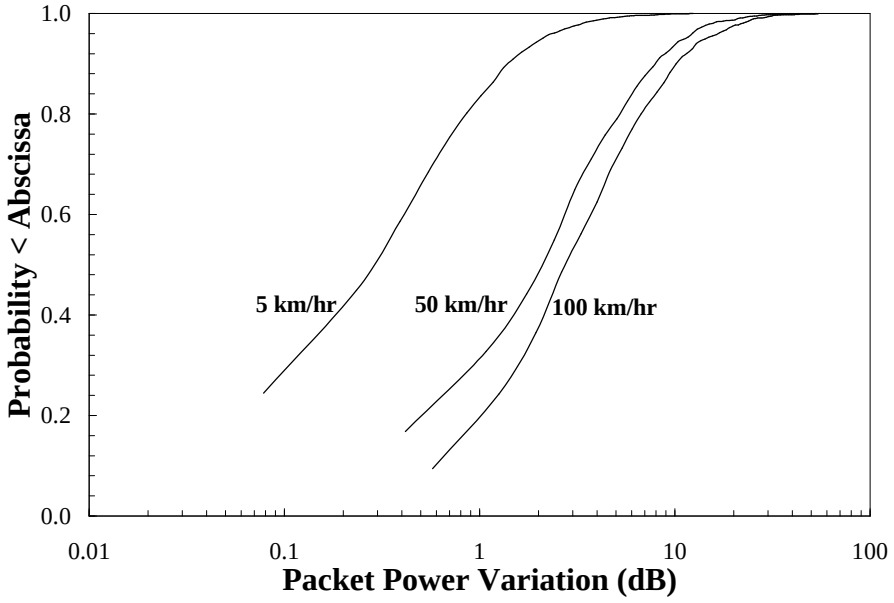

Figure 4.6: *CDF of the variation in power across a packet of duration 1 ms. A Suzuki fading channel is considered, with terminal speeds of 5, 50, and 100 km/hr (f=1.8 GHz).*

It can be observed from Fig. 4.6 that the assumption of constant packet power is valid in an in-building system (5 km/hr) where the rate of fading is slow. However, in an outdoor system, the variation over a packet duration is significantly greater, due to increased terminal speeds. The implication of this phenomenon is that the capture effect may be reduced somewhat in a high speed outdoor system, as the base station may be unable to lock onto a single packet for the duration of a timeslot[8]. In order to investigate this theory more fully, aspects such as error correction and modulation need to be considered. Such consideration is beyond the scope of this thesis. Although this limitation may exist with the capture ratio model, it still provides a relatively robust method for determining the effect of various channel conditions. By evaluating the capture probability for a range of capture ratios, the general effect that different scenarios have on system performance can be determined.

[8] This phenomenon could be accounted for by increasing the capture ratio for higher speeds of mobiles.

4.4 Capture with Multiple Suzuki Fading Packets

Consider the case where m_{cen} packets from terminals within the central cell and m_{coc} packets from terminals in cochannel cells, are received at the central cell base station. Of these m_{cen} packets, one is considered to be the "desired" packet, while the remaining $m_{cen}-1$ packets are intra-cell interferers. Assuming that the momentary voltage of all packets is Rayleigh distributed, then the momentary power of all packets will be exponentially distributed. The pdf of an arbitrary packet's power is, thus, given by

$$f_P(P) = \frac{1}{\overline{P}} \exp\left[\frac{-P}{\overline{P}}\right], \tag{4.11}$$

as presented in (3.13), where $\overline{P}$ is the local mean power. The Laplace transform of (4.11) is given by

$$\mathcal{L}\{f_P(P)\} = \int_0^\infty e^{-sP} f_P(P) dP\,, \tag{4.12}$$

which may be simplified to

$$\mathcal{L}\{f_P(P)\} = \frac{1}{1+s\overline{P}}\,. \tag{4.13}$$

If $f_{P_I}(P_I)$ is the pdf of the sum of $m_{cen}-1$ and m_{coc} exponential random variables then, from [19, p.76], the Laplace transform of $f_{P_I}(P_I)$ is given by

$$\mathcal{L}\{f_{P_I}(P_I)\} = \left(\prod_{x=1}^{m_{cen}-1} \frac{1}{1+s\overline{P_x}}\right)\cdot\left(\prod_{y=m_{cen}}^{m_{cen}-1+m_{coc}} \frac{1}{1+s\overline{P_y}}\right). \tag{4.14}$$

In (4.8), we let $K(zP_I)$ equal the inner integral, such that

$$K(zP_I) = \int_{zP_I}^\infty f_{P_0}(P_0) dP_0\,, \tag{4.15}$$

where $f_{P_0}(P_0)$ is of the form presented in (4.11), $K(zP_I)$ is, therefore, given by

$$K(zP_I) = \exp\left(\frac{-zP_I}{\overline{P_0}}\right). \tag{4.16}$$

Substituting (4.16) into (4.8), it is possible to obtain

$$\Pr[Capture] = \int_0^{\infty} f_{P_I}(P_I) \cdot \exp\left(\frac{-zP_I}{\overline{\overline{P_0}}}\right) dP_I \,. \qquad \textbf{(4.17)}$$

With the substitution, $s = z / \overline{P_0}$, (4.17) is clearly the Laplace transform of $f_{P_I}(P_I)$. Therefore, using (4.14), the probability of capture, as defined in (4.8) can be reduced to

$$\Pr[Capture] = \prod_{x=1}^{m_{cen}-1} \frac{\overline{P_0}}{\overline{P_0} + z\overline{P_x}} \cdot \prod_{y=m_{cen}}^{m_{cen}-1+m_{coc}} \frac{\overline{P_0}}{\overline{P_0} + z\overline{P_y}} \,. \qquad \textbf{(4.18)}$$

In the situation where both lognormal shadowing and Rayleigh fading are considered, the local-mean power, $\overline{P_0}$, of the desired packet in (4.18) may be represented by

$$\overline{P_0} = \overline{\overline{P_0}} \cdot 10^{\frac{x_0}{10}}, \qquad \textbf{(4.19)}$$

where the random variable x_0 represents the random fluctuation around the area-mean power, $\overline{\overline{P_0}}$, due to lognormal shadowing. In this situation, x_0 has a normal probability distribution as presented in Chapter 3, with zero mean (m_0=0) and standard deviation s_0 (dB). In a similar fashion, the local-mean powers, $\overline{P_x}$ and $\overline{P_y}$ of the xth intra-cell and yth inter-cell interferer may be represented by the following two expressions, respectively

$$\overline{P_x} = \overline{\overline{P_x}} \cdot 10^{\frac{x_x}{10}}, \qquad \textbf{(4.20)}$$

$$\overline{P_y} = \overline{\overline{P_y}} \cdot 10^{\frac{x_y}{10}} \,. \qquad \textbf{(4.21)}$$

By substituting (4.19)-(4.21) into (4.18), it is possible to obtain

$$\Pr[Capture] = \prod_{x=1}^{m_{cen}-1} \frac{\overline{\overline{P_0}}}{\overline{\overline{P_0}} + 10^{\frac{x_x - x_0}{10}} z\overline{\overline{P_x}}} \cdot \prod_{y=m_{cen}}^{m_{cen}-1+m_{coc}} \frac{\overline{\overline{P_0}}}{\overline{\overline{P_0}} + 10^{\frac{x_y - x_0}{10}} z\overline{\overline{P_y}}} \,. \qquad \textbf{(4.22)}$$

By including appropriate expressions for the area-mean powers, (4.22) may be used to analyse both outdoor cellular and in-building pico-cellular systems. In this thesis (3.9) is used as a prediction for the area-mean power in outdoor cellular systems, while (3.19) is used in in-building pico-cellular systems. The probability of capture in these two environments is investigated in the following two sub-sections (§4.4.1 and §4.4.2).

4.4.1 Outdoor Cellular Systems

In an outdoor cellular system the area mean power of an individual terminal's packet may be represented by (3.9). Under these circumstances the area-mean power of the desired, xth intra-cell and yth inter-cell interfering packets at the central cell base station are given by

$$\overline{\overline{P_0}} = \frac{P_t}{r_0^{b_0}}, \tag{4.23}$$

$$\overline{\overline{P_x}} = \frac{P_t}{r_x^{b_x}}, \tag{4.24}$$

and

$$\overline{\overline{P_y}} = \frac{P_t}{\left[d_y(r_y,q_y)\right]^{b_y}}, \tag{4.25}$$

respectively. For the meantime, it is assumed that the pathloss exponent experienced by each terminal is independent[9]. Under these circumstances the expression presented in (4.22) may be rewritten as

$$\Pr[Capture] = \prod_{x=1}^{m_{cen}-1} \frac{r_x^{b_x}}{r_x^{b_x} + 10^{\frac{x_x - x_0}{10}} z r_0^{b_0}} \cdot \prod_{y=m_{cen}}^{m_{cen}-1+m_{coc}} \frac{\left[d_y(r_y,q_y)\right]^{b_y}}{\left[d_y(r_y,q_y)\right]^{b_y} + 10^{\frac{x_y - x_0}{10}} z r_0^{b_0}}. \tag{4.26}$$

By integrating over all possible interfering Tx-Rx distances $\{r_x$ and $d_y(r_y,q_y)\}$ and over all possible levels of shadowing $\{x_x$, x_y and $x_0\}$, the probability of the desired terminal capturing the central base station receiver, $q(m_{cen},m_{coc},r_0)$, at a distance r_0 is found to be

$$q(m_{cen},m_{coc},r_0) = \int_{-\infty}^{\infty} \frac{e^{\frac{-x_0^2}{2s_0^2}}}{\sqrt{2p}\,s_0} \left[f(r_0,x_0)\right]^{m_{cen}-1} \left[g(r_0,x_0)\right]^{m_{coc}} dx_0, \tag{4.27}$$

where

$$f(r_0,x_0) = \int_{-\infty}^{\infty} \frac{e^{\frac{-x_x^2}{2s_x^2}}}{\sqrt{2p}\,s_x} \int_0^{R_c} \frac{2r_x}{R_c^2} \cdot \frac{r_x^{b_x}}{r_x^{b_x} + 10^{\frac{x_x - x_0}{10}} z r_0^{b_0}} dr_x dx_x, \tag{4.28}$$

and

$$g(r_0,x_0) = \int_{-\infty}^{\infty} \frac{e^{\frac{-x_y^2}{2s_y^2}}}{\sqrt{2p}\,s_y} \int_0^{R_c} \frac{2r_y}{R_c^2} \int_0^{2p} \frac{1}{2p} \cdot \frac{\left[d_y(r_y,q_y)\right]^{b_y}}{\left[d_y(r_y,q_y)\right]^{b_y} + 10^{\frac{x_y - x_0}{10}} z r_0^{b_0}} dq_y dr_y dx_y. \tag{4.29}$$

As far as the author is aware, no closed form solution to (4.27) exists, hence, numerical integration techniques must be employed to solve this expression. Details of these techniques are presented in Appendix A of this thesis. Having determined $q(m_{cen},m_{coc},r_0)$ from (4.27), it is possible to determine the capture probability expressions $q(m_{cen},m_{coc})$ and $U(m_{cen},m_{coc})$ using the relationships presented in (4.9) and (4.10), respectively.

[9] This assumption will be relaxed in later chapters.

4.4.2 In-Building Pico-Cellular Systems

In an in-building pico-cellular system the area mean powers of the individual packets may be represented by (3.19). In this situation the area-mean power of the desired and *x*th intra-cell interfering packet at the central cell base station are given by (4.23) and (4.24) respectively, while the area-mean power of the *y*th inter-cell interfering packet is given by

$$\overline{\overline{P_y}} = \frac{P_t}{faf_y \cdot \left[d_y(r_y)\right]^{b_y}}. \qquad \textbf{(4.30)}$$

Under these circumstances the capture probability, $q(m_{cen}, m_{coc}, r_0)$, is the same as (4.27) although $g(r_0, x_0)$ is instead given by

$$g(r_0, x_0) = \int_{-\infty}^{\infty} \frac{e^{\frac{-x_y^2}{2\sigma_y^2}}}{\sqrt{2\pi}\,\sigma_y} \int_0^{R_c} \frac{2r_y}{R_c^2} \cdot \frac{faf_y \cdot \left[d_y(r_y)\right]^{b_y}}{faf_y \cdot \left[d_y(r_y)\right]^{b_y} + 10^{\frac{x_y - x_0}{10}} z d_0^{b_0}(r_0)} dr_y dx_y \,. \qquad \textbf{(4.31)}$$

4.5 Capture Probability Results

The expressions derived in the previous two subsections (§4.4.1 and §4.4.2) may be used to determine the probability of capture in either outdoor cellular or in-building pico-cellular systems and for various values of cluster size, capture ratio, lognormal shadowing standard deviation, floor attenuation factor and pathloss exponent. In this section, the effect on the capture probability of these various parameters is determined. Capture probability results are presented for both outdoor cellular and in-building pico-cellular systems.

4.5.1 Outdoor Cellular Systems

In the analysis of outdoor cellular systems, it is assumed that all terminals experience the same pathloss exponent, b, and shadowing standard deviation, σ. In Fig. 4.7, the capture probability, $q(m_{cen}, m_{coc}, r_0)$, in a Suzuki fading cellular system is plotted. It is assumed that N_c=3, z=10 dB, σ =6 dB and b =4. The cases where there are (a) no inter-cell interferers and (b) no intra-cell interferers are presented. It can be observed from Fig. 4.7(a) that as the desired terminal moves further from the central base station and as the number of intra-cell interferers is increased, the probability of the desired terminal successfully capturing the central cell base station is diminished. A similar result is found with Fig. 4.7(b), although in this case the capture probability decreases with increasing numbers of inter-cell interferers. It is evident from Fig. 4.7 that the number of intra-cell interferers has a more significant effect on the capture probability than the number of inter-cell interferers does. This is due to the intra-cell interferers being located closer to the central base station than the inter-cell interferers. This results in a higher power level being received from an intra-cell interferer compared to an inter-cell interferer. However, as the cluster size is reduced, cochannel interferers become more closely located to the central base station, thus reducing the capture probability.

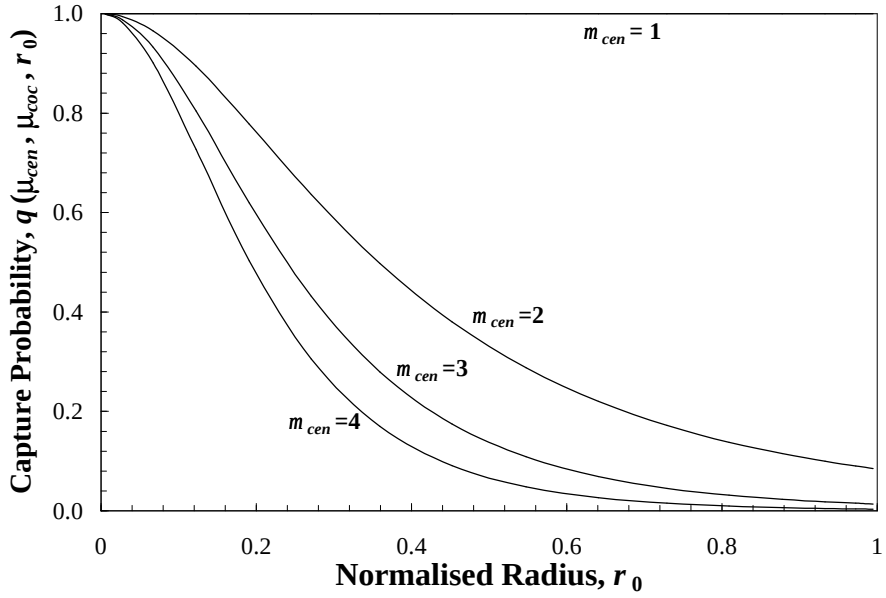

(a) *no inter-cell interferers present (m_{coc} =0).*

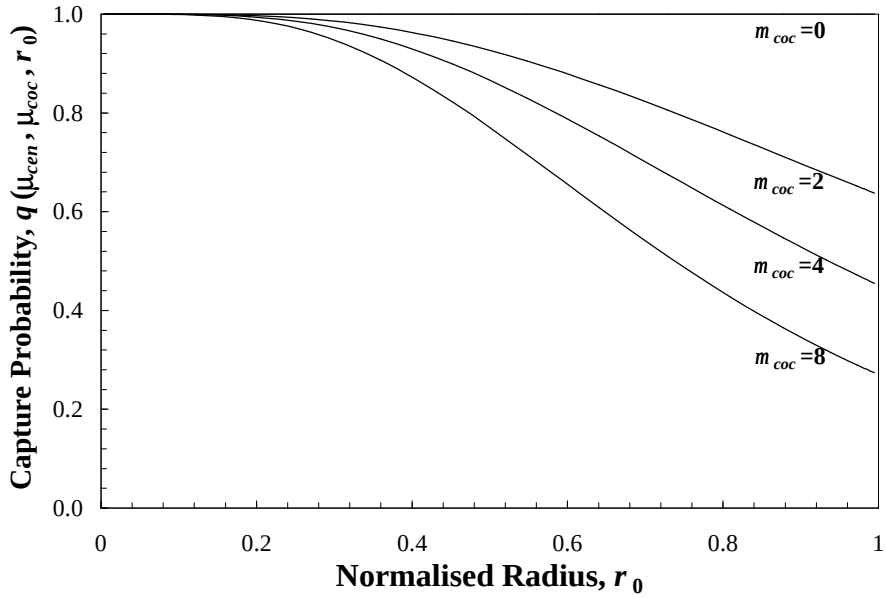

(b) *no intra-cell interferers present (m_{cen} =1).*

Figure 4.7: *Probability of desired terminal capturing the central cell base station from distance r_0 in a Suzuki fading outdoor cellular system (eqn.(4.27)). N_c =3, z=10 dB, s =6 dB, b =4.*

This is illustrated in Fig. 4.8, where instead of considering N_c =3, as was considered in Fig. 4.7 (b), a cluster size of N_c =1 has been assumed. In this situation, the cochannel interference has a more severe effect on the capture probability.

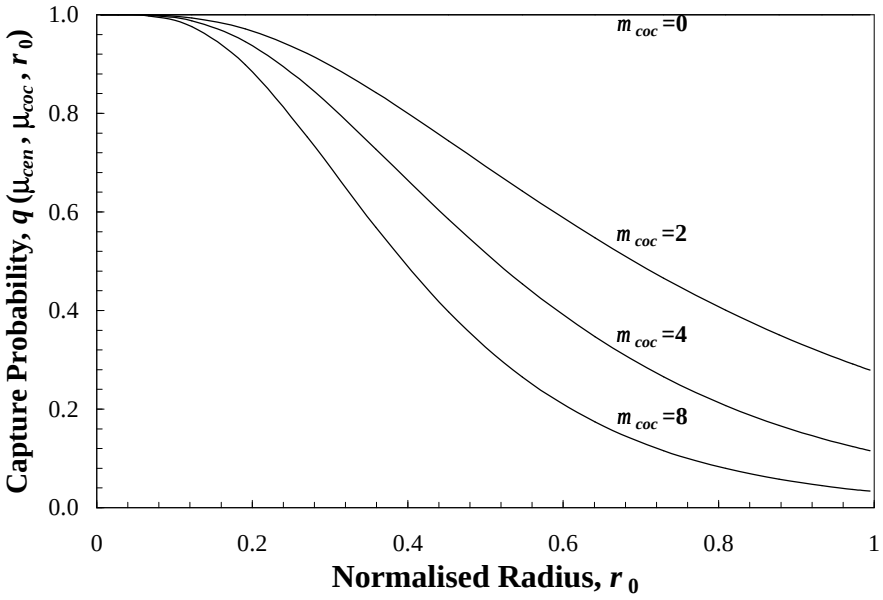

Figure 4.8: *Probability of desired terminal capturing the central cell base station from distance r_0 in a Suzuki fading outdoor cellular system (eqn.(4.27)). m_{cen} =1, N_c =1, z=10 dB, s =6 dB, b =4.*

Fig. 4.9 plots the capture probability, $U(m_{cen}, m_{coc})$, which is the probability that one out of the m_{cen} central cell packets captures the central cell base station, given the presence of m_{coc} inter-cell interferers. This result has been obtained by averaging over the location of the desired and interfering terminals. The system parameters assumed in Fig. 4.7 are also assumed in Fig. 4.9.

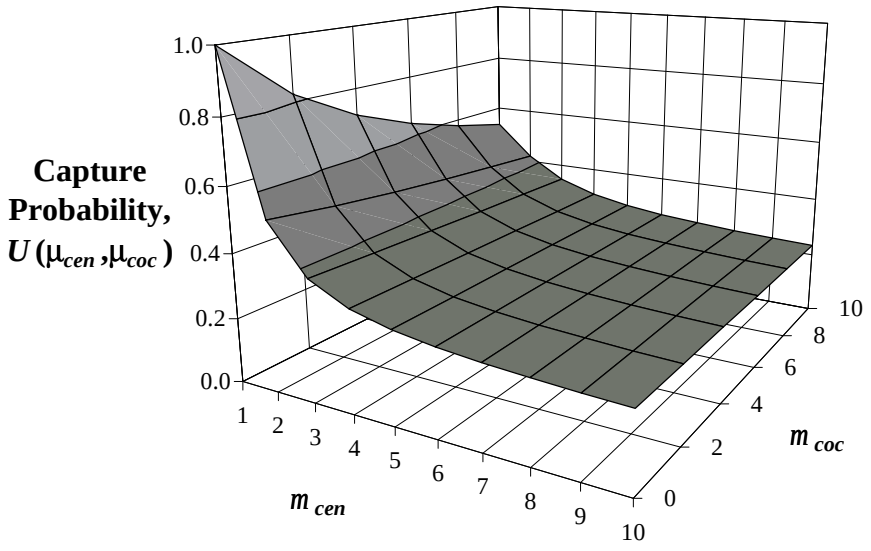

Figure 4.9: *Probability that one of the m_{cen} central cell packets captures the central cell base station in the presence of m_{coc} inter-cell interferers in a Suzuki fading outdoor cellular system (eqn. (4.10)). N_c =3, z=10 dB, s =6 dB, b =4.*

As the number of central cell packets increases, the capture probability approaches a limiting value. In [4, p.256], this limit in a single cell Rayleigh fading only system with $b = 4$, was found to be

$$U(m_{cen})\Big|_{m_{cen}\to\infty} = \frac{2}{p\sqrt{z}}. \qquad \textbf{(4.32)}$$

In [20] and [21], Zorzi and Rao confirmed that even in a single cell Suzuki fading environment, the limiting value of $U(m_{cen})$ is still given by (4.32) for $b = 4$. In addition, it was shown that in the generalised pathloss exponent case, the limiting value of $U(m_{cen})$ is given by

$$U(m_{cen})\Big|_{m_{cen}\to\infty} = \frac{1}{z(b)z^{2/b}}, \qquad \textbf{(4.33)}$$

where

$$z(b) = \frac{2p}{b}\csc\frac{2p}{b}. \qquad \textbf{(4.34)}$$

This means that the limiting capture probability only depends on the capture ratio, *z*, and the pathloss exponent, b, and does not depend on the level of shadowing, determined by the shadowing standard deviation, s. While no rigorous mathematical analysis has been performed, it appears extremely likely from Fig. 4.9 that the limiting value of $U(m_{cen}, m_{coc})$ does not depend on the number of inter-cell interferers. In any case, the limiting value of $U(m_{cen}, m_{coc})$ is only of marginal interest as the probability of a great number of terminals transmitting at the same time would be negligibly small, unless the random access system was severely overloaded.

Fig. 4.10 determines the effect of different cluster sizes on the capture probability, $U(m_{cen}, m_{coc})$, for a fixed number of inter-cell interferers ($m_{coc} = 6$). As the cluster size is decreased, the inter-cell interferers are in closer proximity to the central cell base station, meaning that the capture probability is decreased.

In Fig. 4.11, the effect that the capture ratio, *z*, has on the capture probability $U(m_{cen}, m_{coc})$ is determined for both single cell and multiple cell ($N_c = 3$, $m_{coc} = 6$) systems. It is evident that for both single cell and multiple cell systems, increasing the capture ratio has the effect of decreasing the capture probability. Increasing the capture ratio corresponds to the base station receiver needing a higher signal to interference ratio in order to successfully demodulate a desired packet.

Fig. 4.12 illustrates the effect that the shadowing standard deviation, s, has on the capture probability. When only one packet from a central cell terminal is received at the central base station (m_{cen}=1), there is a greater probability of it capturing with a Rayleigh fading channel (s =0 dB) than for a Suzuki fading channel (s =6, 12 dB). This is because the variability of the composite inter-cell interference power is smaller with Rayleigh fading only, thus, the composite inter-cell interference power is less likely to exceed the power of the desired packet. In the situation where multiple packets are received from central cell terminals at the central base

station (m_{cen} >1), one of the packets is more likely to capture the base station with Suzuki fading than with Rayleigh fading only. This is because one of the m_{cen} packets is more likely to be substantially stronger than the others with the increased variability inherent with Suzuki fading.

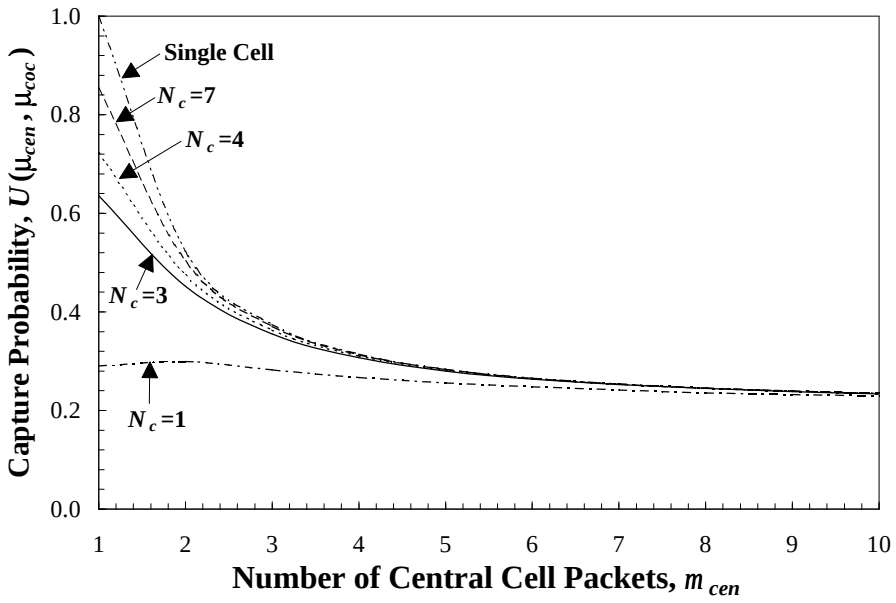

Figure 4.10: *Probability that one of the m_{cen} central cell packets captures the central cell base station in a Suzuki fading outdoor cellular system with various cluster sizes, N_c (eqn. (4.10)). $m_{coc} = 6$, z=10 dB, s =6 dB, b =4.*

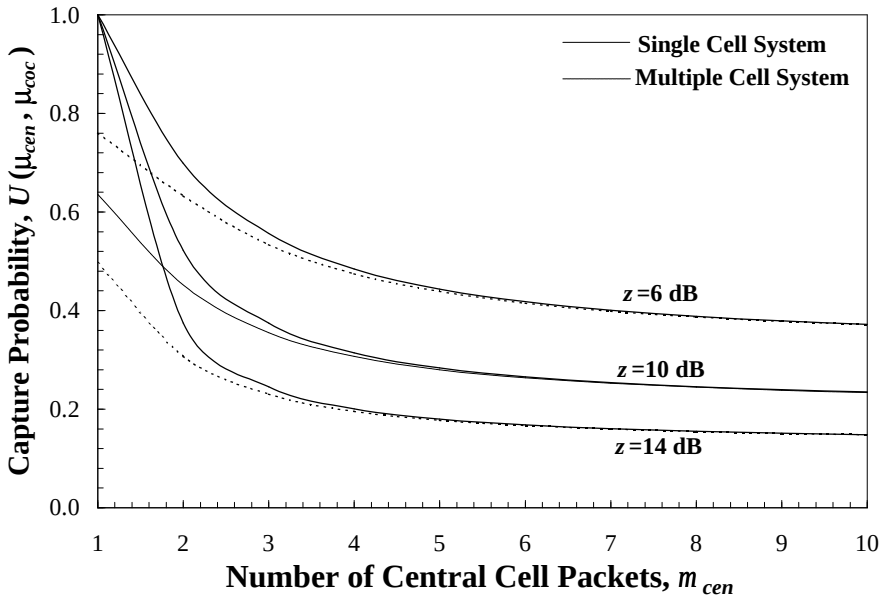

Figure 4.11: *Probability that one of the m_{cen} central cell packets captures the central cell base station in a Suzuki fading outdoor single cell system and multiple cell system (N_c =3, m_{coc} =6) with various capture ratios, z (eqn. (4.10)). s =6 dB, b =4.*

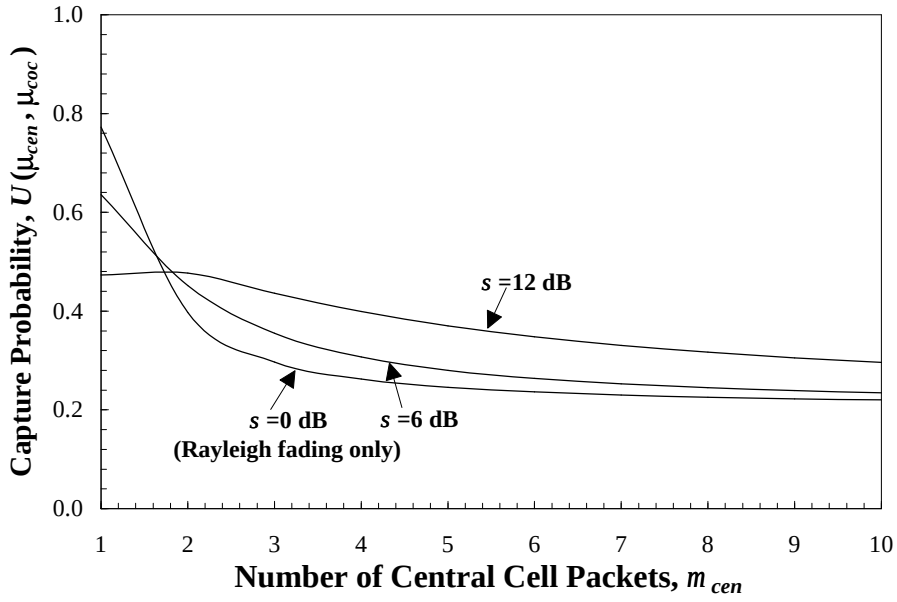

Figure 4.12: *Probability that one of the m_{cen} central cell packets captures the central cell base station in a Suzuki fading outdoor cellular system with various shadowing standard deviations, s (eqn. (4.10)). N_c =3, m_{coc} =6, z=10dB, b =4.*

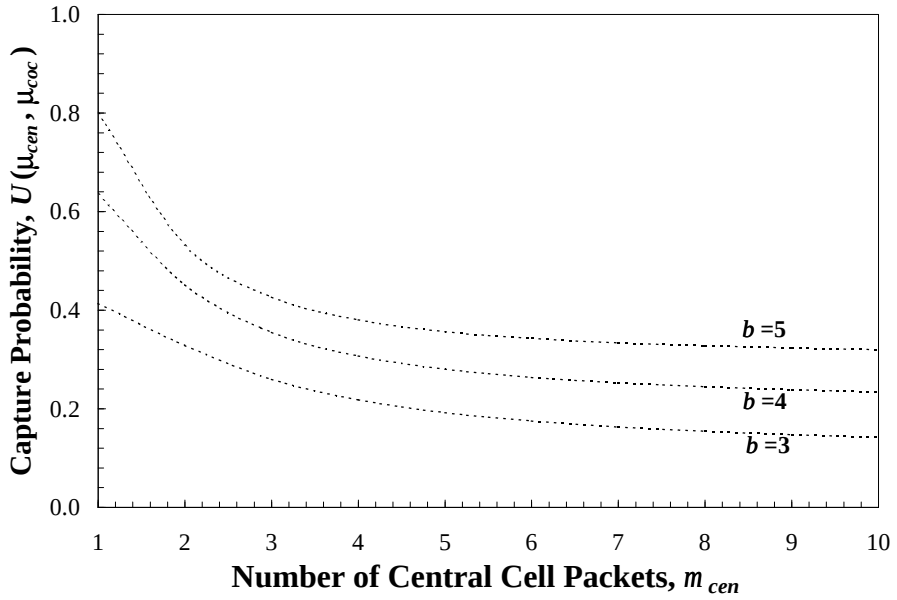

Figure 4.13: *Probability that one of the m_{cen} central cell packets captures the central cell base station in a Suzuki fading multiple cell system with various pathloss exponents, b (eqn. (4.10)). N_c =3, m_{coc} =6, z=10dB, s =6dB.*

In Fig. 4.13, the effect of the pathloss exponent, b, on the capture probability in an outdoor cellular system is determined. As the pathloss exponent is reduced, the capture probability is also

reduced. This is because with a higher pathloss exponent there is a greater level of isolation between cochannel cells, reducing the influence of inter-cell interference. This is especially noticeable when m_{cen}=1. A higher pathloss exponent is also beneficial when m_{cen}>1 as there is increased variability in the power of packets received from central cell terminals, leading to an improvement in capture probability.

4.5.2 In-Building Pico-Cellular Systems

A number of the findings in §4.5.1, derived with respect to outdoor cellular systems, also apply in in-building pico-cellular systems. In particular, the effects of the capture ratio, lognormal shadowing standard deviation and pathloss exponent on the capture probability is similar in both in-building and outdoor systems. In this thesis, the performance of systems operating in the four buildings presented in Table 3.3 is considered. These buildings represent a diverse range of structures. It is not surprising, therefore, that the capture probability varies considerably from one building to another.

Fig. 4.14 illustrates this point by comparing the capture probability for the four individual buildings. In this example, a cluster size of $N_c = 2$ is considered. In the case where only one central cell packet is transmitted, the highest probability of capture occurs in the Walnut Creek building, with the worst performance experienced in the San Francisco PacBell building. The poor performance experienced in the PacBell building is explained by the fact that it has the second lowest floor attenuation factor and the highest shadowing variability compared to the other buildings. With less isolation between floors (as indicated by the floor attenuation factor), cochannel interference has a more significant effect on the performance of the central cell.

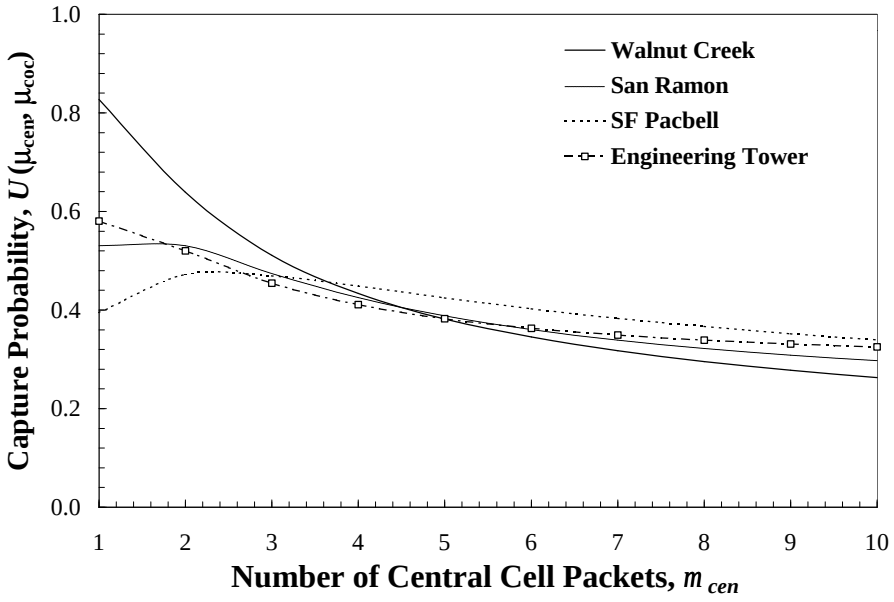

Figure 4.14: *Probability that one of the m_{cen} central cell packets captures the central cell base station for 4 different in-building pico-cellular systems. m_{coc}=6, N_c=2, z=10 dB (eqn. (4.10)). Values of b, s and FAF for the various buildings are presented in Table 3.3.*

4.5.3 Practical Implications of Results

From the results presented in Section 4.4.14.5.1 and 4.5.3, it is clear that the capture probabilities in a multiple cell system are significantly different to those in a 4.4.1single cell system. These differences are due to the effect of inter-cell interference that originates from cochannel users. In the presence of such interference, the central cell users experience a lower capture probability, compared to the performance of users in a single cell system.

The practical implication of this finding is that the performance of users in a realistic multiple cell system is likely to be highly dependent on the level of inter-cell interference present in the system. In the situation where random access systems are considered, it will be necessary to account for this interference when determining the performance of these systems (e.g., the data packet delay and packet dropping probability).

4.6 Effect of Interference on S-ALOHA and PRMA

This thesis is concerned with determining the performance of multiple cell, variable channel S-ALOHA and PRMA systems. In the previous sections of this thesis, a general framework has been developed, which allows such systems to be examined. However, it is still necessary to identify the effect that cochannel interference has on the operation of S-ALOHA and PRMA. There are also additional performance measures that must be considered.

4.6.1 Effect of Cochannel Interference on S-ALOHA

In a multiple cell S-ALOHA system, the central cell base station receives packets from not only terminals in the central cell, but also from terminals in cochannel cells. In this situation, the ability of central cell terminals to have their packets received successfully, is reduced. The consequence of this is that central cell terminals must perform more packet retransmissions before their packets can be received correctly by the central cell base station. This increases the mean data packet delay and reduces the overall system throughput and efficiency. Moreover, the increased rate of packet retransmissions is likely to cause greater interference to neighbouring cochannel cells, thus causing similar problems in these cells (and increasing the total interference even further).

In addition to counteracting interference through packet retransmission, a number of interference mitigation and/or reduction techniques could be employed to improve the performance of multiple cell S-ALOHA systems. These techniques include forward error correction (FEC), receiver diversity, power control and antenna sectorisation. In any realistic multiple cell S-ALOHA implementation some, if not all, of these techniques would be incorporated into the system design. Such approaches are not considered in this thesis with respect to multiple cell S-ALOHA systems, in order to simplify the analysis.

4.6.2 Effect of Cochannel Interference on PRMA

The effect of cochannel interference on the PRMA protocol, depends on whether the current timeslot is available or reserved. During available slots, cochannel interference has the same effect on PRMA as it does on S-ALOHA. In particular, a base station’s ability to decipher a packet from it’s own cell is reduced, due to the presence of packets from cochannel cells. This

leads to greater delay in a packet being received successfully, which increases the probability of speech packet dropping as well as increasing the delay experienced by PRMA data terminals.

During reserved slots, cochannel interference may cause a desired speech packet to be corrupted. Packets from data terminals, on the other hand, are not affected during reserved timeslots as data terminals are not allocated timeslot reservations. If, during a reserved slot, a base station is unable to decipher the desired speech packet, one of two events may have occurred, namely:

- no desired speech packet was transmitted (i.e. the speech talkspurt had finished) and only cochannel interference was received or;
- cochannel interference corrupted the desired speech packet to the extent that it could not be received correctly.

The base station must be capable of discriminating between these two events so that it can take appropriate action. In order to discriminate between the two events a comparison of the total power received in the current slot, with the total power received in the same slot in previous frames could be used. If the desired packet had been transmitted, the total power received would be significantly greater in most cases than if it had not. In this thesis, perfect discrimination between these two events is assumed.

In the first instance, where no desired speech packet was actually transmitted, the base station should relinquish the reservation so that other terminals may contend for access to that timeslot. If, on the other hand, the desired speech packet has been corrupted by cochannel interference the base station and terminal could do several things, as illustrated in Table 4.4.

Scenario	Reservation	Corrupted Packet
A	Retain	Discard
B	Relinquish	Retransmit
C	Retain	Retransmit
D	Relinquish	Discard

Table 4.4: *Possible scenarios for handling cochannel interference in PRMA.*

- **Base Station Response :** Either the base station could continue to allocate the timeslot reservation to the user involved, else it could relinquish it. If the base station believes that a reserved packet has genuinely been corrupted by cochannel interference, it should continue to grant the reservation to the user involved. However, in situations where the base station is unsure whether or not a reserved packet was actually transmitted[10], it may be better for the base station to relinquish the user' s reservation of the timeslot.

- **Speech Terminal Response :** Instead of permanently losing a reserved speech packet due to interference, a speech terminal may decide to return to the contention state and obtain a new timeslot reservation in which to transmit the packet [22]. Retransmitting a corrupted packet may improve the performance of the terminal involved, but may increase the amount of

[10] This situation corresponds to a terminal having already transmitted the last packet in it' s current talkspurt.

interference to other terminals in the system. No packet retransmissions could be considered in circumstances where the information is either non-critical or where doing so would cause unacceptable interference to other terminals.

Scenario C in Table 4.4 represents the most ideal outcome, with respect to the affected speech terminal. In this scenario, the terminal is able to retain it's timeslot reservation as well as being able to attempt retransmission of the corrupted packet. Such an approach, however, may lead to the terminal having two timeslot reservations. As well as increasing the complexity of the access protocol, this approach may lead to speech packets being transmitted in an incorrect order, making re-assembly at the destination more difficult.

Scenario C could, however, be fulfilled via an alternative approach. This approach would involve the affected terminal waiting one frame before retransmitting the corrupted packet using its existing timeslot reservation. This approach ensures that the terminal holds only one timeslot reservation, as well as guaranteeing that packets are transmitted in the correct order. However, with the requirement to wait one frame, it is highly likely that the corrupted packet would have to be dropped before being able to be retransmitted. In addition, subsequent packets transmitted by the terminal would be delayed by one frame. Optimally, corrupted speech packets should be retransmitted as soon as possible, in order to minimise delay variation.

Not only does Scenario C present difficulties in implementation, it is also prohibitively difficult to analyse via mathematical techniques. For these reasons, Scenario C is not considered in the analysis of the multiple cell PRMA systems considered in this thesis. Further research is necessary to determine the best approach for implementing this scenario, although this research is outside the scope of this thesis.

Whereas Scenario C represents the most optimistic approach for handling cochannel interference, Scenario D represents the most pessimistic approach. In particular, Scenario D assumes that the terminal looses both the timeslot reservation as well as the packet that was corrupted. It is unlikely that such an approach would be adopted in any multiple cell implementation of PRMA.

Scenarios A and B in Table 4.4 represent realistic approaches for handling cochannel interference in multiple cell PRMA systems. Scenario A relates to the situation where the speech terminal retains its timeslot reservation, but does not retransmit the corrupted packet, whereas with Scenario B, the terminal relinquishes its reservation and attempts to retransmit the corrupted packet. The performance of multiple cell PRMA systems that employ Scenarios A and B to handle cochannel interference are compared in Chapters 6 and 7, respectively.

As with multiple cell S-ALOHA systems, various interference mitigation and/or reduction techniques can be employed to improve the performance of multiple cell PRMA systems. These techniques are in addition to those presented in Table 4.4, and include forward error correction (FEC), receiver diversity, power control and antenna sectorisation. In Chapter 7 of this thesis, a simple base station receiver selection diversity technique is considered in an attempt to reduce inter-cell interference in various multiple cell PRMA systems.

4.6.3 Additional Performance Measures

System Utilisation Factor : The analysis of multiple cell S-ALOHA and PRMA systems requires that a measure of the spectral efficiency be incorporated. This allows the efficiency of various frequency reuse arrangements to be compared. In this thesis, the overall efficiency of a S-ALOHA or PRMA system is measured using the overall system utilisation factor, y , given by [23-25]

$$y = \frac{h}{N_c}, \tag{4.35}$$

where h is the throughput (per cell) and N_c is the cluster size.

Speech Packet Interference Probability : In PRMA the measure most commonly used to evaluate system performance has been the packet dropping probability. However, when Scenario A in Table 4.4 is considered, it is necessary to also consider the mean speech packet interference probability, P_{int} . This is the probability of a reserved speech packet being corrupted by cochannel interference, denoted by

$$P_{int} = 1 - q(1, \overline{m_{coc}}), \tag{4.36}$$

where $q(1, \overline{m_{coc}})$, given previously in (4.9), represents the probability that one central cell packet (i.e. the reserved packet) captures the central cell base station in the presence of $\overline{m_{coc}}$ inter-cell interfering packets. Under this notation, $\overline{m_{coc}}$ represents the mean inter-cell interference received in a timeslot. Techniques for estimating $\overline{m_{coc}}$ will be presented in following chapters.

Speech Packet Loss Probability : When considering Scenario A, it is necessary to consider the combination of those packets dropped plus those packets interfered. This combination is referred to as the total speech packet loss, P_{loss} , and is given by [24-26]

$$P_{loss} = P_{drop} + \left[1 - P_{drop}\right] P_{int}, \tag{4.37}$$

where P_{int} is given by (4.36). The probability P_{drop} , used for Scenario A, will be defined in Chapter 6 of this thesis. The capacity of PRMA systems can be estimated by the number of users per cell that can be supported at either a 1% or 5% speech packet loss probability (depending on the design requirements). Scenario B considers the case where corrupted speech packets may be retransmitted. In this situation, speech packets are not lost as a direct result of interference. Therefore, P_{int} in (4.37) becomes zero although P_{drop} is likely to increase, as interfered speech packets return to the contention state. A modified expression for P_{drop} , relating to Scenario B, will be defined in Chapter 7 of this thesis.

4.7 Summary

Single cell, simple channel environments have normally been considered in the analysis of random access systems such as S-ALOHA and PRMA. In this chapter the layout of more realistic multiple cell configurations, namely the outdoor cellular and in-building pico-cellular environments have been presented. The particular parameters that will be used in the multiple cell S-ALOHA and PRMA system analyses have also been presented in this chapter. In addition, the variable nature of the radio propagation channel has been incorporated, with the consideration of capture probabilities relevant to multiple cell random access systems. The capture probability model developed, allows for the probability of a desired packet capturing the central cell base station in the presence of both intra-cell and inter-cell interfering packets, to be determined. It is also possible to determine the probability of capture in both outdoor cellular and in-building picocellular systems, for a range of propagation conditions. The effects of cochannel interference on the actual workings of the S-ALOHA and PRMA protocols have been outlined, together with possible approaches for combating this interference. Additional performance measures, required for the analysis of multiple cell S-ALOHA and PRMA systems, have been presented.

References

[1] J.- P. M. G. Linnartz, "Imperfect sector antenna diversity in slotted ALOHA mobile network," *IEEE Trans. Commun.*, vol. 44, no. 10, Oct. 1996, pp. 1322 - 1328.

[2] J.- P. M. G. Linnartz, "Slotted ALOHA land-mobile radio networks with site diversity," *IEE Proceedings-I*, vol. 139, no. 1, Feb. 1992, pp. 58 - 70.

[3] P. M. Cartwright, *Cochannel interference in three-dimensional wireless communication systems*, Ph.D Thesis, Department of Electrical & Electronic Engineering, The University of Auckland, New Zealand, May 1997.

[4] J. P. M. G. Linnartz, *Narrowband land-mobile radio networks*. Massachusetts: Artech House, 1993.

[5] J. J. Metzner, "On improving utilisation in ALOHA channels," *IEEE Trans. Commun.*, vol. 24, no. 4, Apr. 1976, pp. 447 - 448.

[6] N. Abramson, "The throughput of packet broadcasting channels," *IEEE Trans. Commun.*, vol. 25, no. 1, Jan. 1977, pp. 117 - 128.

[7] F. Kuperus, J. Arnbak, "Packet radio in a Rayleigh channel," *Electronics Letters*, vol. 18, no. 12, Jun. 10th 1982, pp. 506 - 507.

[8] R. Sinha, S. C. Gupta, "Mobile packet radio networks: state-of-the-art," *IEEE Commun. Mag.*, vol. 23, no. 3, Mar. 1985, pp. 53 - 61.

[9] D. H. Davis, S. A. Gronemeyer, "Performance of slotted ALOHA random access with delay capture and randomised time of arrival," *IEEE Trans. Commun.*, vol. 28, no. 5, May 1980, pp. 703 - 710.

[10] R. Pluymers, “Computer simulation of a mobile packet radio system, “ *Electronics Letters*, vol. 24, no. 6, Mar. 17, 1988, pp. 316 - 317.

[11] K. Zhang, K. Pahlavan, R. Ganesh, “Slotted ALOHA radio networks with PSK modulation in Rayleigh fading channels,” *Electronics Letters*, vol.25, no.6, Mar.16, 1989, pp. 413-414.

[12] I. M. I. Habbab, M. Kavehrad, C-E. W. Sundberg, “ALOHA with capture over slow and fast fading radio channels with coding and diversity,” *IEEE J. Sel. Commun*., vol. 7, no. 1, Jan. 1989, pp. 79 - 88.

[13] A. U. H. Sheikh, Y. D. Yao, X. Wu, “The ALOHA system in shadowed mobile radio channels with slow and fast fading,” *IEEE Trans. Veh. Technol*., vol. 39, no. 4, Nov. 1990, pp. 289 - 298.

[14] J. Arnbak, W. van Blitterswijk, “Capacity of slotted ALOHA in Rayleigh-fading channels,” *IEEE J. Selected Areas Commun.*, vol. 5, no. 2, Feb. 1987, pp. 261 - 269.

[15] R. Prasad, A. Kegel, “Improved assessment of interference limits in cellular radio performance,” *IEEE Trans. Veh. Technol.*, vol. 40, no. 2, May 1991, pp. 412 - 419.

[16] J. C. -I. Chuang, “Comparison of coherent and differential detection of BPSK and QPSK in a quasi-static fading channel,” *IEEE Trans. Commun.*, vol. 38, no. 5, May 1990, pp. 565 - 567.

[17] J. Walker, *Mobile Information Systems.* Massachusetts: Artech House, 1990.

[18] A. J. Coulson, “The Development of a versatile and robust mobile radio multipath channel simulator,” *Industrial Research Report 410, Industrial Research Ltd.*, Lower Hutt, New Zealand, 29th May 1995.

[19] K. W. Sowerby, *Outage probability in mobile radio systems*. Ph.D Thesis, Department of Electrical & Electronic Engineering, University of Auckland, New Zealand, Feb. 1989.

[20] M. Zorzi, R. R. Rao, “Slotted ALOHA with capture in a mobile radio environment,” *in Proc. 1994 International Zurich Seminar on Digital Communications*, Zurich, Switzerland, Mar. 1994, pp. 452 - 463.

[21] M. Zorzi, R. R. Rao, “Capture and retransmission control in mobile radio,” *IEEE J. Selected Areas Commun.*, vol. 12, no. 8, Oct. 1994, pp. 1289 - 1298.

[22] H. Qi, R. Wyrwas, "Performance analysis of joint voice-data PRMA over random packet error channels," *IEEE Trans. Veh. Technol*., vol. 45, no. 2, May 1996, pp. 332 - 345.

[23] M. D. Orange, K. W. Sowerby, A. J. Coulson, “Markov analysis of an outdoor S-ALOHA system with frequency reuse,” *in Proc. 7th Virginia Tech/MPRG Symposium on Wireless Personal Communications*, Blacksburg, Virginia, Jun. 1997, pp. 13-1 - 13-12.

[24] M. D. Orange, K. W. Sowerby, “The effect of receiver capture and cochannel interference on PRMA,” *in Proc. 46th IEEE Veh. Technol. Conf.*, Atlanta, Georgia, Apr. 1996, pp. 1741 - 1745.

[25] M. D. Orange, K. W. Sowerby, A. J. Coulson, K. S. Butterworth, “Performance of a speech-data PRMA system in an in-building environment,” *in Proc. 47th IEEE Veh. Technol. Conf.*, Phoenix, Arizona, May 1997, pp. 1518 - 1522.

[26] M. Mastroforti, "Up-link capacity evaluation of a PRMA based system in a terrestrial radio mobile environment," *Centro Studi e Laboratori Telecomunicazioni (CSELT) Technical Reports*, Torino, Italy, vol. 24, no. 4, Feb. 1996, pp. 113 - 130.

Chapter 5

Multiple Cell S-ALOHA Data Systems

5.1 Introduction

Previous research relating to S-ALOHA has generally assumed the protocol to be operating under single cell, simple channel conditions. The results obtained under these conditions cannot be applied to the performance of S-ALOHA in a multiple cell system. Base stations in a multiple cell S-ALOHA system receive not only contending packets from terminals within their cell, but also interfering packets from cochannel cells. This has the effect of reducing the performance of the protocol, compared to the performance in an interference-free single-cell system. In Chapter 4, a key component of the theory required to analyse S-ALOHA in multiple cell, fading channel situations was developed, namely capture probability expressions for both outdoor cellular and in-building pico-cellular environments. The performance of S-ALOHA data systems in these environments is determined in this chapter via Markov analysis and computer simulations. The Markov analysis incorporates capture probability expressions developed previously in Chapter 4.

Markov analysis of a multiple cell S-ALOHA system is more complicated than Markov analysis of a single cell S-ALOHA system. However, if the level of cochannel interference can be accurately quantified, it is possible to incorporate it's effect into a single cell Markov analysis, thus, effectively performing a Markov analysis of a multiple cell system. In §5.2 the Markov analysis used to study S-ALOHA in a multiple cell system is outlined. Several techniques for estimating the amount of cochannel interference in such a system are presented in §5.3. In §5.4, details of the Monte Carlo computer simulations are presented. Results are presented in §5.5 and §5.6 for the delay, throughput and stability of interference limited outdoor cellular and in-building pico-cellular S-ALOHA systems, respectively. The effect on the system of various cluster sizes, path loss exponents and shadowing standard deviations is determined. Previous studies have only considered the analysis of single cell S-ALOHA systems, which are shown here to produce more optimistic results than analysis based on more realistic systems.

5.2 Markov Analysis

Markov analysis has frequently been used to analyse S-ALOHA systems because, unlike S-G analysis (infinite population model), it provides information on the dynamic behaviour of the system. Markov analysis of S-ALOHA in a single cell system is well documented [1-4]. In this section the Markov analysis used for single cell systems is extended to consider multiple cell S-ALOHA systems. This Markov analysis does not attempt to incorporate the actual operation of multiple cells as it is mathematically difficult, if not impossible, to include the operation of multiple cells within such an analysis. In order to facilitate the Markov analysis, the problem is constrained so that only the central cell of the system is modeled. However, this approach requires that the expected value of inter-cell interference received at the central cell base station be determined. This expected value, $\overline{m_{coc}}$, is the average number of inter-cell interfering packets,

m_{coc}, received at the central cell base station per timeslot from terminals operating in cochannel cells. Two methods of estimating $\overline{m_{coc}}$ in a multiple cell S-ALOHA system are presented in §5.3.

5.2.1 The State Probability Distribution

The S-ALOHA system under consideration contains M_d data users per cell. Each user can be represented by the tri-state Markov model illustrated in Fig. 2.5. According to this model, each user is either waiting to generate and transmit a new packet (with probability l_d) or else is attempting to retransmit a backlogged packet. A backlogged packet is retransmitted in the current timeslot with probability p_d. From the time a user generates a packet until the time the packet is successfully received, the user is blocked in the sense that it cannot generate (or accept from it's input source) a new packet for transmission.

The global behaviour of the entire S-ALOHA network is modeled by means of a finite Markov chain. The state of the network is represented by the number of terminals, *B*, in the backlogged state. The state probability distribution, $\pi(B)$, is the probability that *B* out of the M_d data terminals are in the backlogged state. Obviously, *B* is in the set $\{0,1,2\ldots M_d\}$. In order to calculate $\pi(B)$, it is necessary to first calculate the one-step state transition probability distribution, $\pi(k|B)$. This is the probability of going from *B* backlogged terminals in one timeslot to *k* backlogged terminals in the following timeslot. This distribution can be determined for a multiple-cell S-ALOHA system by using the single cell S-ALOHA distribution presented in [1] and replacing the capture probability, $U(m_{cen})$, with $U(m_{cen},\overline{m_{coc}})$, namely

$$\pi(k|B)=\begin{cases}0 & k<B-1\\ (1-l_d)^{M_d-B}\displaystyle\sum_{i=0}^{B}\binom{B}{i}p_d{}^{i}(1-p_d)^{B-i}U(i,\overline{m_{coc}}) & k=B-1\\ \binom{M_d-B}{k-B}l_d{}^{k-B}(1-l_d)^{M_d-k-1}\displaystyle\sum_{i=0}^{B}\binom{B}{i}p_d{}^{i}(1-p_d)^{B-i} & \\ \times\left[(1-l_d)\left[1-U(i+k-B,\overline{m_{coc}})\right]+\dfrac{M_d-k}{k-B+1}\,l_dU(i+k-B+1,\overline{m_{coc}})\right] & k\geq B\end{cases} \quad \textbf{(5.1)}$$

$U(m_{cen},\overline{m_{coc}})$ is the probability that one out of m_{cen} intra-cell packets captures the central cell base station, given that, on average, $\overline{m_{coc}}$ unwanted inter-cell packets are also received. Capture probabilities for multiple cell random access systems, such as S-ALOHA, were presented in Chapter 4. From (5.1), it is possible to determine the state probability distribution, $\pi(B)$, by starting with an arbitrary positive $\tilde{\pi}(0)$, and applying the following recursive expression [1]

$$\tilde{\pi}(B)=\frac{1}{\pi(B-1|B)}\left(\tilde{\pi}(B-1)-\sum_{j=0}^{B-1}\tilde{\pi}(j)\cdot\pi(B-1|j)\right), \quad \textbf{(5.2)}$$

and then normalising to obtain

$$\pi(B) = \frac{\tilde{\pi}(B)}{\sum_{s=0}^{M_d} \tilde{\pi}(s)}. \qquad \textbf{(5.3)}$$

A typical state probability distribution obtained from one of the multiple cell S-ALOHA systems considered in this chapter, is presented in Fig. 5.1. The system is assumed to have M_d=60 data terminals per cell. The result presented in Fig. 5.1 shows that the mean number of backlogged terminals is approximately B=50.

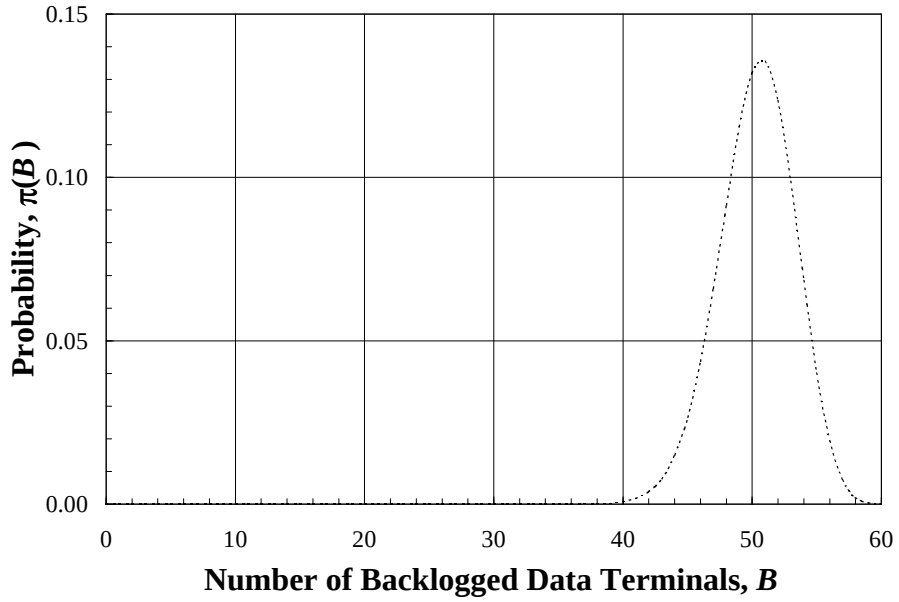

Figure 5.1: *Example of the state probability distribution, $\pi(B)$ (eqn. (5.3)). M_d=60.*

5.2.2 Performance Measures

With knowledge of the distribution $\pi(B)$, it is possible to study other aspects of the multiple cell S-ALOHA system such as the channel throughput per cell, h, data packet delay, W, expected drift, Δ, and system utilisation, y. These performance measures were first introduced in §2.2.4 and §4.6.3. The remainder of this section presents these performance measures in a mathematical form. The expected throughput, $h(B)$, in state B, is given by [1]

$$h(B) = \sum_{j=0}^{M_d-B} \binom{M_d - B}{j} l_d{}^j (1-l_d)^{M_d-B-j} \sum_{i=0}^{B} \binom{B}{i} p_d{}^i (1-p_d)^{B-i} U(i+j, \overline{m_{coc}}), \qquad \textbf{(5.4)}$$

while the overall mean throughput per cell is

$$h = \sum_{B=0}^{M_d} h(B) \cdot \pi(B). \qquad \textbf{(5.5)}$$

By Little's result [5], the average data packet delay (measured in slots), is given by [1,3]

$$W = \frac{\sum_{B=1}^{M_d} B \cdot \pi(B)}{h}. \qquad \textbf{(5.6)}$$

The drift, which can be defined according to [1],

$$\Delta(B) = (M_d - B)\, l_d - h(B), \qquad \textbf{(5.7)}$$

is the difference between the expected number of new packets to be input to the system and the expected number of packets to leave the system within one timeslot. System states B with $\Delta(B)=0$ will be equilibrium states of the network. Each cell in a multiple cell S-ALOHA system has only $1/N_c$ of the total system spectrum allocation, where N_c is the cluster size. A cell with mean throughput, h, equates to an overall system having a utilisation factor, y, given by (4.35).

5.2.3 Performance Study Assumptions

In this chapter, the performance of both outdoor cellular and in-building pico-cellular S-ALOHA systems are compared for various frequency reuse plans. In particular, clusters sizes of N_c=1, 3 and 4 are considered for the outdoor environment and cluster sizes of N_c=1, 2, 3 and 4 are considered for the in-building environment. It is assumed that a total system channel bit rate, R_{sys}, is partitioned amongst the N_c cells per cluster. The appropriate system parameters for these situations were presented in Table 4.1. Each data terminal is assumed to generate information randomly with an average bit rate of R_d b/s. This information is packetised into I bit packets and appended with an H bit header, which contains routing and addressing information. As the cluster size is reduced, the channel bit rate per cell increases while the duration of timeslots reduces. Accordingly, the probability of a terminal generating a new packet in a timeslot is reduced. In general, the packet generation rate, l_d, for a timeslot of length t is given by

$$l_d = \frac{R_d t}{I(\text{bits})}. \qquad \textbf{(5.8)}$$

5.3 Inter-Cell Interference Estimation

In §5.2, the theory required to calculate the state probability distribution and the system performance measures of a multiple cell S-ALOHA system was developed. The calculation of the state probability distribution and the performance measures requires determination of the mean number of inter-cell interfering packets, $\overline{m_{coc}}$, received per timeslot. In a realistic system, the number of inter-cell interfering packets received would not be constant (i.e., equal to $\overline{m_{coc}}$) in every timeslot. Rather, the number of interfering packets, m_{coc}, received at the central cell base station would vary from one timeslot to the next, according to some probability distribution

function, $f_{m_{coc}}(m_{coc})$ [1]. Under these circumstances, the state probability distribution of the terminals in the central cell would depend on the number of inter-cell interfering packets received per timeslot (i.e., $\pi(B|m_{coc})$). The mean inter-cell interference approach, therefore, represents a significant simplification to the analysis.

The results presented in §5.5 and §5.6, however, appear to completely justify the mean inter-cell interference approach, with excellent agreement found between theoretical and simulation results. The results presented in this chapter tend to indicate that it is sufficient to consider $\overline{m_{coc}}$ when analysing a multiple cell S-ALOHA system. While future work could consider the distribution of m_{coc}, this approach would significantly increase the complexity of the analysis. In addition, it is unlikely that more accurate results could be obtained.

In the following subsections, two techniques for estimating $\overline{m_{coc}}$ in a multiple cell S-ALOHA system are presented. The first technique considers interference attributable to newly generated packets only, while the second technique uses an iterative approach to calculate the interference arising from both new as well as retransmitted cochannel cell packets. A new method of applying this latter technique, which is more efficient than previously proposed methods, is introduced.

5.3.1 Technique A: Estimation Based on Newly Arriving Traffic

A simple method for estimating the value of $\overline{m_{coc}}$ is to only consider the mean number of new packets generated by the cochannel interferers. Assuming that the number of data terminals per cell, M_d, is constant for all cells, and that the probability of generating a new data packet in a particular timeslot is l_d (given by (5.8)), then $\overline{m_{coc}}$ can be approximated by

$$\overline{m_{coc}} \approx L\, l_d\, M_d\,, \qquad \textbf{(5.9)}$$

where L is the number of cochannel cells assumed. In this thesis, L=6 is considered for outdoor cellular systems, while for in-building pico-cellular systems, L=2 is considered. This approach does not take into account interference originating from terminals which are retransmitting backlogged packets. This technique is, therefore, expected to be somewhat inaccurate in situations where the system is congested, as confirmed in §5.3.2.

5.3.2 Technique B: Estimation Based on Newly Arriving and Retransmitted Traffic

To more accurately model the expected number of cochannel interfering packets in a single timeslot, it is necessary to consider not only new packets, but also retransmitted packets. In order to determine this total inter-cell interference, an iterative technique has been developed [6]. This technique assumes that the system is homogeneous in so much as each cell experiences identical performance. Based on this assumption, it is reasonable to expect that, on average, an equal number of new and retransmitted packets would be produced in each cell in a given timeslot.

[1] It is likely that the Poisson probability distribution [5] could be used to model the variation of m_{coc} in a multiple cell S-ALOHA system. In this situation, the mean of the Poisson distribution would be given by $\overline{m_{coc}}$.

This means that a particular cell would produce the same average number of packets as it would receive from a single cochannel cell, as illustrated in Fig. 5.2.

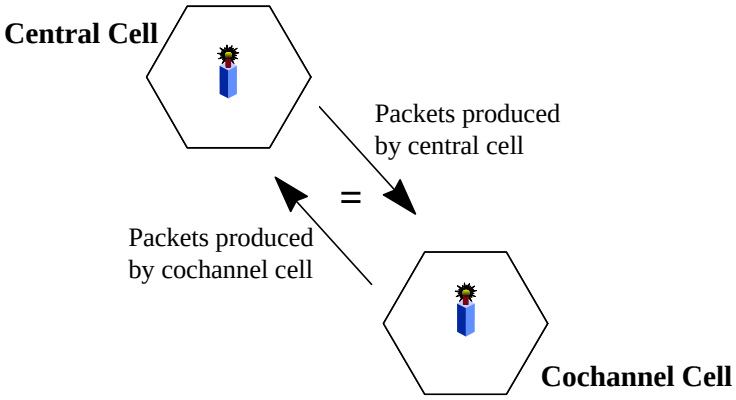

Figure 5.2: *Technique B assumes a homogeneous system whereby the central cell produces the same mean number of new and retransmitted packets per timeslot as it receives from a single cochannel interfering cell.*

Using this approach it is possible to calculate the mean number of cochannel packets produced in a timeslot as being L times the mean number of packets produced in the central cell, namely

$$\overline{m_{coc}} = L \cdot \sum_{m_{cen}=0}^{M_d} m_{cen} \Pr(m_{cen}) . \qquad \textbf{(5.10)}$$

The factor of L accounts for the L nearby cochannel cells and as with Technique A, L=6 and L=2 are assumed for cellular S-ALOHA and pico-cellular S-ALOHA systems, respectively. The summation on the r.h.s. of (5.10) represents the expectation of m_{cen} (i.e., the mean number of central cell packets transmitted per timeslot), where $\Pr(m_{cen})$ is the probability that m_{cen} central cell packets are transmitted per timeslot. $\Pr(m_{cen})$ can be described in terms of the state probability distribution, $\boldsymbol{\pi}(B)$, according to

$$\Pr(m_{cen}) = \sum_{B=0}^{M_d} \Pr(m_{cen}|B)\boldsymbol{\pi}(B) , \qquad \textbf{(5.11)}$$

so that (5.10) can be rewritten as

$$\overline{m_{coc}} - \Omega = 0 , \qquad \textbf{(5.12)}$$

where

$$\Omega = L \cdot \sum_{m_{cen}=0}^{M_d} m_{cen} \sum_{B=0}^{M_d} \Pr(m_{cen}|B)\boldsymbol{\pi}(B) . \qquad \textbf{(5.13)}$$

$\Pr(m_{cen}|B)$ is the probability of m_{cen} packets being produced by the M_d central cell terminals given that B of these terminals are in the re-transmission state. The m_{cen} packets are a combination of i re-transmitted packets and m_{cen}-i new packets such that,

$$\Pr(m_{cen}|B) = \sum_{i=0}^{m_{cen}} \binom{M_d - B}{m_{cen} - i} l_d^{m_{cen}-i} (1 - l_d)^{M_d - B - m_{cen} + i} \binom{B}{i} p_d^i (1 - p_d)^{B-i} \quad . \qquad \textbf{(5.14)}$$

In systems containing traffic hotspots, the assumption of an equal number of packets generated in each cell would not necessarily apply. This analysis, however, is limited to the situation where each cell is assumed to be supporting the same number of users, in which case the assumption is valid.

An iterative procedure is necessary to determine the value of $\overline{m_{coc}}$ which satisfies (5.12). This iterative procedure involves starting with an initial guess and computing step by step approximations of $\overline{m_{coc}}$. In this thesis, the Levenberg-Marquardt method [7] is employed. The following process is, therefore, used to calculate the value of $\overline{m_{coc}}$:

---

a) The iteration number is set to i=0.

b) An estimate of $\overline{m_{coc}}$, denoted $\overline{m_{coc\,i}}$, is provided. In the absence of any better initial estimate, $\overline{m_{coc\,0}}$, is calculated using (5.9).

c) The value of Ω_i, given by (5.13), is evaluated. This calculation requires the capture probability be determined using capture probability theory developed in Chapter 4[2]. In addition, it is also necessary to calculate the state probability distribution using the Markov theory presented in §5.2.

d) The error term, e_i, is determined according to,

$$e_i = \overline{m_{coc\,i}} - \Omega_i \,. \qquad \textbf{(5.18)}$$

e) If e_i is not within an acceptable error range, i is iterated to i= i+1. In addition, $\overline{m_{coc\,i}}$ is iterated to a new value (according to the Levenberg-Marquardt method) and steps *c)* and *d)* are repeated until the equality of (5.12) is satisfied.

f) The value of $\overline{m_{coc\,i}}$ that satisfies (5.12) (denoted by $\overline{m_{coc}}$) can then be used in the calculation of the S-ALOHA performance measures presented in §5.2.2.

Fig. 5.3 presents a comparison of the $\overline{m_{coc}}$ estimates obtained from Techniques A and B for an in-building (Building B) pico-cellular S-ALOHA system. The significant difference between the two techniques is due to Technique B considering both new and retransmitted cochannel

[2] This calculation also requires particular system and propagation parameter values to be included (e.g. cluster size, propagation pathloss exponent, shadowing standard deviation, etc.).

interfering packets, whereas Technique A only considers interference arising from new packets. Technique A appears to seriously underestimate the value of $\overline{m_{coc}}$, especially as M_d is increased.

The main disadvantage of Technique B is the increased complexity in computation, compared with Technique A. For each iteration, the capture probability and state probability distribution must be calculated, with a minimum number of iterations needed to obtain the required accuracy. A simple approach which reduces the need for multiple iterations is presented in the next section.

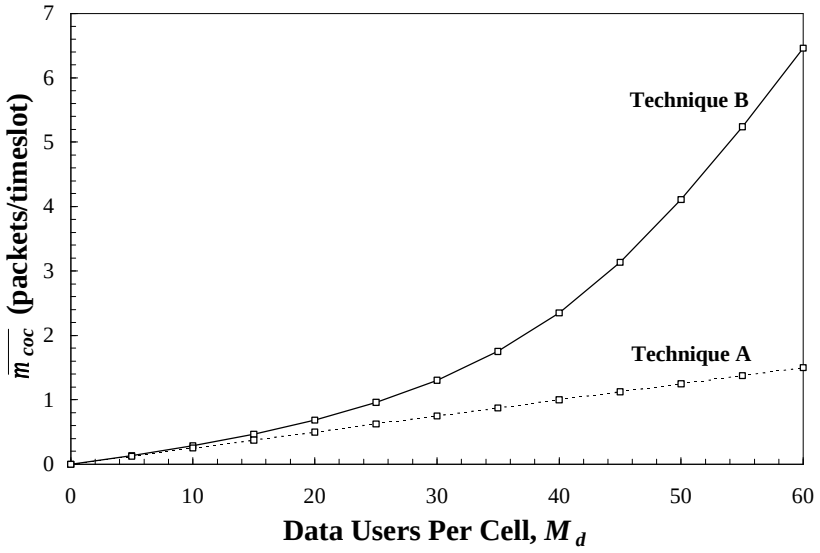

Figure 5.3: *Comparison of $\overline{m_{coc}}$ estimations in an in-building pico-cellular S-ALOHA system (Building B: San Ramon) with N_c =1, z=10 dB.*

5.3.3 Technique B: A More Efficient Approach

The iterative calculation of $\overline{m_{coc}}$ for M_d =5 and M_d =60 in Fig. 5.3, is presented in Fig. 5.4. It can be observed for both examples in Fig. 5.4 that $\overline{m_{coc\,i}}$ initially undergoes some fluctuation before converging to a final value. In the case of M_d =5 (Fig. 5.4(a)) the final estimation is given by $\overline{m_{coc}} = 0.1367$ while for M_d =60 (Fig. 5.4(b)) the final estimation is $\overline{m_{coc}} = 6.461$. An important aspect of Fig. 5.4(a) is that for all *i*,

$$\overline{m_{coc}} \approx \overline{m_{coc\,i}} + e_i \,, \qquad \textbf{(5.16)}$$

where $\overline{m_{coc}}$ represents the final estimation of inter-cell interference, and $\overline{m_{coc\,i}}$ is the value obtained after the *i*-th iteration of Technique B. The expression presented in (5.16) does not, however, agree with the results of Fig. 5.4(b). The reason for this is because the value of $\overline{m_{coc\,0}}$ (obtained from (5.9) and given by $\overline{m_{coc\,0}} = 1.5$) is a poor estimate of the final value ($\overline{m_{coc}} = 6.461$).

This means that only a single iteration may be required, as long as the initial estimate, $\overline{m_{coc\,0}}$, is accurate.

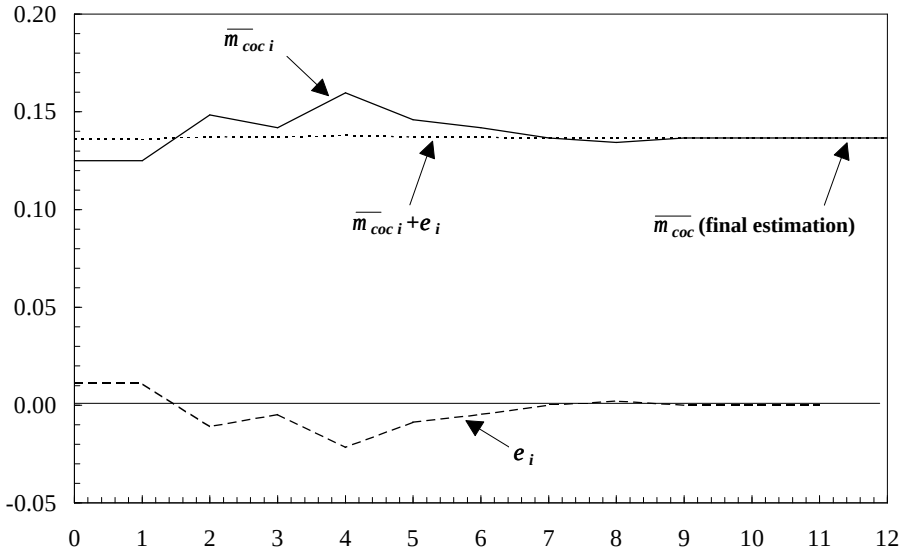

(a)

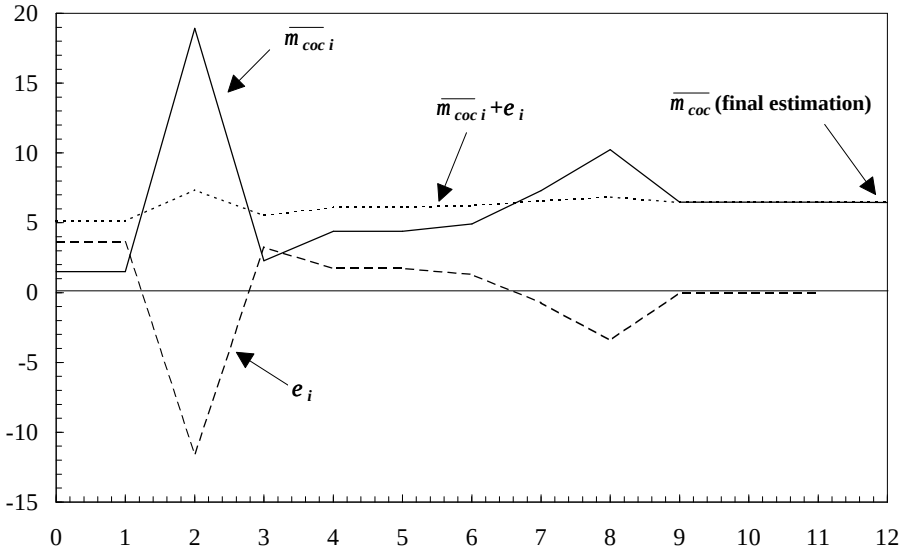

(b)

Figure 5.4: *Calculating $\overline{m_{coc}}$ using iterative process (Technique B, §5.3.2) for* **(a)** *M_d =5 and* **(b)** *M_d =60. N_c =1, z=10 dB. Building B (San Ramon) is considered.*

The value of $\overline{m_{coc\,0}}$, for a given value of M_d, can be improved by considering the value of $\overline{m_{coc}}$ estimated for previous values of M_d. This concept relies on the fact that a reasonably linear relationship exists between $\overline{m_{coc}}$ and M_d over any short interval of the curve in Fig. 5.3 (Technique B). This aspect allows, for example, the value of $\overline{m_{coc\,0}}$ for M_d=60, to be determined based on the values of $\overline{m_{coc}}$ estimated previously for M_d=50 and M_d=55. This particular example is illustrated in Fig. 5.5. The value of $\overline{m_{coc\,0}}$ at M_d=60 is calculated from a linear projection through the coordinates (50, $\overline{m_{coc}}|_{50}$) and (55, $\overline{m_{coc}}|_{55}$).

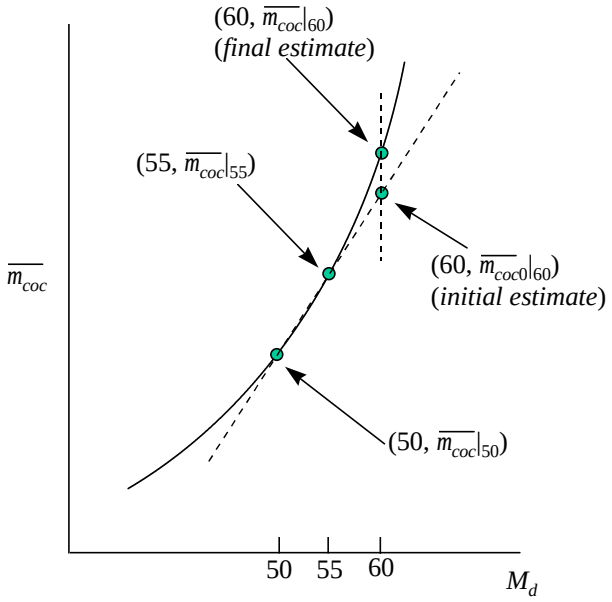

Figure 5.5: *Technique for estimating $\overline{m_{coc\,0}}$ at a particular value of M_d by linear extrapolation from previous calculated values of $\overline{m_{coc}}$ at other values of M_d.*

Assuming that M_d is incremented by 5 terminals/step (as considered in this thesis) then in general,

$$\overline{m_{coc\,0}}\Big|_{M_d} = \begin{cases} 0 & M_d = 0 \\ L\,l_d\,M_d & M_d = 5 \\ 2\overline{m_{coc}}|_{(M_d-5)} - \overline{m_{coc}}|_{(M_d-10)} & M_d = 5n \qquad n = 2,3\ldots \end{cases} \tag{5.17}$$

When M_d=5, the estimate of $\overline{m_{coc\,0}}$ is given by (5.9). In summary, the value of $\overline{m_{coc}}$ which satisfies (5.12) can be more efficiently calculated using the following approach:

a) The iteration number is set to i=0.

b) The initial estimate, $\overline{m_{coc\,0}}$, is calculated using (5.17). This estimate depends on the value of M_d considered.

c) The value of Ω_0, given by (5.13), is evaluated. This calculation requires the capture probability be determined using capture probability theory developed in Chapter 4. In addition, it is also necessary to calculate the state probability distribution using the Markov theory presented in §5.2.

d) The error term, e_0, is determined according to,

$$e_0 = \overline{m_{coc\,0}} - \Omega_0 . \qquad \textbf{(5.18)}$$

e) The final estimate of $\overline{m_{coc}}$ is calculated according to (5.16).

5.4 Computer Simulation Techniques

In addition to determining the performance of multiple cell S-ALOHA systems from Markov analysis, Monte Carlo computer simulations have also been employed. The results obtained from these simulations may be used to validate the Markov analysis results. The simulation results may also be used to examine aspects of the system, which are otherwise too difficult to determine using Markov analysis. This latter aspect will be explained in further detail in Chapters 6 and 7, where Monte Carlo computer simulations will be used to determine the floor-wide performance variations in several in-building PRMA speech systems.

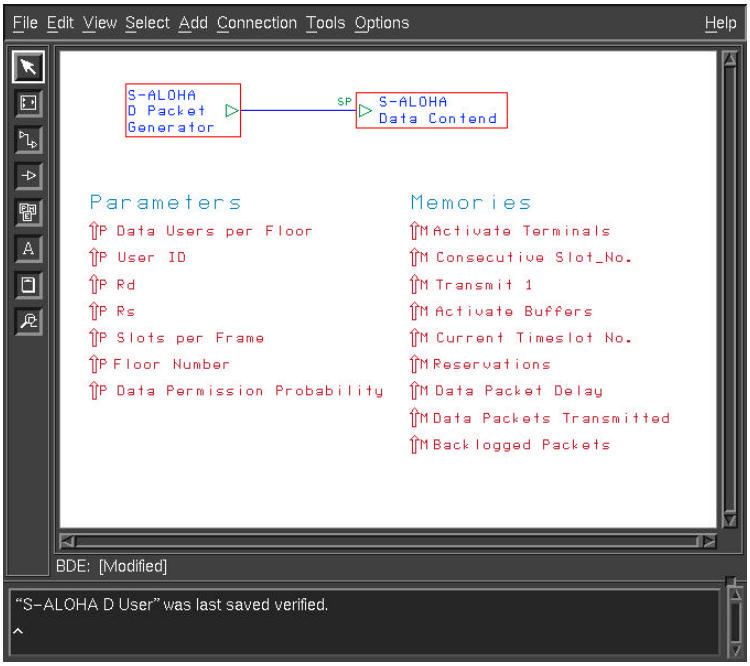

Figure 5.6: *An example of BONeS® Designer©.*

The simulations have been performed using the BONeS® DESIGNER™ software package[3]. BONeS® is designed for modeling and simulating complex communication networks. It provides a graphical environment for modeling a network in terms of its topology, traffic, data (packet) structures and protocol functions. BONeS® translates the network model into a C program, executes an event driven Monte Carlo simulation, computes performance measures, and displays the results graphically. A window from a BONeS® network simulation is illustrated in Fig. 5.6.

Both outdoor cellular and in-building pico-cellular S-ALOHA systems have been simulated using the BONeS® simulation language. These simulations represent realistic scenarios whereby packets transmitted in one cell cause interference to nearby cochannel cells. Two simulation models have been considered in the study of these multiple cell systems. These models are outlined in the following subsections.

5.4.1 Model I : No Cell Wraparound

This model is somewhat simplistic in that not all cells have the same number of cochannel interfering cells surrounding them. This is illustrated in Fig. 5.7 for the outdoor cellular and in-building pico-cellular systems. As this model only considers the first tier of cochannel cells, there is an uneven number of packets transmitted between the central cell and any one of the cochannel cells. For example, in the case of the outdoor cellular system (Fig. 5.7(a)), the central cell receives interference from six nearby cells, whereas a cochannel cell only receives interference from three cells. The effect of this approximation is most noticeable in the case of N_c =1, where high levels of interference occur.

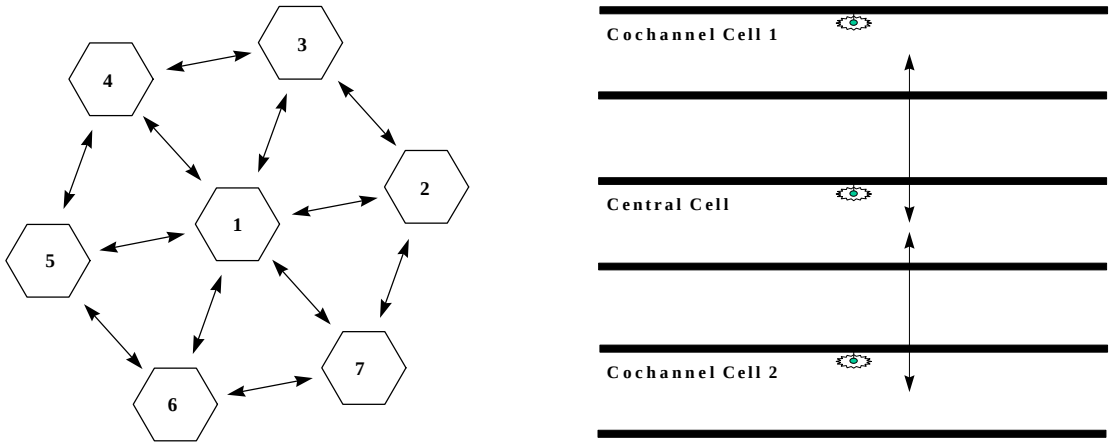

Figure 5.7: *Inter-cell interference patterns considered in Model I simulations of an* **(a)** *outdoor cellular and* **(b)** *in-building pico-cellular S-ALOHA system. Arrows indicate cells which cause interference to each other. The performance of the central cell is evaluated.*

[3] BONeS is an acronym for Block Orientated Network Simulator.

5.4.2 Model II: Cell Wraparound

More accurate results can be obtained by extending the Monte Carlo simulation to include a second tier of cochannel cells, however, this represents a significant increase in the simulation complexity. An alternative approach is to 'wrap' the interference pattern around, so that cells on opposite sides of the central cell interact with each other. This technique is illustrated in Fig. 5.8. For example, in Fig. 5.8(a), cell 4 causes interference to cells 5, 1 and 3 by virtue of the fact that they are nearby cochannel cells. In addition, however, cell 4 is used to represent some of the interference received by cells 6, 7 and 2.

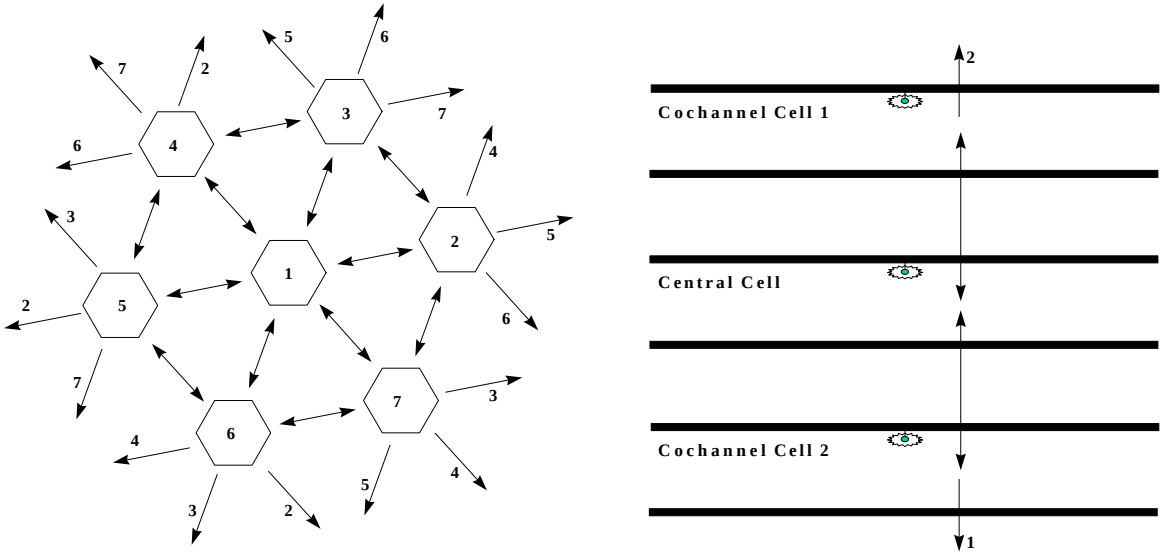

Figure 5.8: *Inter-cell interference patterns considered in Model II simulations of an* **(a)** *outdoor cellular and* **(b)** *in-building pico-cellular S-ALOHA system. Arrows indicate cells which cause interference to each other. The performance of the central cell is evaluated.*

5.4.3 Simulation of Systems with Small Cluster Sizes

The previous simulation models do not consider all possible interdependencies between cells. For example, in the in-building system considered in Fig. 5.8(b), cochannel cell 1 would cause some interference to cochannel cell 2. This is especially true for systems with smaller cluster sizes. In these situations it may be necessary to consider additional cell interdependencies, as illustrated in Fig. 5.9.

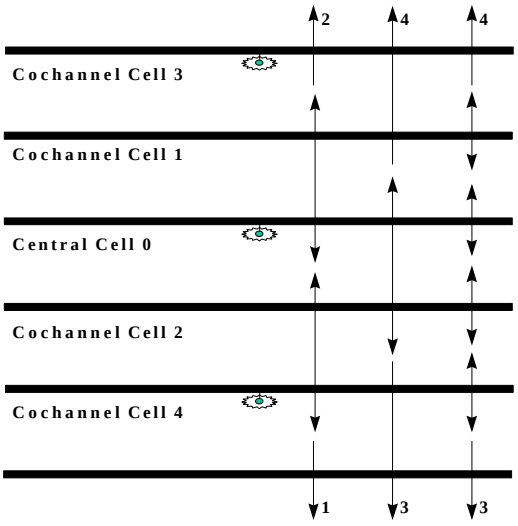

Figure 5.9: *In situations where small cluster sizes are considered (e.g., N_c =1), it may be necessary to include additional interdependencies between cells.*

5.5 Performance of Outdoor Cellular S-ALOHA

In this section, the performance of S-ALOHA in an outdoor cellular system is determined. Analytical results obtained from the Markov analysis are compared to those obtained from Monte Carlo simulations. Clusters sizes of N_c=1, 3 and 4 are considered. It is assumed that a total system channel bit rate, R_{sys}=426.66 kb/s is partitioned amongst the N_c cells per cluster. The system parameters for these various frequency reuse configurations were presented in Table 4.1. Each data terminal is assumed to generate information randomly with an average bit rate of R_d=4800b/s. This information is packetised into I=576 bit packets and appended with an H=64 bit header. A packet retransmission probability, p_d=0.1, is assumed in all cases. The packet generation rate, l_d, for a timeslot of length t is assumed to be given by (5.8).

The propagation parameters chosen in this analysis have a significant influence on the final performance estimates obtained. It is therefore important to estimate the performance for a range of possible operating conditions. In this analysis, a capture ratio, z=10 dB, together with a shadowing standard deviation of s =6 dB and a pathloss exponent of b =4 are considered as median parameters in an outdoor cellular environment. In addition, however, values of z=6 and 14 dB, s =0 and 12 dB and b =3 and 5 are investigated so as to determine the influence of these propagation parameters.

5.5.1 Comparison of Markov and Simulation Techniques

Before the performance of S-ALOHA in an outdoor cellular environment can be determined, it is necessary to compare the results obtained from the various analytical techniques and simulation models proposed in §5.3 and §5.4. This comparison will identify what technique(s) are best suited to particular situations. In Fig. 5.10, the throughput and data packet delay of an outdoor cellular S-ALOHA system are presented. A comparison between the results obtained from Markov analyses based on Techniques A and B are simulations based on Model I and II, are

presented. It is assumed that the system under consideration has N_c=3 cells per cluster and that all packets experience Suzuki fading.

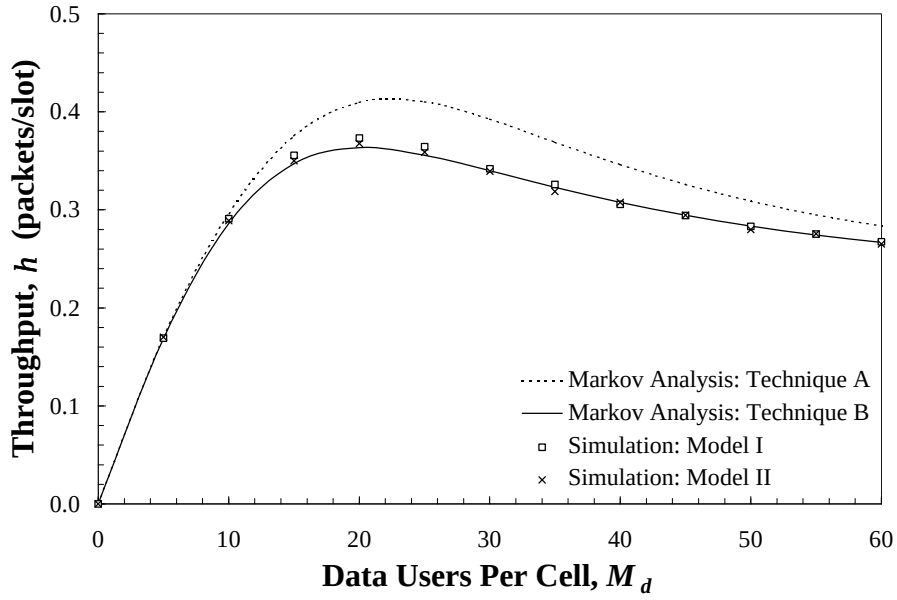

(a)

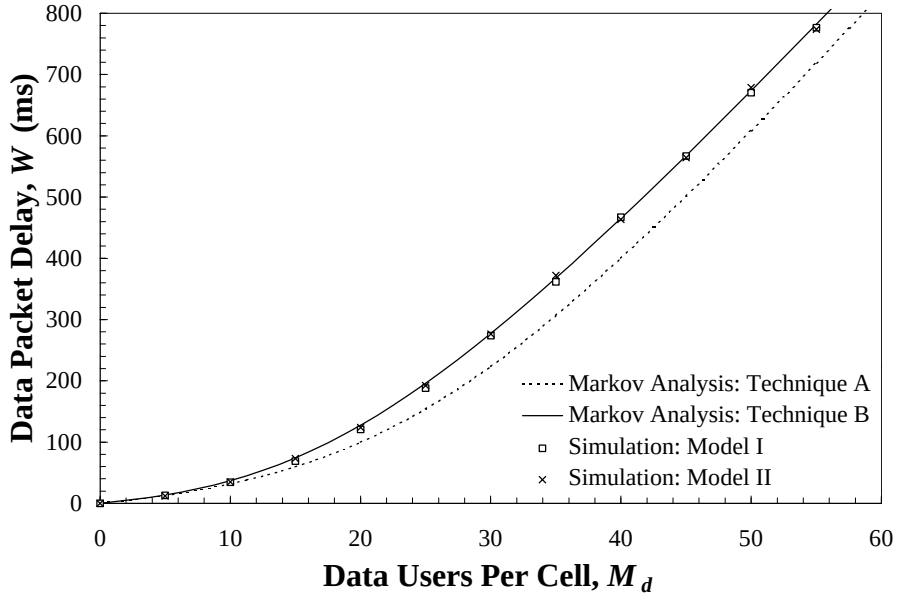

(b)

Figure 5.10: (a) *Throughput per cell and* **(b)** *data packet delay of an outdoor cellular S-ALOHA system with N_c=3. A Suzuki fading channel is considered with s =6 dB, b =4, z=10 dB.*

It can be observed from Fig. 5.10 that there is a significant difference between the results obtained from the two Markov analysis techniques. The computer simulation results obtained from Simulation Model I and II tend to support the Markov analysis results based on Technique

B. Technique A appears to be inadequate in accurately predicting the value of inter-cell interference. This is because the estimation is based only on the amount of newly arriving traffic, with no consideration given to traffic generated from packet retransmissions, as with Technique B. The results of Fig. 5.11 are based on the same system that was considered in Fig. 5.10, although instead of considering N_c=3, a cluster size of N_c=1 is considered. In this situation the disparity between the two Markov analysis techniques is increased considerably. In addition, it can be observed that Simulation Model I becomes increasingly inaccurate in this situation.

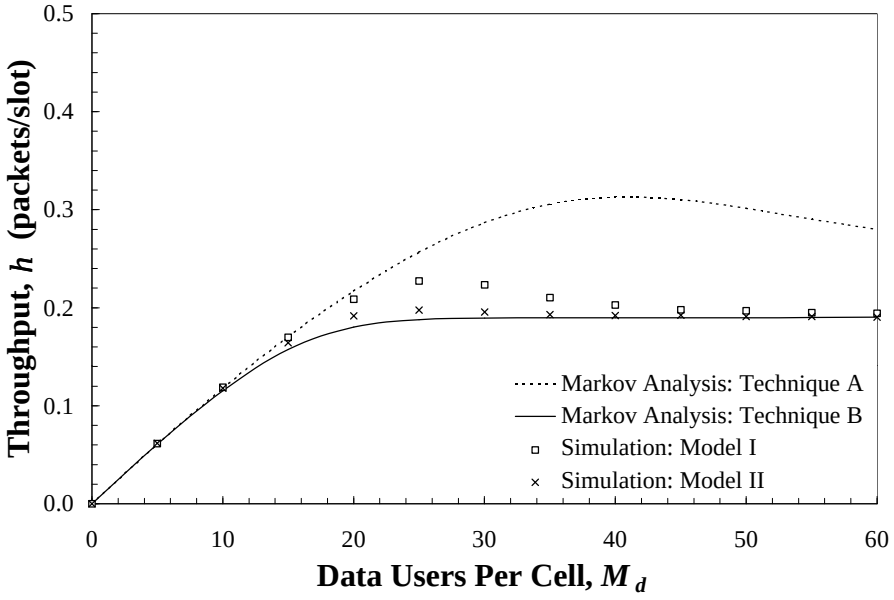

(a)

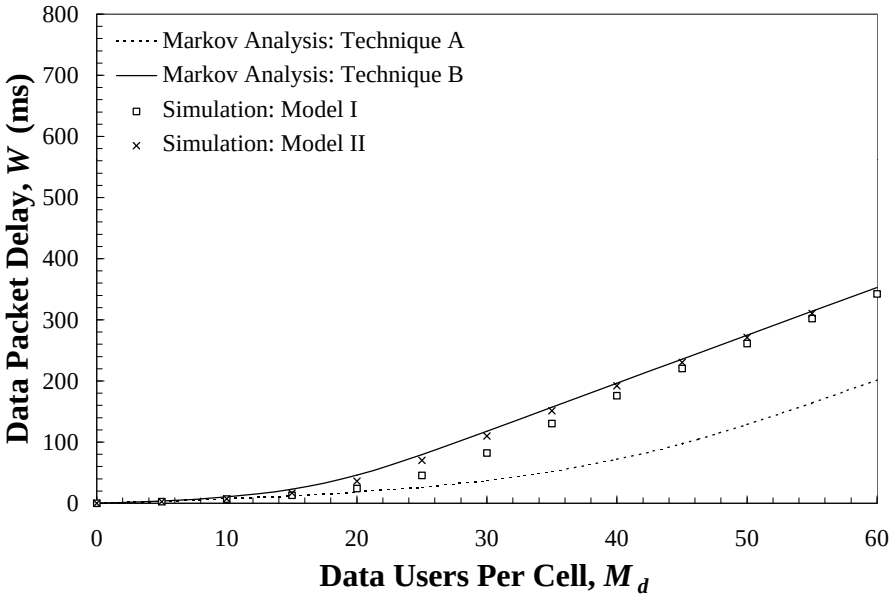

(b)

Figure 5.11: (a) *Throughput per cell and* **(b)** *data packet delay of an outdoor cellular S-ALOHA system with N_c=1. A Suzuki fading channel is considered with s =6 dB, b =4, z=10 dB.*

It appears clear, therefore, that Markov analysis based on Technique B (§5.3.2-§5.3.3) and Monte Carlo simulation based on Simulation Model II (§5.4.2) are the most accurate methods for estimating the performance of outdoor cellular S-ALOHA systems. These methods have also been found to be the most accurate in predicting the performance of in-building pico-cellular S-ALOHA systems. These methods are used throughout the remainder of this chapter.

5.5.2 Single Cell Versus Multiple Cell Performance

The majority of S-ALOHA systems that have been analysed in the published literature have only considered the performance of single-cell, interference-free S-ALOHA systems. This thesis, on the other hand, considers the performance of S-ALOHA in interference limited multiple cell systems. It is useful to compare the performance of these two types of S-ALOHA systems, especially as the performance of S-ALOHA in a single cell represents an upper bound on the performance of multiple cell S-ALOHA systems. The difference between single cell and multiple cell S-ALOHA performance can be attributed to the influence of cochannel interference in the multiple cell environment.

Fig. 5.12 presents the throughput per cell for systems with and without cochannel interference (CCI). The system parameters for the various cluster sizes considered were presented previously in Table 4.1. Suzuki fading is assumed in all cases with s =6 dB, b =4 and z=10 dB. It is clear from Fig. 5.12 that the performance of S-ALOHA is significantly degraded in an outdoor cellular system, compared to an idealised single cell system. This is especially true in the case of N_c=1, where the cochannel interferers are closer to the central cell base station. As the cluster size is increased, the difference in performance of single and multiple cell systems is reduced.

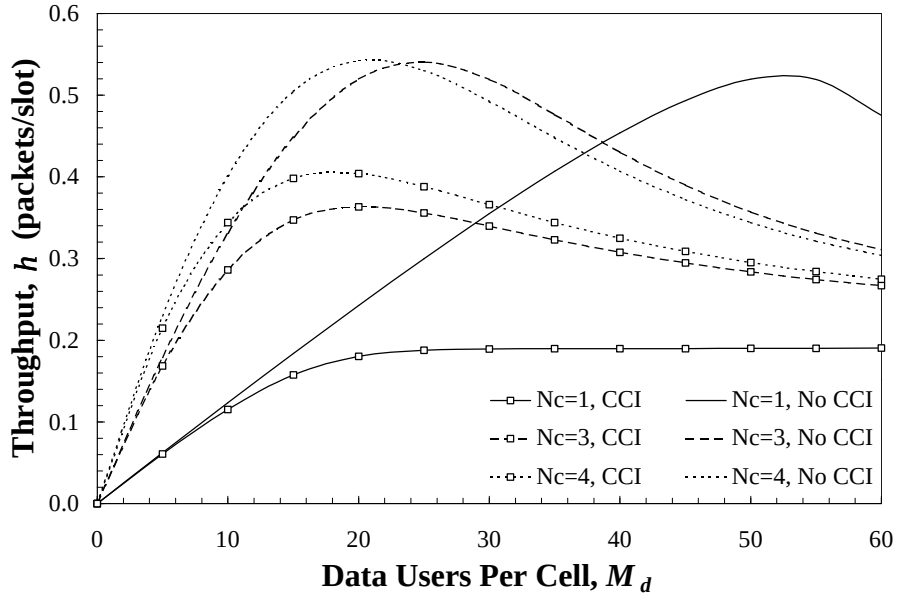

Figure 5.12: *Throughput per cell of single cell and multiple cell (N_c=1, 3 and 4) outdoor S-ALOHA systems. Suzuki fading is considered with s =6 dB, b =4, z=10 dB.*

As M_d is increased in Fig. 5.12, the throughput per cell approaches a limit determined by the limit of the capture probability, $U(m_{cen}, \overline{m_{coc}})$. The limiting value of $U(m_{cen}, \overline{m_{coc}})$ for a pathloss exponent of b=4 is given by (4.32), while for an arbitrary pathloss exponent, the limit is determined by (4.33).

5.5.3 Determination of Optimum Frequency Reuse Plan

According to Fig. 5.12, the optimum throughput per cell for a system with cochannel interference was achieved when N_c=4. This is, however, not necessarily the best choice of frequency plan. Rather, the following points need to be considered:

1. Assuming a fixed allocation of frequency spectrum, systems with N_c=1 have more timeslots per unit time than systems with N_c=3 or N_c=4. This means that small cluster size systems provide more opportunities for terminals to transmit their packets, and hence, the potential to support higher user densities.
2. Smaller cluster sizes, however, suffer more significantly from cochannel interference. This causes more packets to suffer corruption and, hence, require retransmission. The consequence of this is that the throughput of the system is likely to be reduced.

A tradeoff exists, therefore, between the amount of bandwidth allocated to a cell and the resulting throughput. The results in this section present a cost-benefit analysis of these two aspects. The optimum frequency reuse plan may be determined by studying the system utilisation, y, which was given in (4.35). This performance measure is given by the throughput per cell, h, divided by the cluster size, N_c.

Fig. 5.13(a) presents the system utilisation for an outdoor cellular S-ALOHA system with N_c=1, 3, and 4. In this example, a Suzuki fading channel is considered with s =6 dB, b =4 and z=10 dB. It is clear from Fig. 5.13(a) that optimum system utilisation is obtained by allocating the entire bandwidth to each cell (i.e., complete frequency reuse). In addition, it is clear from Fig. 5.13(b) that complete frequency reuse provides the lowest data packet delay of the three frequency plans considered. While a small cluster size leads to increased level of cochannel interference, and therefore, more packet retransmissions, this aspect is outweighed by the significant increase in the number of timeslots per cell which results. When N_c=1, more timeslots are available to terminals, compared to the case where N_c=3 or N_c=4[4], so that packet retransmission does not impose a serious level of congestion on the system.

The same findings are presented in Fig. 5.14 for the case where shadowing is neglected (s = 0 dB, i.e., Rayleigh fading). In particular, a cluster size of N_c=1 produces the optimum system utilisation and data packet delay in a Rayleigh fading environment. Similar findings were presented in [8] for CDPA (Capture Division Packet Access) where it was found that complete frequency reuse, together with random packet retransmission to abate cochannel interference, was more effective than spatial isolation of cells using the same channel, as is usual in FDMA/TDMA systems.

[4] Assuming that the total available system bandwidth is constant.

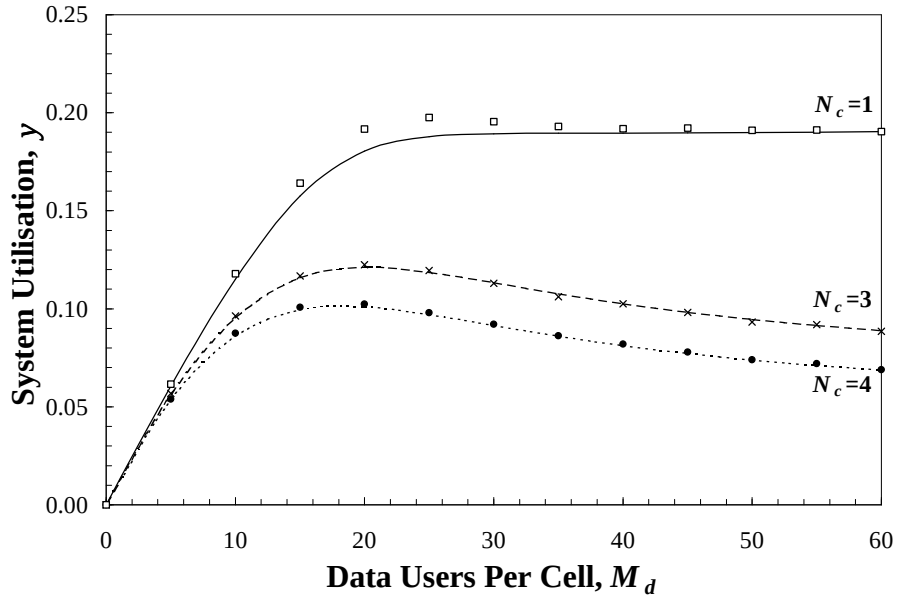

(a)

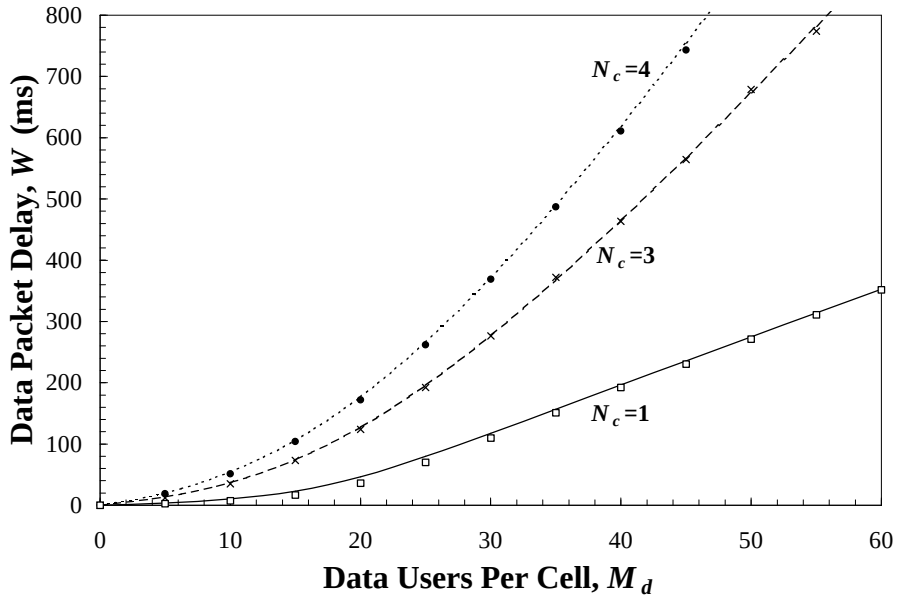

(b)

Figure 5.13: (a) *System utilisation and* **(b)** *data packet delay of an outdoor cellular S-ALOHA system with cluster sizes N_c=1, 3, and 4. A Suzuki fading channel is considered with σ_s =6 dB, b =4, σ_z=10 dB. Markov analysis results (lines) and simulation results (points) are presented.*

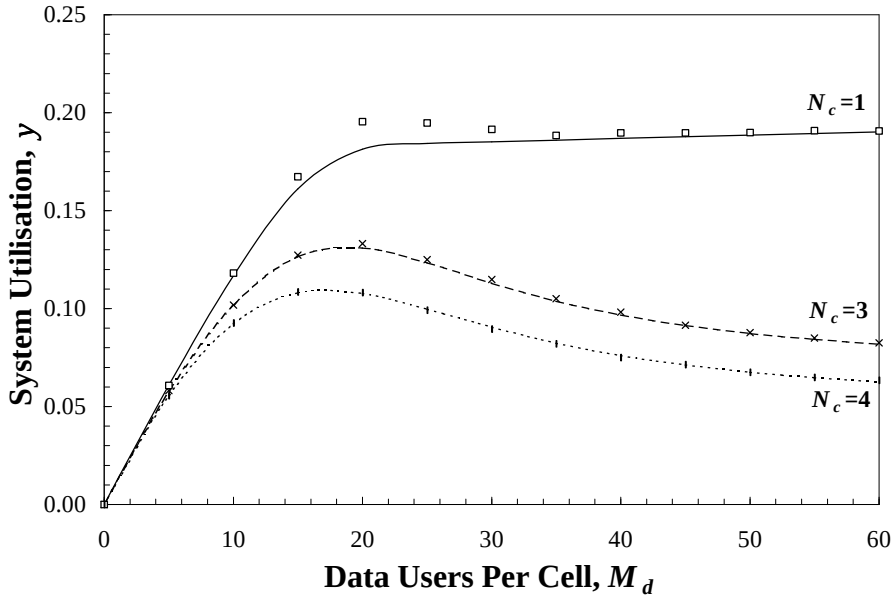

(a)

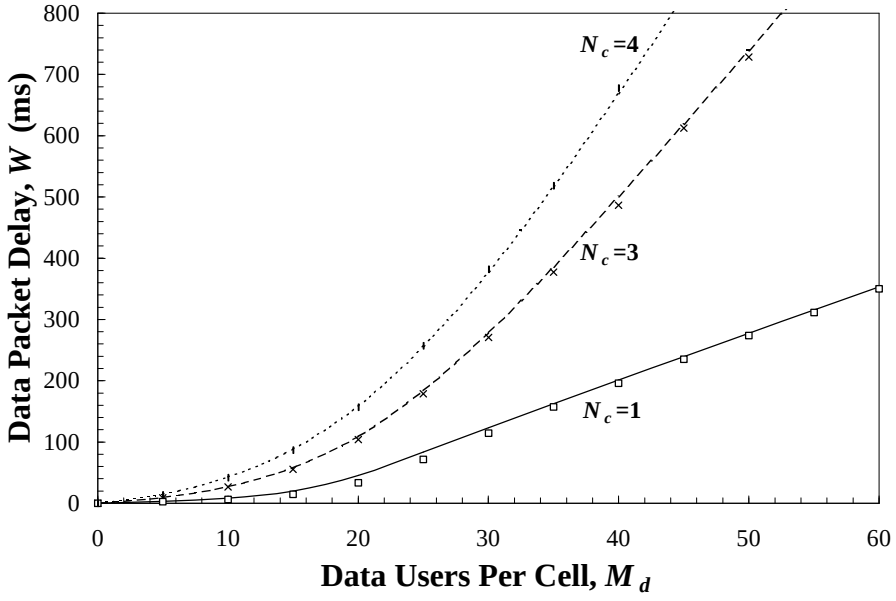

(b)

Figure 5.14: (a) *System utilisation and* **(b)** *data packet delay of an outdoor cellular S-ALOHA system with cluster sizes N_c=1, 3, and 4. A Rayleigh fading channel is considered with b =4, z=10 dB. Markov analysis results (lines) and simulation results (points) are presented.*

5.5.4 Effect of System and Propagation Parameters

Of interest to system planners is the influence that system and propagation parameters have on the performance of a multiple cell S-ALOHA system. Fig. 5.15 compares the performance of an outdoor cellular S-ALOHA system with N_c=3 for various values of the pathloss exponent, b. It is clear from Fig. 5.15 that the pathloss exponent has a significant effect on the performance of

the system, with a higher pathloss exponent resulting in a better performance due to an increased isolation between cochannel cells.

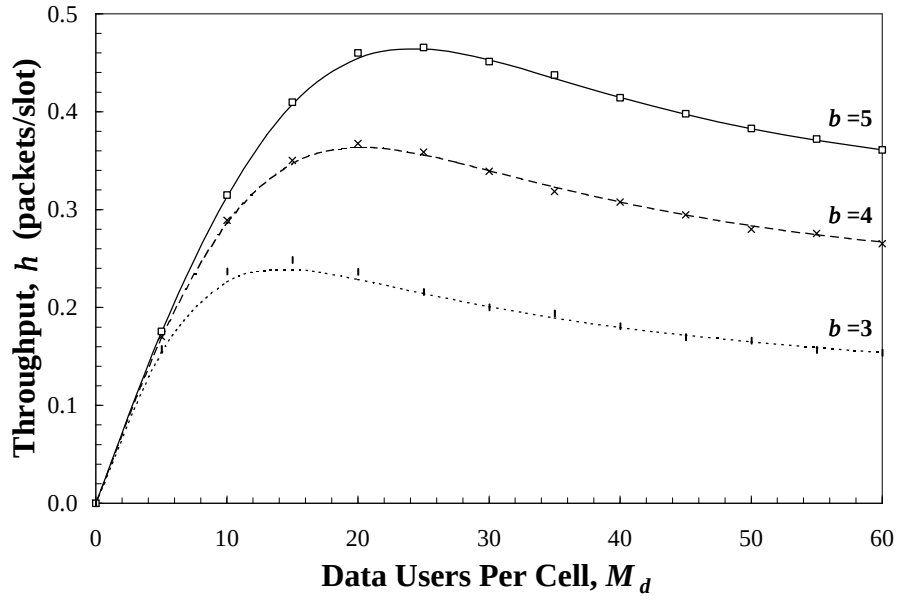

(a)

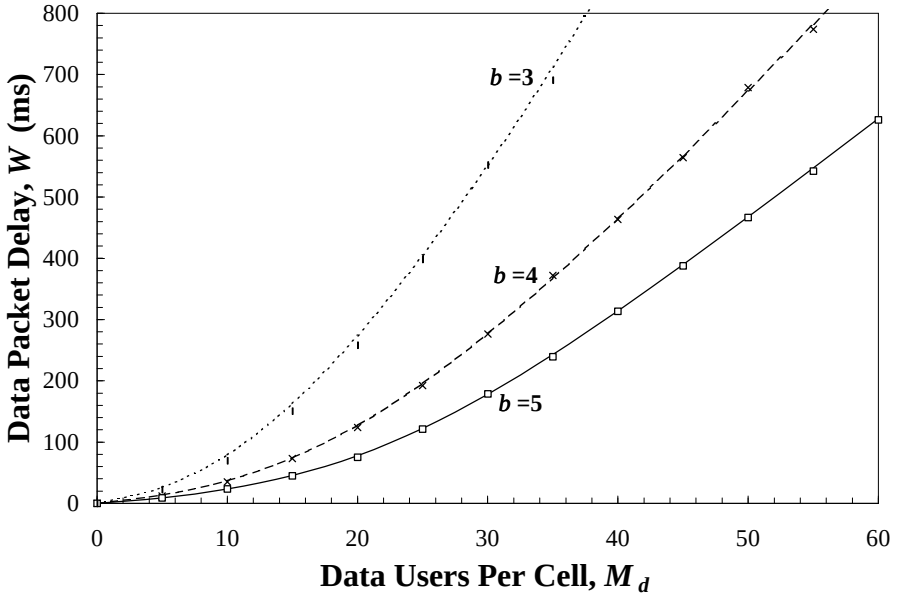

(b)

Figure 5.15: (a) *Throughput per cell and* **(b)** *data packet delay for a multiple cell S-ALOHA system (N_c=3) with pathloss exponent b =3, 4, and 5. s =6 dB and z=10 dB in all cases. Markov analysis results (lines) and simulation results (points) are presented.*

Fig. 5.16 compares the performance of an outdoor cellular S-ALOHA system for various values of the capture ratio, *z*. Like the pathloss exponent, the capture ratio has a significant effect on the performance, with a low capture ratio resulting in an improved throughput and delay response.

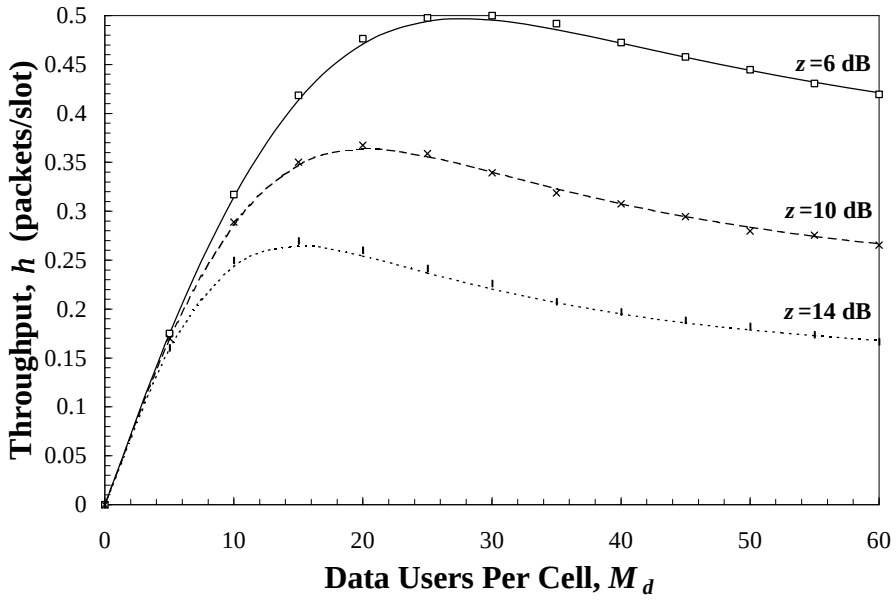

(a)

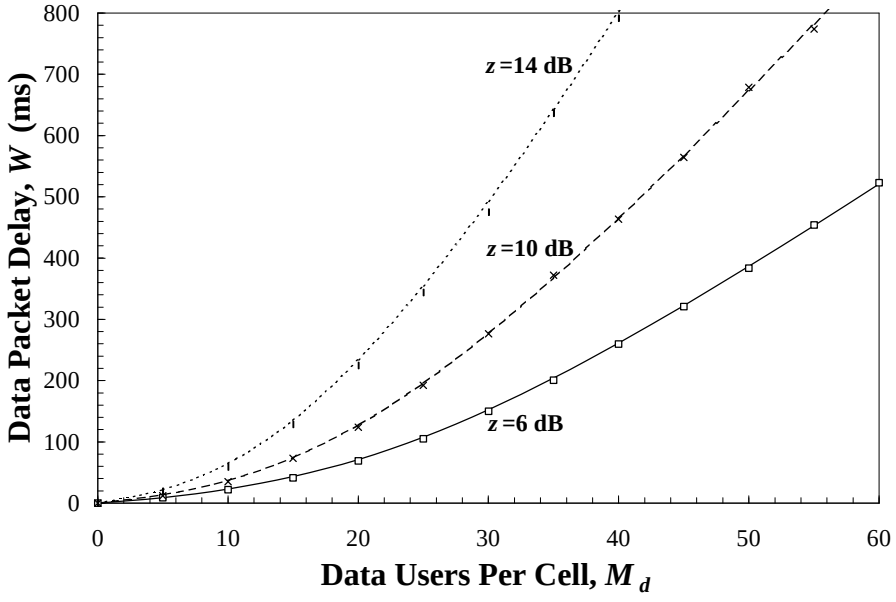

(b)

Figure 5.16: (a) *Throughput per cell and* **(b)** *data packet delay for a multiple cell S-ALOHA system (N_c=3) with capture ratio z=6, 10 and 14 dB. b =4 and s =6 dB in all cases. Markov analysis results (lines) and simulation results (points) are presented.*

Fig. 5.17 compares the performance of an outdoor cellular S-ALOHA system with N_c=3 for various values of the lognormal shadowing standard deviation, s . This parameter does not have the same influence on system performance that parameters such as b and z have. This is contrary to the findings of [9] where shadowing was found to have a considerable effect on the performance of a single cell S-ALOHA system.

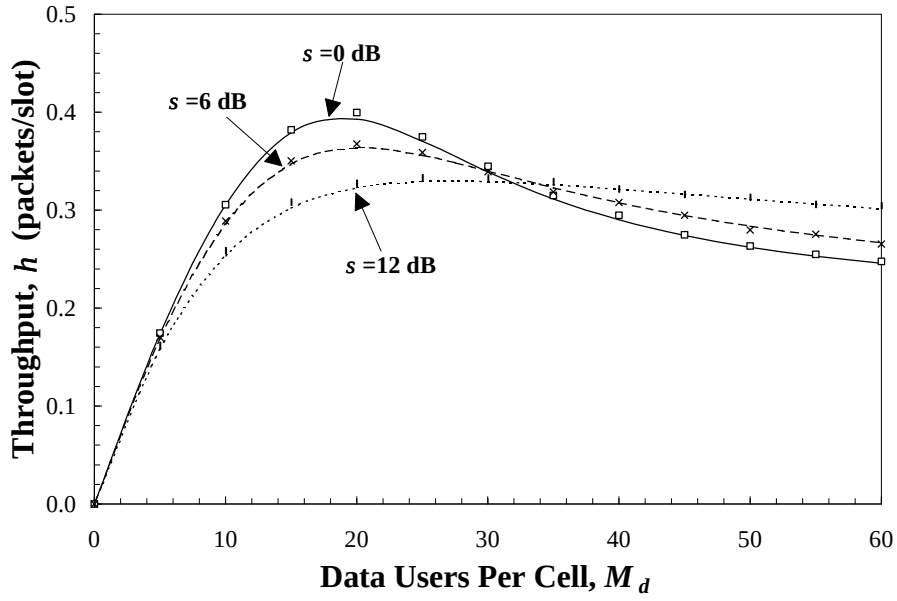

(a)

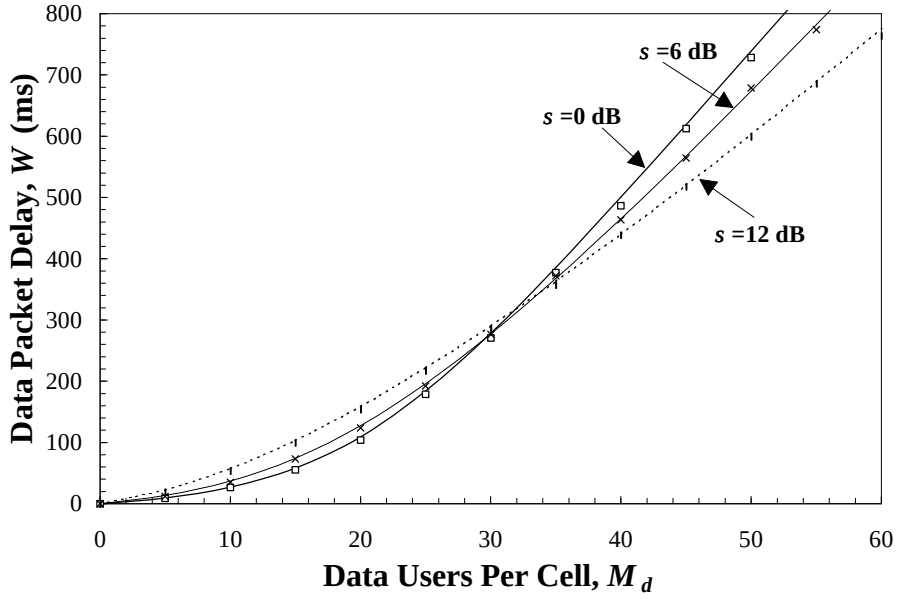

(b)

Figure 5.17: (a) *Throughput per cell and* **(b)** *data packet delay for a multiple cell S-ALOHA system (N_c=3) with shadowing standard deviation s =0, 6, and 12 dB. b =4 and z=10dB in all cases. Markov analysis results (lines) and simulation results (points) are presented.*

From Fig. 5.17, the peak throughput in a heavily shadowed environment is lower than the peak throughput in a shadow-free (i.e. s =0 dB) environment. This is due to the variability of the composite inter-cell interference power being smaller with Rayleigh fading, thus, the composite inter-cell interference is less likely to exceed the desired signal. In the overload region, optimum throughput is achieved with Suzuki fading.

5.5.5 System Stability

In Fig. 5.18 the dynamic behaviour of both single cell and multiple cell (N_c=3) S-ALOHA systems is presented for various propagation models in terms of the expected drift, $\Delta(n)$. A population of M_d=100 data terminals per cell is assumed. The parameters used in [4] for a single cell analysis are also used here in the case of curves (a), (b) and (d). In particular, values of p_d=0.08 and l_d =0.0055 are considered. Curves (c) and (e) are an extension of (b) and (d) to a multiple cell environment. The network is expected to operate in a state near an equilibrium point, i.e., where the expected drift crosses zero with negative derivative [1]. For example, in the case where a single cell without capture is considered (curve (a)), the steady state operation is found at a backlog of nearly B=100 terminals (i.e. all terminals are backlogged). The curves (b) and (d) in Fig. 5.18 for single cell systems with Rayleigh fading and Suzuki fading, respectively, both show a single, almost identical equilibrium at approximately B=6 backlogged data terminals. For the traffic parameters chosen here, network stability is not degraded in operating S-ALOHA in a cellular environment (curves (c) and (e)), in so much as there is still only one equilibrium point. However, by operating S-ALOHA in a cellular environment, the equilibrium point will be moved to the right of the single cell equilibrium point, meaning that there will be a greater fraction of terminals in the retransmission state.

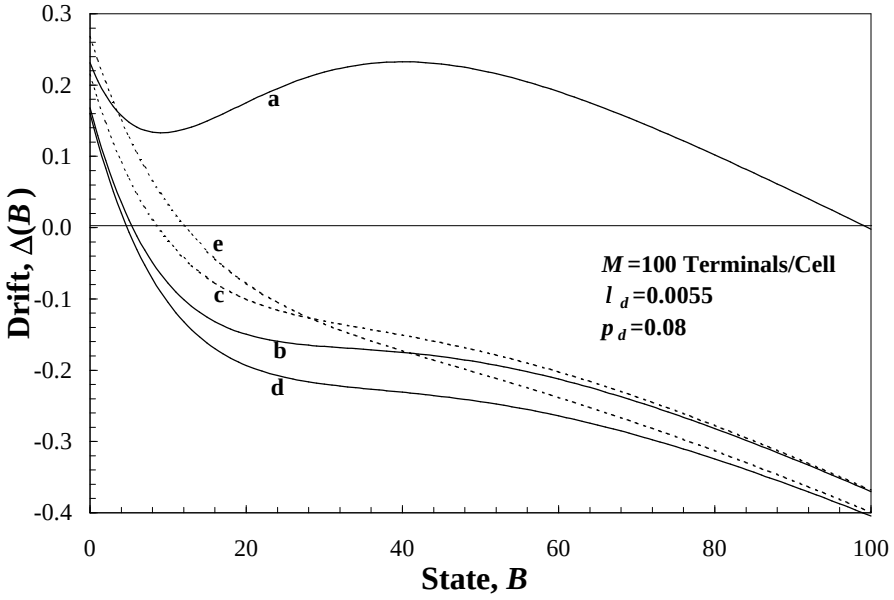

Figure 5.18: *Expected drift for single cell and multiple cell (N_c=3) systems. z=6dB, b =4 in all cases.* **(a)** *single cell, no capture,* **(b)** *single cell, Rayleigh fading,* **(c)** *multiple cell, Rayleigh fading,* **(d)** *single cell, Suzuki fading (s =6dB),* **(e)** *multiple cell, Suzuki fading (s =6dB).*

5.6 Performance of In-Building Pico-Cellular S-ALOHA

In this section, the performance of S-ALOHA in in-building pico-cellular systems is determined. Consideration is given to S-ALOHA systems operating in the four buildings presented previously in Table 3.3. Analytical results obtained from the Markov analysis (Technique B, §5.3.2-§5.3.3) are compared to those obtained from Monte Carlo simulations (Model II, §5.4.2). The same system parameter values considered for outdoor cellular S-ALOHA (§5.5) are considered in this section. In particular, the total system channel bit rate, R_{sys}=426.66 kb/s is assumed to be partitioned amongst the N_c cells per cluster. Clusters sizes of N_c=1, 2, 3 and 4 are considered. Each data terminal is assumed to generate information randomly with an average bit rate of R_d=4800b/s. This information is packetised into I=576 bit packets and appended with a H=64 bit header. A packet retransmission probability, p_d=0.1, is assumed in all cases. The packet generation rate, l_d, for a timeslot of length t is assumed to be given by (5.8). A number of the findings in §5.5, derived for an outdoor cellular S-ALOHA system, also apply to an in-building pico-cellular S-ALOHA system. In particular, the effect of the pathloss exponent, capture ratio and lognormal shadowing standard deviation on system performance is similar in both systems.

In this section, the performance variations that exist from one building to another are identified. Figs. 5.19-5.22 present the system utilisation and data packet delay for Buildings A-D, respectively. The relevant propagation parameter values for these building were presented in Table 3.3. In all cases, a capture ratio of z=10dB is considered. It is evident from Figs. 5.19-5.22 that a cluster size, N_c=1, is optimum for in-building S-ALOHA systems, as was the situation for outdoor cellular S-ALOHA systems. The results presented in Figs. 5.19-5.22 indicate that, for all the buildings considered, the most significant difference exists between cluster sizes N_c=1 and N_c=2. The performance reduction incurred in going from N_c=1 to N_c=2 is generally larger than the performance reduction that occurs in going from N_c=2 to N_c=3. This trend is most noticeable with respect to Building B in Fig. 5.20.

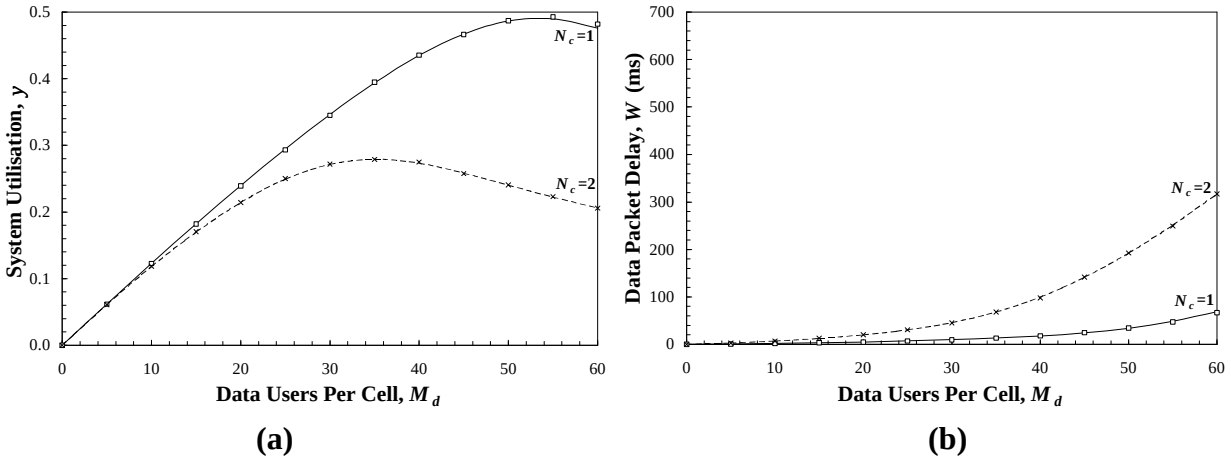

Figure 5.19: (a) *System utilisation and* **(b)** *data packet delay of S-ALOHA system in Building A: Walnut Creek. N_c=1, 2 and z=10dB. Markov analysis results (lines) and simulation results (points) are presented.*

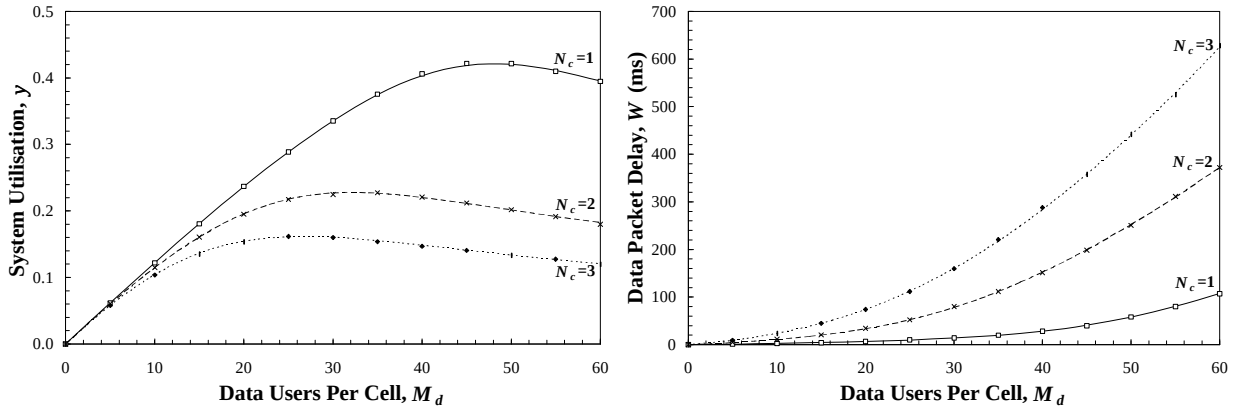

(a) **(b)**

Figure 5.20: (a) *System utilisation and* **(b)** *data packet delay of S-ALOHA system in Building B: San Ramon. N_c=1, 2 and z=10dB. Markov analysis results (lines) and simulation results (points) are presented.*

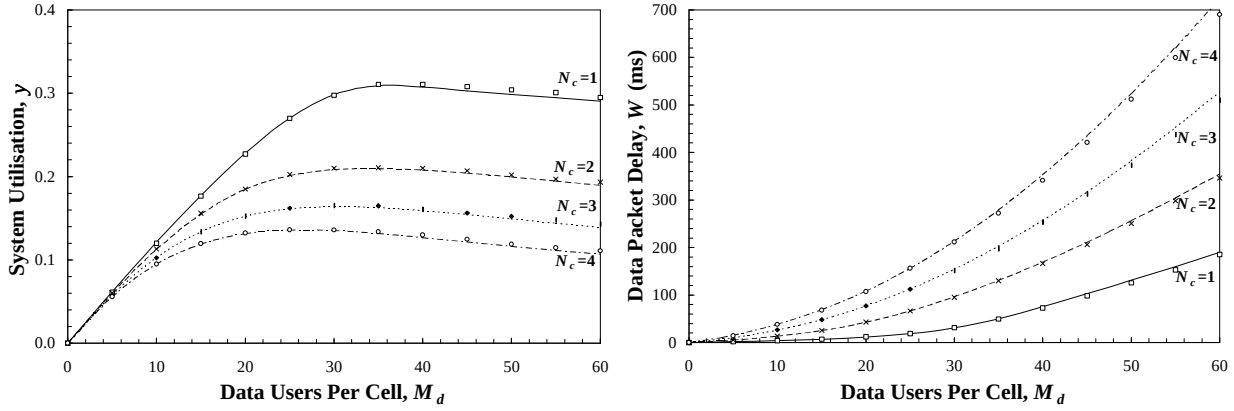

(a) **(b)**

Figure 5.21: (a) *System utilisation and* **(b)** *data packet delay of S-ALOHA system in Building C: SF PacBell. N_c=1, 2 and z=10dB. Markov analysis results (lines) and simulation results (points) are presented.*

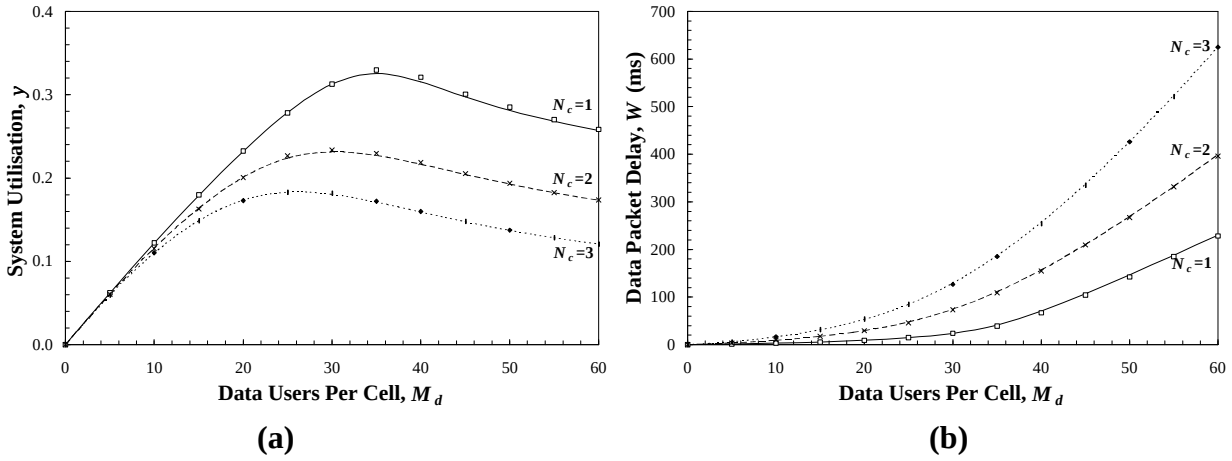

Figure 5.22: (a) *System utilisation and* **(b)** *data packet delay of S-ALOHA system in Building D: Engineering Tower. N_c=1, 2 and z=10dB. Markov analysis results (lines) and simulation results (points) are presented.*

Fig. 5.23 compares the system utilisation of in-building pico-cellular S-ALOHA systems in Buildings A-D. In all situations, it is assumed that complete frequency reuse (i.e. N_c=1) is employed and that z=10 dB. The highest system utilisation occurs in Building A (Walnut Creek), followed by Building B (San Ramon). Buildings C (SF PacBell) and D (Engineering Tower) experience the worst performance. The performance estimates obtained with each building are significantly different. It is likely that the most important cause of this variation is the unique propagation conditions of the buildings involved.

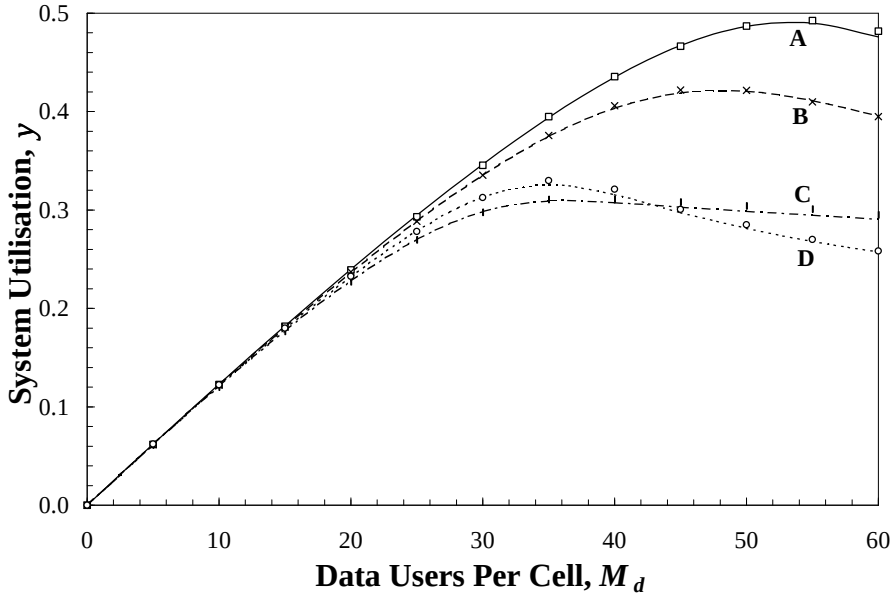

Figure 5.23: *Comparison of system utilisation for in-building pico-cellular S-ALOHA systems in Buildings A-D. N_c=1 and z=10dB in all cases.*

5.7 Summary

In this chapter the performance of both outdoor cellular and in-building pico-cellular S-ALOHA data systems have been determined using Markov analysis and computer simulations. The Markov analysis employed to model the multiple cell S-ALOHA systems is based on a Markov analysis developed previously for use with single cell S-ALOHA systems. This analysis incorporates the effect of cochannel cells, using an estimating of the number of cochannel interfering packets per timeslot, $\overline{m_{coc}}$, received by the central cell base station.

Several techniques for estimating $\overline{m_{coc}}$ have been proposed in this chapter. The most accurate technique (Technique B, §5.3.2) assumes that the multiple cell S-ALOHA system is homogeneous in so much as each cell experiences identical performance. Using this assumption, the average number of new and retransmitted packets produced by cochannel interferers may be determined via an iterative approach. In §5.3.3, a more efficient method for estimating $\overline{m_{coc}}$ using Technique B, was developed. This more efficient method allows the iterative process of Technique B to be eliminated, while still providing highly accurate results. Excellent agreement between Markov analysis and computer simulation results has been obtained, providing confidence in the analytical techniques developed.

Optimum system utilisation, in both outdoor cellular and in-building pico-cellular systems, is achieved when each cell uses all of the available bandwidth (N_c=1, i.e., complete frequency reuse). While this leads to an increased level of cochannel interference, and therefore, more packet retransmissions, this aspect is outweighed by the significant increase in the number of timeslots per cell which results. It should be noted, however, that the performance of a multiple cell S-ALOHA system with N_c=1, is still significantly poorer than that of an identical single cell S-ALOHA system.

While the capture effect has been shown to greatly improve the throughput, delay and stability of S-ALOHA in a single cell system, the improvement in a multiple cell system may not be dramatic, depending on the propagation conditions. Optimum performance is obtained in a multiple cell environment which has a high pathloss exponent, low shadowing variability and with base station receivers which can operate with a low capture ratio. Significant variations in performance have been observed in the in-building S-ALOHA systems considered.

References

[1] C. Namislo, “Analysis of mobile radio slotted ALOHA networks,” *IEEE J. Selected Areas Commun.*, vol. 2, no. 4, Jul. 1984, pp. 583 - 588.

[2] A. B. Carleial, M. E. Hellman, “Bistable behavior of ALOHA-type systems,” *IEEE Trans. Commun.*, vol. 23, no. 4, Apr. 1975, pp. 401 - 409.

[3] L. Kleinrock, S. S. Lam, “Packet switching in a multiaccess broadcast channel: performance evaluation,” *IEEE Trans. Commun.*, vol. 23, no. 4, Apr. 1975, pp. 410 - 422.

[4] C. van der Plas, J. P. M. G. Linnartz, “Stability of mobile slotted ALOHA network with Rayleigh fading, shadowing, and near-far effect,” *IEEE Trans. Veh. Technol.*, vol. 39, no. 4, Nov. 1990, pp. 359 - 366.

[5] L. Kleinrock, *Queueing Systems Volume I: Theory*. John Wiley & Sons, 1975.

[6] M. D. Orange, K. W. Sowerby, A. J. Coulson, “Markov analysis of an outdoor S-ALOHA system with frequency reuse,” *in Proc. 7th Virginia Tech/MPRG Symposium on Wireless Personal Communications*, Blacksburg, Virginia, Jun. 1997, pp. 13-1 - 13-12.

[7] W. H. Press, B. P. Flannery, S. A. Teukolsky, W. T. Vetterling, *Numerical Recipes, The Art of Scientific Computing.* Cambridge University Press.

[8] F. Borgonovo, L. Fratta, M. Zorzi, A. Acampora, "Capture division packet access: a new cellular access architecture for future PCNs," *IEEE Commun. Mag.*, vol. 34, no. 9, Sep. 1996, pp. 154 - 162.

[9] A. U. H. Sheikh, Y.-D. Yao, X. Wu, “The ALOHA systems in shadowed mobile radio channels with slow or fast fading,” *IEEE Trans. Veh. Technol.*, vol. 39, no. 4, Nov. 1990, pp. 289 - 298.

Chapter 6

Multiple Cell PRMA Speech Systems

6.1 Introduction

In the previous chapter the performance of S-ALOHA in various multiple cell systems was determined. Unlike S-ALOHA, which caters purely for data traffic, PRMA is capable of supporting both speech and data traffic. Previously published research into PRMA has normally considered its performance in a single cell, simple channel system. In this chapter, the performance of various multiple cell, variable channel, speech-only PRMA systems are determined from Markov analysis and computer simulations. Base stations in such a system receive packets from not only terminals within their cell, but also interfering packets from terminals operating in cochannel cells, resulting in a reduced system performance. In this chapter, the performance of both outdoor cellular and in-building picocellular PRMA speech systems are determined. Cochannel interference is handled by the PRMA speech terminals according to Scenario A in Table 4.4. In particular, when a reserved speech packet is corrupted by cochannel interference, it is assumed that the terminal which transmitted the packet retains it's reservation. It is assumed, however, that the corrupted packet is not retransmitted. This approach is taken with the view to minimising additional interference to other terminals, which would be caused if the packet was to be retransmitted. The merit of such an approach will be determined in this chapter. The systems considered in this chapter do not incorporate selection diversity.

In §6.2 the Markov analysis of a multiple cell PRMA speech system without retransmission is presented. This Markov analysis incorporates capture probability expressions, which allow both outdoor cellular and in-building pico-cellular scenarios to be considered. These capture probability expressions were developed previously in Chapter 4. As with the Markov analysis of Chapter 5 (multiple cell S-ALOHA), the Markov analysis of multiple cell PRMA requires an estimate of the mean inter-cell interference received at the central cell base station. Several techniques for estimating the amount of inter-cell interference in a multiple cell PRMA system are presented in §6.3. Details of the computer simulation models employed in the study of multiple cell PRMA systems are described in §6.4, with special consideration given to the simulation model used to determine the location dependent performance variations of in-building PRMA systems.

Results are presented in §6.5 and §6.6 in terms of the speech packet dropping probability, speech packet interference probability, total packet loss probability, throughput per cell and system utilisation. These results are presented with respect to both outdoor cellular and in-building pico-cellular PRMA systems. The difference in performance between single cell and multiple cell PRMA systems is determined, with the findings indicating that considerable differences exist between these types of systems. The frequency reuse plan which results in optimum system performance in a multiple cell PRMA system is determined. The findings indicate, however, that no single choice of cluster size is capable of providing optimum performance in all situations. The effect that different path loss exponents, capture ratios and shadowing standard deviations

have on the performance of multiple cell PRMA systems is determined. In addition the location dependent performance of such systems is calculated.

6.2 Markov Analysis

Markov analysis has frequently been used to analyse single cell PRMA systems [1-6]. The operation of single cell PRMA systems was reviewed extensively in Chapter 2. In this section the Markov analysis used for single cell systems is extended to consider multiple cell PRMA. This extension is implemented using an approach similar to that employed in Chapter 5 for S-ALOHA. In particular, the analysis does not explicitly consider the operation of all cells within the multiple cell system. Rather, the analysis only considers the operation of terminals in the central cell. An estimate of the mean number of inter-cell interfering packets, $\overline{m_{coc}}$, received at the central cell base station from cochannel interfering terminals is incorporated into the Markov analysis of the central cell. By applying this approach, it is possible to determine the performance of the multiple cell PRMA system. Two methods of estimating $\overline{m_{coc}}$ in a multiple cell PRMA system will be presented in §6.3. The procedure followed in the Markov analysis is illustrated in Fig. 6.1. Initially, the possible state transitions which can occur at each individual speech terminal are identified, together with the relevant probability expressions. It is then possible to consider the overall system and determine the one-step state transition probability, $\pi(i, j|C, R)$. From $\pi(i, j|C, R)$, the state probability distribution, $\pi(C, R)$, can be calculated. With knowledge of the state probability distribution, the relevant PRMA performance measures may be evaluated.

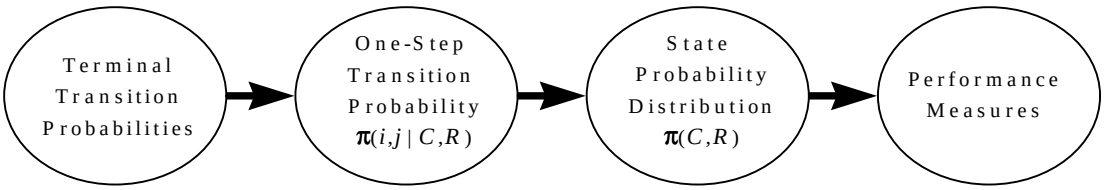

Figure 6.1: *Procedure to complete Markov analysis.*

Before establishing a Markov model, the following definitions are necessary. Let M_s be the number of speech terminals per cell in the PRMA system. C, R, and S are the number of terminals in contention (*CON*), reservation (RES_i $0 \le i \le N-1$) and silent (*SIL*) states at the t-th timeslot, respectively, within the central cell. C, R, and S are random variables in the set of $\{0,1,...,M_s\}$, $\{0,1,...,N\}$ and $\{0,1,...,M_s\}$ respectively, and

$$C + R + S = M_s . \qquad \textbf{(6.1)}$$

6.2.1 Terminal Transition Probabilities

An individual speech terminal can be modeled by the N+2 state Markov chain of Fig. 6.2 with states *SIL*, *CON*, and RES_i ($0 \le i \le N-1$) [7]. This Markov chain is based around the slow speech activity model, which was presented in §2.2.1, and assumes that the speech terminal does not perform retransmissions. With reference to Fig. 6.2, it is possible to denote the seven events, listed in Table 6.1, which may occur at the t-th timeslot at any terminal.

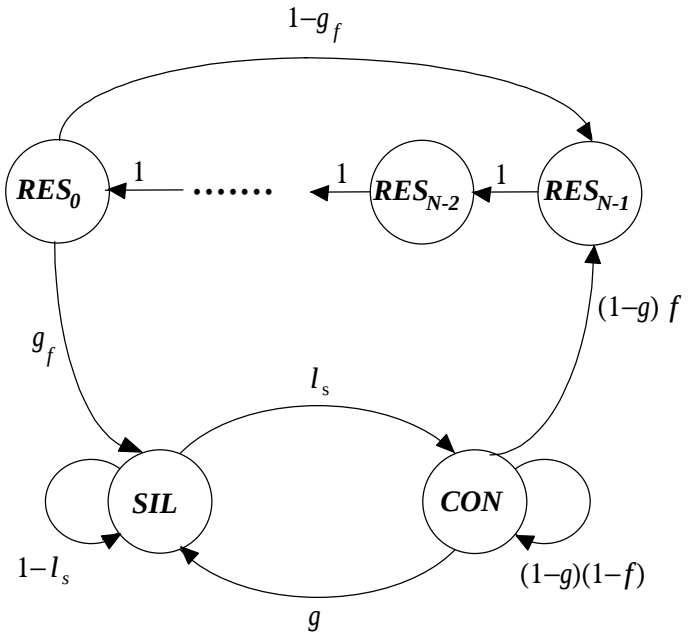

Figure 6.2: *PRMA speech terminal model (no packet retransmissions).*

Event	Transition		Probability
	From	To	
SC	*SIL*	*CON*	l_s
SS	*SIL*	*SIL*	$1-l_s$
CS	*CON*	*SIL*	g
CR	*CON*	RES_{N-1}	$(1-g)f$
CC	*CON*	*CON*	$(1-g)(1-f)$
RS	RES_0	*SIL*	g_f
RR	RES_0	RES_{N-1}	$1-g_f$

Table 6.1: *Terminal events and associated probabilities.*

The probability of an *SC* transition is given by (2.2), namely

$$l_s = 1-\exp(-t/t_2)\,, \qquad \textbf{(6.2)}$$

where t_2 is the mean duration of a silent gap, and t is the duration of a timeslot in seconds. Likewise the probability of a *CS* transition can be obtained using (2.3), namely

$$g = 1-\exp(-t/t_1)\,. \qquad \textbf{(6.3)}$$

The term g was previously defined as the probability of a principal talkspurt with mean duration t_1 seconds ending in a timeslot of duration t seconds. This transition implies that if a talkspurt ends before the terminal obtains a reservation, the terminal stops contending.

In order for a speech terminal to undergo a *CR* transition, the users talkspurt must not end and the user must be successful in obtaining a reservation for the current slot. The probabilities of these events are $(1-g)$ and f, respectively. The probability, f, of a particular user obtaining a reservation for the current slot requires that the following three conditions be simultaneously met:

1) the timeslot must be available;
2) the speech terminal must have permission (p_s) to transmit and;
3) the speech terminal must be successful in capturing the receiver.

The probability that a timeslot is available is given by (1-*R*/*N*), where *R* is the number of terminals in the RES_i states and *N* is the number of timeslots per frame. The probability, f, is therefore

$$f = \left(1-\frac{R}{N}\right) p_s \sum_{t=0}^{C-1} \binom{C-1}{t} p_s^t (1-p_s)^{C-1-t} q(t+1, \overline{m_{coc}}), \qquad \textbf{(6.4)}$$

where *C* is the number of terminals in the *CON* state and $q(t+1, \overline{m_{coc}})$ is the probability of a central cell speech terminal capturing the central cell base station in the presence of t intra-cell interferers and $\overline{m_{coc}}$ inter-cell interferers. In this context, $\overline{m_{coc}}$ is the mean number of inter-cell interfering packets received per timeslot. The appropriate capture probability theory for determining $q(t+1, \overline{m_{coc}})$ in both outdoor cellular and in-building pico-cellular systems was developed in Chapter 4. The probability of a *RS* transition is given by

$$g_f = 1-(1-g)^N \ . \qquad \textbf{(6.5)}$$

Since $\gamma << 1$, it is possible to approximate (6.5) as

$$g_f \approx Ng \ . \qquad \textbf{(6.6)}$$

6.2.2 The One-Step State Transition Probability

Having determined the possible states and associated transition probabilities of a PRMA speech terminal, it is possible to consider the operation of the central cell, which consists of M_s speech terminals. At any particular instant in time, there will be a certain number of terminals in each of the *N*+2 possible, states such that (6.1) is satisfied. Assuming M_s to be time invariant, the system vector $\{C, R, S\}$ is determined when any two of *C*, *R*, or *S* are determined. Without loss of generality, the vector $\{C, R\}$ is selected to serve as the state description.

Before the state probability distribution, $\pi(C,R)$, can be calculated, it is necessary to calculate the one-step state transition probability distribution, $\pi(i,j|C,R)$, defined as the probability of going from system state $\{C_t = C, R_t = R\}$ to $\{C_{t+1} = i, R_{t+1} = j\}$. The one-step state transition probability distribution can be determined by considering the following details:

1) If there are *R* terminals holding reservations in the *t*-th timeslot, then in the (*t*+1)-th timeslot, there will be either *R*+1, *R*, or *R*-1 terminals holding reservations, because only one terminal can lose or receive a reservation in a timeslot.
2) Likewise, if there are *C* terminals in the contention (*CON*) state in the *t*-th timeslot, there will be either $C+x-y-1$ or $C+x-y$ terminals in *CON* in the (*t*+1)-th timeslot. The former case corresponds to *x SC*, *y CS* and one *CR* transitions occuring, whereas the latter case corresponds to *x SC*, *y CS* and no *CR* transitions occuring. The events *SC*, *CS* and *CR* were described previously in §6.2.1.

It is, therefore, possible to list the changes to the system state {*C*,*R*} which can occur in progressing from one timeslot to the next, as follows:

$$\{C,R\} \rightarrow \begin{cases} \{i = C+x-y-1,\ j = R+1\} \\ \{i = C+x-y,\ j = R\} \\ \{i = C+x-y,\ j = R-1\} \end{cases} \qquad 0 \le x \le S,\ 0 \le y \le C \tag{6.7}$$

The situations where the events *SC* and *CS* occur at two or more terminals in the same timeslot are not considered in this thesis. Rather, only those situations where $x \in [0,1]$ and $y \in [0,1]$ are considered. The probability of no *SC* transitions is given by

$$noSC = (1-l_s)^S \approx 1 - Sl_s, \tag{6.8}$$

where l_s is the probability of a single terminal going from the *SIL* to *CON* states and *S* in the number of terminals in the *SIL* state. The corresponding probability of one *SC* transition is, therefore,

$$oneSC = 1 - noSC = Sl_s. \tag{6.9}$$

In a similar fashion, the probability of no *CS* transitions is given according to

$$noCS = (1-g)^C \approx 1 - Cg, \tag{6.10}$$

where g is the probability of a single terminal going from the *CON* to *SIL* states and *C* is the number of terminals in the *CON* state, while the probability of one *CS* transition is defined as

$$oneCS = 1 - noCS = Cg. \tag{6.11}$$

These assumptions, which were made previously in [5], allow the one-step state transition probability distribution to be accurately estimated, although at a significantly reduced complexity. Under these circumstances, $\pi(i, j|C, R)$ is given by,

$$\pi(i, j|C, R) =$$

$$\begin{cases}
\Pr(oneCS, noSC, oneCR) & i = C-2 \quad j = R+1 \\
\Pr(noCS, noSC, oneCR) + \Pr(oneCS, oneSC, oneCR) & i = C-1 \quad j = R+1 \\
\Pr(noCS, oneSC, oneCR) & i = C \quad j = R+1 \\
\Pr(oneCS, noSC, noRS) + \Pr(oneCS, noSC, noCR) & i = C-1 \quad j = R \\
\Pr(noCS, noSC, noRS) + \Pr(oneCS, oneSC, noRS) & \\
+ \Pr(noCS, noSC, noCR) + \Pr(oneCS, oneSC, noCR) & i = C \quad j = R \\
\Pr(noCS, oneSC, noRS) + \Pr(noCS, oneSC, noCR) & i = C+1 \quad j = R \\
\Pr(oneCS, noSC, oneRS) & i = C-1 \quad j = R-1 \\
\Pr(noCS, noSC, oneRS) + \Pr(oneCS, oneSC, oneRS) & i = C \quad j = R-1 \\
\Pr(noCS, oneSC, oneRS) & i = C+1 \quad j = R-1 \\
0 & elsewhere
\end{cases} \tag{6.12}$$

The symbol *noX* in (6.12) means that event *X* does not occur in the next timeslot, while *oneX* means that event *X* happens at one terminal in the next timeslot. The complete expansion of (6.12) is presented in Appendix B. The expressions presented in Appendix B are unique, in that the one-step state transition probability distribution for a multiple cell speech-only PRMA system with receiver capture has not been presented previously in the published literature.

6.2.3 The State Probability Distribution

From the one-step state transition probability distribution, $\pi(i, j|C, R)$, it is possible to derive the state probability distribution, $\pi(C, R)$, which is the probability of having *C* terminals in the *CON* state and *R* terminals in the RES_i states. $\pi(C, R)$ can be obtained by solving the following set of simultaneous linear equations [8],

$$\pi(i, j) = \sum_{R=0}^{N} \sum_{C=0}^{M_s - R} \pi(i, j|C, R)\pi(C, R), \tag{6.13}$$

$$\sum_{j=0}^{N} \sum_{i=0}^{M_s - j} \pi(i, j) = 1. \tag{6.14}$$

In order to solve these linear equations, standard Gaussian elimination or *LU* decomposition techniques can be employed. An example of a state probability distribution, obtained from a multiple cell PRMA system, is presented in Fig. 6.3. The particularly congested system is assumed to have M_s=60 speech terminals per cell, supported by N=8 timeslots per cell. From Fig. 6.3, it can be observed that the system is most likely to have 6-8 terminals with reservations, 16-20 terminals seeking reservations (i.e. in the *CON* state), and the remainder in the silent state.

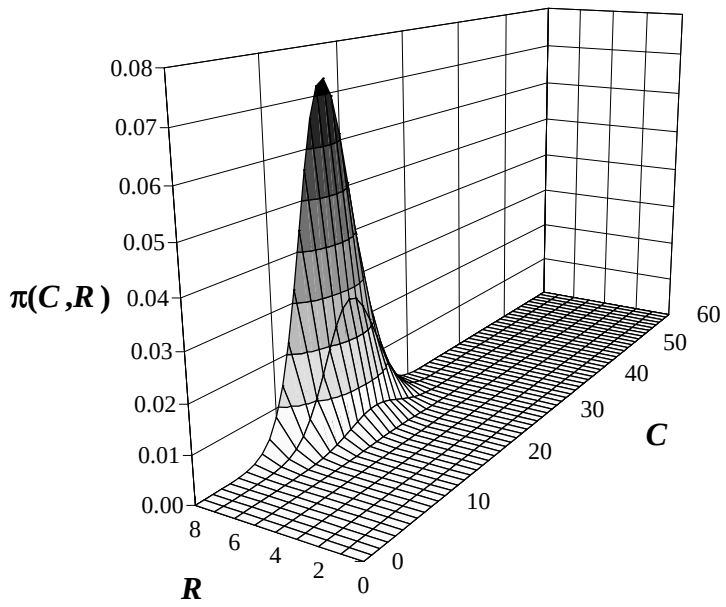

Figure 6.3: *Example of the state probability distribution, $\pi(C,R)$, which describes the probability of having C users in the CON state and R users in the RES_i states. A multiple cell PRMA system with M_s=60, N=8 and no packet retransmissions is considered.*

6.2.4 Performance Measures

With knowledge of the distribution $\pi(C,R)$, it is possible to study other aspects of the multiple cell PRMA speech system such as the speech packet dropping probability, P_{drop}, speech packet interference probability, P_{int}, total speech packet loss probability, P_{loss}, throughput per cell, h, and system utilisation, y. These performance measures were introduced previously in §2.2.4 and §4.6.3. The remainder of this section presents these performance measures in a mathematical form. The average packet dropping probability, for a given number of speech terminals per cell, M_s, can be obtained through calculating the following quantity [7]

$$P_{drop} = \sum_{R=0}^{N} \sum_{C=0}^{M_s - R} P_{drop}(C,R)\pi(C,R), \qquad \textbf{(6.15)}$$

where $P_{drop}(C,R)$ is the packet dropping probability when the system is in state $\{C,R\}$. For a system without speech packet retransmission, $P_{drop}(C,R)$ is given by [7]

$$P_{drop}(C,R) = \frac{g_f \left[v(C,R)\right]^{D_{\max}}}{1-(1-g_f)\left[v(C,R)\right]^{N}}, \qquad \textbf{(6.16)}$$

where $D_{\max}$ is the maximum number of slots that a terminal seeking a reservation can hold a packet before having to drop it. The parameter B is the size of the speech terminal buffer, as presented in (2.6). The term $v(C,R)$ is the probability that a terminal in contention does not gain a reservation in the current timeslot and is given by [6]

$$v(C,R) = 1-(1-g)\left(1-\frac{R}{N}\right)p_s\sum_{t=0}^{C-1}\binom{C-1}{t}p_s^t(1-p_s)^{C-1-t}q(t+1,\overline{m_{coc}}). \qquad \textbf{(6.17)}$$

The speech packet interference probability, P_{int}, on the other hand, is the probability of a reserved speech packet being corrupted by cochannel interference. This performance measure was defined previously in (4.36), namely

$$P_{int} = 1-q(1,\overline{m_{coc}}), \qquad \textbf{(6.18)}$$

where $q(1,\overline{m_{coc}})$ is the probability of a packet transmitted by a central cell terminal (i.e., by the terminal with the timeslot reservation) capturing the central cell base station, given that $\overline{m_{coc}}$ unwanted inter-cell interfering packets are also received.

As has already been presented, the speech information in a multiple cell PRMA system experiences two forms of quality degradation, namely packet dropping and packet interference. This concept is illustrated in Fig. 6.4. The packet dropping mechanism corresponds to packets being lost due to front end clipping of talkspurts, whereas the packet interference mechanism relates to mid-talkspurt clipping. The combined effect of these two phenomena may be represented by the total packet loss probability, P_{loss}, which was given in (4.37), namely

$$P_{loss} = P_{drop} + \left[1-P_{drop}\right]P_{int}. \qquad \textbf{(6.19)}$$

In this thesis, P_{loss} is used as the primary measure of speech terminal quality in multiple cell PRMA systems. Having predetermined a set maximum value of P_{loss}, which can be tolerated by the speech terminals, a wireless system planner is interested in determining the maximum number of terminals that can be supported by the system.

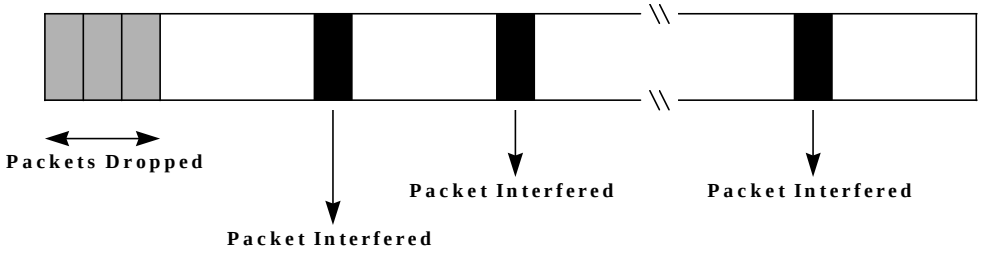

Figure 6.4: *A speech talkspurt suffers both packet dropping and packet interference during transmission in a multiple cell PRMA speech system.*

In the analysis of single cell PRMA systems (e.g., Fig. 2.11), P_{drop} is used in the determination of system capacity. Normally, a maximum packet dropping probability of P_{drop}=0.01 is assumed permissible. In the analysis of multiple cell PRMA systems, in which P_{loss} is the design criterion, it is assumed that maximum values of P_{loss} of either 0.01 or 0.05 are permissible. This level of P_{loss}, comprises both front end clipping (i.e. packet dropping) as well as mid-talkspurt clipping (packet interference). The value of P_{loss}=0.05 is used to represent an upper bound, possible if

speech interpolation [9,10] is incorporated. Based on the design criterion of either 1% or 5% packet loss, the maximum number of speech terminals per cell that can be supported, is denoted by either $M_{s(0.01)}$ or $M_{s(0.05)}$.

To compare different PRMA configurations with one another and with different transmission schemes, a normalised capacity measure was proposed in [11]. This normalised capacity measure is based on the number of conversations per identical TDMA channel. In a perfect TDMA system with no overheads, the number of voice channels per cell is R_{cell}/R_s, the ratio of the channel rate per cell to the speech coding rate. Thus the normalised capacity of a system with a maximum tolerable packet loss rate of P_{loss}=0.01, is defined according to [11]

$$c_{0.01} = \frac{M_{s(0.01)}}{R_{cell}/R_s}. \tag{6.20}$$

Likewise, if the tolerable speech packet loss rate is set at 5% (i.e., systems with speech packet interpolation), then the normalised capacity, $c_{0.05}$, is given according to

$$c_{0.05} = \frac{M_{s(0.05)}}{R_{cell}/R_s}. \tag{6.21}$$

The total throughput per cell for a system with M_s speech terminals per cell is given by [7]

$$h = \sum_{R=0}^{N} \sum_{C=0}^{M_s - R} h(C,R)\pi(C,R), \tag{6.22}$$

where $h(C,R)$ corresponds to the throughput when the system is in state $\{C,R\}$. $h(C,R)$ is given by

$$\begin{aligned} h(C,R) = {} & \frac{R}{N}(1-g_f)q(1,\overline{m_{coc}}) \\ & + (1-g)\left(1-\frac{R}{N}\right)\sum_{m_{cen}=1}^{C}\binom{C}{m_{cen}} p_s^{m_{cen}}(1-p_s)^{C-m_{cen}} U(m_{cen},\overline{m_{coc}}). \end{aligned} \tag{6.23}$$

Finally, each cell in the multiple cell PRMA system has only $1/N_c$ of the total system spectrum allocation, where N_c is the cluster size. Therefore, a cell with mean throughput, h, equates to an overall system having a utilisation factor, y, given by (4.35).

6.2.5 Location Dependent Performance Measures

In a system such as cellular PRMA, the communication quality of a terminal is highly dependent on the terminal's location. Compared to terminals located near cell boundaries, terminals near base stations are more likely to be successful in obtaining timeslot reservations. Terminals near base stations are also less likely to have their packets corrupted by inter-cell interference. With respect to PRMA, it is possible to investigate the packet dropping, packet interference and total packet loss probabilities as a function of terminal location. This requires several slight

modifications to be made in the performance measures presented in §6.2.4. In particular, it is necessary to incorporate capture probabilities which are a function of r_0 (the distance between the desired terminal and the central cell base station) into the performance measures. It should be noted however, that the underlying Markov analysis is not changed. In the case of the packet dropping probability the term $v(C,R)$, presented in (6.17), is modified according to

$$v(C,R,r_0) = 1-(1-g)\left(1-\frac{R}{N}\right)p_s\sum_{t=0}^{C-1}\binom{C-1}{t}p_s^t(1-p_s)^{C-1-t}q(t+1,\overline{m_{coc}},r_0), \qquad \textbf{(6.24)}$$

where $v(C,R,r_0)$ represents the probability that a terminal at a distance r_0 and in the contention state does not gain a reservation in the current timeslot. The capture probability $q(m_{cen},\overline{m_{coc}},r_0)$ was presented previously in Chapter 4 of this thesis. The expression presented in (6.24) is then used in place of $v(C,R)$ in (6.16) to calculate the packet dropping probability at a distance r_0, namely $P_{drop}(r_0)$. In a similar fashion, the speech packet interference probability of a terminal at a distance r_0 is given by

$$P_{int}(r_0) = 1-q(1,\overline{m_{coc}},r_0). \qquad \textbf{(6.25)}$$

It is then a trivial matter to calculate the total packet loss probability, at a distance r_0 using

$$P_{loss}(r_0) = P_{drop}(r_0) + \left[1-P_{drop}(r_0)\right]P_{int}(r_0). \qquad \textbf{(6.26)}$$

6.3 Inter-Cell Interference Estimation

In §6.2, the theory required to calculate the state probability distribution and the system performance measures of a multiple cell PRMA system was presented. The calculation of the state probability distribution and the performance measures requires determination of the mean number of inter-cell interfering packets, $\overline{m_{coc}}$, received per timeslot. In the following subsections, two techniques for estimating $\overline{m_{coc}}$ in a multiple cell PRMA system are presented. The first technique uses the mean speech activity factor to estimate the inter-cell interference, while the second technique uses an iterative approach to estimate the number of cochannel terminals in the contention and reservation states.

6.3.1 Technique A: Estimation Based on Speech Activity Factor

A simple method for estimating the value of $\overline{m_{coc}}$ is to consider the number of speech terminals per cell, M_s, together with the mean speech activity factor, *SAF*. Assuming that M_s is constant for all cells and that the *SAF* is given by (2.4), then $\overline{m_{coc}}$ can be approximated by

$$\overline{m_{coc}} \approx \frac{L\cdot SAF\cdot M_s}{N}, \qquad \textbf{(6.27)}$$

where L is the number of cochannel cells and N is the number of timeslots per frame. In this thesis, L=6 is considered for outdoor cellular systems, while for in-building picocellular systems, L=2 is considered. The *SAF* depends on the mean durations of talkspurts and silent gaps.

The estimation of $\overline{m_{coc}}$ in (6.27) represents the mean number of interfering packets *generated* per timeslot, although this does not necessarily equal the mean number of interfering packets *transmitted* per timeslot, especially in a congested PRMA network. In a congested network, it is possible that the true value of $\overline{m_{coc}}$ could be either less than or greater than the estimate of $\overline{m_{coc}}$ presented in (6.27). The reasons for this possible difference is attributable to two phenomena:

- On one hand, it is unlikely that all generated packets would be transmitted in a congested network, due to the packet dropping mechanism. This would result in a lower value of $\overline{m_{coc}}$.
- On the other hand, terminals in a congested network would perform more packet retransmissions during the contention phase. This would result in an higher value of $\overline{m_{coc}}$.

Because the combined effect of these two phenomena is unknown, the expression presented in (6.27) should be used with some caution, as confirmed in §6.3.2.

6.3.2 Technique B: Estimation Based on Number of Reserved and Contending Terminals

An alternative technique for estimating $\overline{m_{coc}}$ involves determining the respective probabilities of cochannel terminals being in the reservation and contention states. With such knowledge, it is possible to estimate the number of cochannel packets attributable to terminals in the reservation state and the number attributable to terminals in the contention state. The final estimate of inter-cell interference, $\overline{m_{coc}}$, is comprised of both reservation and contention phase interference.

In order to determine the proportion of reserved and contending interferers, a technique similar to that presented in §5.3.2 has been developed. This technique assumes that the system is homogeneous, such that each cell experiences identical performance. Based on this assumption, it is reasonable to expect that, on average, an equal number of reservation and contention packets would be produced in each cell in a given timeslot. This means that a particular cell would produce the same average number of packets as it would receive from a single cochannel cell. This concept was illustrated previously in Fig. 5.2.

In systems containing traffic hotspots, the assumption of an equal number of packets generated in each cell would not necessarily apply. This analysis, however, is limited to the situation where each cell is assumed to be supporting the same number of terminals, in which case the assumption is valid. Using this approach it is possible to calculate the total mean number of cochannel packets produced in a timeslot as being L times the mean number of packets produced in the central cell, namely

$$\overline{m_{coc}} = L \cdot \sum_{m_{cen}=0}^{C} m_{cen} \Pr(m_{cen}) . \qquad \textbf{(6.28)}$$

The factor of L accounts for the L nearby cochannel cells. The summation on the r.h.s. of (6.28) represents the expectation of m_{cen} (i.e., the mean number of central cell packets), where $\Pr(m_{cen})$ is the probability of m_{cen} central cell packets being transmitted. The summation limit in (6.28) is given by C (the number of terminals in the *CON* state) as this represents the maximum number of PRMA packets that may be transmitted in a cell in a given timeslot. $\Pr(m_{cen})$ in (6.28) can be described in terms of the state probability distribution, $\boldsymbol{\pi}(C,R)$, according to

$$\Pr(m_{cen}) = \sum_{R=0}^{N} \sum_{C=0}^{M_s-R} \Pr(m_{cen}|C,R)\boldsymbol{\pi}(C,R), \tag{6.29}$$

so that (6.28) can be rewritten as

$$\overline{m_{coc}} - \Omega = 0, \tag{6.30}$$

where

$$\Omega = L \cdot \sum_{m_{cen}=0}^{C} m_{cen} \sum_{R=0}^{N} \sum_{C=0}^{M_s-R} \Pr(m_{cen}|C,R)\boldsymbol{\pi}(C,R). \tag{6.31}$$

$\Pr(m_{cen}|C,R)$ is the probability of m_{cen} packets being produced in a single timeslot by the M_s central cell speech terminals, given that C of these terminals are in the contention state and R are in the reservation state. $\Pr(m_{cen}|C,R)$ is given by

$$\Pr(m_{cen}|C,R) = \begin{cases} \left(1-\dfrac{R}{N}\right)(1-p_s)^C + \dfrac{R}{N} g_f & m_{cen} = 0 \\ \left(1-\dfrac{R}{N}\right) C p_s (1-p_s)^{C-1} + \dfrac{R}{N}(1-g_f) & m_{cen} = 1 \\ \left(1-\dfrac{R}{N}\right)\binom{C}{m_{cen}} p_s^{m_{cen}} (1-p_s)^{C-m_{cen}} & 1 < m_{cen} \le C \end{cases} \tag{6.32}$$

By means of an example, Fig. 6.5 presents a plot of $\Pr(m_{cen}|C,R)$ for the situation where N=12, R=7 and C=8. Value of g_f = 0.018 and p_s=0.3 are also assumed. It can be observed from Fig. 6.5 that the probability of no packet ($m_{cen} = 0$) being transmitted is small compared to the probability of $m_{cen} = 1$ packet being transmitted. The probability of $m_{cen} > 1$ packets being transmitted reduces as m_{cen} increases. The reason for $m_{cen} = 1$ being the most likely outcome, is due to the high proportion of reserved timeslots (in this example, R/N=0.583) that exist, together with the high number of terminals in the contention state.

An iterative procedure is necessary to determine the value of $\overline{m_{coc}}$ which satisfies (6.30). This iterative procedure involves starting with an initial guess and computing step by step approximations of $\overline{m_{coc}}$. In this thesis, the Levenberg-Marquardt method [12] is employed. For a

particular value of M_s, the following iterative process is employed to calculate the value of $\overline{m_{coc}}$ which satisfies (6.30):

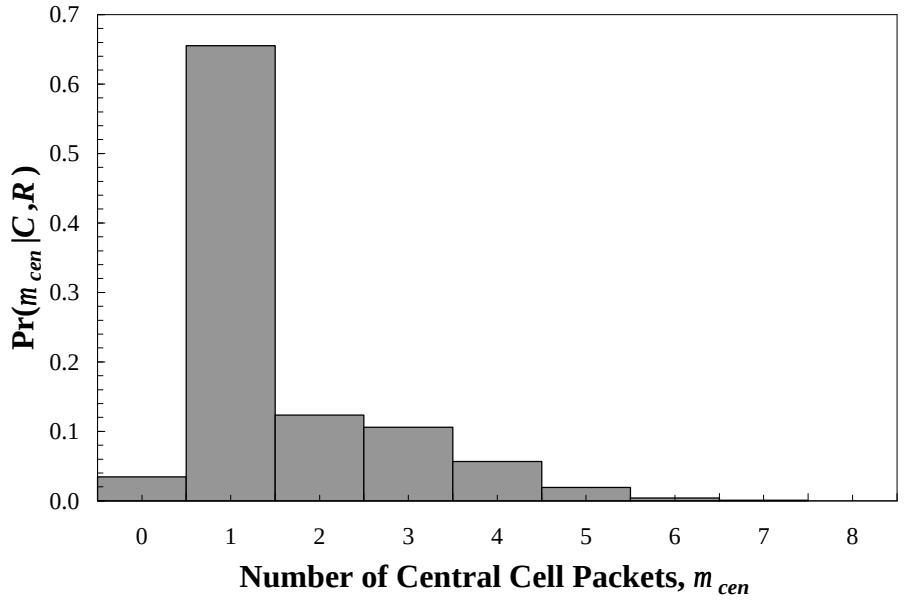

Figure 6.5: *Example of $Pr(m_{cen}|C,R)$ which is the probability that m_{cen} central cell packets are transmitted in a timeslot, given that C of the terminals are in the CON state and R are in the RES_i states. N=12, R=7, C=8, g_f = 0.018 and p_s=0.3 are assumed. See (6.32).*

---

a) The iteration number is set to i=0.

b) An estimate of $\overline{m_{coc}}$, denoted $\overline{m_{coc\,i}}$, is provided. In the absence of any better initial estimate, $\overline{m_{coc\,0}}$, is calculated using (6.27).

c) The value of Ω_i, given by (6.31), is evaluated. This calculation requires the capture probability be determined using capture probability theory developed in Chapter 4. In addition, it is also necessary to calculate the state probability distribution using the Markov theory presented in §6.2.

d) The error term, e_i, is determined according to,

$$e_i = \overline{m_{coc\,i}} - \Omega_i . \qquad \textbf{(6.33)}$$

e) If e_i is not within an acceptable error range, i is iterated to i= i+1. In addition, $\overline{m_{coc\,i}}$ is iterated to a new value (according to the Levenberg-Marquardt method) and steps *c)* and *d)* are repeated until the equality of (6.30) is satisfied.

f) The value of $\overline{m_{coc\,i}}$ that satisfies (6.30) (denoted by $\overline{m_{coc}}$) can then be used in the calculation of the PRMA performance measures presented in §6.2.4 and §6.2.5.

Fig. 6.6 presents comparisons of $\overline{m_{coc}}$, estimated using both Technique A (§6.3.1) and Technique B (§6.3.2). These estimates are based on an in-building (Building B, Table 3.4) pico-cellular PRMA system with cluster sizes, N_c=1 and N_c=3. In the situation where N_c=1 (Fig. 6.6(a)), good agreement is obtained between the respective techniques. However, as M_s is increased, the agreement between the two techniques is diminished, with Technique A predicting a higher value of $\overline{m_{coc}}$ than Technique B.

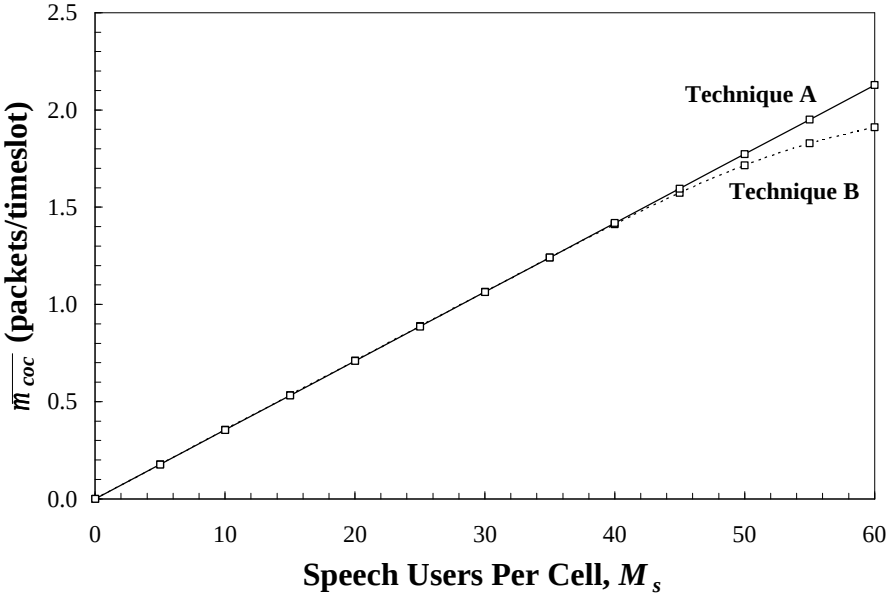

(a)

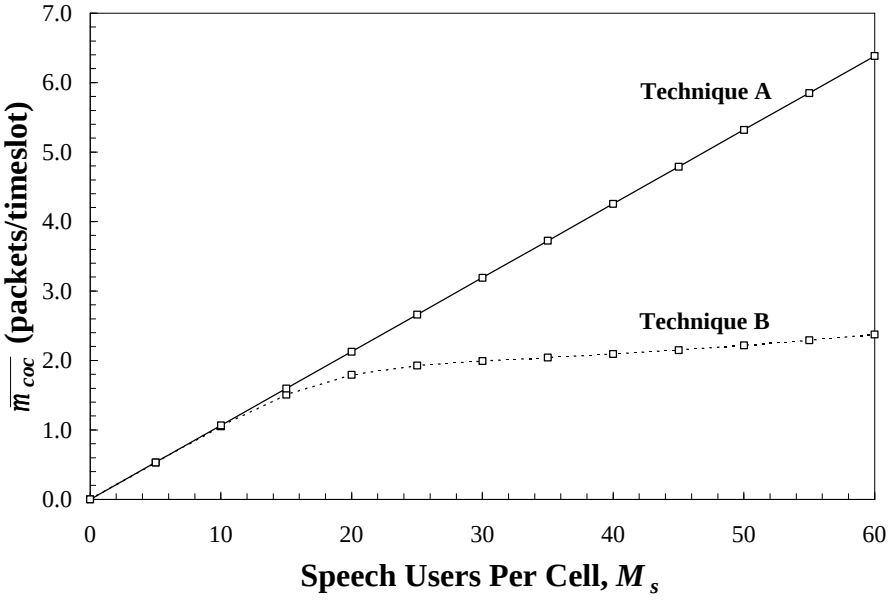

(b)

Figure 6.6: *Comparison of $\overline{m_{coc}}$ estimations in an in-building pico-cellular PRMA system (Building B: San Ramon) with* **(a)** *N_c=1 and* **(b)** *N_c=3. z=10dB. Technique A is described in §6.3.1 while Technique B is described in §6.3.2.*

This is especially true with a larger cluster size (Fig. 6.6(b)), in which case the agreement between the two techniques is reduced considerably. The system presented in Fig. 6.6(b) (N_c=3) is considerably more congested that the system presented in Fig. 6.6(a) (N_c=1). This indicates that Technique A is inadequate for estimating $\overline{m_{coc}}$ in highly overloaded systems.

The result derived using Technique B indicates that inter-cell interference actually flattens off as the network becomes more congested. This is attributable to the increased level of packet dropping that occurs in a congested system. This causes a considerable number of cochannel packets to be dropped at the terminal, making it impossible for them to cause interference to terminals in the central cell. This aspect, which was discussed in §6.3.1, is not considered with Technique A.

6.3.3 Technique B: A More Efficient Approach

The main disadvantage of Technique B is the increased complexity in computation compared with Technique A. This was also the case for Technique B proposed in §5.3.2 for S-ALOHA. It is possible, however, to apply the same method developed in §5.3.3 for S-ALOHA, to the analysis of PRMA. This method allows $\overline{m_{coc}}$ to be more efficiently calculated. As long as an accurate initial estimate of $\overline{m_{coc}}$ is provided, it is possible to estimate the final value of $\overline{m_{coc}}$ after only one iteration. For the case of PRMA, the following approach is used:

---

a) The iteration number is set to i=0.

b) Assuming that M_s is incremented by 5 terminals/step, the initial estimate, $\overline{m_{coc\,0}}$, is calculated using

$$\overline{m_{coc\,0}}\Big|_{M_s} = \begin{cases} 0 & M_s = 0 \\ \dfrac{L \cdot SAF \cdot M_s}{N} & M_s = 5 \\ 2\overline{m_{coc}}|_{(M_s-5)} - \overline{m_{coc}}|_{(M_s-10)} & M_s = 5n \qquad n = 2,3... \end{cases} \tag{6.34}$$

c) The value of Ω_0, given by (6.31), is evaluated.

d) The error term, e_0, is determined according to,

$$e_0 = \overline{m_{coc\,0}} - \Omega_0 . \tag{6.35}$$

e) The final estimate of $\overline{m_{coc}}$ is calculated according to

$$\overline{m_{coc}} = \overline{m_{coc\,0}} + e_0 , \tag{6.36}$$

6.4 Computer Simulation Techniques

In this chapter, as with Chapter 5, the results obtained from Markov analysis are validated using Monte Carlo computer simulation results. Computer simulations of multiple cell PRMA systems have been performed using the BONeS® DESIGNER™ software package, as with the multiple cell S-ALOHA systems of Chapter 5. A brief overview of BONeS® was provided in §5.4. Both outdoor cellular and in-building pico-cellular PRMA systems have been simulated using the BONeS® simulation language. These simulations represent realistic scenarios whereby packets transmitted in one cell cause interference to nearby cochannel cells. Only simulation models, which employ a "*cell wraparound*" approach, are considered in this chapter. Computer simulation results based on Model I (no cell wraparound, §5.4.1) have not been included as it was shown previously in Chapter 5 that this simulation method is inferior to that of Model II (cell wraparound, § 5.4.2).

While the majority of simulations considered in this chapter are used to estimate the 'cell-averaged' performance of the various multiple cell PRMA systems, location dependent simulations have also been performed. These location dependent simulations have been performed with respect to in-building pico-cellular PRMA systems. Location dependent simulations allow the performance of terminals at particular locations within the building to be determined. These simulations rely on a propagation database, such as that compiled in [13]. These simulations are discussed in greater detail in the following section.

6.4.1 Location Dependent Performance of an In-Building System

With floor-averaged simulations, the positions of central cell and cochannel cell users within the building are varied randomly from one trial to another (See Fig. 6.7). For each trial, a floor averaged propagation model, such as that presented in (3.18), is used to estimate the pathloss between individual terminals and that terminal's desired and cochannel base stations. After performing a large number of trials, the average performance of terminals located on the central cell can be calculated. The performance measures include packet dropping, packet interference and total packet loss probabilities, as well as throughput per cell and system utilisation. However, floor-averaged simulations are unable to reveal information relating to the location dependent performance of a particular system.

In [13], a propagation database was presented for the engineering tower block at the University of Auckland. By incorporating these propagation measurements into a Monte Carlo simulation, it is possible to estimate the performance of a PRMA speech terminal at various locations within the building. In order to perform such a simulation, one of the central cell terminals is considered to be the desired terminal while the remaining central cell terminals are considered to be intra-cell interferers. The positions of the intra-cell and inter-cell (i.e. cochannel) interferers are varied randomly from one trial to another, while the position of the desired terminal is assumed to be constant for the duration of the simulation. Instead of employing the floor-averaged propagation model of (3.18), the actual pathloss measurements presented in [13] are incorporated. After a large number of trials the performance of the desired terminal (located at a particular position in the central cell) can be estimated. The simulation is then repeated, with the desired terminal located at a new position.

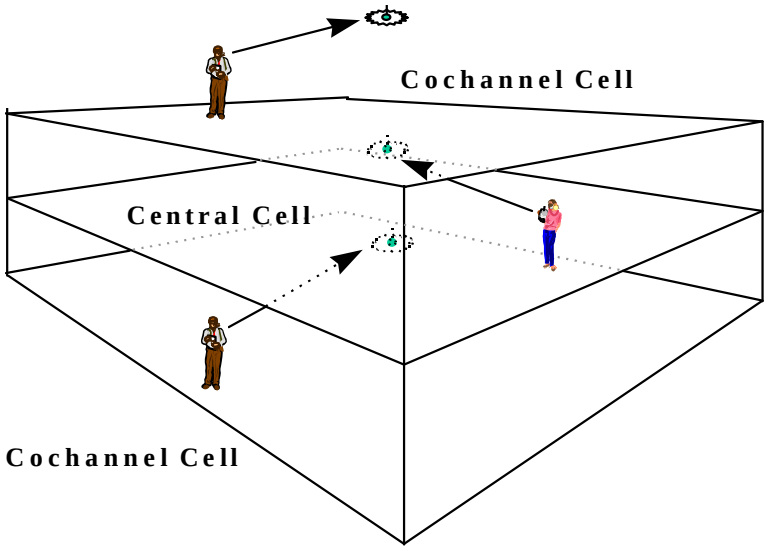

Figure 6.7: *Location dependent computer simulations can be used to estimate the performance of a PRMA speech terminal at various locations within a building.*

6.5 Performance of Outdoor Cellular PRMA

In this section, the performance of PRMA in an outdoor cellular system is determined in terms of P_{drop}, P_{int}, P_{loss}, h and y . Analytical results obtained from Markov analysis are compared to those obtained from Monte Carlo simulations. Clusters sizes of N_c=1, 3 and 4 are considered. It is assumed that a total system channel bit rate, R_{sys}=853.33 kb/s is partitioned amongst the N_c cells per cluster.

The system parameters for these various frequency reuse configurations were presented in Table 4.2. A speech permission probability, p_s=0.3, is assumed in all cases. The speech packet delay limit is assumed to be D_{max}=36 ms, while the mean talkspurt duration is t_1=1.00 sec, and the mean silence duration is t_2=1.35 sec. In this analysis, a capture ratio, z=10 dB, together with a shadowing standard deviation of s =6 dB and a pathloss exponent of b =4 are considered as median parameters in an outdoor cellular environment. In addition, however, values of z=6, 14 dB, s =0, 12 dB and b =3, 5 are investigated so as to determine the influence of these propagation parameters.

6.5.1 Comparison of Markov and Simulation Techniques

Before the performance of PRMA in an outdoor cellular environment can be determined, it is necessary to compare the results obtained from the various analytical techniques and simulation models proposed in §6.2-§6.4. This comparison allows the relative accuracy of the various techniques to be evaluated. In Fig. 6.8 the speech packet loss probability and throughput per cell of an outdoor cellular PRMA system without speech packet retransmission are presented. The results presented in Fig. 6.8 have been obtained from Markov analyses that employ Techniques A and B (§6.3.1 and §6.3.3, respectively) to estimate the inter-cell interference. In addition, computer simulation results based on Model II (cell wraparound, §5.4.2) are included. It is assumed that the outdoor cellular PRMA system has a cluster size of N_c=1 and that all packets

experience Suzuki fading. The results obtained from the two Markov analysis techniques in Fig. 6.8 are almost identical However, for higher values of M_s, the agreement between these two approaches is not as close. The results obtained from the computer simulations show reasonably good agreement with the results obtained from the Markov analyses, with slightly better agreement found with the Markov analysis based on Technique B.

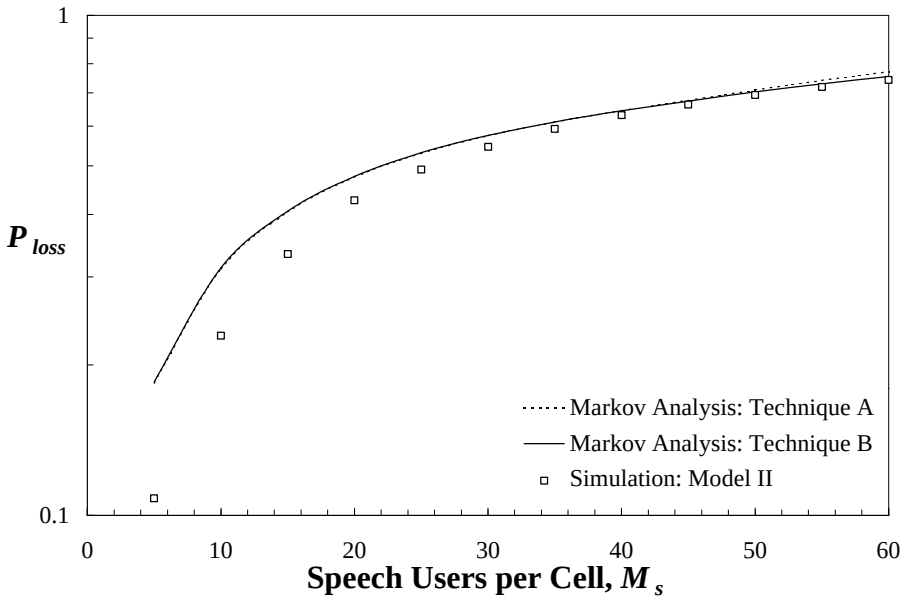

(a)

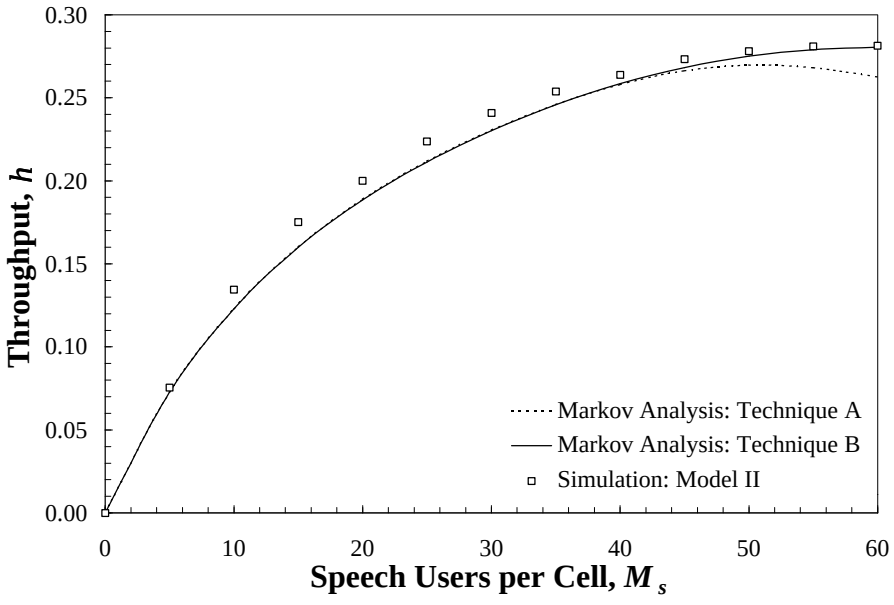

(b)

Figure 6.8: (a) *Speech packet loss probability and* **(b)** *throughput per cell of an outdoor cellular PRMA system with N_c=1. A Suzuki fading channel is considered with s =6 dB, b =4, z=10 dB. Results have been obtained using Markov analyses based on Technique A (§6.3.1) and Technique B (§6.3.2), as well as computer simulations (§ 5.4.2).*

The results of Fig. 6.9 are based on the same system as that considered in Fig. 6.8, although a cluster size of N_c=3 is instead assumed. In this situation, considerably less agreement is found between the two Markov analysis approaches. This is especially true for the estimate of throughput per cell (Fig. 6.9(b)). The simulation results obtained from Simulation Model II tend to support the results obtained from Markov analysis Technique B more strongly than those obtained from Technique A.

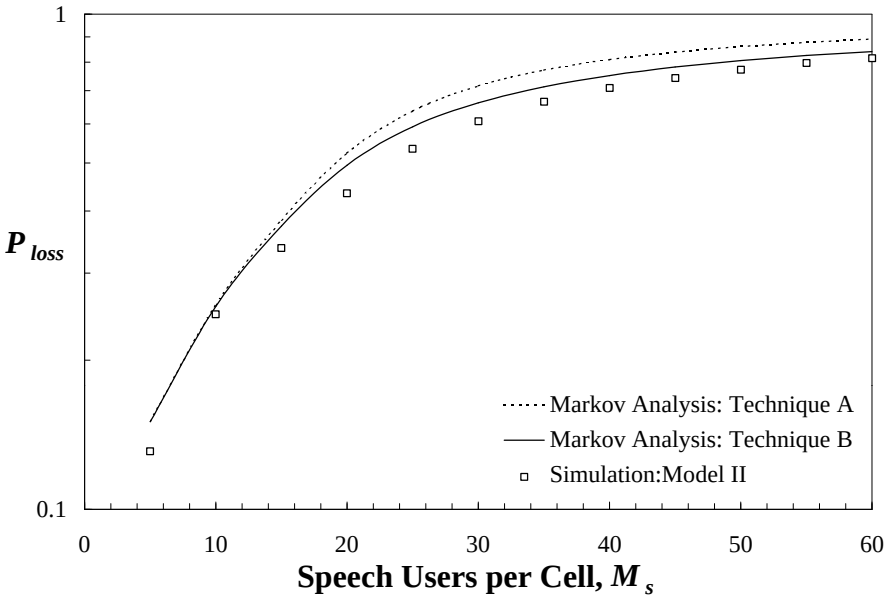

(a)

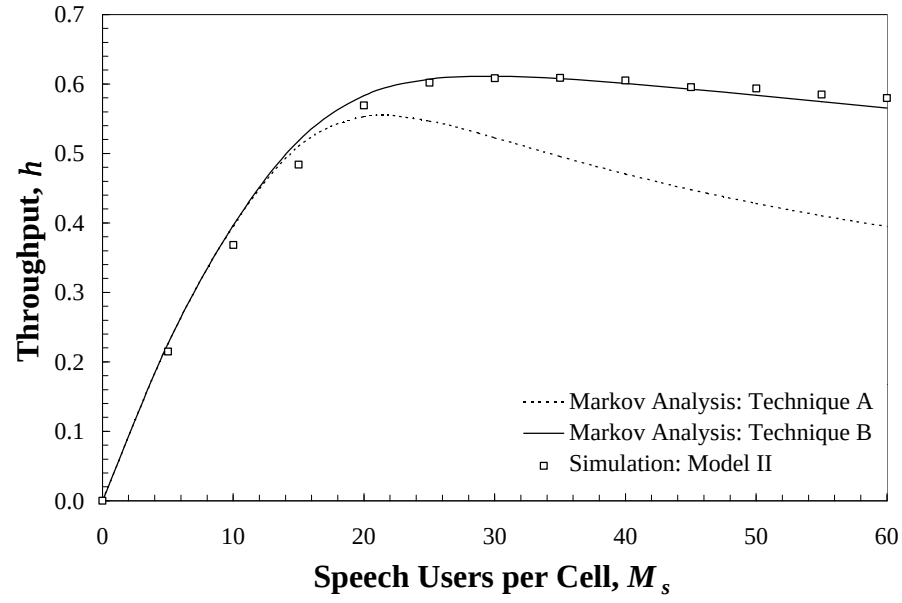

(b)

Figure 6.9: (a) *Speech packet loss probability and* **(b)** *throughput per cell of an outdoor cellular PRMA system with N_c=3. A Suzuki fading channel is considered with s =6 dB, b =4, z=10 dB. Results have been obtained using Markov analyses based on Technique A (§6.3.1) and Technique B (§6.3.2), as well as computer simulations (§ 5.4.2).*

It appears clear, therefore, that Markov analysis based on Technique B (§6.3.3) and Monte Carlo simulation based on Simulation Model II (§5.4.2) are the most accurate methods for estimating the performance of outdoor cellular PRMA systems. These methods have also been found to be the most accurate in predicting the performance of in-building pico-cellular PRMA systems (see §6.6). These methods are used throughout the remainder of this chapter.

6.5.2 Single Cell Versus Multiple Cell Performance

The majority of research relating to PRMA has normally only considered the performance of the protocol in a single cell system. Compared to the performance in a single cell system, the performance of PRMA in a multiple cell system is dominated by the effects of cochannel interference. By comparing the two types of PRMA systems, it is possible to determine the performance reduction attributable to cochannel interference. Fig. 6.10 presents the speech packet loss probability and throughput per cell for single cell and multiple cell PRMA systems. The parameters considered for the single cell systems are identical to those considered for the multiple cell systems (see Table 4.2), although in the case of the single cell systems, $\overline{m_{coc}}$ =0.

It is evident from Fig. 6.10 that in the case where no cochannel interference is considered, a cluster size of N_c=1 provides superior performance, in terms of the speech packet loss probability[1] and throughput. This is because the system parameters for N_c=1, as presented in Table 4.2, provide more bandwidth per cell compared to N_c=3 or N_c=4.

Given that the maximum tolerable packet loss probability is 1%, this single cell system (N_c=1) is capable of supporting $M_{s(0.01)} = 44$ simultaneous speech terminals with the N=24 timeslots per cell allocated to the system. Likewise, for a maximum tolerable packet loss probability of 5%, the system is capable of supporting $M_{s(0.05)} = 52$. With a speech coding rate of $R_s = 32$ kb/s and a bit rate per cell of $R_{cell} = 853.33$ kb/s, 44 speech terminals represents a normalised capacity of $c_{0.01} = 1.65$ conversations per channel, according to (6.20). Accordingly, $M_{s(0.05)} = 52$ corresponds to $c_{0.01} = 1.95$.

Such efficiencies have commonly been proposed for PRMA when operating in a single cell system. Such efficiencies, however, are unable to be substantiated in multiple cell PRMA systems, as evidenced in Fig. 6.10. On the contrary, PRMA is unable to operate in any of the multiple cell configurations presented in Fig. 6.10, as all of the packet loss probability results exceed the 1% and 5% maximum packet loss levels.

This finding indicates that the approach presented in this chapter for handling cochannel interference is over simplistic. This approach assumes that reserved speech packets which suffer cochannel interference are not retransmitted, in order to reduce further interference to other terminals. The benefit obtained from such an approach is unable to be realised as the system is incapable of operation, even for low terminal densities.

[1] For single cell systems, the speech packet loss probability is equal to the speech packet dropping probability.

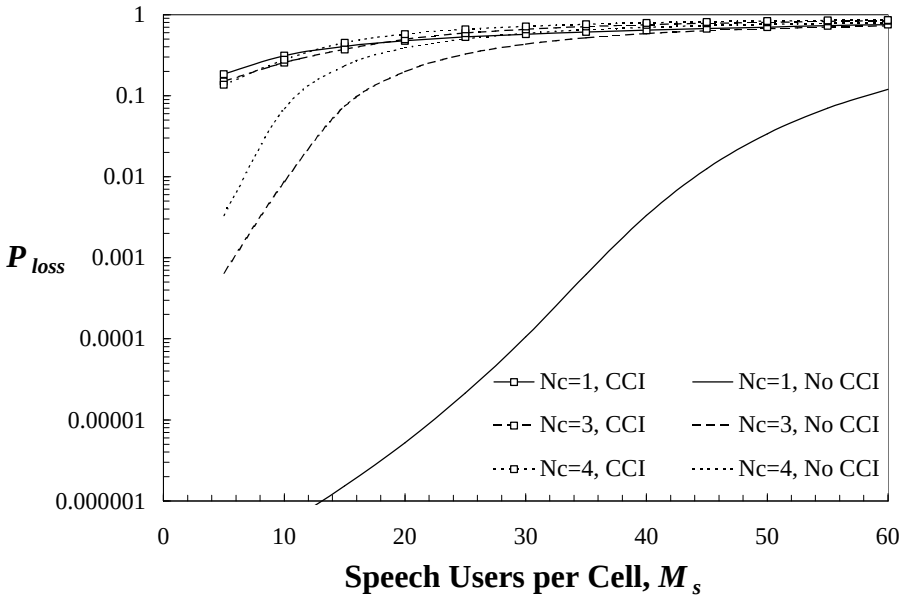

(a)

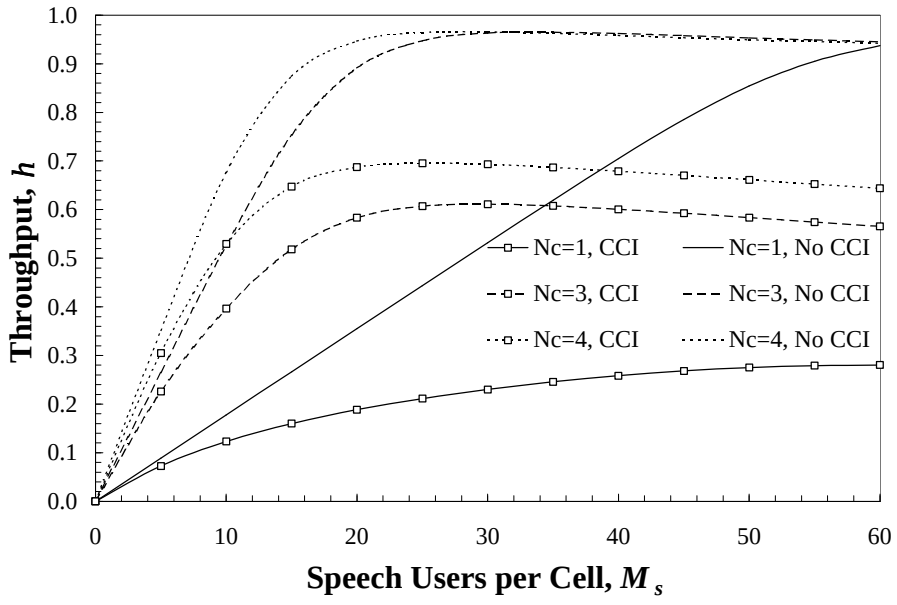

(b)

Figure 6.10: (a) *Speech packet loss probability and* **(b)** *throughput per cell of single cell and multiple cell (N_c=1, 3 and 4) outdoor PRMA systems. Suzuki fading is considered with s =6 dB, b =4, z=10 dB. Results obtained from Markov analysis based on Technique B.*

6.5.3 Determination of Optimum Frequency Reuse Plan

In the previous section, it was found that PRMA systems without speech packet retransmission were incapable of operating in any of the outdoor cellular systems considered. It may appear redundant, therefore, to determine which of these poorly performing systems represents the best choice. Nevertheless, it is useful to identify how the performance of cellular PRMA varies from

one frequency reuse plan to another. Fig. 6.11 and Fig. 6.12 present a number of performance measures for outdoor cellular PRMA systems suffering Suzuki fading (s =6 dB) and Rayleigh fading (s =0 dB), respectively. In particular, the packet dropping, packet interference and total packet loss probabilities are presented, together with the throughput and system utilisation measures. Both Markov analysis (lines) and simulation results (points) are presented. It is assumed that z=10 dB and b =4 in all cases. Cluster sizes of N_c=1, 3 and 4 are considered.

Figs. 6.11(a) and 6.12(a) present the speech packet dropping probability, P_{drop}, for systems suffering Suzuki and Rayleigh fading, respectively. It is clear that N_c=1 provides the best performance for both Suzuki and Rayleigh fading. The level of packet dropping is considerably higher in systems with N_c=3 and N_c=4. The results obtained for Suzuki fading are very close to those obtained for Rayleigh fading, indicating that propagation conditions, on their own, have a limited influence on P_{drop}[2]. Rather, the level of packet dropping appears to be primarily influenced by the number of timeslots allocated to each cell. Systems with N_c=1 have considerably more timeslots per cell than systems with N_c=3 or N_c=4. With N_c=1 there are more opportunities for contending terminals to have packets successfully transmitted during available timeslots. This in turn, minimises the amount of time that packets are held in the terminal buffer.

The results of Fig. 6.11(b) and Fig. 6.12(b) present the speech packet interference probability, P_{int}, for systems suffering Suzuki fading and Rayleigh fading, respectively. In contrast to the results presented for P_{drop}, the worst performing systems in terms of P_{int} are those with a cluster size of N_c=1. Systems with N_c=3 and N_c=4 have considerably lower levels of packet interference, although these levels still prohibit these systems operating satisfactorily. The level of P_{int} is determined primarily by the propagation conditions that exist, together with the geographic spacing of cochannel cells from the central cell. The close proximity of cochannel interferers in a system with complete frequency reuse (N_c=1) leads to a greater probability of reserved packets suffering corruption, as the power level of the interferers is substantially higher in this scenario, compared to if N_c=3 or N_c=4. The results indicate that systems suffering Suzuki fading experience a greater probability of packet interference. This result (discussed previously in Chapter 4, pg. 69) is due to a larger variability in the composite inter-cell interference signal with Suzuki fading, which increases the likelihood of signal outages.

In Fig. 6.11(c) and Fig. 6.12(c), the combination of the packet dropping and packet interference probabilities are presented in terms of the speech packet loss probability, P_{loss}. None of the frequency reuse plans presented have a clear advantage over the range of M_s values evaluated. However, when the number of terminals per cell is low, N_c=4 is a slightly better choice. As the number of terminals is increased, a cluster size of N_c=3 becomes optimum and for high terminal loading, N_c=1 is clearly the best choice. This finding is a result of the tradeoff between cell capacity and inter-cell interference. In particular, when the value of M_s is low, all systems have sufficient capacity to support the terminals, although systems with N_c=3 and N_c=4 experience significantly lower levels of inter-cell interference. This leads to the performance of these systems being better than those which have a cluster size of N_c=1. On the other hand, when the

[2] In [3] it was shown that the value of P_{drop} can be influenced by propagation conditions, providing that the speech permission probability (p_s) is also varied.

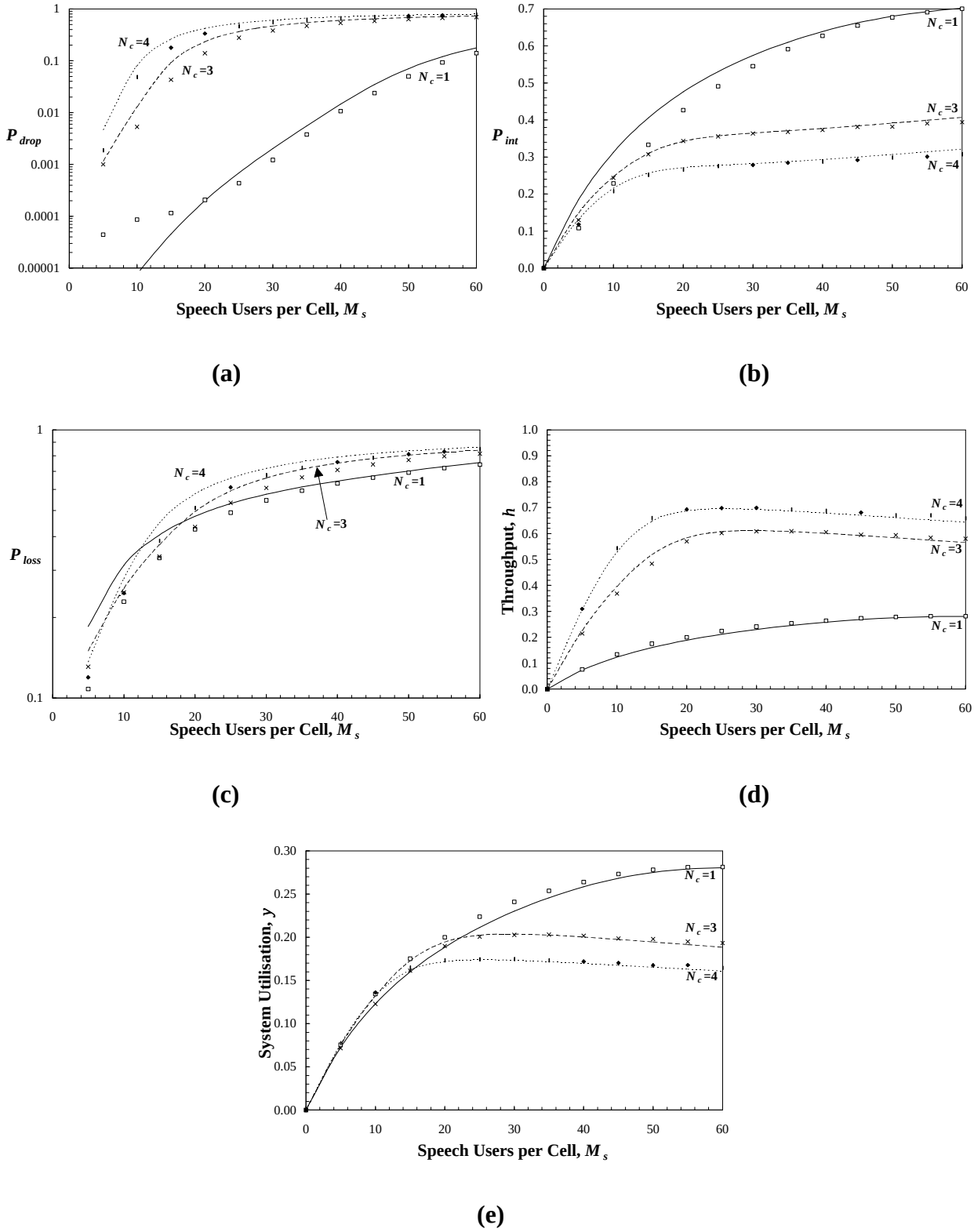

Figure 6.11: (a) *Speech packet dropping probability,* **(b)** *speech packet interference probability,* **(c)** *speech packet loss probability,* **(d)** *throughput per cell and* **(e)** *system utilisation of an outdoor cellular PRMA system with cluster sizes N_c=1, 3, and 4. A Suzuki fading channel is considered with s =6 dB, b =4, z=10 dB. Markov analysis results (lines) and simulation results (points) are presented.*

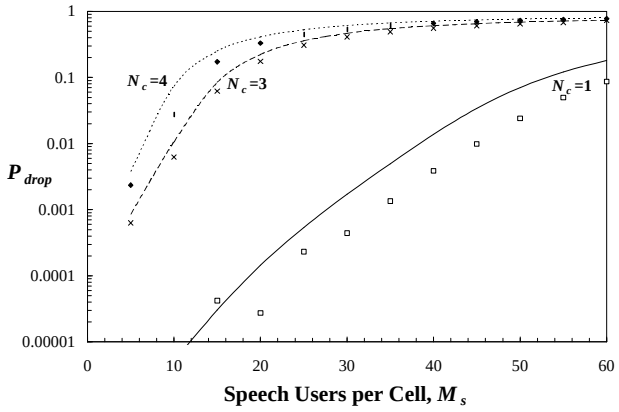

(a)

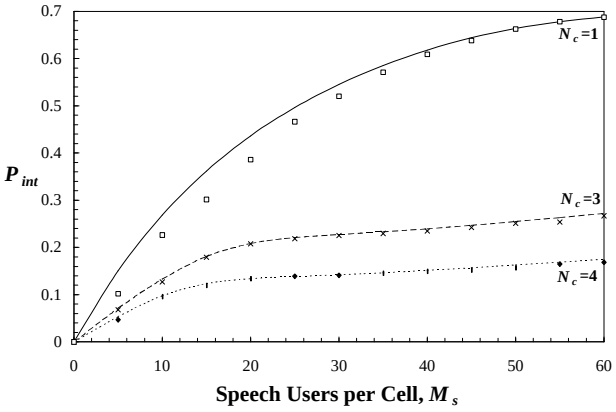

(b)

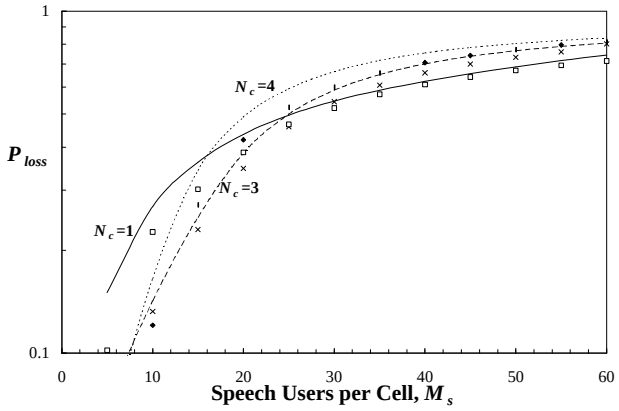

(c)

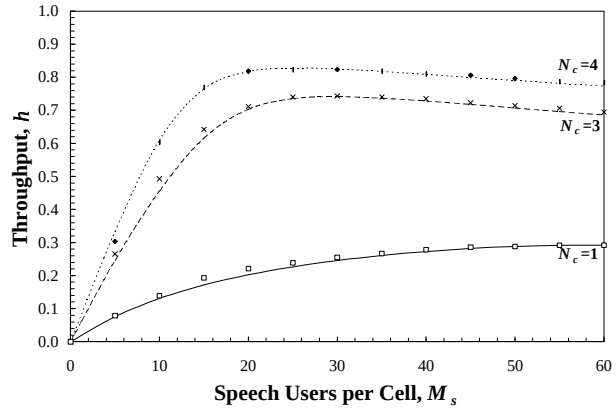

(d)

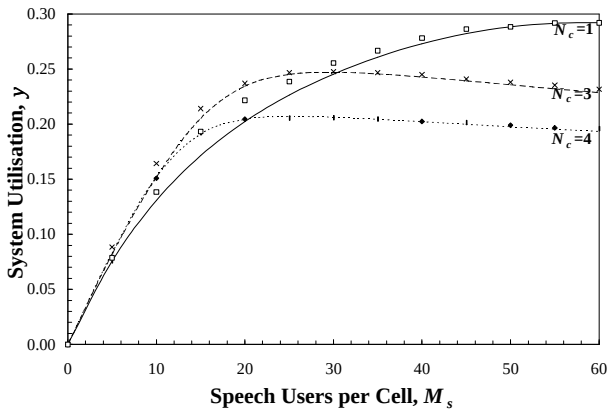

(e)

Figure 6.12: (a) *Speech packet dropping probability,* **(b)** *speech packet interference probability,* **(c)** *speech packet loss probability,* **(d)** *throughput per cell and* **(e)** *system utilisation of an outdoor cellular PRMA system with cluster sizes N_c=1, 3, and 4. A Rayleigh fading channel is considered with b =4, z=10 dB. Markov analysis results (lines) and simulation results (points) are presented.*

value of M_s is high, systems with N_c=3 and N_c=4 have insufficient capacity (i.e. timeslots) and as a result suffer from high packet dropping probabilities, whereas systems with N_c=1 are not affected to the same extent. It should be noted, however, that none of the systems presented in Fig. 6.11(c) or Fig. 6.12(c) are capable of supporting a significant number of users, based on the maximum tolerable packet loss probability constraint. Actual capacity estimations are presented in the following section.

Fig. 6.11(d) and Fig. 6.12(d) present the throughputs per cell, h, of the respective systems. The throughput of those systems suffering Rayleigh fading is noticeably better than those which suffer Suzuki fading. The throughput of systems with N_c=3 and N_c=4 are considerably greater than those with N_c=1. This does not necessarily imply that systems with N_c=3 and N_c=4 have a superior performance, but merely that the timeslots in these systems are more highly utilised. It should be recognised that systems with N_c=3 or N_c=4 have less timeslots per cell than systems with N_c=1, but must support the same number of users.

Finally, Figs. 6.11(e) and 6.12(e) present the system utilisation, y, for systems suffering Suzuki and Rayleigh fading, respectively. This performance measure gives a better understanding of system efficiency, because unlike the throughput per cell, h, it considers the operation of the overall system. It can be observed that the most efficient choice of system depends on the level of terminal loading (i.e., the value of M_s) considered.

6.5.4 Capacity Estimations

Based on the results presented in the previous section, it is possible to estimate the capacities of the outdoor cellular PRMA systems presented in Fig. 6.11 and Fig. 6.12. These capacity estimations have been obtained from the Markov analysis and computer simulation results and are in terms of the maximum number of speech terminals, M_s, able to be supported per cell. These estimations, presented in Table 6.2, consider clusters sizes of N_c=1, 3, and 4, for both Suzuki fading and Rayleigh fading environments.

It is evident from Table 6.2 that the performance of the various outdoor PRMA systems is extremely poor. The best scenario appears to involve a cluster size of N_c=4, a Rayleigh fading channel, together with reliance on the inclusion of speech interpolation techniques (P_{loss}=0.05). In this situation the system is capable of supporting five terminals per cell.

N_c:	1	3	4
Suzuki (P_{loss}=0.01)	0	0	0
Suzuki (P_{loss}=0.05)	2	2	2
Rayleigh (P_{loss}=0.01)	0	0	1
Rayleigh (P_{loss}=0.05)	2	3	5

Table 6.2: *Number of speech terminals per cell, M_s, able to be supported at 1% and 5% total packet loss, P_{loss}, rates in an outdoor cellular PRMA system without retransmission. Both Suzuki fading ($s = 6$ dB) and Rayleigh fading ($s = 0$ dB) environments are considered for cluster sizes of N_c=1, 3, and 4. z=10 dB, $b = 4$.*

6.5.5 Effect of System and Propagation Parameters

In this section, the effect of the pathloss exponent, b, the lognormal shadowing standard deviation, s, and the capture ratio, z, on the performance of an outdoor cellular PRMA system is determined. For example, Fig. 6.13 compares the performance of an outdoor cellular PRMA system with N_c=3 in terms of the total speech packet loss probability, P_{loss}, for various values of the pathloss exponent, b. It is clear from Fig. 6.13 that the pathloss exponent has a significant effect on the performance of the system, with a higher pathloss exponent resulting in a better performance due to an increased isolation between cochannel cells.

Fig. 6.14 compares the performance of an outdoor cellular PRMA system for various values of the capture ratio, z. Like the pathloss exponent, the capture ratio has a significant effect on the performance, with a low capture ratio resulting in an improved speech packet loss probability.

Fig. 6.15 compares the performance of a cellular PRMA system with N_c=3 for various values of the lognormal shadowing standard deviation, s. From Fig. **6.15**, it can be noted that the performance of PRMA in an outdoor cellular system is especially poor in a highly shadowed environment. This is unlike the finding presented in [3] for a single cell PRMA system, which found that a high level of shadowing was responsible for an improved system performance. The improvement obtained with increased shadowing in a single cell system is attributable to a higher capture probability, which increases the ability of contending terminals to obtain timeslot reservations. In addition, terminals in a single cell system are not affected by inter-cell interference. In a multiple cell system, however, terminals that transmit reserved packets are more susceptible to interference from inter-cell interferers when the shadowing level is high.

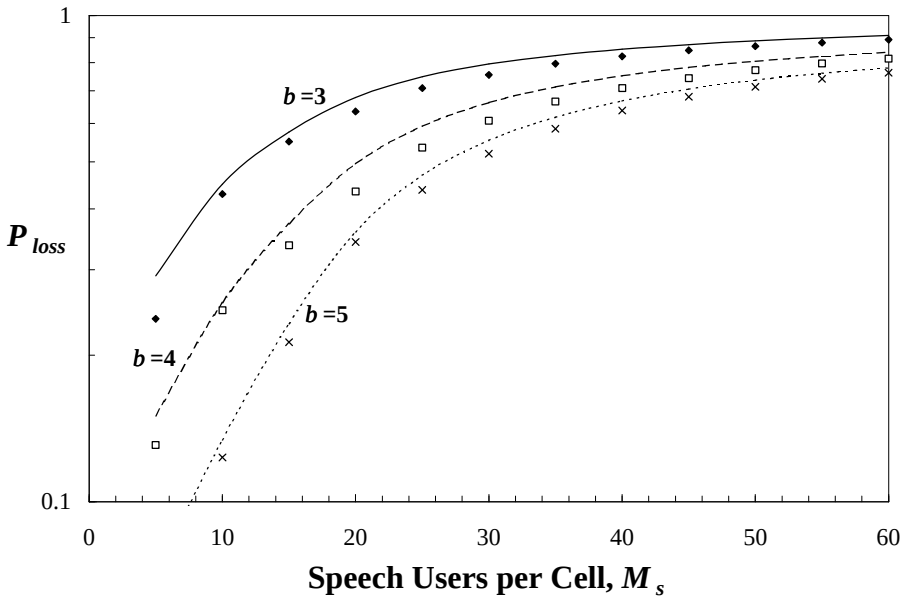

Figure 6.13: *Speech packet loss probability for an outdoor cellular PRMA system (N_c=3) with pathloss exponent b =3, 4, and 5. s =6 dB and z=10 dB in all cases. Markov analysis results (lines) and simulation results (points) are presented.*

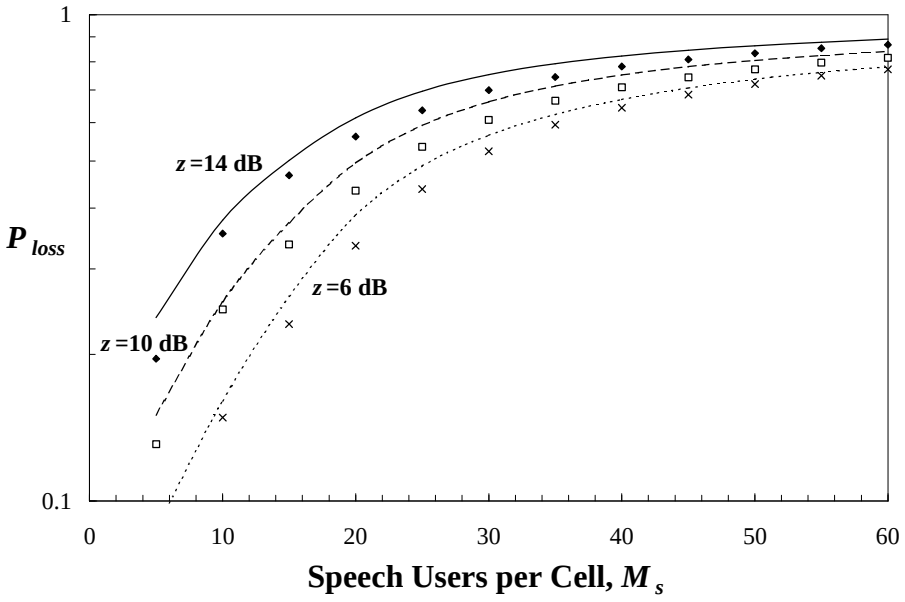

Figure 6.14: *Speech packet loss probability for an outdoor cellular PRMA system (N_c=3) with capture ratio z=6, 10 and 14 dB. b =4 and s =6 dB in all cases. Markov analysis results (lines) and simulation results (points) are presented.*

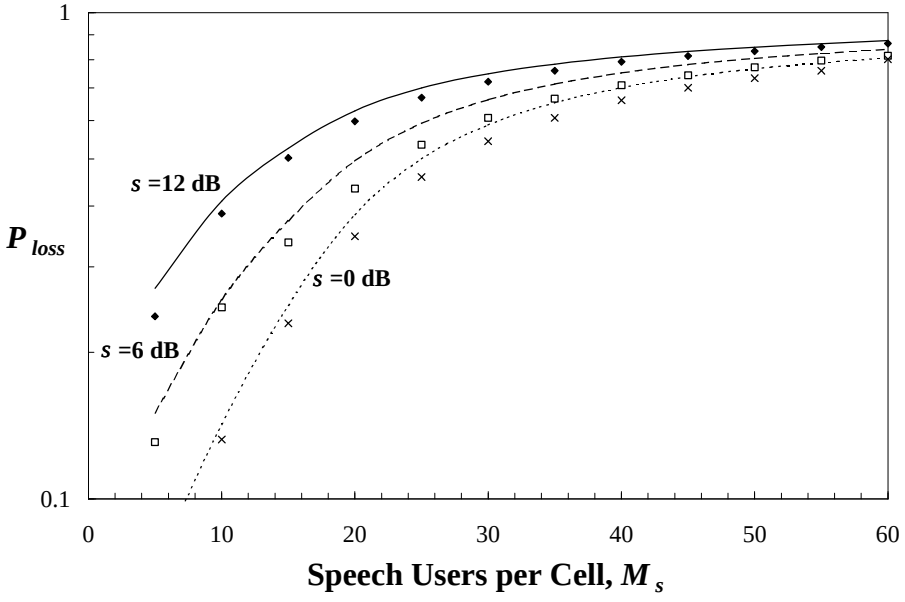

Figure 6.15: *Speech packet loss probability for an outdoor cellular PRMA system (N_c=3) with shadowing standard deviation s =0, 6, and 12 dB. b =4 and z=10dB in all cases. Markov analysis results (lines) and simulation results (points) are presented.*

6.5.6 Location Dependent Performance

Throughout §6.5, the cell averaged performance of various outdoor cellular PRMA systems has been determined. Such an approach is analogous to calculating the performance of a speech terminal at each location within the cell and then averaging these calculations over the probability that the terminal is at these particular locations. In this section, the location dependent performance of an outdoor cellular PRMA is investigated. In particular, the variations in the packet dropping, packet interference and total packet loss probabilities are determined as a function of the terminal to base station separation distance, r_0.

Fig. 6.16 presents the distance dependent performance of an outdoor cellular PRMA system with N_c=3 and M_s=20 speech terminals per cell. A Suzuki fading channel is assumed with b=4, z=10 dB and s=6 dB. Cell averaged performance results for this system have already been presented on a number of occasions throughout §6.6 (e.g. Fig. 6.11). Cell averaged values of P_{drop}, P_{int} and P_{loss} for this system when M_s=20 have been estimated and are presented in Table 6.3.

	P_{drop}	P_{int}	P_{loss}
M_s=30	0.233	0.343	0.496

Table 6.3: *Cell averaged performance of an outdoor cellular PRMA system (N_c=3) with M_s=20 terminals/cell. b=4, z=10 dB and s=6 dB.*

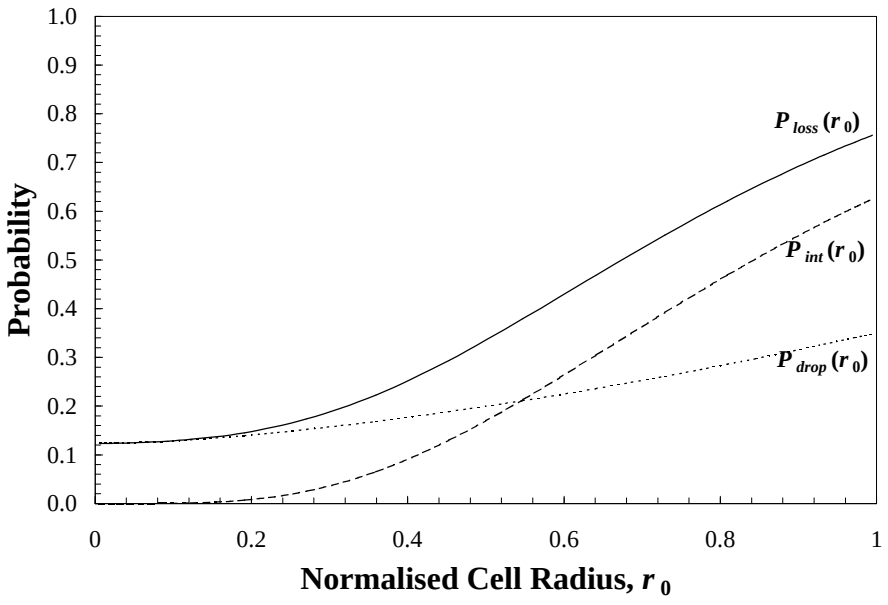

Figure 6.16: *Distance dependency of P_{drop}, P_{int} and P_{loss} for an outdoor cellular PRMA system (Nc=3) with M_s=20 terminals/cell. b=4, z=10 dB and s=6 dB. Results obtained using Markov analysis based on Technique B.*

From Fig. 6.16, it can be observed that the performance experienced by a speech terminal is highly dependent on the terminals distance from the central cell base station and is not simply given by the performance estimates presented in Table 6.3.

As a terminal moves from the centre of the cell (r_0=0) to the cell boundary (r_0=1), there is an increase in the levels of the three performance measures plotted. When the terminal is close to the base station, the packet dropping mechanism is the dominant source of degradation, whereas for terminals closer to the cell boundary, packet interference is the main source of packet loss. It can also be observed that P_{drop} is somewhat less influenced by the speech terminal's location compared to P_{loss}, which increases rapidly as a function of r_0.

6.6 Performance of In-Building Pico-Cellular PRMA

In this section the performance of PRMA in the in-building environment is determined. Consideration is given to PRMA systems operating in the four buildings presented in Table 3.3. Analytical results obtained from Markov analyses are compared with those obtained from Monte Carlo simulations. The same system parameter values considered for outdoor cellular PRMA (§6.5) are also considered in this section.

A number of the findings in §6.5, derived with respect to an outdoor cellular PRMA system, also apply to an in-building pico-cellular PRMA system. In particular, the effect of the pathloss exponent, capture ratio and lognormal shadowing standard deviation on system performance is similar in both in-building and outdoor systems. There are, however, several issues that can be explored with respect to the in-building environment. The first of these relates to the in-homogeneity of the in-building wireless propagation environment, with different buildings having different propagation characteristics. This uniqueness is attributable to variations in building structure and it leads to the performance of in-building wireless systems being dependent on the building in which they are implemented. The variations in performance of the four in-building PRMA systems are investigated in §6.6.1. The actual capacities of the PRMA systems operating in these four buildings are presented in §6.6.2.

Another aspect that requires consideration is the location dependent performance of PRMA in an in-building environment, as presented in §6.6.3. By employing the detailed propagation information of [13], it is possible to estimate the location dependent performance of an in-building pico-cellular PRMA system, assumed to be operating in Building D (Engineering Tower).

6.6.1 Performance Variations Between Buildings

In this section, the performance variations that exist from one building to another are identified. Figs. 6.17 to 6.20 present the speech packet loss probability, P_{loss}, and system utilisation, y , for Buildings A-D, respectively. The relevant propagation parameter values for these building were presented in Table 3.3. In all cases, a capture ratio of z=10dB is considered. It is evident from Figs. 6.17 to 6.20 that PRMA is unable to operate successfully in any of these in-building environments, as the packet loss probability exceeds the 1% threshold, as well as the 5% threshold, in many situations.

From the results of Figs. 6.17 to 6.20, it is clear that no single choice of cluster size is able to provide optimum performance in all situations. As with the outdoor cellular PRMA systems presented in §6.5.3, the choice of optimum cluster size in Buildings A and D depends on the number of terminals per cell to be simultaneously supported. In particular, when the number of terminals per cell is low, larger cluster sizes provide optimum performance, whereas when the number of terminals per cell is high, the smallest cluster size is optimum. This trend, however, is not found for the in-building PRMA system operating in Building B. In this situation, it appears that a cluster size of N_c=1 is always optimum, irrespective of the value of M_s.

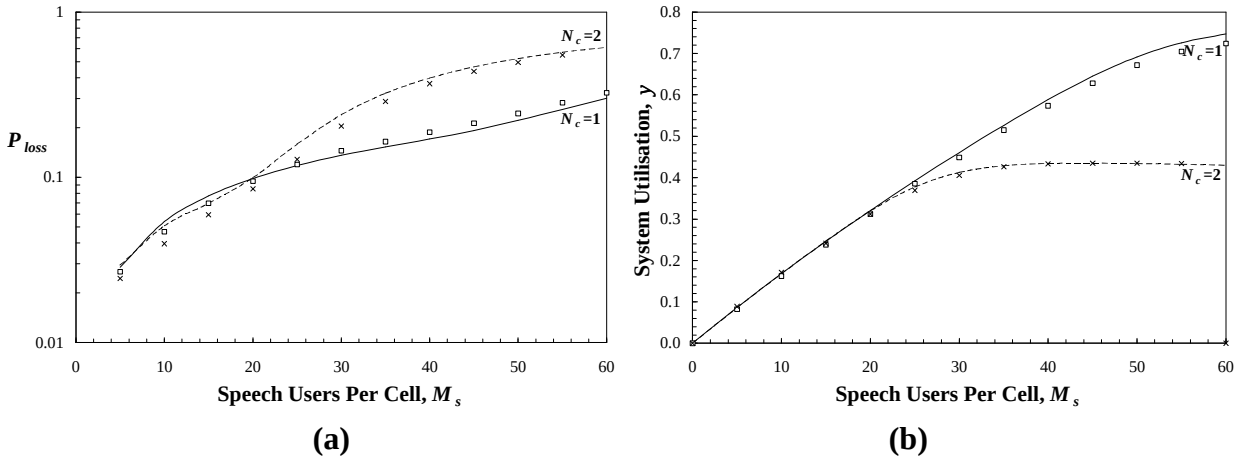

(a) **(b)**

Figure 6.17: *Packet loss probability* **(a)** *and system utilisation* **(b)** *of a PRMA system in Building A: Walnut Creek. N_c=1, 2 and z=10dB. Markov analysis results (lines) and simulation results (points) are presented.*

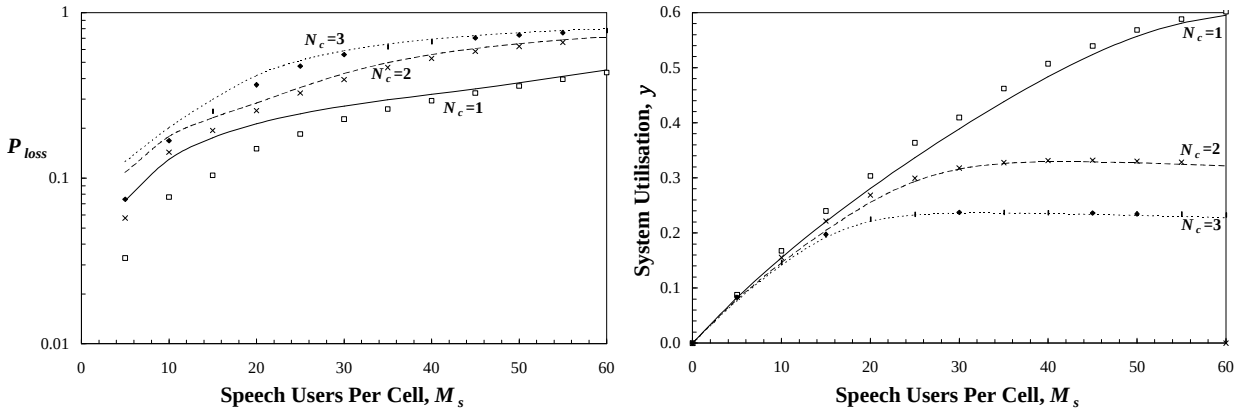

(a) **(b)**

Figure 6.18: *Packet loss probability* **(a)** *and system utilisation* **(b)** *of a PRMA system in Building B: San Ramon. N_c=1, 2, 3 and z=10dB. Markov analysis results (lines) and simulation results (points) are presented.*

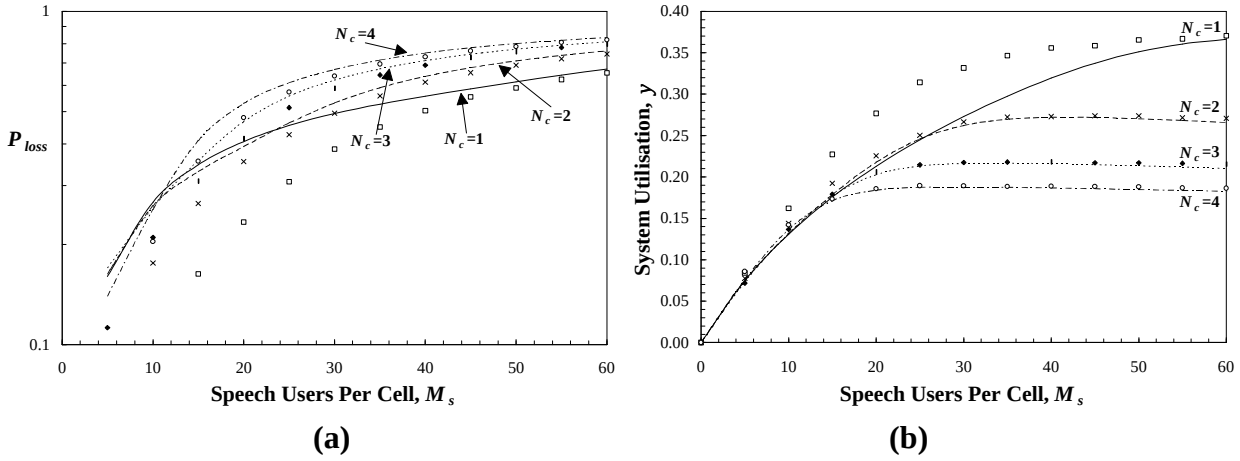

(a) **(b)**

Figure 6.19: *Packet loss probability* **(a)** *and system utilisation* **(b)** *of a PRMA system in Building C: SF Pacbell. N_c=1, 2, 3, 4 and z=10dB. Markov analysis results (lines) and simulation results (points) are presented.*

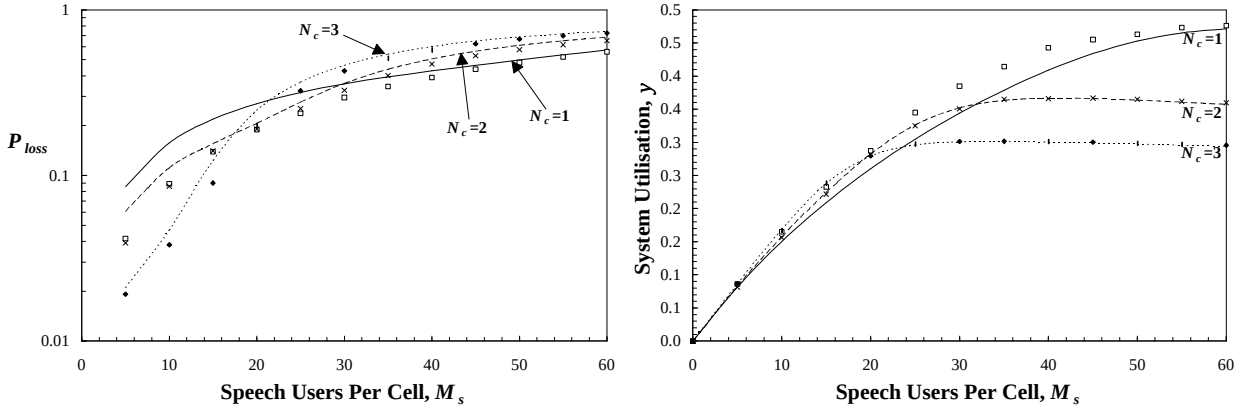

(a) **(b)**

Figure 6.20: *Packet loss probability* **(a)** *and system utilisation* **(b)** *of a PRMA system in Building D: Engineering Tower. N_c=1, 2, 3 and z=10dB. Markov analysis results (lines) and simulation results (points) are presented.*

Fig. 6.21 presents a comparison of the packet dropping, packet interference and total packet loss probabilities for the four in-building PRMA systems considered. These results are based on systems with cluster sizes of N_c=1 and a capture ratio of z=10 dB. It can be observed from Fig. 6.21(a), that the level of speech packet dropping is almost entirely unaffected by the physical location of the system, with similar estimates obtained in all buildings considered. Fig. 6.21(b) compares the estimates of speech packet interference probability, P_{int}, obtained in the various buildings. In this situation, it can be observed that this performance measure is strongly influenced by the building propagation parameters, with the estimates varying significantly between the four buildings.

The highest packet loss probability occurs in Building C. This is attributable to the combined effect of the floor attenuation factors, path loss exponents and the environmental shadowing. All three of these parameters are important when estimating the performance of a particular system. The findings of Fig. 6.21 indicate that, for the systems investigated, specific propagation characteristics must be known before an efficient wireless system can be deployed in a particular building.

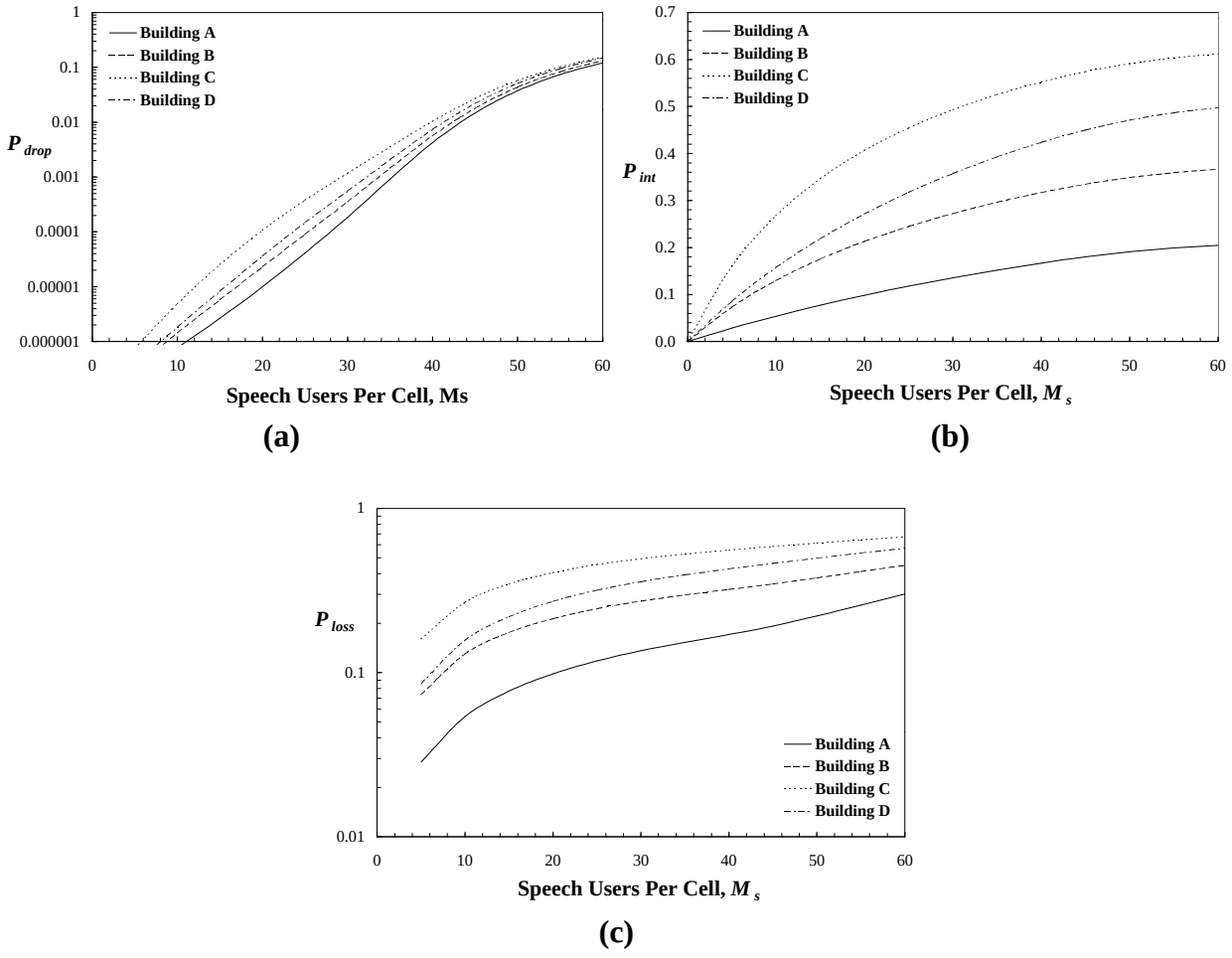

Figure 6.21: *Comparison of* **(a)** *packet dropping probability,* **(b)** *packet interference probability and* **(c)** *total packet loss probability between Buildings A-D. N_c=1 and z=10dB in all cases. Results obtained from Markov analyses based on inter-cell interference Technique B.*

6.6.2 Capacity Estimations

Based on the results presented in Figs. 6.17 - 6.20, it is possible to estimate the capacities of the four in-building pico-cellular PRMA systems. These capacity estimations have been obtained from the Markov analysis and computer simulation results and are in terms of the maximum number of speech terminals, M_s, able to be supported per cell. These estimations, presented in Table 6.4, consider clusters sizes of N_c=1, 2, 3, and 4.

It is clear from Table 6.4 that the performance of the various in-building PRMA systems, as with the outdoor cellular PRMA systems of §6.5.3, is poor. The best performance is experienced in buildings A and D, with an estimated capacity of M_s=10 users per floor for cluster sizes of 2 and 3, respectively. This finding relies on the inclusion of speech interpolation techniques (P_{loss}=0.05). Without speech interpolation, the performance would be extremely poor.

Building	N_c:	1	2	3	4
A	P_{loss}=0.01	1	1	-	-
	P_{loss}=0.05	9	10	-	-
B	P_{loss}=0.01	0	0	0	-
	P_{loss}=0.05	3	1	0	-
C	P_{loss}=0.01	0	0	0	0
	P_{loss}=0.05	0	0	0	1
D	P_{loss}=0.01	0	0	2	-
	P_{loss}=0.05	3	4	10	-

Table 6.4: *Number of speech terminals per cell, M_s, able to be supported at 1% and 5% total packet loss, P_{loss}, rates in 4 in-building pico-cellular PRMA system without retransmission. Cluster sizes of N_c=1, 2, 3, and 4 are considered. z=10 dB.*

6.6.3 Location Dependent Performance of Building D

The variation in performance that exist over the coverage area of an in-building wireless system is of considerable interest to system planners. With the aid of detailed propagation information, it is possible to determine the location dependent performance of an in-building system. The location dependent performance of an in-building pico-cellular PRMA speech system is determined in this section using the propagation database of [13] (Building D, Engineering Tower). This performance analysis is accomplished via Monte Carlo simulation, as described in §6.4.1.

Fig. 6.22 plots the variation in packet loss probability over the central cell of Building D for a speech only PRMA system with N_c=1 and M_s=20 users/floor. For this particular building, the central core has a significant effect on the performance at certain locations. In particular, terminals in the shadow region of the floor (opposite side from transmitter) experience significantly worse performance compared to terminals on the same side as the transmitter. Clearly this information is unavailable in the floor-averaged results of §6.6.1.

An appreciation of these performance variations is especially relevant in indoor systems, where users are normally confined to a single area (e.g., office room) permanently or semi-permanently. In this situation, users could conceivably experience consistently good or consistently bad communication, depending on their location.

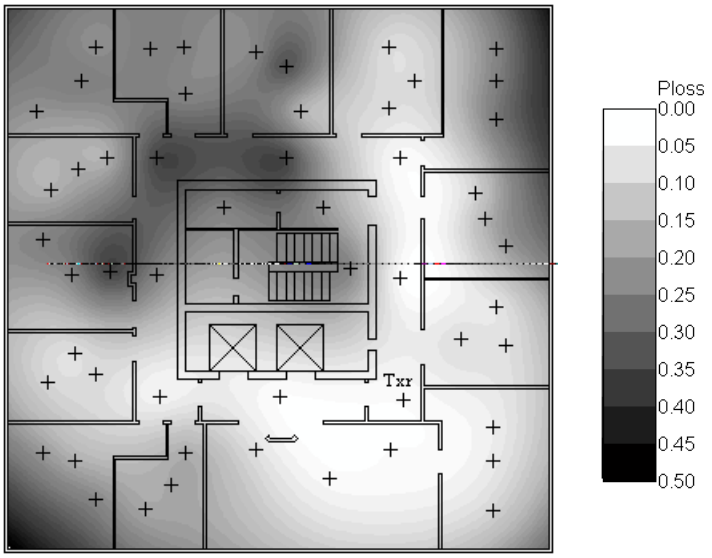

Figure 6.22: *Floor-wide variation in packet loss probability, P_{loss}, for an in-building pico-cellular PRMA system (Building D: Engineering Tower). M_s=20 users/floor, N_c=1.*

6.7 Summary

In this chapter the performance of both outdoor cellular and in-building pico-cellular PRMA speech systems have been determined using Markov analysis and computer simulations. It is assumed that reserved speech packets which suffer cochannel interference are not retransmitted, in order to reduce further interference to other terminals.

The Markov analysis employed to model the multiple cell PRMA systems is based on a single cell PRMA Markov analysis. This analysis requires determination of the mean number of cochannel interfering packets, $\overline{m_{coc}}$, received by the central cell base station per timeslot. Several techniques for estimating $\overline{m_{coc}}$ have been proposed in this chapter. The most accurate technique (Technique B, §6.3.2) assumes that the multiple cell PRMA system is homogeneous in so much as each cell experiences identical performance. Using this assumption, the average number of contending and reserved packets produced by cochannel interferers may be determined via an iterative approach. A similar technique was developed in Chapter 5 for the analysis of multiple cell S-ALOHA systems. Excellent agreement between Markov analysis and computer simulation results has been obtained, providing confidence in the analytical techniques developed.

From the results presented in §6.5 and §6.6 it has been found that PRMA is unable to operate particularly successfully in any of the multiple cell configurations considered. A comparison between single cell and multiple cell PRMA systems has revealed significant variations in system performance. These finding indicates that the approach presented in this chapter for handling cochannel interference is over simplistic. In particular, the benefit obtained by not retransmitting packets (in terms of reduced interference to other terminals) is unable to be realised as the system is incapable of operation, even for low terminal densities. Chapter 7 will investigate an alternative approach for handling cochannel interference, which is based on speech packet

retransmission. In addition, a simple base station receiver selection diversity technique, which can reduce the impact of inter-cell interference will be considered in Chapter 7.

Optimum performance is obtained in a cellular environment which has a high pathloss exponent, low shadowing variability and with base station receivers which can operate with a low capture ratio.

The location dependent performance of both outdoor cellular and in-building pico-cellular PRMA systems have been investigated. In the outdoor environment, the variations in the packet dropping, packet interference and total packet loss probabilities were determined as a function of the terminal to base station separation distance. The performance experienced by a central cell speech terminal was found to be highly dependent on their distance from the central cell base station. When the terminal was close to the base station, the packet dropping mechanism was the dominant source of degradation, whereas for terminals closer to the cell boundary, packet interference was the main source of packet loss. The variations in performance that exist over the coverage area of an in-building wireless system was also investigated. For the particular building considered, the central core was found to have a significant effect on the performance at certain locations. In particular, terminals in the shadow region of the floor experienced significantly worse performance compared to terminals on the same side as the transmitter.

References

[1] G. Wu, K. Mukumoto, A. Fukuda, "Analysis of an integrated voice and data transmission system using packet reservation multiple access," *IEEE Trans. Veh. Technol*., vol. 43, no. 2, May 1994, pp. 289 - 297.

[2] H. Qi, R. Wyrwas, “Markov analysis for PRMA performance study,” in *Proc. 44th IEEE Veh. Technol. Conf.*, Stockholm, Sweden, May 1994, pp.1184-1188.

[3] H. Qi, R. Wyrwas, “Capture effects on PRMA stability and performance,” *Electronics Letters*, vol. 30, no. 7, Mar. 31st 1994, pp. 539 - 540.

[4] C. van den Broek, R. Prasad, “Effect of capture on the performance of the PRMA protocol in an indoor radio environment with BPSK modulation,” *in Proc. 44th IEEE Veh. Technol. Conf.*, Stockholm, Sweden, May 1994, pp. 1223 - 1227.

[5] H. Qi, R. Wyrwas, "Performance analysis of joint voice-data PRMA over random packet error channels," *IEEE Trans. Veh. Technol*., vol. 45, no. 2, May 1996, pp. 332 - 345.

[6] X. Qiu, V. O. K. Li, “On the capacity of packet reservation multiple access with capture in personal communication systems,” *IEEE Trans. Veh. Technol.*, vol. 45, no. 4, Nov. 1996, pp. 666 - 675.

[7] S. Nanda, D. J. Goodman, U. Timor, “Performance of PRMA: a packet voice protocol for cellular systems,” *IEEE Trans. Veh. Technol.*, vol. 40, no. 3, Aug. 1991, pp. 584 - 598.

[8] L. Kleinrock, S. S. Lam, “Packet switching in a multi-access broadcast channel: performance evaluation,” *IEEE Trans. Commun.*, vol. 23, no. 4, Apr. 1975, pp. 410 - 422.

[9] N. S. Jayant, S. W. Christensen, "Effects of packet losses in waveform coded speech and improvements due to an odd-even sample interpolation procedure," *IEEE Trans. Commun.*, vol. 29, Feb. 1981, pp. 101-109.

[10] O. J. Wasem, D. J. Goodman, C. A. Dvorak, H. G. Page, "The effect of waveform substitution on the quality of PCM packet communications," *IEEE Trans. Commun.*, vol. 36, Mar. 1988, pp. 342-348.

[11] D. J. Goodman, S. X. Wei, "Efficiency of packet reservation multiple access," *IEEE Trans. Veh. Technol.*, vol. 40, no. 1, Feb. 1991, pp. 170 - 176.

[12] W. H. Press, B. P. Flannery, S. A. Teukolsky, W. T. Vetterling, *Numerical Recipes, The Art of Scientific Computing.* Cambridge University Press.

[13] K. S. Butterworth, K. W. Sowerby, A. G. Williamson, "A 1.8 GHz indoor wideband propagation study at The University of Auckland," *in School of Engineering Report No. 569, The University of Auckland*, Auckland, New Zealand, Sep. 1996.

Chapter 7

Multiple Cell PRMA Speech Systems with Packet Retransmission and Selection Diversity

7.1 Introduction

In the previous chapter the performance of speech only PRMA systems without packet retransmission in various multiple cell environments was determined. The performance of PRMA in these systems was found to be extremely poor, to the extent that the protocol was unable to operate in any of the multiple cell environments that were examined. Inter-cell interference was identified as the leading contributor towards this poor performance.

In an attempt to overcome the effects of inter-cell interference, an ideal base station antenna diversity scheme is considered in this chapter. This ideal selection diversity technique is capable of reducing the number of reserved speech packets corrupted by inter-cell interference. In addition to employing selection diversity, reserved speech packets that suffer corruption are retransmitted according to Scenario B, which was presented in Table 4.4. In particular, when a reserved PRMA speech packet encounters cochannel interference, the terminal that transmitted the packet loses it's reservation. In addition, the terminal is given an opportunity to retransmit the corrupted packet, providing it is not older than the packet delay limit.

As with Chapter 6, the performance of PRMA speech systems in both outdoor cellular and in-building pico-cellular environments are considered. The performance of these systems is determined using Markov analysis and computer simulation techniques.

In §7.2, appropriate capture probability expressions that include the effect of ideal selection diversity are developed. These capture probability expressions may be used to determine the probability of a desired (i.e. reserved) packet capturing a base station with selection diversity, in the presence of inter-cell interfering packets. The theory presented in §7.2 is based on the work presented in Chapter 4, where capture probability expressions without selection diversity were developed.

In §7.3 the Markov analysis for a multiple cell PRMA speech-only system with retransmission is presented. This analysis is similar to that presented in Chapter 6 for a multiple cell PRMA system without retransmission. As with the Markov analyses of Chapters 5 and 6, an estimate of the mean level of inter-cell interference is required in order to make the analysis tractable. The inter-cell interference estimation techniques developed previously in §6.3.2 and §6.3.3 can also be used to estimate the interference in a PRMA system with retransmission (see §7.4).

Results are presented in §7.5 and §7.6 in terms of the total speech packet loss probability, throughput per cell and system utilisation. These results are presented in relation to both outdoor cellular and in-building pico-cellular PRMA systems. Comparisons are made between systems

with and without speech packet retransmission and selection diversity. Systems suffering both Rayleigh fading and Suzuki fading are considered. Performance comparisons between PRMA systems and a number of TDMA systems are presented.

7.2 Selection Diversity

In Chapter 6, PRMA was found to perform poorly in all of the multiple cell systems examined due to the effect of inter-cell interference during reserved timeslots. In order to reduce the effect of inter-cell interference, selection diversity may be incorporated into the system design [1].

In a fading environment, selection diversity exploits the fact that if two or more independent inputs (branches) to a radio receiver are available it is possible, by switching between inputs, to achieve better reception quality than is possible with just a single input [2, p.183]. The improvement in reception quality depends on the number of branches that are employed, but dual branch receiving systems are probably the most attractive due to the increased cost and complexity of systems with more input branches. The diversity scheme considered in this chapter is based on a two-branch system. The most ideal form of selection diversity, namely *S*/*I diversity*[1] is considered. This selection diversity scheme assumes that the branch with the largest momentary SIR is selected in order to provide the largest possible SIR to the input of the base station receiver[2].

In the following section, capture probability expressions are presented for the situation where a desired (i.e., reserved) packet is received at a base station with two receiving branches, in the presence of m_{coc} inter-cell interfering packets. It is assumed that each packet undergoes Suzuki fading (see § 3.3.5).

7.2.1 Capture Probability Expressions

The capture probability for the situation where a single reserved packet is received (i.e., $m_{cen} = 1$) at a base station without selection diversity, in the presence of m_{coc} inter-cell interfering packets is given according to (4.22), namely

$$\Pr[Capture] = \prod_{y=1}^{m_{coc}} \frac{\overline{\overline{P_0}}}{\overline{\overline{P_0}} + 10^{\frac{x_y - x_0}{10}} z \overline{\overline{P_y}}}, \qquad \textbf{(7.1)}$$

where $\overline{\overline{P_0}}$ is the area mean power of the desired (i.e. reserved) packet, $\overline{\overline{P_y}}$ is the area mean power of the *y*th inter-cell interfering packet and z is the receiver capture ratio. The random variables, x_0 and x_y, represent the random fluctuation about the area mean powers of the desired and *y*th inter-cell interfering packets, respectively. These various terms where presented previously in Chapters 3 and 4 of this thesis. The complement of the capture probability is the outage probability, i.e.,

[1] Signal to Interference Ratio (SIR) diversity.

[2] In reality it is very difficult to measure the momentary SIR of each individual branch continuously. Fortunately, the branch with the largest SIR is also likely to have the largest total received power. A selection diversity system that selects the branch with the greatest received power is known as *S*+*I* diversity.

$$\Pr[Outage] = 1 - \Pr[Capture]. \qquad \textbf{(7.2)}$$

If $\Pr[Outage]$ is the same for each branch and each branch is independent, then the outage probability, $\Pr^m[Outage]$, for an *m*-branch selection diversity system is given by

$$\Pr^m[Outage] = \left[1 - \prod_{y=1}^{m_{coc}} \frac{\overline{\overline{P_0}}}{\overline{\overline{P_0}} + 10^{\frac{x_y - x_0}{10}} z\overline{\overline{P_y}}}\right]^m. \qquad \textbf{(7.3)}$$

For the specific case where *m*=2, the expression presented in (7.3) may be rewritten as

$$\Pr^2[Outage] = 1 - 2 \cdot \prod_{y=1}^{m_{coc}} \frac{\overline{\overline{P_0}}}{\overline{\overline{P_0}} + 10^{\frac{x_y - x_0}{10}} z\overline{\overline{P_y}}} + \left[\prod_{y=1}^{m_{coc}} \frac{\overline{\overline{P_0}}}{\overline{\overline{P_0}} + 10^{\frac{x_y - x_0}{10}} z\overline{\overline{P_y}}}\right]^2. \qquad \textbf{(7.5)}$$

The corresponding probability of capture, for a dual branch diversity system is therefore given by

$$\Pr^2[Capture] = 2 \cdot \prod_{y=1}^{m_{coc}} \frac{\overline{\overline{P_0}}}{\overline{\overline{P_0}} + 10^{\frac{x_y - x_0}{10}} z\overline{\overline{P_y}}} - \left[\prod_{y=1}^{m_{coc}} \frac{\overline{\overline{P_0}}}{\overline{\overline{P_0}} + 10^{\frac{x_y - x_0}{10}} z\overline{\overline{P_y}}}\right]^2. \qquad \textbf{(7.5)}$$

By including appropriate expressions for the area-mean powers, (7.5) may be used to analyse both outdoor cellular and in-building pico-cellular systems.

Outdoor Cellular Systems : In an outdoor cellular system the area mean power of an individual terminal's packet may be represented by (3.9). Under these circumstances the area-mean power of the desired and *y*th inter-cell interfering packet at the central cell base station is given by (4.23) and (4.25), respectively. By integrating over the joint random variable, $d_y(r_y, q_y)$, and over all possible levels of shadowing $\{x_y$ and $x_0\}$, the probability of the reserved speech packet capturing the central base station receiver from a distance r_0 (assuming 2-branch selection diversity) is found to be,

$$q^2(1, m_{coc}, r_0) = \int_{-\infty}^{\infty} \frac{e^{\frac{-x_0^2}{2\sigma_0^2}}}{\sqrt{2\pi}\,\sigma_0} \left[2 \cdot \left[g(r_0, x_0)\right]^{m_{coc}} - \left[h(r_0, x_0)\right]^{m_{coc}}\right] dx_0, \qquad \textbf{(7.6)}$$

where $g(r_0, x_0)$ was given in (4.29) and where

$$h(r_0, x_0) = \int_{-\infty}^{\infty} \frac{e^{\frac{-x_y^2}{2\sigma_y^2}}}{\sqrt{2\pi}\,\sigma_y} \int_0^{R_c} \frac{2r_y}{R_c^2} \int_0^{2\pi} \frac{1}{2\pi} \cdot \left[\frac{\left[d_y(r_y, q_y)\right]^{\beta_y}}{\left[d_y(r_y, q_y)\right]^{\beta_y} + 10^{\frac{x_y - x_0}{10}} z r_0^{b_0}}\right]^2 dq_y\, dr_y\, dx_y. \qquad \textbf{(7.7)}$$

The superscript in the term $q^2(1, m_{coc}, r_0)$ refers to a system with 2-branch selection diversity. As with the capture probability expressions presented in Chapter 4, (7.6) must be solved using numerical integration techniques, such as those presented in Appendix A. Having determined $q^2(1, m_{coc}, r_0)$, it is possible to determine the capture probability expression $q^2(1, m_{coc})$ using the relationship presented in (4.9), i.e.,

$$q^2(1, m_{coc}) = \int_0^{R_c} q^2(1, m_{coc}, r_0)\, f_r(r_0) dr_0, \qquad \textbf{(7.8)}$$

where $f_r(r_0)$ was presented in (4.2). $q^2(1, m_{coc})$ represents the probability of a reserved packet, transmitted by a central cell terminal, capturing the central cell base station in the presence of m_{coc} inter-cell interfering packets, assuming the base station has 2-branch selection diversity.

In-Building Pico-Cellular Systems : In an in-building pico-cellular system the area mean power of an individual terminal's packet may be represented by (3.19). In this situation the area-mean power of the desired and *y*th inter-cell interfering packet is given by (4.23) and (4.30), respectively. Under these circumstances, the capture probability for an in-building system with 2-branch ideal selection diversity is also given by (7.6), although $g(r_0, x_0)$ is given in (4.31) and $h(r_0, x_0)$ is given by

$$h(r_0, x_0) = \int_{-\infty}^{\infty} \frac{e^{\frac{-x_y^2}{2s_y^2}}}{\sqrt{2p}\, s_y} \int_0^{R_c} \frac{2r_y}{R_c^2} \cdot \left[\frac{faf_y \cdot \left[d_y(r_y)\right]^{p_y}}{faf_y \cdot \left[d_y(r_y)\right]^{p_y} + 10^{\frac{x_y - x_0}{10}} z d_0^{b_0}(r_0)} \right]^2 dr_y dx_y \,. \qquad \textbf{(7.9)}$$

7.2.2 Capture Probability Results

Fig. 7.1 illustrates how two-branch selection diversity can be used in increase the probability of a desired packet capturing the central cell base station. In this example, an outdoor cellular system (N_c=3) suffering Rayleigh fading ($s = 0$ dB) and Suzuki fading ($s = 6$ dB) is considered. The capture probability, $q^m(1, m_{coc})$, is presented as a function of the number of inter-cell interfering packets, m_{coc}, received in a timeslot. The probability of capture is compared for a central cell base station with both single branch (i.e., *m*=1) and dual-branch (*m*=2) receiving antennas. Both analytical results (lines) and simulation results (points) are presented in Fig. 7.1.

It can be observed from Fig. 7.1 that irrespective of whether or not selection diversity is employed, the probability of capture is higher in a Rayleigh fading only environment than in a Suzuki fading environment. This result, which was discussed previously in Chapter 4, is attributable to the increased variability associated with Suzuki fading. The dual-branch selection diversity system results in an improvement in the capture probability for both Rayleigh fading and Suzuki fading environments. For the example illustrated in Fig. 7.1, the capture probability is approximately 10 % greater with a dual-branch system, compared to a single branch system. Capture probability expressions, such as those developed in this section, will be incorporated in the Markov analysis of the following section.

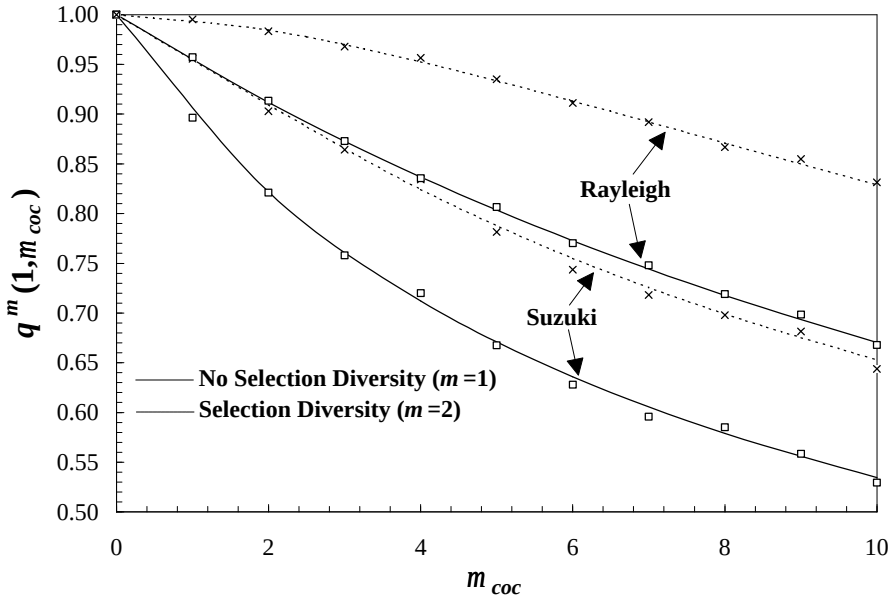

Figure 7.1: *Probability of desired terminal capturing the central cell base station in Suzuki fading (s =6 dB) and Rayleigh fading (s =0 dB) outdoor cellular systems with and without 2-branch selection diversity. N_c=3, z=10 dB, b =4. Analytical results (lines) and simulation results (points) are presented.*

7.3 Markov Analysis

In this section, the Markov analysis of a multiple cell PRMA speech system with retransmission is presented. The procedure used in the Markov analysis of Chapter 6 (Fig. 6.1) is also used in this chapter. Several differences exist between the Markov analysis of this chapter and that of Chapter 6. These differences are attributable to the way that cochannel interference is handled by speech terminals during the reservation state. These differences require several modifications be made to the speech terminal model, the one-step state transition probability distribution and the system performance measures, which are presented in the following sections.

7.3.1 Terminal Transition Probabilities

In this chapter, it is assumed that speech terminals attempt retransmission of any packets corrupted by inter-cell interference. In particular, the terminal involved returns to the contention state and re-contends for a new timeslot reservation. The speech terminal model for this scenario is presented in Fig. 7.2. Compared with Fig. 6.2, Fig. 7.2 incorporates an additional state transition from state RES_0 to *CON*. This event models the probability of a reserved speech packet suffering cochannel interference and returning to the contention state (denoted as a *RC* transition). This probability is given by $P_{int}(1-g_f)$, where P_{int} is the speech packet interference probability, defined previously in (6.14), namely

$$P_{int} = 1 - q^1(1, \overline{m_{coc}}). \qquad \textbf{(7.10)}$$

The term $q^1(1,\overline{m_{coc}})$ is the probability that a reserved speech packet captures a single branch base station in the presence of $\overline{m_{coc}}$ (mean value) inter-cell interfering packets. If 2-branch selection diversity is incorporated into the system design, the term $q^2(1,\overline{m_{coc}})$ (given by (7.8)) should be used. All other terminal transition probabilities in Fig. 7.2 are the same as those presented previously in § 6.2.1.

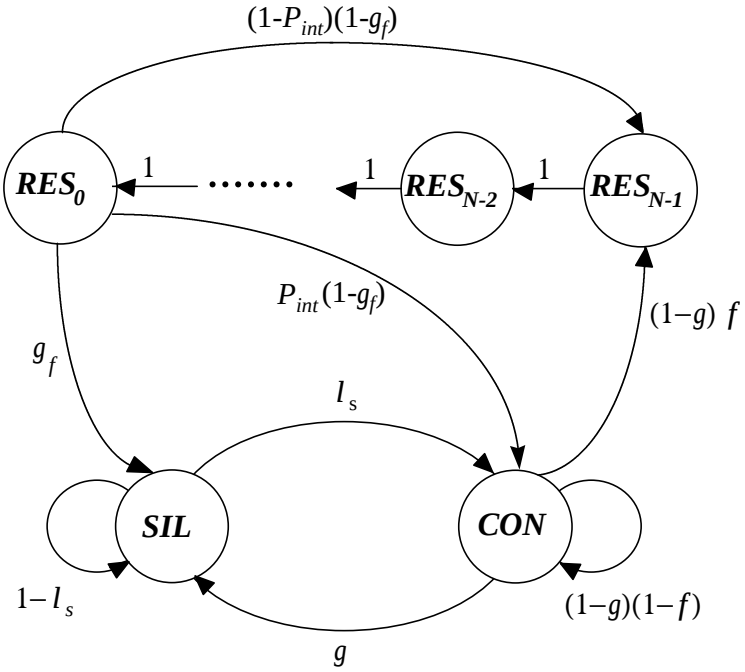

Figure 7.2: *PRMA speech terminal model (packet retransmissions)*

7.3.2 The One-Step State Transition Probability

Based on the PRMA speech terminal model presented in Fig. 7.2, it is possible to determine the one-step state transition probability distribution, $\pi(i, j|C, R)$. This distribution is similar to that presented in Chapter 6 for a system without speech retransmission. For a system with packet retransmission, the following basic rules apply:

1) If there are *R* terminals holding reservations in the *t*-th timeslot, then in the (*t*+1)-th timeslot, there can be either *R*+1, *R*, or *R*-1 terminals holding reservations, because only one terminal can lose or receive a reservation in a timeslot.
2) Likewise, if there are *C* terminals in the contention (*CON*) state in the *t*-th timeslot, there will be either $C+x-y-1$, $C+x-y$ or $C+x-y+1$ terminals in *CON* in the (*t*+1)-th timeslot. The first case corresponds to *x SC*, *y CS*, one *CR* and no *RC* transitions occuring, the second case corresponds to *x SC*, *y CS*, no *CR* and no *RC* transitions occuring, while the final case corresponds to *x SC*, *y CS*, no *CR* and one *RC* transitions. The events *SC*, *CS* and *CR* were described previously in § 6.2.1 and the event*RC* was discussed in §7.3.1.

It is therefore possible to list the changes to the system state $\{C,R\}$ which can occur in progressing from one timeslot to the next, as follows:

$$\{C,R\} \rightarrow \begin{cases} \{i = C + x - y - 1,\ j = R + 1\} \\ \{i = C + x - y,\ j = R\} \\ \{i = C + x - y,\ j = R - 1\} \\ \{i = C + x - y + 1,\ j = R - 1\} \end{cases} \qquad 0 \le x \le S,\ 0 \le y \le C \tag{7.11}$$

Only those situations where the events *SC* and *CS* occur at one or less terminals per timeslot are considered in this chapter. Therefore, only those situations where $x \in [0,1]$ and $y \in [0,1]$ are considered. The probabilities of no *SC*, one *SC*, no *CS* and one *CS* transitions were presented previously in (6.8) to (6.11). Under these circumstances, the one-step state transition probability distribution is given by

$$\pi(i, j|C, R) =$$

$\Pr(oneCS, noSC, oneCR)$	$i = C - 2$	$j = R + 1$
$\Pr(noCS, noSC, oneCR) + \Pr(oneCS, oneSC, oneCR)$	$i = C - 1$	$j = R + 1$
$\Pr(noCS, oneSC, oneCR)$	$i = C$	$j = R + 1$
$\Pr(oneCS, noSC, noRS, noRC) + \Pr(oneCS, noSC, noCR)$	$i = C - 1$	$j = R$
$\Pr(noCS, noSC, noRS, noRC) + \Pr(oneCS, oneSC, noRS, noRC)$ $+ \Pr(noCS, noSC, noCR) + \Pr(oneCS, oneSC, noCR)$	$i = C$	$j = R$
$\Pr(noCS, oneSC, noRS, noRC) + \Pr(noCS, oneSC, noCR)$	$i = C + 1$	$j = R$
$\Pr(oneCS, noSC, oneRS)$	$i = C - 1$	$j = R - 1$
$\Pr(noCS, noSC, oneRS) + \Pr(oneCS, oneSC, oneRS)$ $+ \Pr(oneCS, noSC, oneRC)$	$i = C$	$j = R - 1$
$\Pr(noCS, oneSC, oneRS) + \Pr(noCS, noSC, oneRC)$ $+ \Pr(oneCS, oneSC, oneRC)$	$i = C + 1$	$j = R - 1$
$\Pr(noCS, oneSC, oneRC)$	$i = C + 2$	$j = R - 1$
0	*elsewhere*	

(7.12)

The symbol *noX* in (7.12) means that event *X* does not occur in the next timeslot, while *oneX* means that event *X* happens at one terminal in the next timeslot. The complete expansion of (7.12) is presented in Appendix B.

7.3.3 State Probability Distribution

Having determined $\pi(i, j|C, R)$, it is possible to calculate the state probability distribution, $\pi(C, R)$, using the procedure presented in §6.2.3. Fig. 7.3 presents the state probability distribution, $\pi(C, R)$, for a multiple cell PRMA system with packet retransmission. The same parameters that were considered in Fig. 6.3, namely M_s=60 and N=8, are also considered for the result presented in Fig. 7.3. The state probability distribution for a system with retransmission is significantly different from that obtained for a system without retransmission. From Fig. 7.3, it is

clear that speech terminals in a PRMA system with speech packet retransmission are far more likely to be in the contention state and less likely to be in the reservation state.

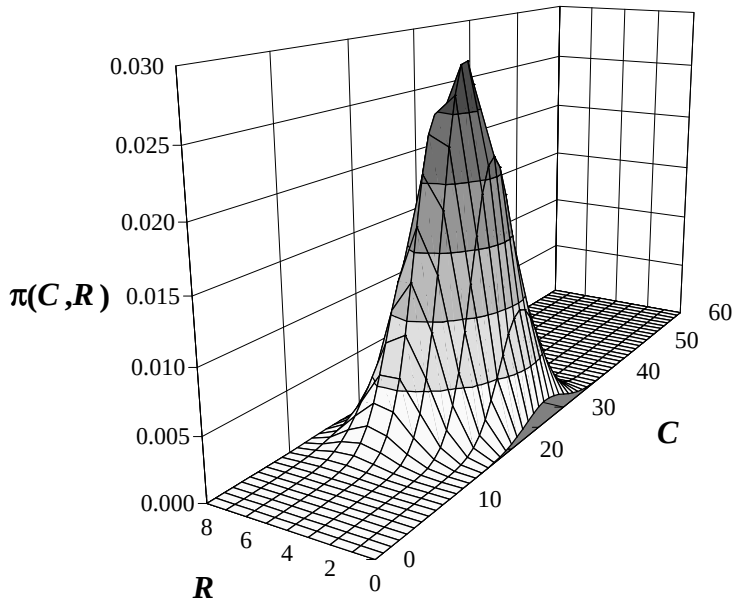

Figure 7.3: *Example of the state probability distribution, $\pi(C,R)$, which describes the probability of having C users in the CON state and R users in the RES_i states. A multiple cell PRMA system with M_s=60, N=8, packet retransmissions and no selection diversity is considered.*

7.3.4 Performance Measures

A number of the performance measures presented in §6.2.4 for a system without retransmission can also be considered for a multiple cell PRMA system with retransmission. In particular, the normalised capacity, c, the throughput per cell, h, and the system utilisation, y remain unchanged. However, it is necessary to reconsider the expressions presented in Chapter 6 for the packet dropping probability, P_{drop}, and the total packet loss probability, P_{loss}.

In a system with packet retransmission, packets are not lost directly as a result of inter-cell interference, as packets that suffer interference have a chance to be retransmitted in a subsequent timeslot. However, it is possible for the packet to be subsequently dropped due to delay in obtaining a new timeslot reservation. This phenomenon is illustrated in Fig. 7.4. The packet dropping probability, P_{drop}, is therefore, comprised of two components namely

$$P_{drop} = P_{drop0} + P_{drop1}, \qquad \textbf{(7.13)}$$

where P_{drop0} is the probability of packets being dropped during the initial contention period, (i.e., at the start of the talkspurt) and P_{drop1} is the probability of packets being dropped during subsequent re-contention periods (i.e., following packet transmission errors). A speech users

perception of these impairments would consist of both front-end and mid-talkspurt clipping, as was the case in Chapter 6.

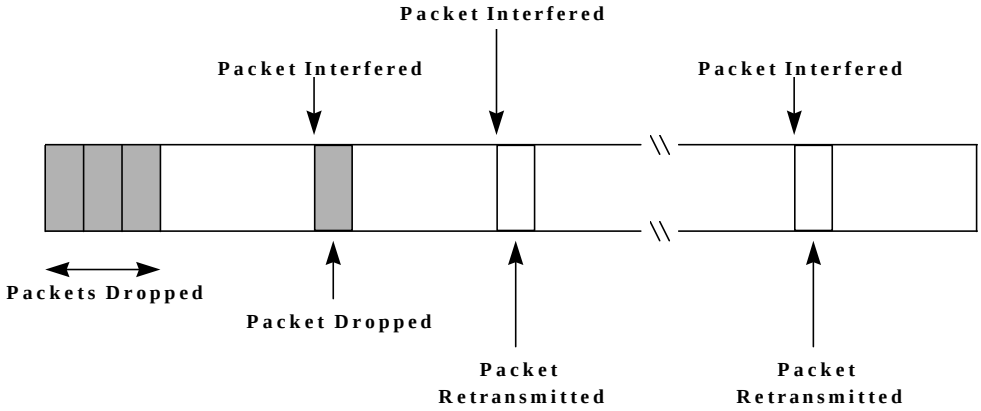

Figure 7.4: *A speech talkspurt may suffer packet dropping at the beginning of the talkspurt as well as after some packet interference instances.*

Expressions for P_{drop0} and P_{drop1} have been presented previously in [3] and [4]. Investigation into these expressions has revealed significant variations in the estimations, not only between the various expressions, but when the analytical results are compared to computer simulation results. An alternative packet dropping probability expression for systems with speech packet retransmission has been developed during the course of the research, namely

$$P_{drop} = \frac{\overline{P_{Gen}} - \overline{P_{Txd}}}{\overline{P_{Gen}}}, \tag{7.14}$$

where $\overline{P_{Gen}}$ represents the mean number of packets generated per timeslot and $\overline{P_{Txd}}$ represents the mean number of packets successfully transmitted per timeslot. The mean number of packets generated per timeslot can be approximated using the speech activity factor presented in (2.4), together with the number of users per cell, M_s and the number of timeslots per cell, N, such that

$$\overline{P_{Gen}} = \frac{SAF \cdot M_s}{N}. \tag{7.15}$$

The mean number of successfully transmitted packets per timeslot, $\overline{P_{Txd}}$, is equivalent to the throughput per cell, h. The throughput per cell for a system without selection diversity can be calculated using the expressions presented in (6.31) and (6.32). If two-branch selection diversity is considered, then the term $q(1, \overline{m_{coc}})$ in (6.32) should be replaced with $q^2(1, \overline{m_{coc}})$, which was presented in (7.8). The packet dropping probability expression presented in (7.14) can, therefore, be rewritten as

$$P_{drop} = 1 - \frac{N \cdot h}{SAF \cdot M_s} . \quad \textbf{(7.16)}$$

The expression presented in (7.16) for P_{drop} is considerably simpler than that presented in [3] or [4] and, as will be shown in the following sections of this chapter, provides excellent agreement with results obtained from computer simulations. The total packet loss, P_{loss}, in a multiple cell PRMA system with retransmission, is comprised solely of dropped packets, i.e.,

$$P_{loss} = P_{drop} . \quad \textbf{(7.17)}$$

Maximum speech packet loss probabilities of either P_{loss}=1% or P_{loss}=5% are considered, as in Chapter 6. A maximum packet loss probability of 5% corresponds to a system that incorporates speech packet interpolation techniques. The capacities of various multiple cell PRMA systems will be determined in the following sections of this chapter, based on these constraining values.

7.4 Inter-Cell Interference Estimation

In the Markov analyses of Chapters 5 and 6, estimates of the mean level of inter-cell interference, $\overline{m_{coc}}$, were made in order to simplify the analysis. These estimates meant that the analysis of a multiple cell system could be performed by considering only a single cell Markov analysis. The inter-cell interference techniques considered in Chapter 6 are also considered in this chapter. These techniques are summarised as follows:

- **Technique A** (*Estimation Based on Speech Activity Factor*)**:** This technique, which was described previously in §6.3.1, assumes that $\overline{m_{coc}}$ is dependent only on the number of speech terminals per cell, M_s, the mean speech activity factor, *SAF*, and *L*, the number of cochannel interfering cells. For systems without retransmission, this technique was found, in most cases, to be capable of accurately predicting $\overline{m_{coc}}$. However, in situations where the system was congested this technique over-estimated the level of inter-cell interference.

- **Technique B (***Estimation based on Number of Reserved and Contending Terminals*)**:** This technique, which was described previously in §6.3.2 and §6.3.3, assumes that the system is homogeneous, such that each cell has identical performance. Based on this assumption, it is possible to estimate the number of cochannel terminals in the contention and reservation states, from which a more accurate estimate of $\overline{m_{coc}}$ can be obtained. This technique was found to be superior in terms of accuracy, compared to Technique A, although the complexity was somewhat greater.

Techniques A and B can be applied to multiple cell PRMA systems with retransmission in exactly the same way as they were applied in Chapter 6 to systems without retransmission. By way of an example, Fig. 7.5 presents the inter-cell interference, $\overline{m_{coc}}$, in an in-building pico-cellular PRMA system with retransmission (Building B, N_c=3). These estimates have been obtained using analytical techniques (Techniques A and B) as well as computer-based

simulations (Model II, §5.4.2). An estimate of $\overline{m_{coc}}$ obtained for an identical system, but without speech packet retransmission, is also included in Fig. 7.5 for reference.

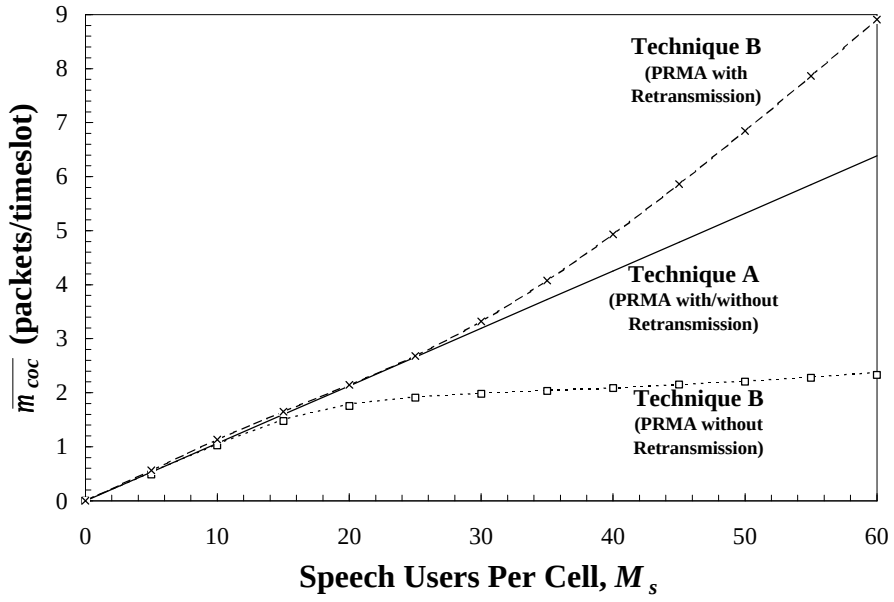

Figure 7.5: *Comparison of $\overline{m_{coc}}$ estimations in an in-building pico-cellular PRMA system (Building B: San Ramon, Nc=3) with and without packet retransmission. z=10 dB, no selection diversity. Markov analysis results (lines) and simulation results (points) are presented.*

It can be observed from Fig. 7.5 that a significant difference exists between the estimates of $\overline{m_{coc}}$ obtained for the system with packet retransmission. In particular, the inter-cell interference estimated according to Technique B is significantly greater than that estimated using Technique A. Computer simulation results closely agree with the estimation provided by Technique B. This indicates that Technique A may not be suitable for predicting the level of $\overline{m_{coc}}$ in a PRMA system with retransmission. This is due to Technique A not explicitly considering the number of cochannel speech terminals in the respective contention and reservation states. Rather, Technique A is based on the mean speech activity factor, which represents the mean number of speech packets generated by terminals, as opposed to the actual number of speech packets transmitted by terminals.

A significant feature of Fig. 7.5 is the comparison that can be made between the respective estimates of $\overline{m_{coc}}$ for systems with and without speech packet retransmission. In systems without retransmission, the level of inter-cell interference plateaus off after a certain number of users are added to the cell. This effect, which was discussed in Chapter 6, is due to the packet dropping mechanism, which reduces the number of transmitted packets. In addition, in a system without retransmission any reserved packets that suffer interference are not retransmitted, therefore reducing the amount of inter-cell interference. It can be seen, however, that in a system with retransmission the level of inter-cell interference increases significantly with an increasing number of users per cell. This indicates that for high user densities, the performance of PRMA

systems with packet retransmission is likely to be poorer than equivalent systems without retransmission. This finding will be presented in §7.5.2.

7.5 Performance of Outdoor Cellular PRMA

In this section, the performance of PRMA in an outdoor cellular system is determined in terms of P_{loss}, h and y. Analytical results obtained from Markov analysis are compared to those obtained from Monte Carlo simulations. Systems with and without selection diversity and packet retransmission are compared. The frequency reuse plan that results in optimum performance is determined for systems with packet retransmission and selection diversity, for both Suzuki and Rayleigh fading environments. Clusters sizes of N_c=1, 3 and 4 are considered, as in Chapter 6. The system parameters for these various frequency reuse configurations were presented previously in Table 4.2. As with Chapter 6, it is assumed that the speech coding rate, R_s=32 kb/s, while the speech packet information size, I=576 bits and the speech packet header size, H=64 bits. In addition, it is assumed that the speech permission probability, p_s=0.3, the speech packet delay limit, D_{max}=36 ms. Finally, it is assumed that the mean talkspurt duration, t_1=1.00 s and mean silence duration, t_2=1.35 s.

7.5.1 Comparison of Markov and Simulation Techniques

In this section, the effectiveness of the various Markov analysis and computer simulation techniques to accurately estimate the system performance is determined. In particular, Markov analyses that use the inter-cell interference estimation techniques discussed in §7.4 (Technique A and B) are compared with computer simulation results (Model II, § 5.4.2).

Fig. 7.6 presents the speech packet loss probability, P_{loss}, for an outdoor cellular PRMA system (N_c=1) with packet retransmission, operating in a Suzuki fading environment. It can be observed that there is a significant difference between the results predicted using Markov analyses based on Technique A and B. In addition, the computer simulation results tend to support the Markov analysis based on Technique B. This finding was also found to be true in the case of Fig. 7.5, where the mean inter-cell interference, $\overline{m_{coc}}$, was considered.

Fig. 7.7 presents the throughput per cell, h, for the same system considered in Fig. 7.6. As with Fig. 7.6, the variation between the two Markov analyses is significant, with the computer simulation results supporting the Markov analysis based on inter-cell interference estimation Technique B. The remainder of the results presented in this chapter will rely on Markov analysis using Technique B, together with simulation results obtained using Simulation Model II.

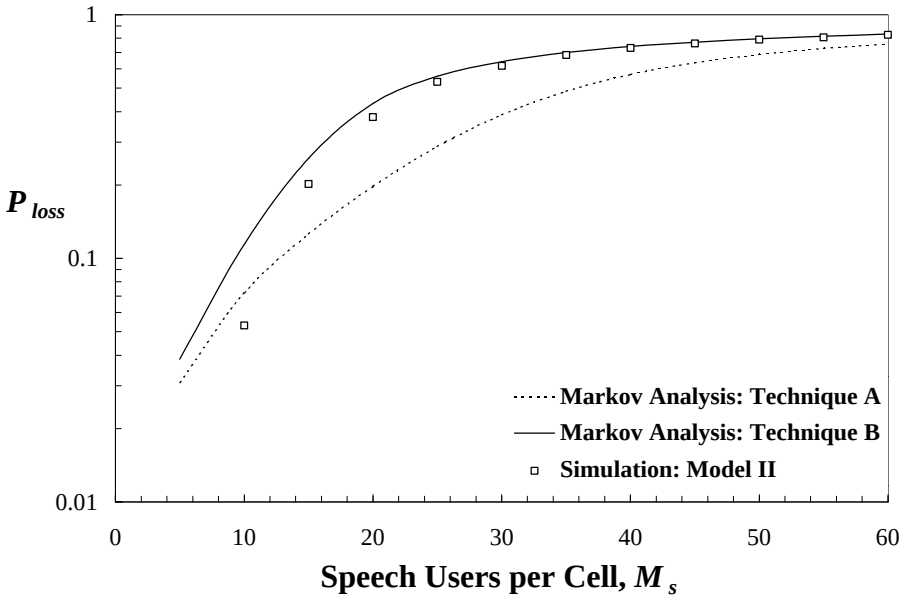

Figure 7.6: *Speech packet loss probability, P_{loss}, of an outdoor cellular PRMA system (N_c=1) with packet retransmission and no selection diversity. Suzuki fading is considered, s =6 dB, b =4, z=10 dB.*

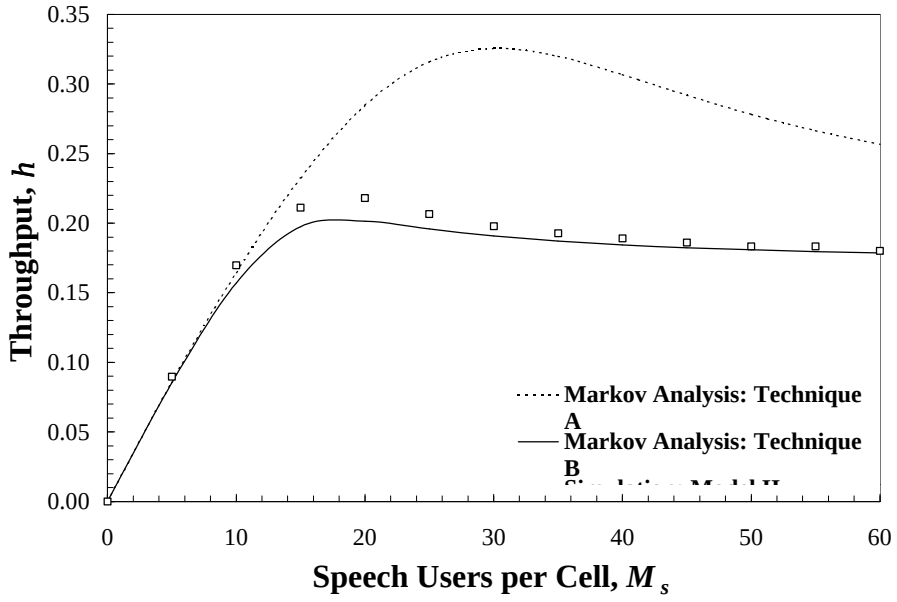

Figure 7.7: *Throughput per cell, h, of an outdoor cellular PRMA system (N_c=1) with packet retransmission and no selection diversity. Suzuki fading is considered, s =6 dB, b =4, z=10 dB.*

7.5.2 Effect of Packet Retransmission

In this section, the effect of packet retransmission on the performance of outdoor cellular PRMA systems is examined. In particular, the performance of PRMA systems with and without speech packet retransmission are compared. This comparison will determine when, if at all, it is appropriate to employ such retransmission. Systems without selection diversity are considered.

In Fig. 7.8(a), the speech packet loss probability, P_{loss}, for an outdoor cellular PRMA system (N_c=1) with and without packet retransmission is presented, while in Fig. 7.8(b) the throughput per cell, h, for this system is presented.

It can be observed that for the scenario considered, packet retransmission is beneficial to system performance providing the number of users per cell is low (in the case of Fig. 7.8(a), for $M_s < 22$). In this situation, retransmission can be performed with a higher probability of success, therefore minimising the effect of the additional interference to other PRMA users. In situations, however, where there are a large number of users per cell, packet retransmission results in a reduced system performance, in terms of P_{loss} and h. This is due to the probability of successfully retransmitting a packet on the first attempt being low in a highly congested network. In practice, a packet may need to be retransmitted multiple times before being successfully received at it's respective base station. This, in turn, increases the interference to other terminals, resulting in reduced system performance.

Fig. 7.9 presents results for the same systems considered in Fig. 7.8 although a cluster size of N_c=3 is considered. In this situation, the benefit of employing packet retransmission appears to have disappeared almost completely, even though a cluster size of N_c=3 has a greater frequency reuse separation distance, D, compared to a system with N_c=1. A system with N_c=3 has, however, fewer timeslots per cell compared to a system with N_c=1. This leads to terminals in the retransmission mode experiencing increased difficulty (and therefore delay) in obtaining available timeslots in which to retransmit. This situation is true even for low user densities.

It appears clear that a tradeoff exists between the choice of cluster size and the level of retransmission. As the cluster size is decreased, speech packet retransmission becomes increasingly more attractive, although the results indicate that an improvement in PRMA performance can only be obtained if the user density is between low to moderate.

It should be made clear that the performance of PRMA in a multiple cell system is still disappointing, even with packet retransmission incorporated into the system design, when compared to the performance of single cell PRMA systems presented previously in the literature.

7.5.3 Effect of Selection Diversity

The results of §7.5.2 indicated that even with packet retransmission, the performance of PRMA in an outdoor cellular system was, at best, extremely poor. In an effort to improve the performance, 2-branch selection diversity (see §7.2) has been incorporated in the system design.

Fig. 7.10 presents the speech packet loss probability, P_{loss}, and the throughput per cell, h, for an outdoor cellular PRMA system (N_c=3) with packet retransmissions. Systems with and without selection diversity are considered, for both Rayleigh fading and Suzuki fading scenarios.

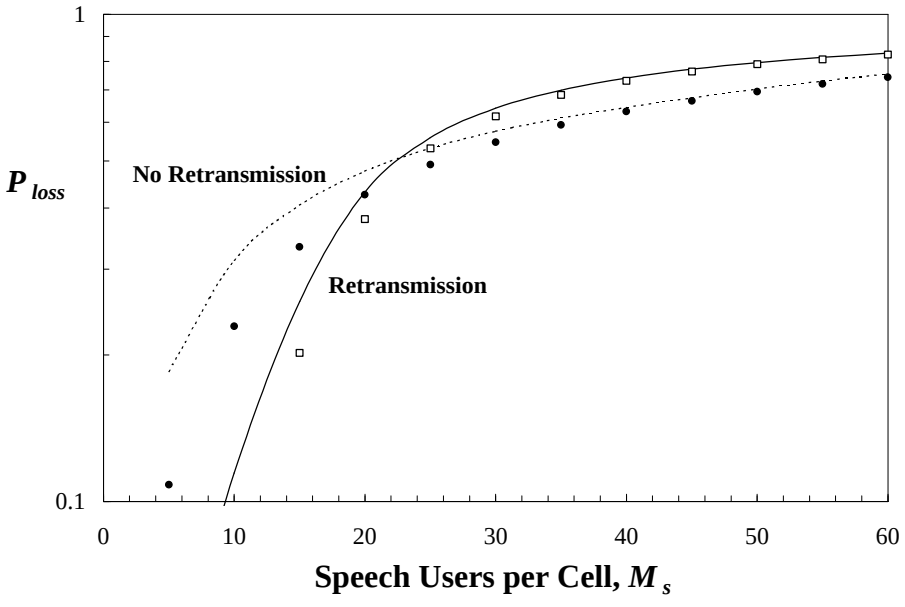

(a)

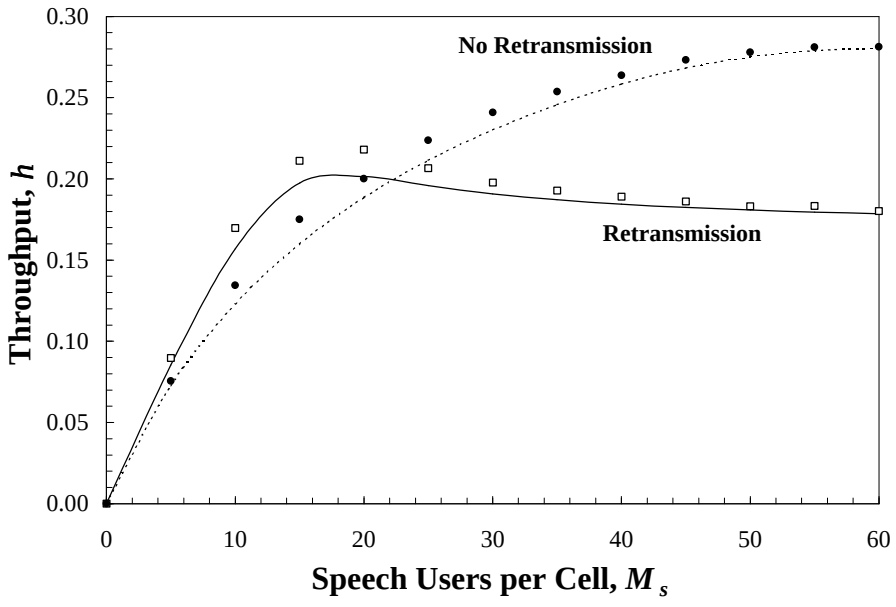

(b)

Figure 7.8: (a) *Speech packet loss probability, P_{loss}, and* **(b)** *throughput per cell, h, of an outdoor cellular PRMA system with and without packet retransmission. N_c=1, s =6 dB, b =4, z=10 dB, no selection diversity. Markov analysis results (lines) and simulation results (points) are presented.*

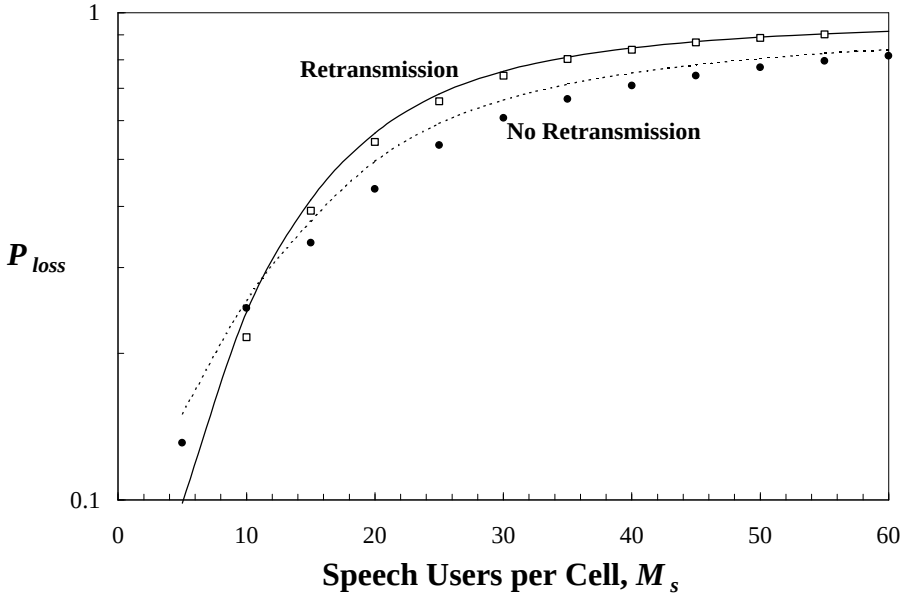

(a)

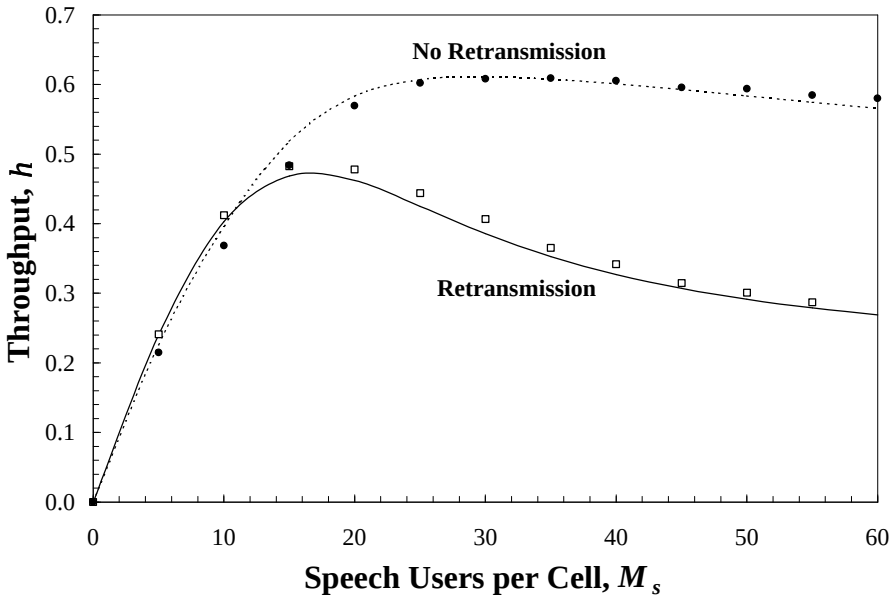

(b)

Figure 7.9: (a) *Speech packet loss probability, P_{loss}, and* **(b)** *throughput per cell, h, of an outdoor cellular PRMA system with and without packet retransmission. N_c=3, s =6 dB, b =4, z=10 dB, no selection diversity. Markov analysis results (lines) and simulation results (points) are presented.*

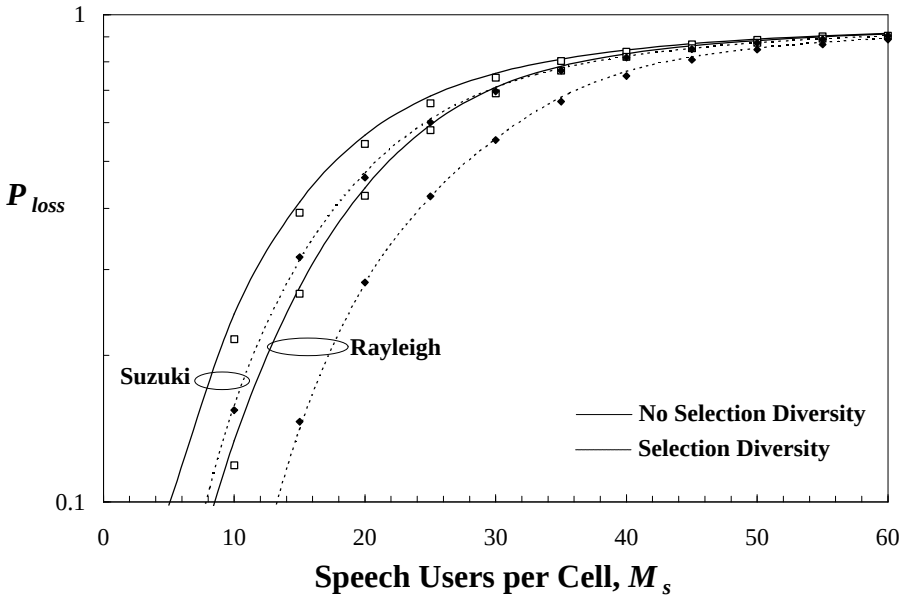

(a)

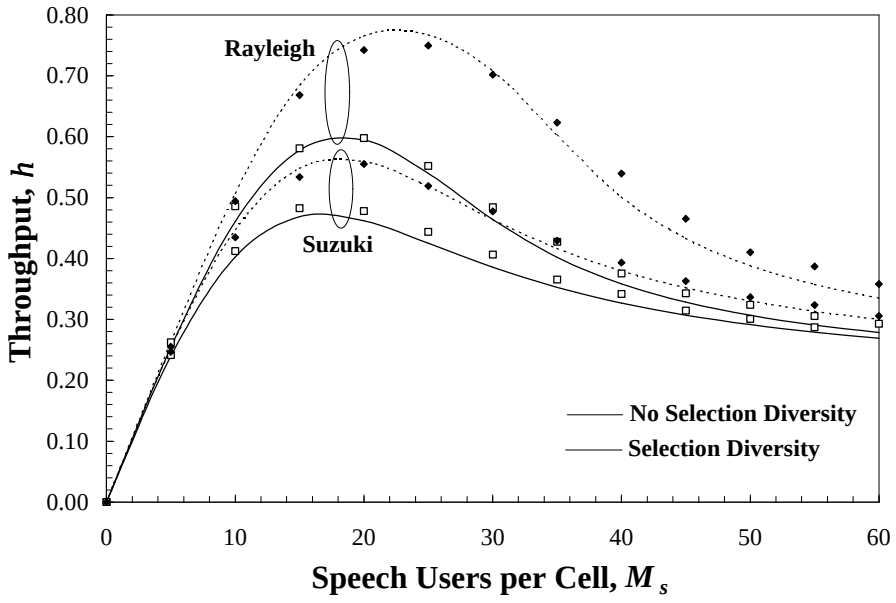

(b)

Figure 7.10: (a) *Speech packet loss probability, P_{loss}, and* **(b)** *throughput per cell, h, of an outdoor cellular PRMA system with packet retransmission and with/without selection diversity. N_c=3, s =0, 6 dB, b =4, z=10 dB. Markov analysis results (lines) and simulation results (points) are presented.*

It can be observed from Fig. 7.10 that selection diversity is capable of combating the effect of inter-cell interference, resulting in a lower number of lost packets and an improved throughput. Selection diversity is able to provide the greatest benefit in a Rayleigh fading environment, although it is still beneficial in a Suzuki fading environment.

7.5.4 Determination of Optimum Frequency Reuse Plan

In this section, the optimum frequency reuse plan for an outdoor cellular PRMA system with packet retransmission and selection diversity is determined. Fig. 7.11 and Fig. 7.12 present the total packet loss probability and system utilisation for such a system in Suzuki fading (s =6 dB) and Rayleigh fading (s =0 dB) environments, respectively. In order to determine the optimum frequency reuse plan, cluster sizes of N_c=1, 3 and 4 are considered. Both Markov analysis (lines) and simulation results (points) are presented. It is assumed that z=10 dB and b =4 in all cases.

Fig. 7.11 presents the speech packet loss probability, P_{loss}, and system utilisation, y , for a system suffering Suzuki fading. It is clear that N_c=1 provides the best performance in such an environment over the range of M_s values evaluated. The level of packet loss is considerably higher and the system utilisation is considerably lower in systems with N_c=3 and N_c=4. This finding is in sharp contrast to that of Fig. 6.11, where no cluster size was able to provide a clear advantage[3]. Systems with N_c=1 have considerably more timeslots per cell than systems with N_c=3 or N_c=4. With N_c=1, there are more opportunities for contending terminals to have packets successfully retransmitted during available timeslots. Re-using the spectrum in each cell and employing retransmission is therefore a better option than employing a fixed frequency reuse plan PRMA system without retransmission.

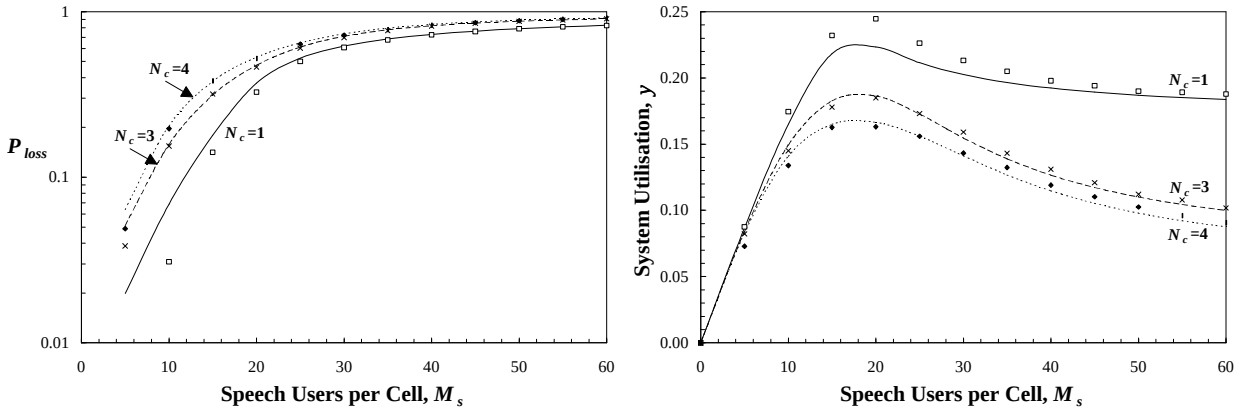

Figure 7.11: (a) *Speech packet loss probability, P_{loss}, and* **(b)** *system utilisation, y , of an outdoor cellular PRMA system with packet retransmission and selection diversity. N_c=1, 3, 4. s = 6 dB, b =4, z=10 dB. Markov analysis results (lines) and simulation results (points) are presented.*

Fig. 7.12 presents the speech packet loss probability, P_{loss}, and system utilisation, y , for a identical system to that considered in Fig. 7.11, although Rayleigh fading is considered. In this situation, the probability of packet loss is reduced and the system utilisation is increased, compared to an identical system operating in a Suzuki fading environment. Unlike Fig. 7.11, a

[3] The results of Fig. 6.11 were based on an identical system to Fig. 7.11, although neither speech packet retransmissions or selection diversity were considered.

cluster size of N_c=1 is no longer clearly the best choice of frequency plan for all user densities (i.e., across all values of M_s). However, such a configuration still provides the highest system capacity, based on both the 1% or 5% maximum tolerable packet loss levels.

It should be noted that none of the configurations presented in Fig. 7.11 or Fig. 7.12 are capable of supporting a significant number of users, based on the total packet loss probability constraint of either 1% or 5%. Actual capacity estimations are presented in the following section. Even with speech packet retransmission and selection diversity, the performance of PRMA in an outdoor cellular system is not as promising as earlier research, based on the analysis of single cell PRMA systems, has suggested.

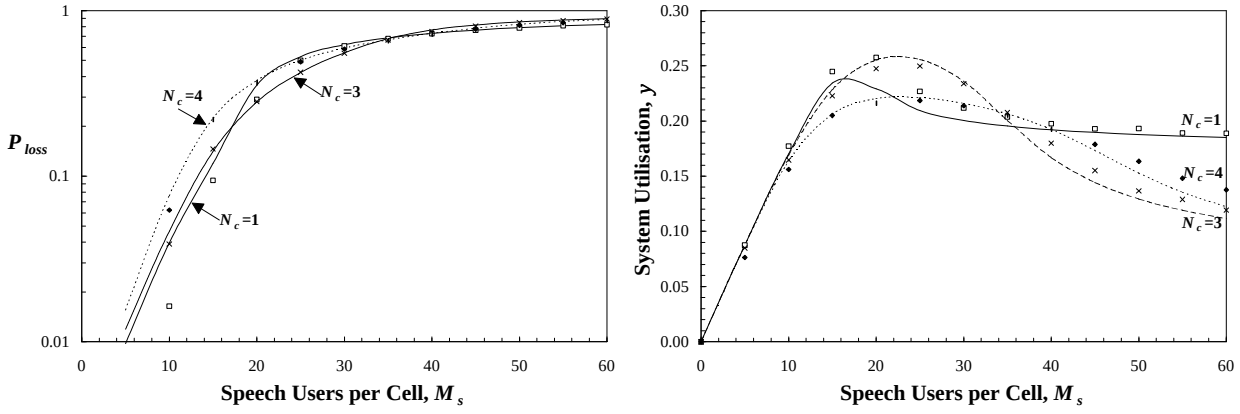

Figure 7.12: (a) *Speech packet loss probability, P_{loss}, and* **(b)** *system utilisation, y, of an outdoor cellular PRMA system with packet retransmission and selection diversity. N_c=1, 3, 4. s = 0 dB, b =4, z=10 dB. Markov analysis results (lines) and simulation results (points) are presented.*

7.5.5 Capacity Estimations

Based on the results presented in the previous section, it is possible to estimate the capacities of the outdoor cellular PRMA systems presented in Fig. 7.11 and Fig. 7.12. These capacity estimations have been obtained by extrapolating the Markov analysis and computer simulation results and are in terms of the maximum number of speech terminals, M_s, able to be supported per cell. Capacity estimations are presented in Table 7.1. Consideration is given to clusters sizes of N_c=1, 3, and 4, for both Suzuki fading and Rayleigh fading environments. Comparison with Chapter 6 system capacities can be made using Table 6.2.

Fig. 7.13 provides comparison of the estimated system capacities for the various outdoor cellular PRMA systems considered in Chapters 6 and 7 of this thesis. Fig. 7.13 presents system capacities based on the max{P_{loss}}=0.05 criterion. In general, it can be stated that a system that incorporates packet retransmission and selection diversity and has a cluster size of N_c=1, provides superior performance over any other configuration. In addition, speech packet interpolation techniques are needed in order for the system to support a moderate number of users.

N_c	1	3	4
Suzuki (P_{loss}=0.01)	5	3	3
Suzuki (P_{loss}=0.05)	11	5	5
Rayleigh (P_{loss}=0.01)	5	5	5
Rayleigh (P_{loss}=0.05)	12	10	9

Table 7.1: *Number of speech terminals per cell, M_s, able to be supported at 1% and 5% total packet loss, P_{loss}, rates in an outdoor cellular PRMA system with retransmission and selection diversity. Both Suzuki fading ($\sigma_s = 6$ dB) and Rayleigh fading ($\sigma_s = 0$ dB) environments are considered for cluster sizes of N_c=1, 3, and 4. z=10 dB, $b = 4$.*

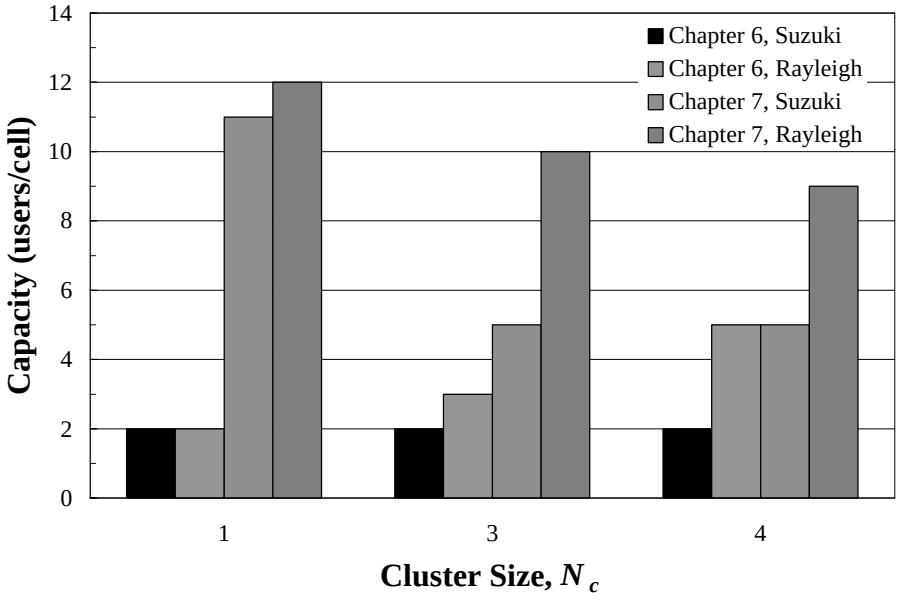

Figure 7.13: *Comparison of Chapters 6 and 7 outdoor cellular PRMA system capacities (P_{loss}=0.05) for Suzuki fading (σ_s=6dB) and Rayleigh fading (σ_s=0dB) channels. Chapter 6 systems are without packet retransmission or selection diversity; Chapter 7 systems have both packet retransmission and selection diversity. z=10dB and b=4 in all cases.*

7.5.6 Comparison with TDMA Systems

The results of Table 7.1 may appear relatively poor and indeed they are when compared against results for a single cell PRMA system (see §6.5.2). However, it is of interest to compare the results presented for PRMA in Table 7.1, with similar TDMA (Time Division Multiple Access) systems to see if PRMA is able to provide an advantage over more conventional multiple access techniques. In this section, a comparison between the performance of outdoor cellular PRMA and TDMA systems is presented. The details of the individual systems are given in Table 7.2. The PRMA system considered is that which was found to provide optimum performance in §7.5.5, namely a system with complete frequency reuse (N=24 timeslots per cell), packet retransmission and selection diversity. It is assumed that speech packet interpolation techniques are also included, so that the design constraint is a 5% maximum speech packet loss probability.

In this situation, the user capacities, which were given in Table 7.1, are M_s=11 users/cell for Suzuki fading and M_s=12 users/cell for Rayleigh fading.

System:	PRMA	TDMA
Parameters	N_c=1 (N=24 timeslots) {*optimum scenario*}	N_c=1 (N=26.66 timeslots) N_c=3 (N=8.88 timeslots) N_c=4 (N=6.66 timeslots)
Features	1. Selection Diversity 2. Packet Retransmit 3. Packet Interpolation	1. Selection Diversity 2. Speech Activity Detect.
Design Constraint	$P_{loss} \leq 0.05$	$P_{out} \leq 0.05$

Table 7.2: *Parameters, features and design constraints of outdoor cellular PRMA and TDMA systems considered for performance comparison.*

TDMA systems traditionally overcome cochannel interference by engineering the frequency reuse plan to ensure adequate separation distances between cochannel cells. TDMA systems with cluster sizes of N_c=1, 3 and 4 are considered in this comparison. A TDMA system with a cluster size of N_c=1 has N=26.66 timeslots/cell, a system with a cluster size of N_c=3 has N=8.88 timeslots/cell, while a system with a cluster size of N_c=4 would have N=6.66 timeslots/cell[4]. The value of N, which can be calculated according to the expression,

$$N = \frac{R_{sys}}{R_s \cdot N_c} \quad \text{(TDMA)}, \tag{7.18}$$

takes into account the removal of packet headers from TDMA timeslot transmissions. Values of total system bitrate, R_{sys},=853.33 kb/s and speech coding rate, Rs=32 kb/s, apply for the speech only systems considered here (see Table 4.2). Both Suzuki fading ($s = 6$ dB) and Rayleigh fading ($s = 0$ dB) environments are considered, with z=10 dB and b=4 in all cases. It is assumed that the TDMA systems incorporate two-branch selection diversity. In addition, it is assumed that TDMA terminals have speech activity detection capability, so that the TDMA terminals only transmit during speech activity (i.e., talkspurt) periods. In this situation the level of inter-cell interference received per timeslot can be accurately estimated using (6.27), namely

$$\overline{m_{coc}} = \frac{L \cdot SAF \cdot M_s}{N}, \tag{7.19}$$

where L is the number of cochannel cell (L=6), SAF is the speech activity factor (SAF=0.426), M_s is the number of TDMA speech users per cell and N is the number of timeslots per cell, given by (7.18). A common design tool for TDMA based systems is the outage probability [5]. The outage probability for the TDMA systems examined in this section is given by

$$P_{out} = 1 - q^2(1, \overline{m_{coc}}), \tag{7.20}$$

[4] While these values of N are not physically realisable, they can be used in this performance comparison to represent the *average* number of timeslots per cell.

where $q^2(1,\overline{m_{coc}})$ is the capture probability presented previously in (7.8). (7.20) is equivalent to the speech packet interference probability, P_{int}, presented in (7.10). It is assumed that an outage probability of P_{out}=0.05 is tolerable for the TDMA systems considered. The value of M_s that results in the right hand side of (7.20) being equal to 0.05 (i.e., the design constraint) also represents the cell capacity.

Table 7.3 presents a comparison of the optimum PRMA system and three TDMA systems. In particular, the value of the design criteria (P_{loss} or P_{out}), together with the associated system capacities, for each system are presented. It is clear from Table 7.3 that the PRMA system has a superior performance over all three TDMA systems considered. In the case of a Rayleigh fading environment, the capacity of the PRMA system of 12 users/cell compares with a maximum TDMA system capacity of 8.88 users/cell (N_c=3). In the case of Suzuki fading, the margin between the systems is increased, with the capacity of the PRMA system equal to 11 users/cell and the maximum capacity of the TDMA systems equal to 4.71 users/cell (N_c=4).

		PRMA	TDMA		
	N_c:	1	1	3	4
Rayleigh	Users/Cell	12	4.66	8.88	6.66
	P_{loss}/P_{out}	0.05	0.05	2.2×10^{-2}	8×10^{-3}
Suzuki	Users/Cell	11	2.7	4	4.71
	P_{loss}/P_{out}	0.05	0.05	0.05	0.05

Table 7.3: *Comparison between optimum PRMA (with packet retransmission and selection diversity) and three TDMA (with selection diversity and speech activity detection) outdoor cellular systems. Suzuki fading and Rayleigh fading is considered. z=10dB and b =4.*

7.6 Performance of In-Building Pico-Cellular PRMA

In this section, performance results for various in-building PRMA systems with packet retransmission and selection diversity are presented. Consideration is given to PRMA systems operating in the four buildings presented in Table 3.3. Analytical results obtained from Markov analysis are compared with those obtained from Monte Carlo simulations. The same system parameter values considered for the outdoor cellular PRMA systems of §7.5 are also considered in this section.

Comparisons of the floor-averaged performance of the four in-building pico-cellular PRMA systems are presented in §7.6.1. This comparison identifies how systems operating in different buildings respond to the inclusion of packet retransmission. Actual capacity estimations are presented in §7.6.2, with comparison between PRMA and TDMA systems presented in §7.6.3. Location dependent performance variations over a typical floor of an in-building PRMA system operating in Building D (Engineering Tower), are presented in §7.6.4. This location dependency study is made possible by considering the detailed propagation information presented in [6].

7.6.1 Performance Variations Between Buildings

Figs. 7.14-7.17, present the speech packet loss probability, P_{loss}, and system utilisation, y , for in-building pico-cellular PRMA systems with packet retransmission and selection diversity, operating in Buildings A-D, respectively. The relevant propagation parameter values for these building were presented in Table 3.3. In all cases, a capture ratio of z=10dB is considered.

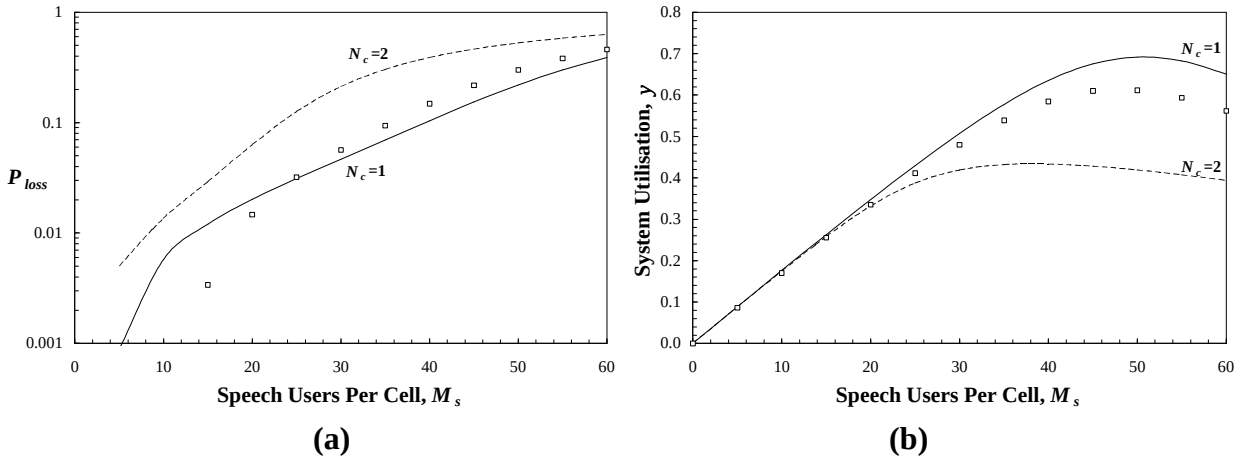

(a) **(b)**

Figure 7.14: *Packet loss probability* **(a)** *and system utilisation* **(b)** *of a PRMA system in Building A: Walnut Creek. System N_c=1, 2, z=10dB, packet retransmission and selection diversity. Markov analysis results (lines) and simulation results (points) are presented.*

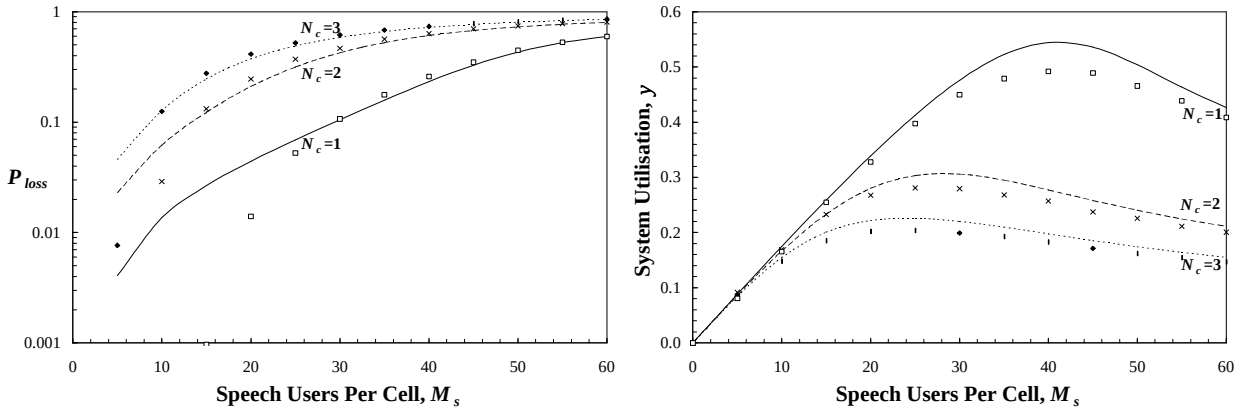

(a) **(b)**

Figure 7.15: *Packet loss probability* **(a)** *and system utilisation* **(b)** *of a PRMA system in Building B: San Ramon. N_c=1, 2, 3, z=10dB, packet retransmission and selection diversity. Markov analysis results (lines) and simulation results (points) are presented.*

Fig. 7.14 considers the performance of PRMA in the Walnut Creek building (Building A, Table 3.3). In this environment, a cluster size of N_c=1 provides considerably better performance, compared to N_c=2. A cluster size of N_c=1 also proves to be the best choice of frequency reuse plan in Buildings B-D (Figs. 7.15-7.17).

In §7.5, outdoor cellular PRMA systems with packet retransmission and selection diversity were also found to perform optimally in systems with complete frequency reuse. This finding is, however, in sharp contrast to that of §6.6, where no single choice of cluster size was able to provide optimum performance in all situations. Actual capacity estimations, based on the results presented in this section, are presented in the following section.

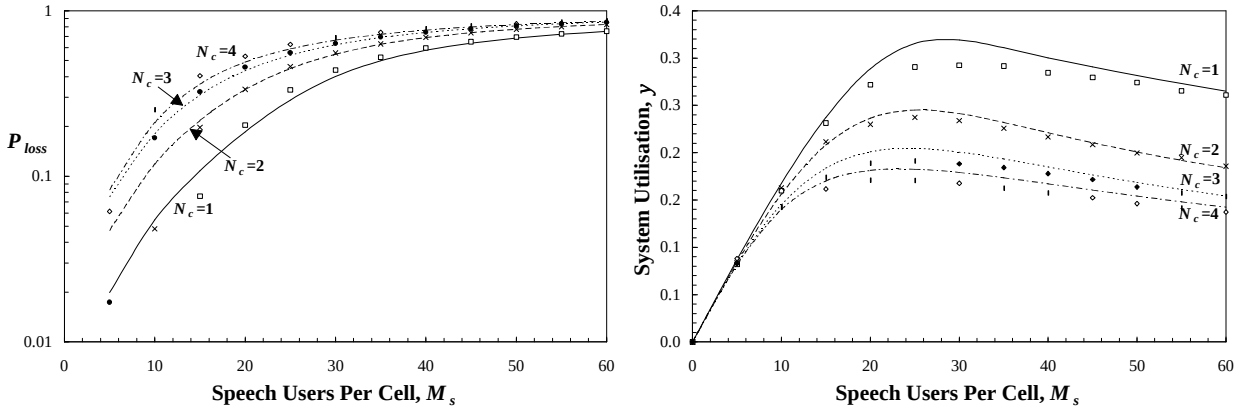

(a) **(b)**

Figure 7.16: *Packet loss probability* **(a)** *and system utilisation* **(b)** *of a PRMA system in Building C: SF Pacbell. N_c=1, 2, 3, 4, z=10dB, packet retransmission and selection diversity. Markov analysis results (lines) and simulation results (points) are presented.*

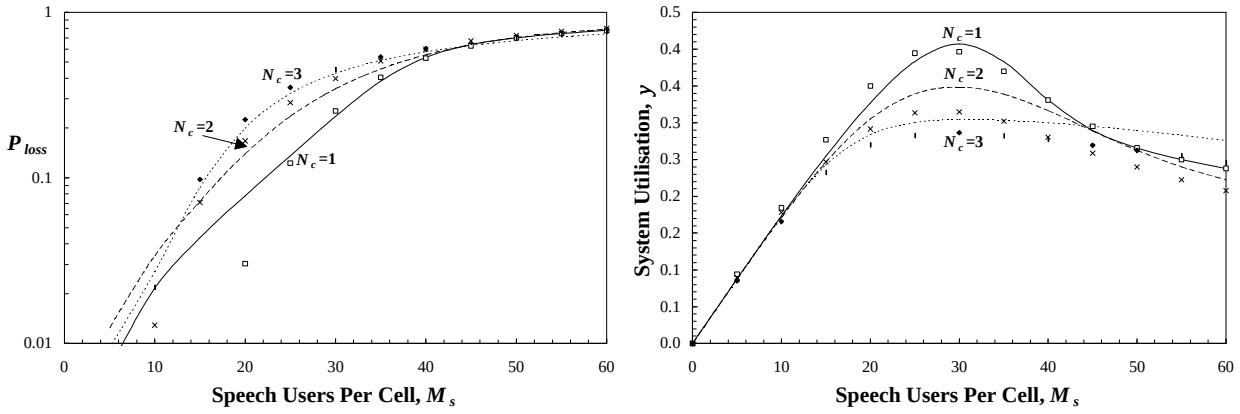

(a) **(b)**

Figure 7.17: *Packet loss probability* **(a)** *and system utilisation* **(b)** *of a PRMA system in Building D: Engineering Tower. N_c=1, 2, 3, z=10dB, packet retransmission and selection diversity. Markov analysis results (lines) and simulation results (points) are presented.*

7.6.2 Capacity Estimations

Based on the results presented in the previous section, it is possible to estimate the capacities of the four in-building pico-cellular PRMA systems presented in Figs. 7.14-7.17. These capacity estimations have been obtained by extrapolating the Markov analysis and computer simulation

results and are in terms of the maximum number of speech terminals, M_s, able to be supported per cell. Capacity estimations are presented in Table 7.4. Consideration is given to clusters sizes of N_c=1, 2, 3, and 4. The results of Table 7.4 are also presented graphically in Fig. 7.18.

	N_c:	1	2	3	4
A	P_{loss}=0.01	13	8	-	-
	P_{loss}=0.05	31	19	-	-
B	P_{loss}=0.01	9	3	2	-
	P_{loss}=0.05	21	9	5	-
C	P_{loss}=0.01	3	1	1	1
	P_{loss}=0.05	10	5	4	4
D	P_{loss}=0.01	6	5	4	-
	P_{loss}=0.05	16	14	14	-

Table 7.4: *Number of speech terminals per cell, M_s, able to be supported at a 1% and 5% total packet loss, P_{loss}, in 4 in-building pico-cellular PRMA system with retransmission and selection diversity. Cluster sizes of N_c=1, 2, 3, and 4 are considered. z=10 dB.*

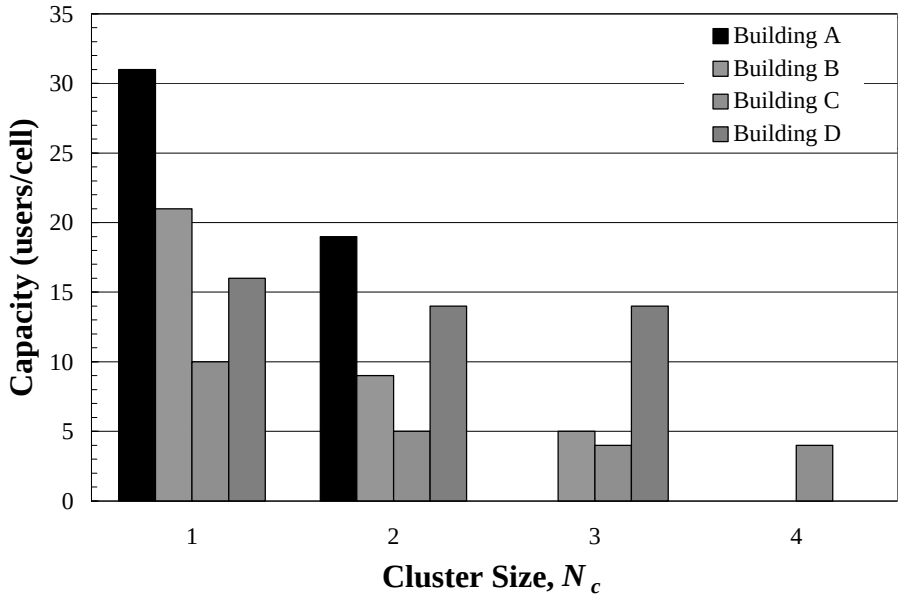

Figure 7.18: *System capacities of four in-building pico-cellular PRMA systems assuming a maximum packet loss probability, P_{loss}=0.05. Systems incorporate packet retransmission and selection diversity. z=10dB in all cases.*

The performance of PRMA in an in-building system is enhanced significantly with the inclusion of packet retransmission and selection diversity. This is especially noticeable when the results of Table 7.4 are compared with those presented in Table 6.4, for identical systems but without packet retransmission or selection diversity. The best performance is experienced in Buildings A and B, with estimated capacities of M_s=31 users/floor and M_s=21 users/floor, respectively. This

finding relies on the inclusion of speech interpolation techniques (P_{loss}=0.05). Without speech interpolation, the performance is reduced considerably.

7.6.3 Comparison with TDMA Systems

In §7.5.6 the performance of an outdoor cellular PRMA system was compared with a number of similar outdoor cellular TDMA systems. In this section the same comparison is made, although in-building PRMA and TDMA systems are considered. In particular, a PRMA system operating in Building B with a cluster size of N_c=1 is compared against TDMA systems in Building B, with cluster sizes of N_c=1, 2 or 3. This comparison will identify what, if any, performance improvements can be obtained with PRMA over more conventional TDMA schemes. The details of the individual systems are presented in Table 7.5. An approach identical to that of §7.5.6 is applied in this section in determining the performance of the TDMA systems.

System:	PRMA (Building B)	TDMA (Building B)
Parameters	N_c=1 (N=24 timeslots) {*optimum scenario for Building B*}	N_c=1 (N=26.66 timeslots) N_c=2 (N=13.33 timeslots) N_c=3 (N=8.88 timeslots)
Features	1. Selection Diversity 2. Packet Retransmit 3. Packet Interpolation	1. Selection Diversity 2. Speech Activity Detect.
Design Constraint	$P_{loss} \leq 0.05$	$P_{out} \leq 0.05$

Table 7.5: *Parameters, features and design constraints of in-building pico-cellular PRMA and TDMA systems considered for performance comparison.*

The PRMA system considered is that which was found to provide optimum performance in §7.6.2 for Building B, namely a system with complete frequency reuse (N=24 timeslots per cell), packet retransmission and selection diversity. A design constraint of 5% maximum speech packet loss probability is imposed so that the user capacity is 21 users/cell, as presented in Table 7.4.

TDMA systems with cluster sizes of N_c=1, 2 and 3 are considered in this comparison. A TDMA system with a cluster size of N_c=1 has N=26.66 timeslots/cell, a system with a cluster size of N_c=2 has N=13.33 timeslots/cell, while a system with a cluster size of N_c=3 would have N=8.88 timeslots/cell. These values are calculated according to (7.18). It is assumed that the TDMA systems incorporate two-branch selection diversity and that the TDMA terminals have speech activity detection capability, as in §7.5.6. The number of inter-cell interfering signals received per timeslot, $\overline{m_{coc}}$, can be estimated according to (6.27). The outage probability, presented in (7.20), is used to estimate the system capacity, with P_{out}=5% used as the design criteria.

Table 7.6 presents a comparison of the optimum PRMA system and three TDMA systems. It can be observed from Table 7.6 that the PRMA system has superior performance over all three TDMA systems considered. The capacity of the PRMA system with 21 users/cell compares with a maximum TDMA system capacity of 7.4 users/cell (N_c=1).

		PRMA	TDMA		
	N_c:	**1**	**1**	**2**	**3**
Building B	Users/Cell	21	7.4	4.8	4.2
	P_{loss}/P_{out}	0.05	0.05	0.05	0.05

Table 7.6: *Comparison between optimum in-building pico-cellular PRMA system (with packet retransmission and selection diversity) and three in-building pico-cellular TDMA systems (with selection diversity and speech activity detection). Building B is considered. z=10dB.*

7.6.4 Location Dependent Performance of Building D

The location dependent performance of an in-building pico-cellular PRMA speech system (Building D, Engineering Tower) with packet retransmission and selection diversity is presented in Fig. 7.19. In particular, the variation in packet loss probability over the central cell is considered. It is assumed that N_c=1 and M_s=20 users/floor. The results of Fig. 7.19 have been obtained via Monte Carlo simulation (§6.4.1) and with the use of the propagation database of [6]. The contour plot of Fig. 7.19 can be compared with that of Fig. 6.22, where an identical system without packet retransmission or selection diversity was considered.

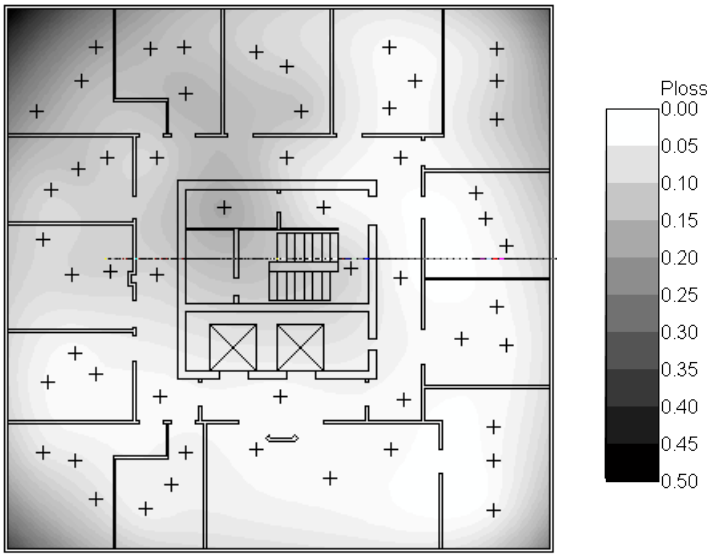

Figure 7.19: *Floor-wide variation in packet loss probability, P_{loss}, for an in-building pico-cellular PRMA system (Building D: Engineering Tower) with packet retransmission and selection diversity. M_s=20 users/floor, N_c=1.*

Compared with Fig. 6.22, the results of Fig. 7.19 indicate that the performance of terminals at all locations on the central floor is improved with packet retransmission and selection diversity. The central core still has a significant effect on the performance of terminals in the shadow region of the floor (opposite side from transmitter).

Fig. 7.20 plots the cumulative distribution function of the P_{loss} contours presented in Fig. 6.22 (no packet retransmission or selection diversity) and Fig. 7.19 (packet retransmission and

selection diversity). While speech packet retransmission and selection diversity improve the performance of speech terminals at all floor locations, analysis has shown that the improvement is considerably greater for terminals in the non-shadowed region of the floor, with terminals there experiencing approximately a 75% reduction in P_{loss}. Terminals in the shadowed region obtain up to a 30% reduction in P_{loss} with packet retransmission and selection diversity. The average reduction in P_{loss} over all locations is 54%.

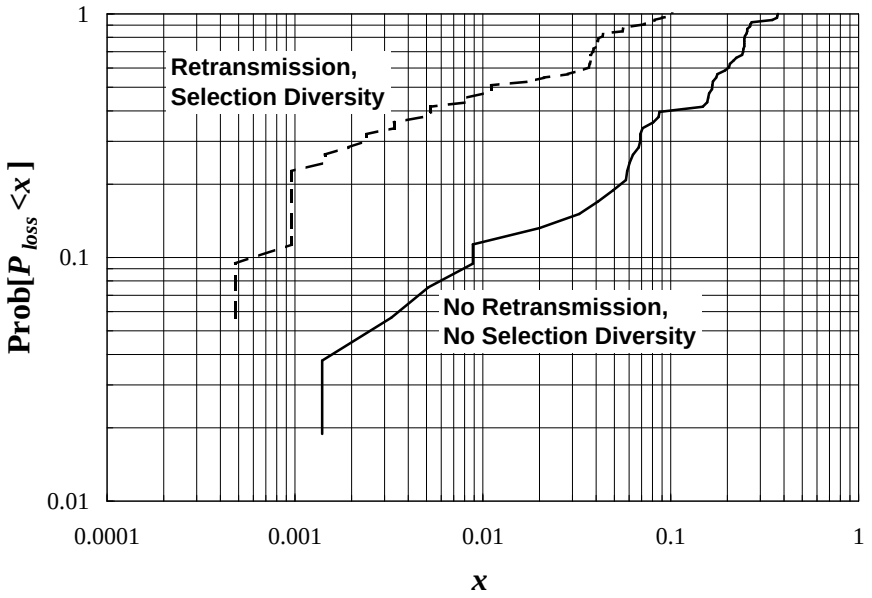

Figure 7.20: *CDF of total packet loss probability, P_{loss}, for two speech only PRMA systems operating in Building B. M_s=20 users/floor, N_c=1, z=10 dB.*

7.7 Summary

In an attempt to extract a more satisfactory performance from the multiple cell PRMA systems considered in Chapter 6, packet retransmission and selection diversity techniques have been incorporated in the PRMA systems considered in this chapter. In particular, reserved speech packets that suffer cochannel interference during transmission to the base station, are able to be retransmitted by their terminals. The simple base station receiver selection diversity technique is used to increase the likelihood of packet success, even in the presence of cochannel interference.

The performance of outdoor cellular and in-building pico-cellular PRMA speech systems with packet retransmission and selection diversity has been determined using both Markov analysis and computer simulations. The Markov analysis employed to model multiple cell PRMA with packet retransmission and selection diversity is similar to that of Chapter 6. The inter-cell interference technique developed previously in §6.3.2 for a system without packet retransmission or selection diversity is also able to accurately predict the amount of interference in the systems considered in this chapter. Confidence in this interference prediction method has been obtained after comparison with results obtained from detailed computer simulations.

The results of this chapter indicate that packet retransmission is beneficial, provided complete frequency reuse is also implemented. Complete frequency reuse provides more opportunities for contending terminals to have packets successfully retransmitted during available timeslots. Selection diversity can also be used to combat the effect of inter-cell interference, resulting in a lower number of lost packets and an improved throughput. Selection diversity provides the greatest benefit in a Rayleigh fading environment, although it is still beneficial in a Suzuki fading environment.

An improvement in PRMA system capacity can be obtained with the inclusion of packet retransmission and selection diversity. However, the system capacity is still relatively poor when compared to the capacity of single cell PRMA systems considered in earlier research. This comparison highlights the danger of relying on capacity estimations obtained from ideal system models. Realistic estimations can only be obtained by considering realistic propagation models and system configurations, as in this chapter.

Comparisons have been made between PRMA and TDMA systems, for both outdoor and in-building environments. These comparisons have revealed that the capacity of PRMA is significantly greater than that of TDMA.

References

[1] W. C. Jakes, "A comparison of specific space diversity techniques for reduction of fast fading in UHF mobile radio systems," *IEEE Trans. Veh. Technol.*, vol. 20, no. 4, Nov. 1971, pp. 81 - 92.

[2] K. W. Sowerby, A. G. Williamson, "Selection diversity in multiple interferer mobile radio systems," *Electronics Letters*, vol. 24, no. 24, Nov. 24th 1988, pp. 1511 - 1513.

[3] X. Qiu, V. O. K. Li, "On the capacity of packet reservation multiple access with capture in personal communication systems," *IEEE Trans. Veh. Technol.*, vol. 45, no. 4, Nov. 1996, pp. 666 - 675.

[4] H. Qi, R. Wyrwas, "Performance analysis of joint voice-data PRMA over random packet error channels," *IEEE Trans. Veh. Technol.*, vol. 45, no. 2, May 1996, pp. 332 - 345.

[5] K. W. Sowerby, *Outage probability in mobile radio systems*. Ph.D Thesis, Department of Electrical & Electronic Engineering, The University of Auckland, New Zealand, Feb. 1989.

[6] K. S. Butterworth, K. W. Sowerby, A. G. Williamson, "A 1.8 GHz indoor wideband propagation study at The University of Auckland," *in School of Engineering Report No. 569, The University of Auckland*, Auckland, New Zealand, Sep. 1996.

Chapter 8

Multiple Cell PRMA Speech-Data Systems

8.1 Introduction

In Chapter 5 of this thesis, the performance of various data-only S-ALOHA systems operating in interference limited outdoor cellular and in-building pico-cellular environments was investigated. Likewise, in Chapters 6 and 7 of this thesis, the performance of various speech-only PRMA systems operating in these same environments was determined. Having examined these individual speech and data systems in considerable detail, it is now appropriate to consider the performance of various integrated speech-data PRMA systems. These systems incorporate speech packet retransmission and selection diversity, as these techniques were found to improve performance in Chapter 7.

Integration of disparate speech and data systems is of considerable interest to system planners, as the potential exists to minimise the necessary system infrastructure, increase the network manageability, and to provide a range of integrated services to the users. However, a critical aspect of this chapter will be the comparison of integrated speech-data systems with separate speech and data systems. This comparison will resolve whether or not the integration of speech and data into a unified system provides improved performance over disparate speech and data systems. In addition, the effect that data terminals have on the performance of PRMA speech terminals, and vice versa, is determined for various multiple cell PRMA systems.

In determining the performance of the various multiple cell speech-data systems in this chapter, both Markov analysis and computer simulation techniques have been considered. The Markov analysis considered in this chapter combines the Markov analyses of Chapters 5 and 7. It is, however, mathematically and computationally complex, meaning that the determination of performance results is restricted to simple cases only. An overview of the Markov analysis is presented in §8.2 with the complete Markov analysis theory presented in Appendix C. It is envisaged that future simplifications to this theory, coupled with increased computing power, will result in more efficient determination of performance results.

In §8.3, the performance of an outdoor cellular speech-data PRMA system with speech packet retransmission and selection diversity is determined. Unlike previous chapters, no consideration of in-building pico-cellular systems is made in this chapter. This is due to the findings derived from the in-building results being the same as those derived from the outdoor cellular results. The performance of an in-building speech-data PRMA system was determined previously in the simulation study of [1]. A determination of the optimum frequency reuse plan is made, together with a comparison of various stand-alone speech and data systems (presented previously in Chapters 5 and 7) and the integrated system of this chapter.

8.2 Markov Analysis

In the previous PRMA Markov analyses of Chapter 6 and 7, theory was presented to calculate the state probability distribution, $\pi(C,R)$. This distribution describes the probability of having C speech terminals in the contention state and R speech terminals in the reservation state. Similarly, the state probability distribution, $\pi(B)$, determined in Chapter 5 for S-ALOHA, describes the probability of having B data terminals in the backlogged state.

In this section, theory is presented for the calculation of the state probability distribution, $\pi(C,R,B)$, for a joint speech-data multiple cell PRMA system. The direct calculation of $\pi(C,R,B)$ is shown in §8.2.1 to be, in many situations, computationally very difficult. In §8.2.2, an overview of the approach taken in [2] for the Markov analysis of a single cell speech-data PRMA system is presented. The approach presented in §8.2.2 is, however, unable to be applied with any accuracy to the analysis of a multiple cell PRMA system in which the receiver capture effect is considered. In §8.2.2, a new analytical approach is presented, which involves performing separate Markov analyses on the data and speech subsystems. While this analysis represents a simplification over the direct calculation, it is still computationally difficult to calculate integrated speech-data system performance in a multiple cell environment using this analysis.

8.2.1 Rigorous Approach

The Markov analysis of a joint speech-data PRMA system requires, ultimately, that the state probability distribution, $\pi(C,R,B)$, be determined. Using a similar approach to that taken in [3], $\pi(C,R,B)$ could be obtained by solving the following set of simultaneous linear equations,

$$\pi(i,j,k) = \sum_{C=0}^{M_d} \sum_{R=0}^{N} \sum_{C=0}^{M_s-R} \pi(i,j,k|C,R,B)\pi(C,R,B), \tag{8.1}$$

$$\sum_{k=0}^{M_d} \sum_{j=0}^{N} \sum_{i=0}^{M_s-j} \pi(i,j,k) = 1, \tag{8.2}$$

where $\pi(i,j,k|C,R,B)$ represents the one-step state transition probability distribution for a joint speech-data system. M_d and M_s are the number of data and speech terminals per cell, respectively, and N is the number of timeslots per cell. It is possible to arrange (8.1) and (8.2) into a matrix of the form

$$\mathbf{A} \cdot \boldsymbol{\pi} = \mathbf{b}, \tag{8.3}$$

where $\mathbf{A}$ is a n+1×n matrix and $\mathbf{b}$ is a n+1 column vector. The n+1 column vector, $\boldsymbol{\pi}$, represents the state probability distribution. This transformation assumes that the 6-dimensional entity of $\pi(i,j,k|C,R,B)$ is represented in 2-dimensional matrix form.

Evaluation of $\boldsymbol{\pi}$ is prohibitively difficult due to the large number of simultaneous equations that must be solved. In particular, the matrix dimension, n, increases significantly as M_s and M_d are increased. The matrix dimension, n, for a joint-speech data PRMA system is given according to

$$n = \begin{cases} \left[M_s - \dfrac{N}{2} + 1 \right] \cdot (N+1) \cdot (M_d + 1) & M_s \geq N \\ \dfrac{1}{2}(M_s + 2) \cdot (M_s + 1) \cdot (M_d + 1) & M_s < N \end{cases} \qquad \textbf{(8.4)}$$

Fig. 8.1 presents the matrix dimension, *n*, versus the number of speech and data terminals per cell. In this situation, the number of data terminals per cell is assumed to equal the number of speech terminals per cell. It is assumed that N=36 timeslots per cell, which is the value of N considered for speech-data PRMA systems with a cluster size of N_c=1 (See Table 4.3). It is obvious that the number of simultaneous equations that must be solved for a speech-data PRMA system is significantly greater than the number that must be solved for a speech-only PRMA system.

For example, for M_s=M_d=60, the matrix dimension for a speech-data PRMA system is n=97,051. In the case of matrix **A** (dimensions n+1×n), the memory storage required is 70 Gbytes. This compares with 19.3 Mbytes for a speech only system[1]. The memory requirements of this approach make analysis almost completely unfeasible. There is, in addition to memory requirements, significant computing requirements associated with this approach.

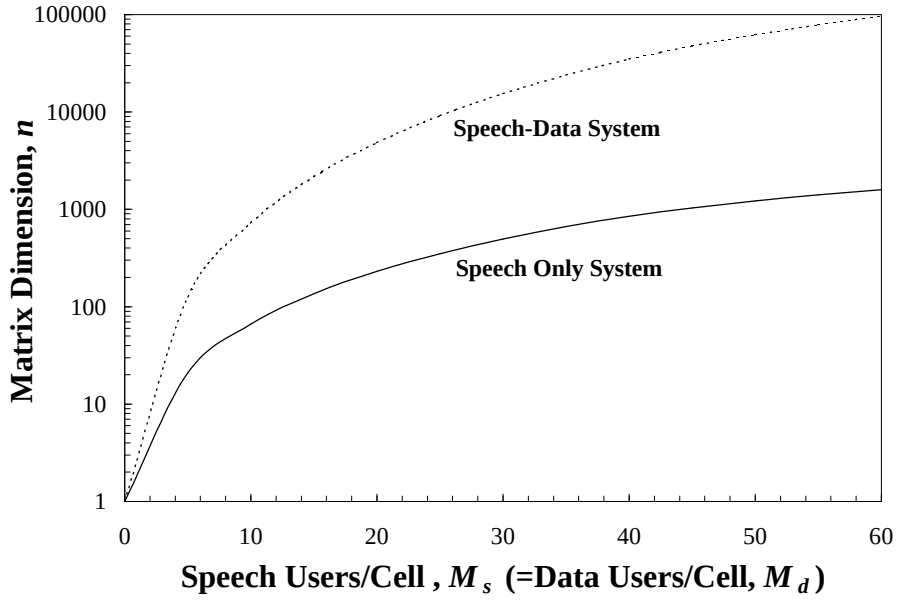

Figure 8.1: *The matrix dimension, n, involved in calculating the state probability distribution for speech only PRMA systems ($\mathbf{p}(C,R)$), and speech-data PRMA systems ($\mathbf{p}(C,R,B)$). An expression for n was presented in (8.4). It is assumed that N=36 timeslots per cell.*

[1] These figures are based on the assumption that each element in the matrix occupies 8 bytes of computer memory, as commonly used in commercial software packages such as MATLAB® (© The Mathworks Inc.).

8.2.2 Markov Analysis of Single Cell Speech-Data PRMA System

In [2], Markov analysis was used to analyse a single cell speech-data PRMA system. This analysis was discussed previously in the literature review of §2.5.2. The analysis assumed the presence of random packet errors and speech packet retransmission. Instead of calculating the state probability distribution directly, $\pi(C,R,B)$ was determined in [2] according to

$$\pi(C,R,B) = \pi(C,R|B)\pi(B), \tag{8.5}$$

where $\pi(C,R|B)$ is the conditional state probability distribution of $\{C,R\}$, given the number of backlogged data terminals, B. Two approximation methods were considered in [2] for calculating $\pi(C,R,B)$, both of which gave comparable results. Method A was a combined EPA[2] and Markov analysis, while Method B was a Markov analysis which used an approximate marginal distribution of backlogged data terminals. The simplest of these methods, namely Method A, involves calculating the equilibrium number of backlogged data terminals, $\overline{B}$, from EPA theory. EPA assumes that the system is always at a stable equilibrium point. The system is, therefore, assumed to always have $\overline{B}$ backlogged data terminals, that is $\pi(B=\overline{B})=1$. The state probability distribution is then calculated according to[3]

$$\begin{aligned}\pi(C,R,B) &= \pi(C,R|B)\pi(B)\\ &= \pi(C,R|\overline{B}).\end{aligned} \tag{8.6}$$

This approach greatly reduces the computational requirements involved in calculating $\pi(C,R,B)$, compared to the direct approach presented in §8.2.1. If Method A is considered, the computational requirements of the joint speech-data PRMA system is approximately the same as that required for the speech only situation. If, however, Method B is considered, the analysis is (M_d+1) times more complex than Method A. This additional complexity does not relate to an increase in the size of the matrix dimension, n, but rather an increase in the number of matrix operations that must be performed. In effect, Method B is equivalent to M_d+1 single cell speech only PRMA analyses.

The approach considered in [2], while not rigorous, is suitable for the analysis of single cell speech-data PRMA systems when considering a simple channel model. However, this approach is unsuitable if cochannel interference (associated with a multiple cell system) or the capture effect (associated with more realistic propagation conditions) are considered. The incorporation of these aspects within a joint-speech data PRMA Markov analysis represents a considerable challenge. In such situations, accurate estimation of $\overline{B}$ becomes difficult to obtain, especially if an EPA analysis is considered.

[2] Equilibrium Point Analysis.
[3] The expression presented in [2, pg. 336] is incorrect. It's correct form is given by (8.6).

8.2.3 Proposed Markov Analysis for Multiple Cell PRMA Speech-Data System

In this section, a proposed strategy for analysing a multiple cell PRMA speech-data system is presented. Considerable more detail is presented in Appendix C. The analysis involves performing two Markov analyses; one for the data subsystem and; a second for the speech subsystem. The procedure to complete this analysis for a particular number of speech terminals, M_s, and data terminals, M_d, per cell, is summarised in Fig. 8.2.

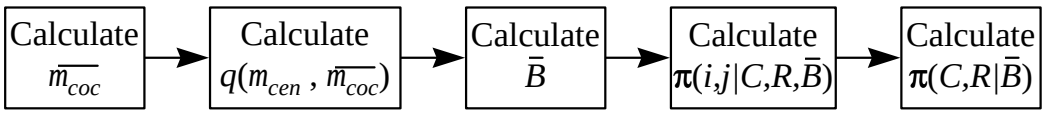

Figure 8.2: *Proposed Markov analysis for a multiple cell PRMA speech-data system.*

The first requirement of the analysis is to estimate the number of inter-cell interfering packets, $\overline{m_{coc}}$, received per timeslot at the central cell base station. This interference consists of packets from both inter-cell interfering speech and data terminals. An iterative procedure to estimate the value of $\overline{m_{coc}}$ is presented in §C.6. Having determined $\overline{m_{coc}}$ it is possible to calculate the capture probability, $q(m_{cen}, \overline{m_{coc}})$ for the particular system under consideration.

The next step involves calculating the mean number of backlogged data terminals, $\overline{B}$, for a given number of reserved, R, and contending, C, speech terminals. A technique for estimating $\overline{B}$ is presented in §C.3. This technique involves a separate Markov analysis of the data subsystem. Having calculated the number of backlogged data terminals, $\overline{B}$, for particular values of C and R, a Markov analysis of the speech subsystem is initiated. In particular, the one-step state transition probability distribution is determined, $\pi(i, j|C, R, \overline{B})$, as well as the state probability distribution, $\pi(C, R, B)$. According to (8.6), $\pi(C, R, B)$ can be estimated using $\pi(C, R|\overline{B})$. With knowledge of the state probability distribution, various performance measures can be evaluated (see §C.7). While the analysis presented in this section is more computationally feasible than the rigorous approach presented in §8.2.1, it is still difficult to obtain performance results using this technique. This is due to a separate Markov analysis of the data subsystem being required for each value of $\{C,R\}$. In addition, the iterative procedure to calculate $\overline{m_{coc}}$ is more computationally difficult for a multiple cell speech-data PRMA system.

8.3 Performance of Outdoor Cellular PRMA

In this section, the performance of various outdoor cellular speech-data PRMA systems are determined in terms of P_{loss}, W, h and y. Analytical results are not considered in this section, due to the complexity of the analysis. Instead, the results obtained from Monte Carlo simulations are presented. Systems with selection diversity and speech packet retransmission are considered. The frequency reuse plan that results in optimum performance is determined for both Suzuki and Rayleigh fading environments. Clusters sizes of N_c=1, 3 and 4 are considered, as in Chapter 6

and Chapter 7. The system parameters for these various frequency reuse configurations were presented previously in Table 4.3. A number of comparisons are made between the performance of separate data and speech systems (i.e., those considered in Chapters 5 and 7, respectively) and the integrated speech-data systems considered in this chapter. This comparison is intended to highlight the effect that traffic integration has on system performance.

As with previous chapters, it is assumed that the speech coding rate, R_s=32 kb/s, while each data terminal is assumed to generate information randomly with an average bit rate of R_d=4800b/s. The packet information size is, I=576 bits and the packet header size is, H=64 bits. In addition, it is assumed that the speech permission probability, p_s=0.3 and the data permission probability, p_d=0.1. The speech packet delay limit is given by, D_{max}=36 ms. The packet generation rate, l_d, for a timeslot of length t is assumed to be given by (5.8). It is assumed that the mean talkspurt duration, t_1=1.00 s and mean silence duration, t_2=1.35 s. In this analysis, a capture ratio, z=10 dB, together with a shadowing standard deviation of s =6 dB and a pathloss exponent of b =4 are considered as median parameters in an outdoor cellular environment.

8.3.1 Determination of Optimum Frequency Reuse Plan

In this section, the optimum frequency reuse plan for an outdoor cellular speech-data PRMA system with packet retransmission and selection diversity is determined. It is assumed in all cases that the number of speech terminals per cell, M_s, is equal to the number of data terminals per cell, M_d. Fig. 8.3 and Fig. 8.4 present the total speech packet loss probability, P_{loss}, data packet delay, W, throughput per cell, h, mean number of inter-cell interfering packets per timeslot, $\overline{m_{coc}}$, and system utilisation, y, for such a system in Suzuki fading (s =6 dB) and Rayleigh fading (s =0 dB) environments, respectively. In order to determine the optimum frequency reuse plan, cluster sizes of N_c=1, 3 and 4 are considered.

Fig. 8.3 presents the various performance measures for a system suffering Suzuki fading. It is clear that a speech-data PRMA system with N_c=1 provides optimum performance. A similar finding was presented in Chapter 7 for a speech-only PRMA system. Systems with N_c=1 have considerably more timeslots per cell than systems with N_c=3 or N_c=4. This leads to more opportunities for contending speech and data terminals to have packets successfully transmitted during available timeslots.

Fig. 8.4 presents the same performance measures presented in Fig. 8.3, but for a system suffering Rayleigh fading. In this situation, the packet loss probability is reduced, while the data packet delay is increased, compared to an identical system operating in a Suzuki fading environment. With Rayleigh fading, less reserved speech packets are corrupted by cochannel interference, resulting in a lower speech packet loss probability. However, as a consequence there are less available timeslots for data terminals to transmit their packets. This results in the average data packet delay increasing. A cluster size of N_c=1 is clearly the best choice of frequency plan for data terminals in a system suffering Rayleigh fading. A cluster size of N_c=1 also provides marginally superior performance for speech terminals in a system with Rayleigh fading.

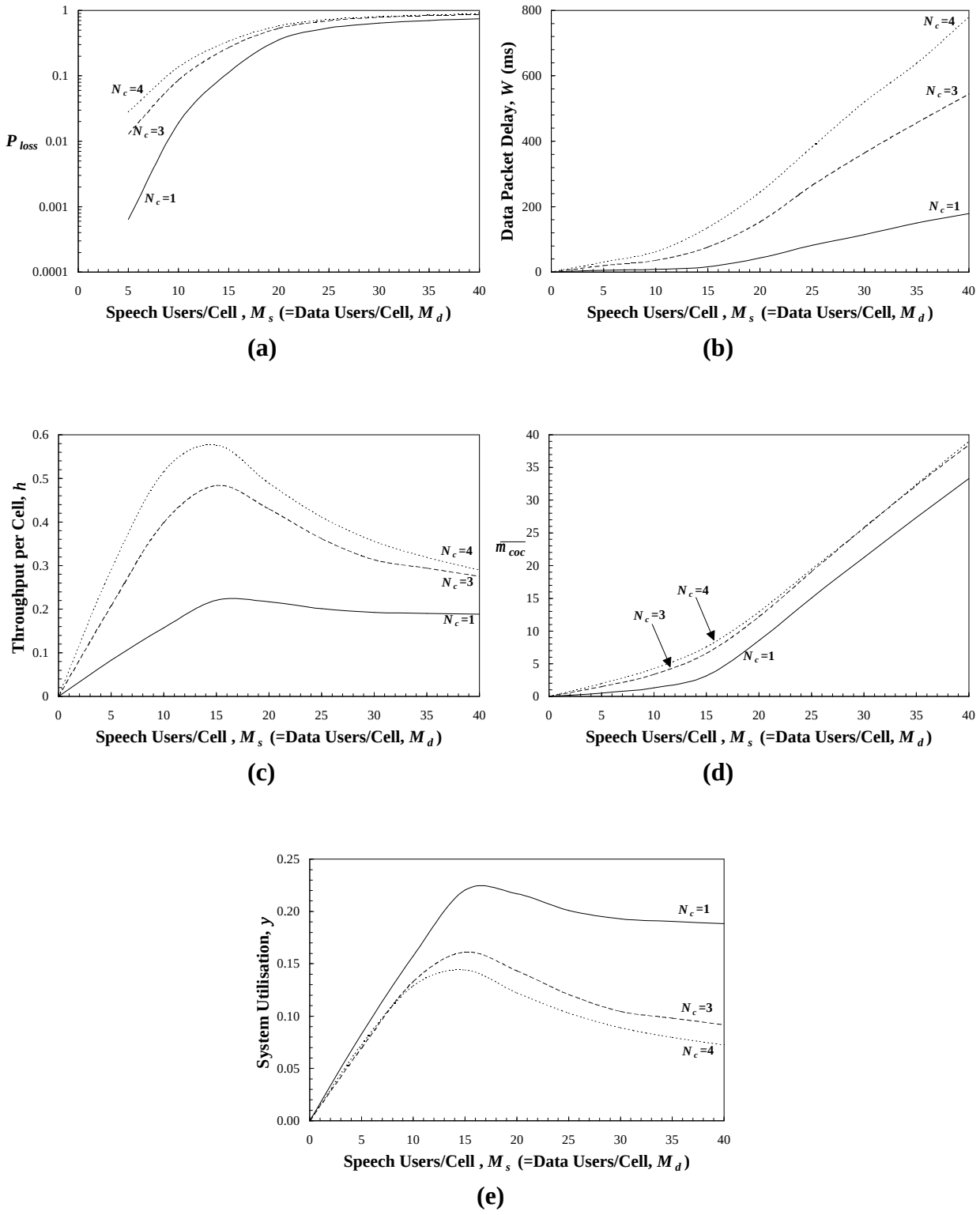

Figure 8.3: (a) *Speech packet loss probability,* P_{loss} , **(b)** *data packet delay, W,* **(c)** *throughput per cell,* h , **(d)** *inter-cell interfering packets per timeslot,* $\overline{m_{coc}}$ *and* **(e)** *system utilisation,* y *, of an outdoor cellular speech-data PRMA system with speech packet retransmission and selection diversity.* N_c*=1, 3, 4.* s *= 6 dB,* b *=4, z=10 dB. Simulation results are presented.*

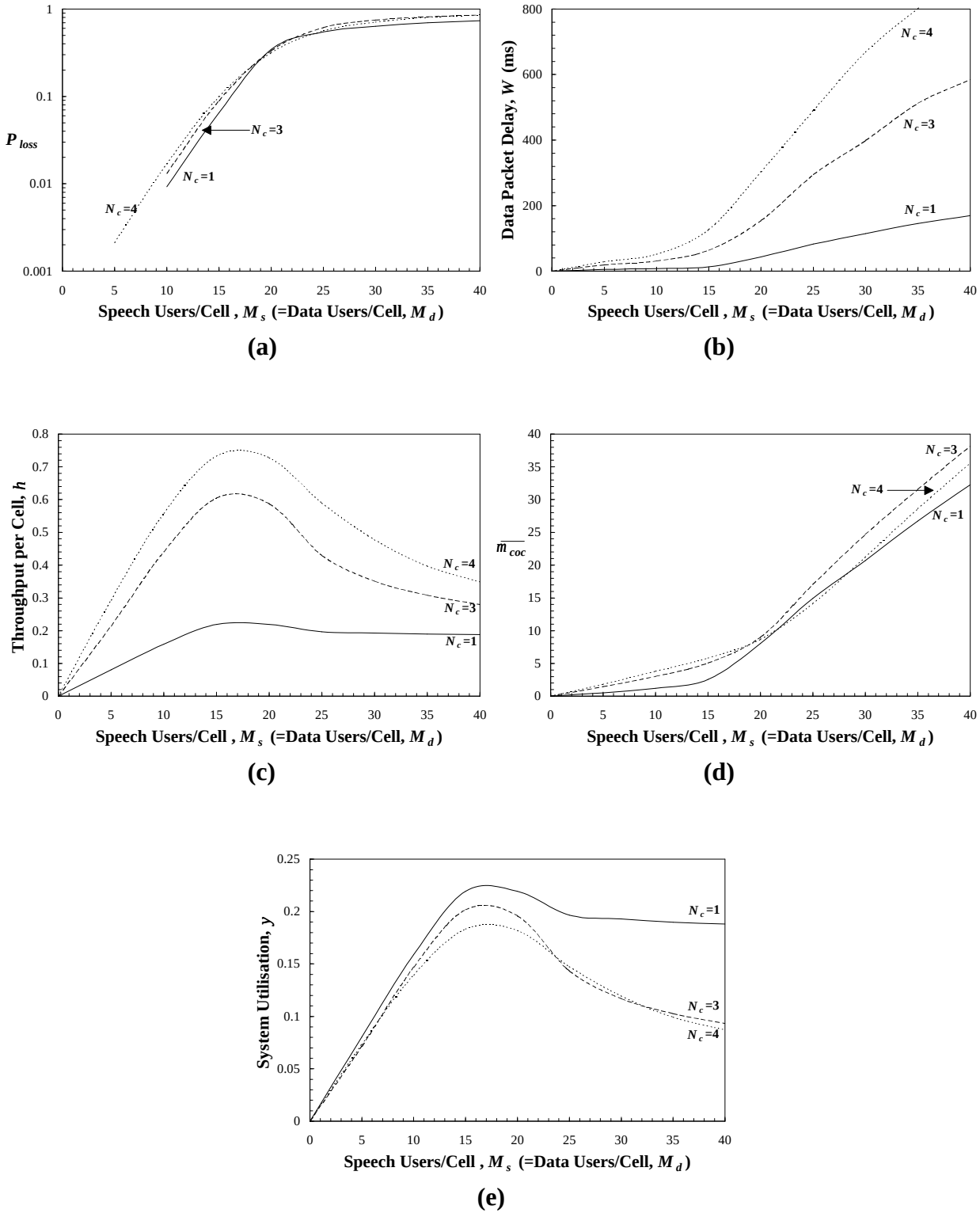

Figure 8.4: (a) *Speech packet loss probability,* P_{loss}, **(b)** *data packet delay, W,* **(c)** *throughput per cell,* h , **(d)** *inter-cell interfering packets per timeslot,* $\overline{m_{coc}}$ *and* **(e)** *system utilisation,* y , *of an outdoor cellular speech-data PRMA system with speech packet retransmission and selection diversity.* N_c*=1, 3, 4.* s *= 0 dB,* b *=4, z=10 dB. Simulation results are presented.*

8.3.2 Integrated Versus Separate Speech-Data Systems

In this section, comparisons are made between integrated and separate outdoor cellular speech and data systems. Separate speech and data systems were considered in earlier chapters of this thesis. In particular, Chapter 5 considered the performance of an outdoor cellular S-ALOHA data system, while Chapter 7 considered the performance of an outdoor cellular PRMA speech system with speech packet retransmission and selection diversity. In this chapter, consideration is given to an outdoor cellular speech-data PRMA system with speech packet retransmission and selection diversity. Of interest to system planners is the performance comparison of integrated speech-data systems with disparate speech and data systems. A central assumption in this analysis is that the available system bandwidth of the integrated speech-data PRMA system is equal to the sum of the separate speech and data system bandwidths. These various system configurations were presented previously in Tables 4.1 to 4.3. In the results of the following section, a Suzuki fading channel is assumed with $s = 6$ dB, $b = 4$ and z=10 dB.

Fig. **8.5** presents the speech packet loss probability, P_{loss}, and data packet delay, W, for various outdoor cellular speech and data systems with a cluster size of N_c=1. In Fig. 8.5(a), the speech packet loss probability in an integrated speech-data PRMA system is compared with that of a separate speech PRMA system (see Fig. 7.11). Fig. 8.5(b) compares the data packet delay of an integrated speech-data PRMA system with that of a separate data S-ALOHA system (Fig. 5.13).

It can be observed that there is little difference in performance between the separate and integrated systems when the cluster size is N_c=1. This is encouraging, in so much as overall performance is not degraded by integrating the separate speech and data systems. It is clear that the speech terminals have little or no effect on the performance of data terminals, and vice-versa. Figs. 8.6 and 8.7 present the same performance measures as those presented in Fig. 8.5, although cluster sizes of N_c=3 and N_c=4 are considered, respectively.

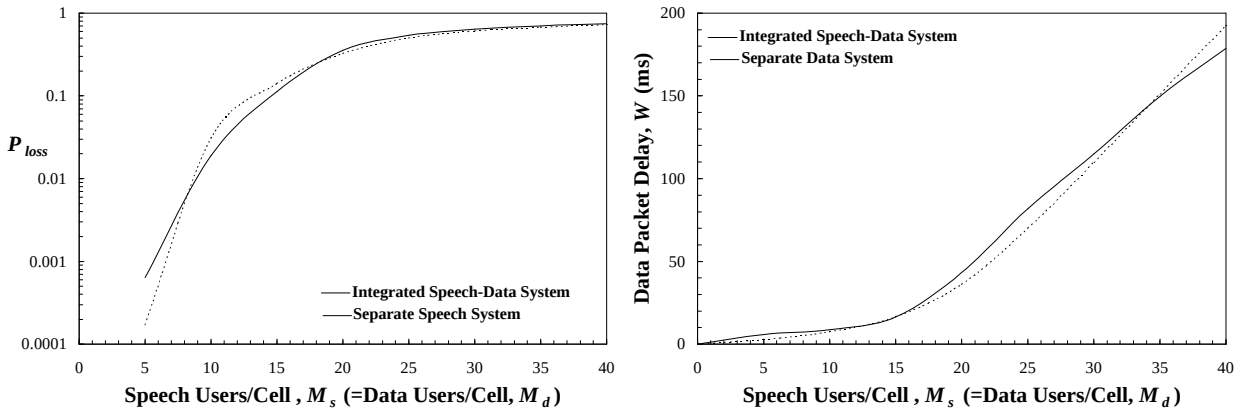

Figure 8.5: (a) *Speech packet loss probability, P_{loss}, and* **(b)** *data packet delay, W, for outdoor cellular speech and data systems (N_c=1). Comparison is made between an integrated speech-data PRMA system, a data-only S-ALOHA system (see Chapter 5) and a speech-only PRMA system (see Chapter 7). The PRMA systems are assumed to operate with speech packet retransmissions and selection diversity. s = 6 dB, b =4, z=10 dB.*

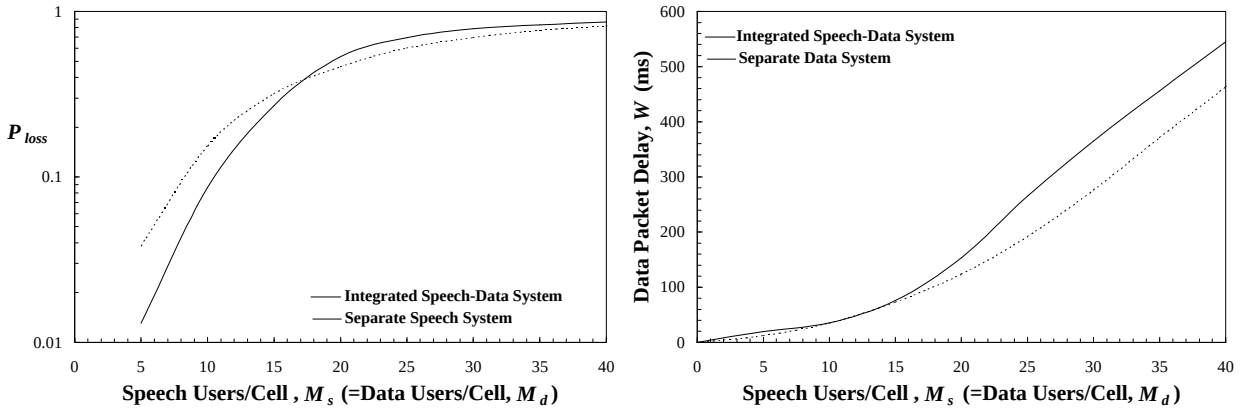

Figure 8.6: (a) *Speech packet loss probability, P_{loss}, and* **(b)** *data packet delay, W, for outdoor cellular speech and data systems (N_c=3). Comparison is made between an integrated speech-data PRMA system, a data-only S-ALOHA system (see Chapter 5) and a speech-only PRMA system (see Chapter 7). The PRMA systems are assumed to operate with speech packet retransmissions and selection diversity. s = 6 dB, b =4, z=10 dB.*

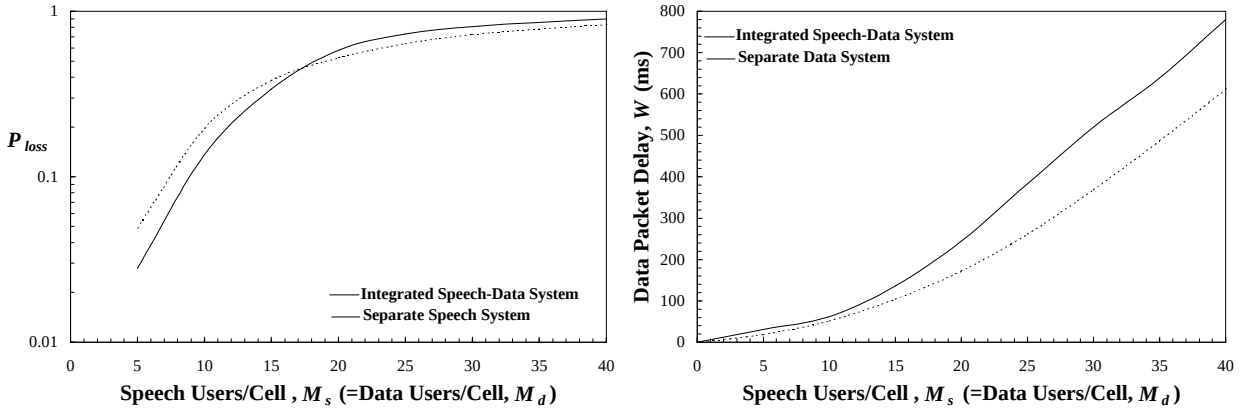

Figure 8.7: (a) *Speech packet loss probability, P_{loss}, and* **(b)** *data packet delay, W, for outdoor cellular speech and data systems (N_c=4). Comparison is made between an integrated speech-data PRMA system, a data-only S-ALOHA system (see Chapter 5) and a speech-only PRMA system (see Chapter 7). The PRMA systems are assumed to operate with speech packet retransmissions and selection diversity. s = 6 dB, b =4, z=10 dB.*

In each case, it can be observed that a difference in performance exists between the integrated and separate systems. In particular, speech terminals benefit from a reduced P_{loss} in an integrated speech-data system for low to moderate numbers of speech and data terminals per cell. At the same time, however, data terminals suffer from an increased data packet delay. Under the assumption that data terminals could cope with a slight increase in packet delay, the integration of speech and data systems would be beneficial in allowing for a greater system capacity.

If an increase in data packet delay could not be tolerated by the data terminals, it would be possible to adjust the respective speech and data permission probabilities (p_s and p_d), to accommodate a greater number of data terminals to access the common channel. In particular, it would be necessary to decrease the speech permission probability, p_s and increase the data permission probability, p_d. Under these circumstances, it should be possible to extract the same, if not slightly better performance from an integrated speech-data PRMA system. With additional benefits of integration such as a minimised system infrastructure, increased network manageability, and the ability to provide integrated services to users, system integration appears to be the most viable long term strategy for packet based wireless networks.

8.3.3 Capacity Estimations

Based on the results presented in §8.3.1, it is possible to estimate the capacities of the outdoor cellular speech-data PRMA systems presented in Fig. 8.3 and Fig. 8.4. These capacity estimations have been obtained by extrapolating the computer simulation results and are in terms of the maximum number of speech terminals, M_s, and data terminals, M_d, able to be supported per cell. These capacity estimations are presented in Table 8.1 and are based on the number of speech and data terminals able to be supported at maximum tolerable P_{loss} levels of 1% and 5%. In addition, the data packet delay for the corresponding number of data terminals per cell is presented. Consideration is given to clusters sizes of N_c=1, 3, and 4, for both Suzuki fading and Rayleigh fading environments.

	N_c	1	3	4
Suzuki (P_{loss}=0.01)	Terminals/Cell, M_s (=M_d)	9	5	4
	Data Packet Delay, W	8 ms	21 ms	25 ms
Suzuki (P_{loss}=0.05)	Terminals/Cell, M_s (=M_d)	12	8	6
	Data Packet Delay, W	12 ms	28 ms	38 ms
Rayleigh (P_{loss}=0.01)	Terminals/Cell, M_s (=M_d)	10	10	9
	Data Packet Delay, W	8 ms	29 ms	44 ms
Rayleigh (P_{loss}=0.05)	Terminals/Cell, M_s (=M_d)	14	13	13
	Data Packet Delay, W	10 ms	45 ms	90 ms

Table 8.1: *Number of speech terminals per cell, M_s, (=number of data terminals per cell, Md) able to be supported at 1% and 5% total speech packet loss, P_{loss}, rates in an outdoor cellular PRMA system with retransmission and selection diversity. The corresponding data packet delay, W, is also presented. Both Suzuki fading ($s = 6$ dB) and Rayleigh fading ($s = 0$ dB) environments are considered for cluster sizes of N_c=1, 3, and 4. z=10 dB, $b = 4$.*

It can be noted from Table 8.1 that the optimum performance is obtained for a speech-data PRMA system with a cluster size of N_c=1, operating in a Rayleigh fading channel, and employing speech packet interpolation techniques. The system capacities presented in Table 8.1 for an integrated speech-data PRMA system are slightly greater than those presented in Table 7.1 for a speech-only system.

8.4 Summary

The performance of an outdoor cellular speech-data PRMA system has been considered in this chapter. Such a system represents the integration of the data-only S-ALOHA system considered in Chapter 5 and the speech-only PRMA system considered in Chapter 7. The integrated system considered in this chapter incorporates speech packet retransmission and selection diversity during reserved timeslots, as these techniques were found to improve performance in Chapter 7. Unlike previous chapters, no consideration of in-building pico-cellular systems has been made in this chapter. This is due to the findings derived from the in-building results being the same as those derived from the outdoor cellular results.

In considering the performance of this system, both Markov analysis and computer simulation approaches have been investigated. It was shown in §8.2, that a complete Markov analysis of the system is mathematically very difficult to perform. It was recognised that a more simplified approach, such as that taken in [2], was required for the Markov analysis. An overview of a more simplified Markov analysis was presented in §8.2.3, with considerable detail also presented in Appendix C. This analysis involves performing separate Markov analyses on the data and speech subsystems. While this analysis represents a simplification over the rigorous analysis, it is still computationally difficult, to the point that it is more efficient to use computer based simulation techniques to obtain performance results. It is envisaged that future simplifications to this theory, coupled with increased computing power, will result in more efficient calculation of performance results.

Computer simulations have been used to investigate the optimum frequency reuse plan in an outdoor cellular speech-data PRMA system. It has been found that a cluster size of N_c=1 provides the optimum performance for both speech and data terminals, in both Rayleigh fading and Suzuki fading environments. This finding is the same as those presented in Chapters 5 and 7 for the individual speech and data systems. The benefit of integrating disparate speech and data systems has also been examined in this chapter. In terms of system performance it has been found that the performance of an integrated system is the same or slightly better than the performance of individual speech and data systems. This improvement is due largely to the increase in available bandwidth, which is able to be shared effectively between speech and data terminals using the PRMA protocol. It was found that speech terminals did not adversely affect the performance of data terminals, and vice-versa.

References

[1] M. D. Orange, K. W. Sowerby, A. J. Coulson, K. S. Butterworth, “Performance of a speech-data PRMA system in an in-building environment,” *in Proc. 47th IEEE Veh. Technol. Conf.*, Phoenix, Arizona, May 1997, pp. 1518 - 1522.

[2] H. Qi, R. Wyrwas, “Performance analysis of joint voice-data PRMA over random packet error channels,” *IEEE Trans. Veh. Technol.*, vol. 45, no. 2, May 1996, pp. 332 - 345.

[3] L. Kleinrock, S. S. Lam, “Packet switching in a multi-access broadcast channel: performance evaluation,” *IEEE Trans. Commun.*, vol. 23, no. 4, Apr. 1975, pp. 410 - 422.

Chapter 9

Summary

There is a strong likelihood that third generation wireless communication systems will employ packetised transmission techniques. Such an approach would provide a number of benefits, including the ability to integrate with emerging wired systems based on Asynchronous Transfer Mode (ATM). In addition, packet-based wireless networks would allow for diverse traffic types and in particular, speech and data traffic, to be integrated more readily. The merging of speech and data within a single unified and seamless wireless network would present significant benefits to users and network providers alike. This thesis has presented theoretical models, together with performance studies for various interference-limited, multiple-cell packet-based, speech and data wireless communication systems.

The significant differences between speech and data traffic present challenges when designing wireless transmission protocols that are capable of integrating both traffic types in an efficient and accurate manner. In this thesis, two packet-based random access protocols have been considered for investigation, namely S-ALOHA and PRMA. The S-ALOHA protocol is designed specifically for data traffic, whereas the PRMA protocol is optimised for speech traffic. However, the PRMA protocol can also cater for the integrated transmission of speech and data traffic, by allowing the data users to communicate with the base station using a S-ALOHA approach.

By far the majority of previously published research into S-ALOHA and PRMA has focused on the performance of these protocols in idealised single cell systems, free from cochannel interference. Future wireless communication systems are, however, likely to employ small frequency reuse distances in order to maximise system capacity, meaning that the effect of cochannel interference cannot be excluded. In this thesis, the performance of S-ALOHA and PRMA in more realistic multiple cell configurations, namely the outdoor cellular and in-building pico-cellular environments, have been considered.

Previous analyses of S-ALOHA and PRMA have often only considered simple signal propagation models that give little or no consideration to signal variability. Received signal strength measurements taken in outdoor and in-building environments indicate, however, that significant fluctuations exist. These fluctuations have been modeled in this thesis using narrowband statistical propagation models. In particular, the variability in signal strength has been modeled as the superposition of three independent phenomena, namely distance dependent pathloss, environmental shadowing and envelope fading. Environmental shadowing is modeled in this thesis using the Suzuki distribution, while envelope fading is described using the Rayleigh distribution.

Previous analyses of S-ALOHA and PRMA have often assumed that all packets involved in collisions with other packets are lost, while those packets received in the absence of other packets are received successfully. This assumption has been reconsidered in this thesis because practical receivers are often capable of locking onto one packet in the presence of other intra-cell

and inter-cell interfering packets, due to the receiver capture effect. The capture probability, which is the probability of a desired packet capturing the base station in the presence of other intra-cell and inter-cell interfering packets, is the underlying performance measure used in this thesis. The capture probability model developed in this thesis, defines the probability of a desired packet capturing the central cell base station in the presence of both intra-cell and inter-cell interfering packets. By utilising this model, it is possible, to calculate the probability of capture in both outdoor cellular and in-building picocellular systems, for a range of propagation conditions. The capture probability expressions developed in this thesis can also be applied to the analysis of many other multiple cell random access systems.

The performance of single cell S-ALOHA and PRMA systems has been determined by previous researchers using Markov analysis theory. This analytical approach has been found to be more accurate than alternative techniques, such as the equilibrium point analysis technique. In this thesis, Markov analysis theory has been applied to the analysis of multiple cell S-ALOHA and PRMA systems. The Markov analyses considered in this thesis do not attempt to incorporate the actual operation of the cochannel cells, as it is mathematically difficult, if not impossible, to include this operation within such analyses. Rather the problem has been constrained so that only the central cell of a particular system is modeled. This approach requires that the expected level of cochannel interference received at the central cell base station be determined and incorporated into the analysis of the central cell. Performance results have also been obtained by utilising Monte Carlo simulation techniques. With respect to this thesis, the simulation results have been used primarily as a validation tool for the Markov analysis results.

Having developed the necessary framework, namely the capture probability and Markov analysis theory, it has been possible to successfully analyse various multiple cell S-ALOHA and PRMA systems.

The initial performance study presented in this thesis related to a multiple cell data-only S-ALOHA system. Both outdoor cellular and in-building pico-cellular S-ALOHA systems were considered. These systems were analysed using both Markov analysis and computer simulation techniques. The Markov analysis theory relied on an accurate estimate of inter-cell interference in order for system performance to be determined. A novel technique for estimating the number of inter-cell interfering packets in a multiple cell S-ALOHA system has been developed in this thesis. This technique assumes that the multiple cell S-ALOHA system is homogeneous in so much as each cell is assumed to experience identical performance. Using this assumption, the average number of new and retransmitted packets produced by cochannel interferers may be determined via an iterative approach. Excellent agreement between Markov analysis and computer simulation results has been obtained, providing confidence in the analytical technique developed.

The difference in performance between single cell S-ALOHA and multiple cell S-ALOHA systems has been determined, with the findings indicating that significant differences in performance exist, due to the impact of inter-cell interference. The effect of the receiver capture ratio, the level of shadowing variability and pathloss exponent on the performance of multiple cell S-ALOHA systems has been determined. While the capture effect has been shown to greatly improve the performance of S-ALOHA in single cell systems, the improvement in multiple cell S-ALOHA systems may not be dramatic, depending on the propagation conditions. Optimum performance is obtained in a multiple cell S-ALOHA system which has a high pathloss exponent,

low shadowing variability and which has base station receivers that can operate with a low capture ratio. Significant variations in performance have been observed between the different in-building S-ALOHA systems considered. It is likely that the most important cause for this variation is the unique propagation conditions of the buildings involved.

In this thesis, a number of frequency reuse plans have been considered and the optimum arrangement has been determined for each system considered. In this thesis it has been assumed that the total system bandwidth allocated to a particular system is constant. Further, it has been assumed that this bandwidth is partitioned equally amongst the N_c cells per cluster to form a particular reuse pattern. Optimum system utilisation, in both outdoor cellular and in-building pico-cellular S-ALOHA systems, is achieved when each cell uses all of the available bandwidth (i.e., complete frequency reuse, N_c=1). While this leads to an increased level of cochannel interference, and therefore, more packet retransmissions, this aspect is outweighed by the significant increase in the number of timeslots per cell that results. It should be noted, however, that the performance of a multiple cell S-ALOHA system with N_c=1, is still significantly poorer than that of an identical single cell S-ALOHA system.

The second performance study presented in this thesis considered a multiple cell speech-only PRMA system without selection diversity or speech packet retransmission. In particular, when a reserved speech packet was corrupted by cochannel interference, it was assumed that the terminal which transmitted the packet retained it's reservation. It was assumed, however, that the corrupted packet was not retransmitted. This approach was taken with the view to minimising additional interference to other terminals, which would be caused if the packet was retransmitted. Both outdoor cellular and in-building pico-cellular PRMA systems have been considered. These systems have been analysed using both Markov analysis and computer simulation techniques. As with the data-only S-ALOHA system, an estimate of the inter-cell interference was required in order for the PRMA Markov analysis to be completed. The estimation technique used for a multiple cell S-ALOHA system was able to be successfully implemented with respect to this PRMA system. This was highlighted with the excellent agreement obtained between analytical and simulation results.

A comparison between single cell and multiple cell PRMA systems has revealed a significant reduction in performance in a multiple cell system. This finding indicates that the approach presented for handling cochannel interference is over simplistic. In particular, the benefit obtained by not retransmitting packets (in terms of reduced interference to other terminals) is unable to be realised as the system is incapable of operation, even for low terminal densities. It was found that the PRMA system was unable to operate particularly successfully in any of the multiple cell configurations considered. The findings indicated that no single choice of cluster size was capable of providing optimum performance in all situations.

The location dependent performance of both outdoor cellular and in-building pico-cellular PRMA systems has been investigated. The performance experienced by a speech terminal in the outdoor environment was found to be highly dependent on their distance from the central cell base station. When the terminal was close to the base station, the packet dropping mechanism was the dominant source of degradation, whereas packet interference was the main source of packet loss for terminals closer to the cell boundary. Obstacles in the in-building environment were found to play a significant role in determining the location dependent performance of

PRMA terminals. Significant variations in performance were found to exist over the area of a single floor.

The third performance study presented in this thesis considered a multiple cell speech-only PRMA system with selection diversity and speech packet retransmission. This ideal selection diversity technique was utilised to reduce the number of reserved speech packets corrupted by inter-cell interference. It was assumed that when a reserved PRMA speech packet encountered cochannel interference, the terminal which transmitted the packet returned to the contention state to attempt retransmission of the corrupted packet in a subsequent available timeslot. As with the previous performance studies, the results of this performance study were obtained from both Markov analysis and computer simulation techniques. The inter-cell interference technique considered for a PRMA system without selection diversity or packet retransmission was successfully extended for use in this analysis.

Appropriate capture probability expressions that include the effect of ideal selection diversity in a multiple cell packet-based system have been developed in this thesis. These capture probability expressions may be used to determine the probability of a desired (i.e. reserved) packet capturing a base station with selection diversity, in the presence of inter-cell interfering packets.

The results of this performance study indicated that packet retransmission is beneficial, provided complete frequency reuse is also implemented. Complete frequency reuse provides more opportunities for contending terminals to have packets successfully retransmitted during available timeslots. Selection diversity can be used to combat the effect of inter-cell interference, resulting in a lower number of lost packets and an improved throughput. Selection diversity provides the greatest benefit in a Rayleigh fading environment, although it is still beneficial in a Suzuki fading environment.

While improvements in PRMA system capacity can be obtained with the inclusion of packet retransmission and selection diversity, system capacity is still relatively poor when compared to the capacity of single cell PRMA systems considered in earlier research. This finding highlights the danger of relying on capacity estimations obtained from ideal system analyses. Realistic estimations can only be obtained by considering realistic propagation models and system configurations. Comparisons between the optimum PRMA system and a number of TDMA systems, have revealed that the capacity of PRMA is significantly greater than that of TDMA. This comparison has been made with respect to both outdoor cellular and in-building pico-cellular systems.

Having examined individual speech and data systems in considerable detail, the final performance study considered the performance of an integrated speech-data multiple cell PRMA system with selection diversity and speech packet retransmission. It was assumed that the bandwidth of this system was the composite of the individual data and speech systems considered in the previous performance studies. No consideration of in-building pico-cellular systems was given in this performance study due to the findings derived in this environment being essentially the same as those derived in the outdoor cellular case.

In considering the performance of this integrated system, both Markov analysis and computer simulation approaches have been investigated. This Markov analysis is a combination of the previous data-only S-ALOHA and speech-only PRMA Markov analyses. It is, however,

mathematically and computationally complex, meaning that the determination of performance results is restricted to simple cases only and it is more efficient to use computer based simulation techniques to obtain performance results. It is envisaged that future simplifications to this theory, coupled with increased computing power, could result in more efficient determination of performance results.

It has been found that a cluster size of N_c=1 provides the optimum performance for both speech and data terminals in an integrated speech-data system. This finding holds true for both Rayleigh fading and Suzuki fading environments. The benefit of integrating disparate speech and data systems has also been examined. In terms of system performance it has been found that the performance of an integrated system is the same or slightly better than the performance of individual speech and data systems. This improvement is due largely to the increase in available bandwidth, which is able to be shared effectively between speech and data terminals using the PRMA protocol. It was found that speech terminals did not adversely affect the performance of data terminals, and vice-versa.

9.1.1 Future Areas of Research

There are a number of areas with potential for further research. The first of these involves the consideration of alternative propagation channel models from those considered in this thesis. Alternative propagation models that could be considered in the outdoor cellular environment include the Nakagami-*m*, Rice, and Weibull distributions. Alternative in-building propagation models that include the effect of obstacle and wall losses, in addition to the effect of floors losses, could also be considered.

Further research exists in developing a more tractable Markov analysis for the joint speech-data multiple cell PRMA system. While the theory presented in Chapter 8 goes some way towards addressing this issue, there is still some scope to improve the accuracy and computability of this theory.

An area for considerable research is the development of random access protocols that minimise the effect of cochannel interference on protocol performance. In this thesis, two relatively simple approaches for handling cochannel interference in PRMA were considered in Chapters 6 and 7. A more advanced PRMA protocol in which terminals retransmit any corrupted packets in available timeslots, as well as retain any existing timeslot reservations for their other packets, could be designed. The decision to retransmit should be based on the level of congestion in the network. In a more congested network, it is likely that improved performance would be obtained if only a portion of the corrupted packets were retransmitted.

One of the primary aims of any protocol enhancement should be a reduction in the number of packet retransmissions by speech and data terminals. Techniques whereby speech terminals are only permitted to retransmit a certain number of times should be investigated.

Given that a central finding of this thesis involves PRMA operating with complete frequency reuse, it is important that base station diversity techniques be investigated as a method for significantly enhancing the performance of PRMA in a multiple cell system. Such techniques would allow speech terminals to receive a timeslot reservation from any of the surrounding base

stations. This is unlike the approach taken in this thesis, where terminals are considered to only communicate with their nearby base station.

In addition to the selection diversity technique investigated in this thesis, consideration of appropriate power control algorithms that allow for improved system performance need to be investigated. A number of other performance improvement measures could be considered, including cell sectorisation and dynamic channel allocation.

Appendix A

Numerical Integration Using Gaussian Quadrature Techniques

A.1 Introduction

Many analytical expressions presented in this thesis contain integral equations which cannot be expressed in a closed form. These integral equations can be solved numerically using Gaussian quadrature numerical integration techniques. These techniques approximate the integral of a particular function from the ordinates of the function, (*y* values) at particular abscissae (*x* values), which are weighted and summed to give an approximate evaluation of the integral.

The accuracy of the Gauss quadrature techniques depends on the number of abscissae (points) at which the ordinates are evaluated, and the nature of the integrand. The integral expressions in this thesis are generally reasonably well suited to Gauss quadrature integration and accurate estimates can usually be achieved using between 8 to 20 points.

A.2 Gaussian Integration Over Finite Limits

Integrals having finite limits can be evaluated using the Gauss-Legendre integration technique. This technique is based on a Gauss' classical result which demonstrates that the integral of a function, $f(x)$ in the range $(-1<x<1)$ can be evaluated with greatest accuracy using n ordinates, when they are obtained from the abscissae at the zeros $x_1,...x_n$ of the Legendre polynomials $L_n(x)$. With each x_i there is an associated constant (weight), w_i, such that [1-3],

$$\int_{-1}^{1} f(x)dx \approx \sum_{i=1}^{n} w_i f(x_i). \qquad \textbf{(A.1)}$$

Appropriate values for x_i and w_i are tabulated in [3]. An integral with arbitrary limits (a,b) can be evaluated using [4]

$$\int_{a}^{b} f(x)dx \approx \frac{b-a}{2}\sum_{i=1}^{n} w_i \cdot f\left(x_i \frac{(b-a)}{2} + \frac{(b-a)}{2} \right). \qquad \textbf{(A.2)}$$

A.3 Gaussian Integration Over Infinite and Semi-Infinite Intervals

For numerical integration over infinite and semi-infinite intervals, (i.e. one limit which is finite and the other which is infinite), it is convenient to use a weight function, $w(x)$, which ensures the convergence of the integral of $w(x)f(x)$. An integral equation with a semi-infinite interval can be evaluated using the Gauss-Laguerre method with a weight function given by, $w(x)=\exp(-x)$. This method is similar to Gauss-Legendre integration except that the weights (w_i) are derived from the *Christoffel-Darboux* identity and the associated abscissae (x_i) correspond to the zeros of the Laguerre polynomial [4]. Accordingly, the Gaussian quadrature formula associated with integration in the range $(0,\infty)$ is given by [1],

$$\int_0^\infty e^{-x} f(x)dx \approx \sum_{i=1}^{n} w_i f(x_i) \qquad \textbf{(A.3)}$$

When a semi-infinite integral has an arbitrary lower limit, *a*, the variable *x* in (A.3) can be changed to $x+a$, so that [1],

$$\int_a^\infty e^{-x} f(x)dx \approx e^{-a}\sum_{i=1}^{n} w_i f(x_i+a) \qquad \textbf{(A.4)}$$

Appropriate values for x_i, w_i and $w_i e^{x_i}$ are tabulated in [3]. An integral with an infinite interval in the range $(-\infty,\infty)$ can be solved using the Gauss-Hermite method with a weight function, $w(x)=e^{-x^2}$. This method is similar to the Gauss-Laguerre method except the weights and abscissae are derived from Hermite polynomials [4]. The Gaussian quadrature formula associated with integration in the range $(-\infty,\infty)$ is given by [1]

$$\int_{-\infty}^\infty e^{-x^2} f(x)dx \approx \sum_{i=1}^{n} w_i f(x_i) \qquad \textbf{(A.5)}$$

Appropriate values for x_i, w_i and $w_i e^{x_i^2}$ are tabulated in [3].

References

[1] P. J. Davis, P. Rabinowitz, *Methods of Numerical Integration*. Academic Press, California, 1984.

[2] A. N. Lowan, *et. al.* "Table of the zeros of the Legendre Polynomials of order 1-16 and the weight coefficients for Gauss' mechanical quadrature formula', *Bull. Amer. Math. Soc.*, Vol. 48, No. 10, Oct. 1942, pp. 739-743.

[3] M. Abramowitz and A. Stegun, *Handbook of mathematical functions*. Dover Publications, New York, 1964.

[4] A. Ralston, *A first course in numerical analysis*. McGraw-Hill, Japan, 1964.

Appendix B

One-Step State Transition Probability Distributions

B.1 Introduction

This appendix presents full mathematical descriptions of the one-step state transition probability distributions, $\pi(i, j|C, R)$, that have been considered in the analyses of Chapter 6 and Chapter 7 of this thesis. The distribution, $\pi(i, j|C, R)$, describes the probability that there are *j* terminals in the reservation state and *i* terminals in the contention state in the current timeslot, given that there were *R* terminals in the reservation state and *C* terminals in the contention state in the previous timeslot.

B.2 Multiple Cell PRMA Speech Systems

This section provides a full expansion of the one-step state transition probability distribution presented in (6.12) for multiple cell PRMA speech systems, namely,

$$\pi(i, j|C, R) = \begin{cases} \Pr(oneCS, noSC, oneCR) & i = C-2 \quad j = R+1 \\ \Pr(noCS, noSC, oneCR) + \Pr(oneCS, oneSC, oneCR) & i = C-1 \quad j = R+1 \\ \Pr(noCS, oneSC, oneCR) & i = C \quad j = R+1 \\ \Pr(oneCS, noSC, noRS) + \Pr(oneCS, noSC, noCR) & i = C-1 \quad j = R \\ \Pr(noCS, noSC, noRS) + \Pr(oneCS, oneSC, noRS) & \\ \quad + \Pr(noCS, noSC, noCR) + \Pr(oneCS, oneSC, noCR) & i = C \quad j = R \\ \Pr(noCS, oneSC, noRS) + \Pr(noCS, oneSC, noCR) & i = C+1 \quad j = R \\ \Pr(oneCS, noSC, oneRS) & i = C-1 \quad j = R-1 \\ \Pr(noCS, noSC, oneRS) + \Pr(oneCS, oneSC, oneRS) & i = C \quad j = R-1 \\ \Pr(noCS, oneSC, oneRS) & i = C+1 \quad j = R-1 \\ 0 & elsewhere \end{cases} \tag{B.1}$$

B.2.1 Case 1 : *i*=*C*-2, *j*=*R*+1

In this situation, the number of contending terminals will decrease by two (*i*=*C*-2) and the number of terminals with reservations will increase by one (*j*=*R*+1) in going from the current timeslot to the next timeslot. In order for this situation to occur, the current timeslot must be available. One *CS* transition must occur and no *SC* transitions must occur. In addition, one of the remaining *C*-1 terminals in the *CON* state must successfully obtain a reservation for the current timeslot. The one-step transition probability in this case is, therefore, given by

$$\pi(i, j|C, R) = \Pr(oneCS, noSC, oneCR)$$
$$= \left(1 - \frac{R}{N}\right) \cdot Cg \cdot (1 - Sl_s) \cdot (1 - g) \sum_{n=1}^{C-1} \binom{C-1}{n} p_s^n (1 - p_s)^{C-1-n} U(n, \overline{m_{coc}})$$

$$i = C - 2, j = R + 1 \qquad \textbf{(B.2)}$$

B.2.2 Case 2 : *i*=*C*-1, *j*=*R*+1

In this situation, the number of contending terminals will decrease by one (*i*=*C*-1) and the number of terminals with reservations will increase by one (*j*=*R*+1) in going from the current timeslot to the next timeslot. In order for this situation to occur, the current timeslot must be available. In addition, either

1. no *CS* transitions and no *SC* transitions must occur. One of the *C* terminals in the *CON* state must successfully obtain a reservation for the current timeslot;
2. one *CS* transition and one *SC* transition must occur. One of the remaining *C*-1 terminals in the *CON* state must successfully obtain a reservation for the current timeslot.

The one-step transition probability in this case is, therefore, given by

$$\pi(i, j|C, R) = \Pr(noCS, noSC, oneCR)$$
$$+ \Pr(oneCS, oneSC, oneCR)$$
$$= \left(1 - \frac{R}{N}\right) \cdot (1 - Cg) \cdot (1 - Sl_s) \cdot (1 - g) \sum_{n=1}^{C} \binom{C}{n} p_s^n (1 - p_s)^{C-n} U(n, \overline{m_{coc}})$$
$$+ \left(1 - \frac{R}{N}\right) \cdot Cg \cdot Sl_s \cdot (1 - g) \sum_{n=1}^{C-1} \binom{C-1}{n} p_s^n (1 - p_s)^{C-1-n} U(n, \overline{m_{coc}})$$

$$i = C - 1, j = R + 1 \qquad \textbf{(B.3)}$$

B.2.3 Case 3 : *i*=*C*, *j*=*R*+1

In this situation, the number of contending terminals will remain the same (*i*=*C*) and the number of terminals with reservations will increase by one (*j*=*R*+1) in going from the current timeslot to the next timeslot. In order for this situation to occur, the current timeslot must be available. No *CS* transitions must occur and one *SC* transition must occur. In addition, one of the *C* terminals in the *CON* state must successfully obtain a reservation for the current timeslot. The one-step transition probability in this case is, therefore, given by

$$\pi(i, j|C, R) = \Pr(noCS, oneSC, oneCR)$$
$$= \left(1 - \frac{R}{N}\right) \cdot (1 - Cg) \cdot Sl_s \cdot (1 - g) \sum_{n=1}^{C} \binom{C}{n} p_s^n (1 - p_s)^{C-n} U(n, \overline{m_{coc}})$$

$$i = C, j = R + 1 \qquad \textbf{(B.4)}$$

B.2.4 Case 4 : *i*=*C*-1, *j*=*R*

In this situation, the number of contending terminals will decrease by one (*i*=*C*-1) and the number of terminals with reservations will remain the same (*j*=*R*) in going from the current timeslot to the next timeslot. In order for this situation to occur, the current timeslot can be either reserved or available.

In the case where the timeslot is reserved, one *CS* transition and no *SC* transitions must occur. In addition, the terminal that holds the reservation for the current timeslot must successfully transmit a packet to the base station. The probability of this occurring is given by $(1 - g_f)$, where g_f is the probability of terminal returning to the *SIL* state. In the case where the timeslot is available one *CS* transition and no *SC* transitions must occur. In addition, none of the remaining *C*-1 terminals in the *CON* state must successfully obtain a reservation for the current timeslot. The one-step transition probability in this case is, therefore, given by

$$\pi(i, j|C, R) = \Pr(oneCS, noSC, noRS)$$
$$+ \Pr(oneCS, noSC, noCR)$$
$$= \frac{R}{N} \cdot Cg \cdot (1 - Sl_s) \cdot (1 - g_f)$$
$$+ \left(1 - \frac{R}{N}\right) \cdot Cg \cdot (1 - Sl_s) \cdot \left(1 - (1 - g) \sum_{n=1}^{C-1} \binom{C-1}{n} p_s^n (1 - p_s)^{C-1-n} U(n, \overline{m_{coc}})\right)$$

$$i = C - 1, j = R \qquad \textbf{(B.5)}$$

B.2.5 Case 5 : *i*=*C*, *j*=*R*

In this situation, the number of contending terminals remains the same (*i*=*C*) and the number of terminals with reservations also remains the same (*j*=*R*) in going from the current timeslot to the next timeslot. In order for this situation to occur, the current timeslot can be either reserved or available.

In the case where the timeslot is reserved, either no *CS* transitions and no *SC* transitions must occur, else one *CS* and one *SC* transitions must occur. In addition, the terminal that holds the reservation for the current timeslot must successfully transmit a packet to the base station. The probability of this occurring is given by $(1 - g_f)$. In the case where the timeslot is available, either:

1. no *CS* transitions and no *SC* transitions must occur. In addition, none of the *C* terminals in the *CON* state must successfully obtain a reservation for the current timeslot;
2. one *CS* and one *SC* transitions must occur. In addition none of the remaining *C*-1 terminals in the *CON* state must successfully obtain a reservation for the current timeslot.

The one-step transition probability in this case is, therefore, given by

$$\begin{aligned}\pi(i,j|C,R) &= \Pr(noCS,noSC,noRS) + \Pr(oneCS,oneSC,noRS) \\ &\quad + \Pr(noCS,noSC,noCR) \\ &\quad + \Pr(oneCS,oneSC,noCR) \\ &= \frac{R}{N}\cdot\left[(1-Cg)\cdot(1-Sl_s)+Cg\cdot Sl_s\right]\cdot(1-g_f) \\ &\quad + \left(1-\frac{R}{N}\right)\cdot(1-Cg)\cdot(1-Sl_s)\cdot\left(1-(1-g)\sum_{n=1}^{C}\binom{C}{n}p_s^n(1-p_s)^{C-n}U(n,\overline{m_{coc}})\right) \\ &\quad + \left(1-\frac{R}{N}\right)\cdot Cg\cdot Sl_s\cdot\left(1-(1-g)\sum_{n=1}^{C-1}\binom{C-1}{n}p_s^n(1-p_s)^{C-1-n}U(n,\overline{m_{coc}})\right)\end{aligned}$$

$$i = C,\ j = R \qquad \textbf{(B.6)}$$

B.2.6 Case 6 : *i*=*C*+1, *j*=*R*

In this situation, the number of contending terminals will increase by one (*i*=*C*+1) and the number of terminals with reservations will remain the same (*j*=*R*) in going from the current timeslot to the next timeslot. In order for this situation to occur, the current timeslot can be either reserved or available.

In the case where the timeslot is reserved, no *CS* transitions and one *SC* transition must occur. In addition, the terminal that holds the reservation for the current timeslot must successfully transmit a packet to the base station. The probability of this occurring is given by $(1-g_f)$. In the case where the timeslot is available no *CS* transitions and one *SC* transition must occur. In addition, none of the *C* terminals in the *CON* state must successfully obtain a reservation for the current timeslot. The one-step transition probability in this case is, therefore, given by

$$\begin{aligned}\pi(i,j|C,R) &= \Pr(noCS,oneSC,noRS) \\ &\quad + \Pr(noCS,oneSC,noCR) \\ &= \frac{R}{N}\cdot(1-Cg)\cdot Sl_s\cdot(1-g_f) \\ &\quad + \left(1-\frac{R}{N}\right)\cdot(1-Cg)\cdot Sl_s\cdot\left(1-(1-g)\sum_{n=1}^{C}\binom{C}{n}p_s^n(1-p_s)^{C-n}U(n,\overline{m_{coc}})\right)\end{aligned}$$

$$i = C+1,\ j = R \qquad \textbf{(B.7)}$$

B.2.7 Case 7 : *i*=*C*-1, *j*=*R*-1

In this situation, the number of contending terminals will reduce by one (*i*=*C*-1) and the number of terminals with reservations will also reduce by one (*j*=*R*-1) in going from the current timeslot to the next timeslot. In order for this situation to occur, the current timeslot must be reserved. One *CS* transition and no *SC* transitions must occur. In addition, the terminal that holds the reservation for the current timeslot must have no more packets to transmit and, therefore, return to the *SIL* state (with probability g_f). The one-step transition probability in this case is, therefore, given by

$$\begin{aligned}\pi(i, j|C, R) &= \Pr(oneCS, noSC, oneRS) \\ &= \frac{R}{N} \cdot Cg \cdot (1 - Sl_s) \cdot g_f\end{aligned}$$

$$i = C - 1, j = R - 1 \qquad \textbf{(B.8)}$$

B.2.8 Case 8 : *i*=*C*, *j*=*R*-1

In this situation, the number of contending terminals will remain the same (*i*=*C*) and the number of terminals with reservations will reduce by one (*j*=*R*-1) in going from the current timeslot to the next timeslot. In order for this situation to occur, the current timeslot must be reserved. In addition, no *CS* transitions and no *SC* transitions must occur, else one *CS* transition and one *SC* transition must occur. The terminal that holds the reservation for the current timeslot must have no more packets to transmit and, thus, return to the *SIL* state (with probability g_f). The one-step transition probability in this case is therefore given by

$$\begin{aligned}\pi(i, j|C, R) &= \Pr(noCS, noSC, oneRS) + \Pr(oneCS, oneSC, oneRS) \\ &= \frac{R}{N}\left[(1 - Cg) \cdot (1 - Sl_s) + Cg \cdot Sl_s\right] \cdot g_f\end{aligned}$$

$$i = C, j = R - 1$$

(B.9)

B.2.9 Case 9 : *i*=*C*+1, *j*=*R*-1

In this situation, the number of contending terminals will increase by one (*i*=*C*+1) and the number of terminals with reservations will reduce by one (*j*=*R*-1) in going from the current timeslot to the next timeslot. In order for this situation to occur, the current timeslot must be reserved. In addition, no *CS* transitions and one *SC* transition must occur. The terminal that holds the reservation for the current timeslot must have no more packets to transmit and, thus, return to the *SIL* state (with probability g_f). The one-step transition probability in this case is therefore given by

$$\pi(i, j|C, R) = \Pr(noCS, oneSC, oneRS)$$
$$= \frac{R}{N} \cdot (1 - Cg) \cdot Sl_s \cdot g_f$$

$$i = C + 1,\ j = R - 1$$

(B.10)

B.3 Multiple Cell PRMA Speech System with Packet Retransmission & Selection Diversity

This section provides a full expansion of the one-step state transition probability distribution presented in (7.12) for a multiple cell PRMA speech system with speech packet retransmission and selection diversity, namely,

$\pi(i, j|C, R) =$

$\Pr(oneCS, noSC, oneCR)$	$i = C - 2$	$j = R + 1$
$\Pr(noCS, noSC, oneCR) + \Pr(oneCS, oneSC, oneCR)$	$i = C - 1$	$j = R + 1$
$\Pr(noCS, oneSC, oneCR)$	$i = C$	$j = R + 1$
$\Pr(oneCS, noSC, noRS, noRC) + \Pr(oneCS, noSC, noCR)$	$i = C - 1$	$j = R$
$\Pr(noCS, noSC, noRS, noRC) + \Pr(oneCS, oneSC, noRS, noRC)$ $+ \Pr(noCS, noSC, noCR) + \Pr(oneCS, oneSC, noCR)$	$i = C$	$j = R$
$\Pr(noCS, oneSC, noRS, noRC) + \Pr(noCS, oneSC, noCR)$	$i = C + 1$	$j = R$
$\Pr(oneCS, noSC, oneRS)$	$i = C - 1$	$j = R - 1$
$\Pr(noCS, noSC, oneRS) + \Pr(oneCS, oneSC, oneRS)$ $+ \Pr(oneCS, noSC, oneRC)$	$i = C$	$j = R - 1$
$\Pr(noCS, oneSC, oneRS) + \Pr(noCS, noSC, oneRC)$ $+ \Pr(oneCS, oneSC, oneRC)$	$i = C + 1$	$j = R - 1$
$\Pr(noCS, oneSC, oneRC)$	$i = C + 2$	$j = R - 1$
0	*elsewhere*	

(B.11)

B.3.1 Case 1 : *i*=*C*-2, *j*=*R*+1

In this situation, the number of contending terminals will decrease by two ($i=C-2$) and the number of terminals with reservations will increase by one ($j=R+1$) in going from the current timeslot to the next timeslot. In order for this situation to occur, the current timeslot must be available. One *CS* transition must occur and no *SC* transitions must occur. In addition, one of the remaining $C-1$ terminals in the *CON* state must successfully obtain a reservation for the current timeslot. The one-step transition probability in this case is, therefore, given by

$$\pi(i, j|C, R) = \Pr(oneCS, noSC, oneCR)$$
$$= \left(1 - \frac{R}{N}\right) \cdot Cg \cdot (1 - Sl_s) \cdot (1 - g) \sum_{n=1}^{C-1} \binom{C-1}{n} p_s^n (1 - p_s)^{C-1-n} U(n, \overline{m_{coc}})$$

$$i = C - 2, j = R + 1 \quad \textbf{(B.12)}$$

B.3.2 Case 2 : *i*=*C*-1, *j*=*R*+1

In this situation, the number of contending terminals will decrease by one ($i=C-1$) and the number of terminals with reservations will increase by one ($j=R+1$) in going from the current timeslot to the next timeslot. In order for this situation to occur, the current timeslot must be available. In addition, either

1. no *CS* transitions and no *SC* transitions must occur. One of the *C* terminals in the *CON* state must successfully obtain a reservation for the current timeslot;
2. one *CS* transition and one *SC* transition must occur. One of the remaining *C*-1 terminals in the *CON* state must successfully obtain a reservation for the current timeslot.

The one-step transition probability in this case is, therefore, given by

$$\pi(i, j|C, R) = \Pr(noCS, noSC, oneCR)$$
$$+ \Pr(oneCS, oneSC, oneCR)$$
$$= \left(1 - \frac{R}{N}\right) \cdot (1 - Cg) \cdot (1 - Sl_s) \cdot (1 - g) \sum_{n=1}^{C} \binom{C}{n} p_s^n (1 - p_s)^{C-n} U(n, \overline{m_{coc}})$$
$$+ \left(1 - \frac{R}{N}\right) \cdot Cg \cdot Sl_s \cdot (1 - g) \sum_{n=1}^{C-1} \binom{C-1}{n} p_s^n (1 - p_s)^{C-1-n} U(n, \overline{m_{coc}})$$

$$i = C - 1, j = R + 1 \quad \textbf{(B.13)}$$

B.3.3 Case 3 : *i*=*C*, *j*=*R*+1

In this situation, the number of contending terminals will remain the same ($i=C$) and the number of terminals with reservations will increase by one ($j=R+1$) in going from the current timeslot to the next timeslot. In order for this situation to occur, the current timeslot must be available. No *CS* transitions must occur and one *SC* transition must occur. In addition, one of the *C* terminals in the *CON* state must successfully obtain a reservation for the current timeslot. The one-step transition probability in this case is, therefore, given by

$$\pi(i, j|C,R) = \Pr(noCS, oneSC, oneCR)$$
$$= \left(1-\frac{R}{N}\right)\cdot(1-Cg)\cdot Sl_s\cdot(1-g)\sum_{n=1}^{C}\binom{C}{n}p_s^n(1-p_s)^{C-n}U(n,\overline{m_{coc}})$$

$$i = C, j = R+1 \qquad \textbf{(B.14)}$$

B.3.4 Case 4 : *i*=*C*-1, *j*=*R*

In this situation, the number of contending terminals will decrease by one (*i*=*C*-1) and the number of terminals with reservations will remain the same (*j*=*R*) in going from the current timeslot to the next timeslot. In order for this situation to occur, the current timeslot can be either reserved or available.

In the case where the timeslot is reserved, one *CS* transition and no *SC* transitions must occur. In addition, the terminal that holds the reservation for the current timeslot must successfully transmit a packet to the base station. The probability of this occurring is given by $(1-g_f)(1-P_{int})$, where P_{int} is the speech packet interference probability, defined previously in (7.10) and g_f is the probability of terminal returning to the *SIL* state.

In the case where the timeslot is available one *CS* transition and no *SC* transitions must occur. In addition, none of the remaining *C*-1 terminals in the *CON* state must successfully obtain a reservation for the current timeslot. The one-step transition probability in this case is, therefore, given by

$$\pi(i, j|C,R) = \Pr(oneCS, noSC, noRS, noRC)$$
$$+ \Pr(oneCS, noSC, noCR)$$
$$= \frac{R}{N}\cdot Cg\cdot(1-Sl_s)\cdot(1-g_f)(1-P_{int})$$
$$+\left(1-\frac{R}{N}\right)\cdot Cg\cdot(1-Sl_s)\cdot\left(1-(1-g)\sum_{n=1}^{C-1}\binom{C-1}{n}p_s^n(1-p_s)^{C-1-n}U(n,\overline{m_{coc}})\right)$$

$$i = C-1, j = R \qquad \textbf{(B.15)}$$

B.3.5 Case 5 : *i*=*C*, *j*=*R*

In this situation, the number of contending terminals remains the same (*i*=*C*) and the number of terminals with reservations also remains the same (*j*=*R*) in going from the current timeslot to the next timeslot. In order for this situation to occur, the current timeslot can be either reserved or available.

In the case where the timeslot is reserved, either no *CS* transitions and no *SC* transitions must occur, else one *CS* and one *SC* transitions must occur. In addition, the terminal that holds the

reservation for the current timeslot must successfully transmit a packet to the base station. The probability of this occurring is given by $(1-g_f)(1-P_{int})$.

In the case where the timeslot is available, either:

1. no *CS* transitions and no *SC* transitions must occur. In addition, none of the *C* terminals in the *CON* state must successfully obtain a reservation for the current timeslot;
2. one *CS* and one *SC* transitions must occur. In addition none of the remaining *C*-1 terminals in the *CON* state must successfully obtain a reservation for the current timeslot.

The one-step transition probability in this case is, therefore, given by

$$\begin{aligned}\pi(i,j|C,R) &= \Pr(noCS,noSC,noRS,noRC) + \Pr(oneCS,oneSC,noRS,noRC) \\ &\quad + \Pr(noCS,noSC,noCR) \\ &\quad + \Pr(oneCS,oneSC,noCR) \\ &= \frac{R}{N}\cdot\left[(1-Cg)\cdot(1-Sl_s)+Cg\cdot Sl_s\right]\cdot(1-g_f)(1-P_{int}) \\ &\quad + \left(1-\frac{R}{N}\right)\cdot(1-Cg)\cdot(1-Sl_s)\cdot\left(1-(1-g)\sum_{n=1}^{C}\binom{C}{n}p_s^n(1-p_s)^{C-n}U(n,\overline{m_{coc}})\right) \\ &\quad + \left(1-\frac{R}{N}\right)\cdot Cg\cdot Sl_s\cdot\left(1-(1-g)\sum_{n=1}^{C-1}\binom{C-1}{n}p_s^n(1-p_s)^{C-1-n}U(n,\overline{m_{coc}})\right)\end{aligned}$$

$$i = C, j = R \qquad \textbf{(B.16)}$$

B.3.6 Case 6 : *i*=*C*+1, *j*=*R*

In this situation, the number of contending terminals will increase by one (*i*=*C*+1) and the number of terminals with reservations will remain the same (*j*=*R*) in going from the current timeslot to the next timeslot. In order for this situation to occur, the current timeslot can be either reserved or available.

In the case where the timeslot is reserved, no *CS* transitions and one *SC* transition must occur. In addition, the terminal that holds the reservation for the current timeslot must successfully transmit a packet to the base station. The probability of this occurring is given by $(1-g_f)(1-P_{int})$.

In the case where the timeslot is available no *CS* transitions and one *SC* transition must occur. In addition, none of the *C* terminals in the *CON* state must successfully obtain a reservation for the current timeslot. The one-step transition probability in this case is, therefore, given by

$$\begin{aligned}\pi(i, j|C, R) &= \Pr(noCS, oneSC, noRS, noRC) \\ &\quad + \Pr(noCS, oneSC, noCR) \\ &= \frac{R}{N} \cdot (1 - Cg) \cdot Sl_s \cdot (1 - g_f)(1 - P_{int}) \\ &\quad + \left(1 - \frac{R}{N}\right) \cdot (1 - Cg) \cdot Sl_s \cdot \left(1 - (1 - g) \sum_{n=1}^{C} \binom{C}{n} p_s^n (1 - p_s)^{C-n} U(n, \overline{m_{coc}})\right)\end{aligned}$$

$$i = C + 1, j = R \qquad \textbf{(B.17)}$$

B.3.7 Case 7 : *i*=*C*-1, *j*=*R*-1

In this situation, the number of contending terminals will reduce by one (*i*=*C*-1) and the number of terminals with reservations will also reduce by one (*j*=*R*-1) in going from the current timeslot to the next timeslot. In order for this situation to occur, the current timeslot must be reserved. One *CS* transition and no *SC* transitions must occur. In addition, the terminal that holds the reservation for the current timeslot must have no more packets to transmit and, therefore, return to the *SIL* state (with probability g_f). The one-step transition probability in this case is, therefore, given by

$$\begin{aligned}\pi(i, j|C, R) &= \Pr(oneCS, noSC, oneRS) \\ &= \frac{R}{N} \cdot Cg \cdot (1 - Sl_s) \cdot g_f\end{aligned}$$

$$i = C - 1, j = R - 1 \qquad \textbf{(B.18)}$$

B.3.8 Case 8 : *i*=*C*, *j*=*R*-1

In this situation, the number of contending terminals will remain the same (*i*=*C*) and the number of terminals with reservations will reduce by one (*j*=*R*-1) in going from the current timeslot to the next timeslot. In order for this situation to occur, the current timeslot must be reserved. In addition, either

1. no *CS* transitions and no *SC* transitions must occur, else one *CS* transition and one *SC* transition must occur. The terminal that holds the reservation for the current timeslot must have no more packets to transmit and, thus, return to the *SIL* state (with probability g_f);
2. one *CS* transition and no *SC* transitions must occur. The terminal that holds the reservation for the current timeslot must have a transmitted packet corrupted by inter-cell interference and, therefore, return to the contention state to attempt to have the packet retransmitted. The probability of this occurring is given by $(1 - g_f) P_{int}$.

The one-step transition probability in this case is therefore given by

$$\begin{aligned}\pi(i,\, j|C,R) &= \Pr(noCS, noSC, oneRS) + \Pr(oneCS, oneSC, oneRS) \\ &\quad + \Pr(oneCS, noSC, oneRC) \\ &= \frac{R}{N}\left[(1-Cg)\cdot(1-Sl_s) + Cg\cdot Sl_s\right]\cdot g_f \\ &\quad + \frac{R}{N}\cdot Cg\cdot(1-Sl_s)\cdot(1-g_f)\cdot P_{int}\end{aligned}$$

$$i = C,\, j = R-1 \qquad \textbf{(B.19)}$$

B.3.9 Case 9 : *i*=*C*+1, *j*=*R*-1

In this situation, the number of contending terminals will increase by one (*i*=*C*+1) and the number of terminals with reservations will reduce by one (*j*=*R*-1) in going from the current timeslot to the next timeslot. In order for this situation to occur, the current timeslot must be reserved. In addition, either:

1. no *CS* transitions and one *SC* transition must occur. The terminal that holds the reservation for the current timeslot must have no more packets to transmit and, thus, return to the *SIL* state (with probability g_f);
2. no *CS* or *SC* transitions must occur, else one *CS* and one *SC* transitions must occur. The terminal that holds the reservation for the current timeslot must have a transmitted packet corrupted by inter-cell interference and, therefore, return to the contention state to attempt to have the packet retransmitted. The probability of this occurring is given by $(1-g_f)P_{int}$.

The one-step transition probability in this case is therefore given by

$$\begin{aligned}\pi(i,\, j|C,R) &= \Pr(noCS, oneSC, oneRS) \\ &\quad + \Pr(noCS, noSC, oneRC) + \Pr(oneCS, oneSC, oneRC) \\ &= \frac{R}{N}\cdot(1-Cg)\cdot Sl_s\cdot g_f \\ &\quad + \frac{R}{N}\cdot\left[(1-Cg)\cdot(1-Sl_s) + Cg\cdot Sl_s\right]\cdot(1-g_f)P_{int}\end{aligned}$$

$$i = C+1,\, j = R-1 \qquad \textbf{(B.20)}$$

B.3.10 Case 10 : *i*=*C*+2, *j*=*R*-1

In this situation, the number of contending terminals will increase by two (*i*=*C*+2) and the number of terminals with reservations will reduce by one (*j*=*R*-1) in going from the current timeslot to the next timeslot. In order for this situation to occur, the current timeslot must be reserved. No *CS* transitions and one *SC* transition must occur. In addition, the terminal that holds the reservation for the current timeslot must have a transmitted packet corrupted by inter-cell interference and, therefore, return to the contention state to attempt to have the packet

retransmitted. The probability of this occurring is given by $(1-g_f)P_{int}$. The one-step transition probability in this case is, therefore, given by

$$\begin{aligned}\pi(i, j|C, R) &= \Pr(noCS, oneSC, oneRC) \\ &= \frac{R}{N} \cdot (1-Cg) \cdot Sl_s \cdot (1-g_f) \cdot P_{int}\end{aligned}$$

$$i = C+2, j = R-1 \qquad \textbf{(B.21)}$$

Appendix C

Markov Analysis of Multiple Cell PRMA Speech-Data System with Packet Retransmission

C.1 Introduction

In this appendix, Markov analysis theory for a multiple cell speech-data PRMA system with speech packet retransmission and capture is presented. This theory was outlined previously in § 8.2.3.

In §C.2, the speech and data Markov models are presented, together with associated state transition probabilities. Section §C.3 presents a technique for calculating the mean number of backlogged data terminals, $\overline{B}$, given that there are C speech terminals in the contention state and R terminals in the reservation state. This is derived from a Markov analysis of the data subsystem of the joint speech-data PRMA system. With knowledge of $\overline{B}$, it is possible to derive the one step state transition probability distribution, $p(i, j|C, R, \overline{B})$ of the speech subsystem. This distribution is presented in §C.4. Theory for calculating the state probability distribution is presented in §C.5. The estimation of the inter-cell interference is provided via the technique presented in § C6. Several performance measures are given in § C7.

C.2 Terminal Transition Probabilities

C.2.1 Speech Terminals

The speech terminal model for an integrated speech-data PRMA system is the same as that presented in §7.3.1, where a speech-only PRMA system was considered. However, the transition probability, f, for a *CR* (contention to reservation) transition requires modification. This transition probability still requires that:

1. the timeslot is available (with probability (1-R/N));
2. the speech terminal has permission (p_s) to transmit and;
3. the terminal is successful in capturing the base station receiver.

However, in capturing the base station, the desired speech packet must not only succeed in the presence of t other contending speech packets (as in Chapters 6 and 7) but also u contending data packets. The probability, f, is therefore

$$f = \left(1-\frac{R}{N}\right) p_s \sum_{t=0}^{C-1} \binom{C-1}{t} p_s^t (1-p_s)^{C-1-t} \sum_{u=0}^{B} \binom{B}{u} p_d^u (1-p_d)^{B-u} q(t+u+1, \overline{m_{coc}}), \qquad \textbf{(C.1)}$$

where $q(t+u+1,\overline{m_{coc}})$ is the probability of a central cell speech terminal capturing the central cell base station in the presence of t intra-cell speech interferers and u intra-cell data interferers and $\overline{m_{coc}}$ inter-cell interferers. Under this notation, $\overline{m_{coc}}$ represents the mean number of inter-cell interferers received at the central cell base station, per timeslot. Relevant theory for the determination of $\overline{m_{coc}}$ in a multiple cell speech-data PRMA system will be presented in §C.6. The inter-cell interference in such a system consists of packets from both speech and data cochannel interferers.

C.2.2 Data Terminals

The data terminal model considered in this analysis is the two-state Markov model presented in Fig. C.1 and is based closely on that considered in the analysis of S-ALOHA in Chapter 5. New packets are generated in the origination state (*ORG*) with probability l_d and enter the backlogged state (*BKL*). The data packet generation probability, l_d, was defined previously in (5.8). Terminals in the *BKL* state continue to retransmit packets until they are successful, at which point they return to the *ORG* state. A backlogged terminal is blocked in the sense that no new messages can arrive when the terminal is in state *BKL*. This implies the absence of a buffer for more than one packet in a data terminal. *B* is the number of data terminals in the backlogged (*BKL*) state at the *t*-th timeslot, within the central cell. *B* is a random variable in the set of $\{0,1,...,M_d\}$.

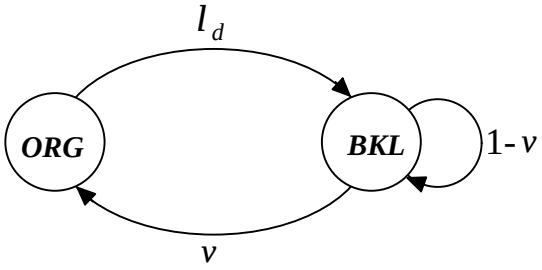

Figure C.1: *Data terminal model with finite buffer.*

PRMA data packets are not transmitted immediately after being generated. Instead, they must use the same contention process as PRMA speech packets to access the base station[1]. In order for data packets to be successfully received at the base station, the following conditions must be met:

1. the timeslot must be available (with probability (1-*R*/*N*)),
2. the data terminal must have permission (p_d) to transmit and;
3. the data terminal must be successful in capturing the base station receiver.

In order to capture the base station, the desired data packet must not only succeed in the presence of *u* other contending data packets but also *t* contending speech packets. The probability of terminal successfully transmitting a packet to the base station, denoted by v, is given by

[1] This differs from S-ALOHA, where new packets are transmitted immediately be the data terminals.

$$v = \left(1-\frac{R}{N}\right) p_d \sum_{u=0}^{B-1} \binom{B-1}{u} p_d^u (1-p_d)^{B-1-u} \sum_{t=0}^{C} \binom{C}{t} p_s^t (1-p_s)^{C-t} q(t+u+1, \overline{m_{coc}}), \qquad \textbf{(C.2)}$$

where $q(t+u+1, \overline{m_{coc}})$ is the probability of a central cell data terminal capturing the central cell base station in the presence of t intra-cell speech interferers and u intra-cell data interferers and $\overline{m_{coc}}$ inter-cell interferers.

C.3 Mean Backlogged Data Terminals, $\overline{B}$

This section presents a Markov analysis of the data subsystem of the joint speech-data PRMA system. The analysis is used for deriving the mean number of backlogged data terminals, $\overline{B}$, for a given number of contending and reserved speech terminals. The value of $\overline{B}$ will then be used in the Markov analysis of the speech subsystem presented in the next section.

The behaviour of the PRMA data subsystem can be modeled by means of a finite Markov chain. The state of the data subsystem is represented by the number of terminals, *B*, in the backlogged (*BKL*) state. The number of backlogged data terminals depends intrinsically on the number of reserved speech terminals, *R*, and contending speech terminals, *C*. The state probability distribution, $\pi_{C,R}(B)$, is the probability that *B* out of the M_d data terminals are in the backlogged state, given that *C* speech terminals are in the contention state and *R* speech terminals are in the reservation state. Having obtained the state probability distribution, $\pi_{C,R}(B)$, it is possible to determine the mean number of backlogged data terminals, $\overline{B}$, from the following relationship

$$\overline{B} = round\left[\sum_{B=1}^{M_d} B \cdot \pi_{C,R}(B)\right]. \qquad \textbf{(C.3)}$$

The rounded value[2] in (C.3) is taken to allow $\overline{B}$ to be used in summations in the next section.

In order to calculate $\pi_{C,R}(B)$, it is necessary to first calculate the one-step state transition probability distribution, $\pi_{C,R}(k|B)$. This is the probability of going from *B* backlogged data terminals in one timeslot to *k* backlogged data terminals in the following timeslot, given the condition that there are *C* speech terminals in the contention state and *R* speech terminals in the reservation state. The distribution, $\pi_{C,R}(k|B)$, is similar in several respects to the one-step state transition probability distribution presented for a multiple cell S-ALOHA system in (5.1). $\pi_{C,R}(k|B)$ is given according to

[2] *round*[*x*] rounds *x* to the nearest integer.

$$\pi_{C,R}(k|B) =$$

$$\begin{cases} 0 & k < B-1 \\ (1-l_d)^{M_d-B}\left(1-\frac{R}{N}\right)\sum_{i=1}^{B}\binom{B}{i}p_d{}^{i}(1-p_d)^{B-i}\sum_{j=0}^{C}\binom{C}{j}p_s{}^{j}(1-p_s)^{C-j}\cdot i\cdot q(i+j,\overline{m_{coc}}) & k = B-1 \\ \left(\frac{R}{N}\right)\binom{M_d-B}{k-B}l_d{}^{k-B}(1-l_d)^{M_d-k} & \\ +\left(1-\frac{R}{N}\right)\binom{M_d-B}{k-B}l_d{}^{k-B}(1-l_d)^{M_d-k-1}\sum_{i=0}^{B}\binom{B}{i}p_d{}^{i}(1-p_d)^{B-i}\sum_{j=0}^{C}\binom{C}{j}p_s{}^{j}(1-p_s)^{C-j} & \\ \times\left[(1-l_d)\left[1-i\cdot q(i+j,\overline{m_{coc}})\right]+\frac{M_d-k}{k-B+1}l_d\cdot i\cdot q(i+k,\overline{m_{coc}})\right] & k \geq B \end{cases} \quad \textbf{(C.4)}$$

From (C.4), it is possible to determine the state probability distribution, $\pi_{C,R}(B)$, by starting with an arbitrary positive $\tilde{\pi}(0)$, and applying the following recursive expression [1]

$$\tilde{\pi}_{C,R}(B) = \frac{1}{\pi_{C,R}(B-1|B)}\left(\tilde{\pi}_{C,R}(B-1) - \sum_{j=0}^{B-1}\tilde{\pi}_{C,R}(j)\cdot\pi_{C,R}(B-1|j)\right), \quad \textbf{(C.5)}$$

and then normalising to obtain

$$\pi_{C,R}(B) = \frac{\tilde{\pi}_{C,R}(B)}{\sum_{s=0}^{M_d}\tilde{\pi}_{C,R}(s)}. \quad \textbf{(C.6)}$$

The approach presented in (C.5) and (C.6) was also followed in Chapter 5 for a multiple cell data-only S-ALOHA system. The mean number of backlogged data terminals, $\overline{B}$, can be calculated according to (C.3).

C.4 The One-Step State Transition Probability

Having calculated $\overline{B}$ for particular values of *C* and *R*, it is possible to calculate the one-step state transition probability distribution, $\pi(i, j|C, R, \overline{B})$, of the speech subsystem. This distribution describes the probability of going from *C* contending and *R* reserved speech terminals in the current timeslot to *i* contending and *j* reservation speech terminals in the next timeslot, with the prerequisite that there are (on average) $\overline{B}$ backlogged data terminals also present in the system.

The one-step state transition probability distribution for a speech-data PRMA system with speech packet retransmission and selection diversity is similar to that presented in Chapter 7 for a speech only system. Indeed, the form of the distribution is exactly the same as that presented in (7.12), namely

$$\pi(i, j|C, R, \overline{B}) =$$

$$\begin{cases}
\Pr(oneCS, noSC, oneCR) & i = C-2 \quad j = R+1 \\
\Pr(noCS, noSC, oneCR) + \Pr(oneCS, oneSC, oneCR) & i = C-1 \quad j = R+1 \\
\Pr(noCS, oneSC, oneCR) & i = C \quad j = R+1 \\
\Pr(oneCS, noSC, noRS, noRC) + \Pr(oneCS, noSC, noCR) & i = C-1 \quad j = R \\
\Pr(noCS, noSC, noRS, noRC) + \Pr(oneCS, oneSC, noRS, noRC) & \\
\quad + \Pr(noCS, noSC, noCR) + \Pr(oneCS, oneSC, noCR) & i = C \quad j = R \\
\Pr(noCS, oneSC, noRS, noRC) + \Pr(noCS, oneSC, noCR) & i = C+1 \quad j = R \\
\Pr(oneCS, noSC, oneRS) & i = C-1 \quad j = R-1 \\
\Pr(noCS, noSC, oneRS) + \Pr(oneCS, oneSC, oneRS) & \\
\quad + \Pr(oneCS, noSC, oneRC) & i = C \quad j = R-1 \\
\Pr(noCS, oneSC, oneRS) + \Pr(noCS, noSC, oneRC) & \\
\quad + \Pr(oneCS, oneSC, oneRC) & i = C+1 \quad j = R-1 \\
\Pr(noCS, oneSC, oneRC) & i = C+2 \quad j = R-1 \\
0 & elsewhere
\end{cases} \tag{C.7}$$

However, the nature of the transition probabilities, such as *oneCR* and *noCR*, are different from those presented in Chapter 7. Only those situations where the events *SC* and *CS* occur at one or less terminals per timeslot are considered in this chapter. The complete expansion of $\pi(i, j|C, R, \overline{B})$ is presented in the following subsections.

C.4.1 Case 1 : *i*=*C*-2, *j*=*R*+1

In this situation, the number of contending terminals will decrease by two (*i*=*C*-2) and the number of terminals with reservations will increase by one (*j*=*R*+1) in going from the current timeslot to the next timeslot. In order for this situation to occur, the current timeslot must be available. One *CS* transition must occur and no *SC* transitions must occur. In addition, one of the remaining *C*-1 terminals in the *CON* state must successfully obtain a reservation for the current timeslot. The one-step transition probability in this case is, therefore, given by

$$\begin{aligned}
\pi(i, j|C, R, \overline{B}) &= \Pr(oneCS, noSC, oneCR) \\
&= \left(1 - \frac{R}{N}\right) \cdot Cg \cdot (1 - Sl_s)(1-g) \sum_{t=1}^{C-1} \binom{C-1}{t} p_s^t (1-p_s)^{C-1-t} \\
&\times \sum_{u=1}^{\overline{B}} \binom{\overline{B}}{u} p_d^u (1-p_d)^{\overline{B}-u} \cdot t \cdot q(t+u, \overline{m_{coc}})
\end{aligned}$$

$$i = C-2, j = R+1 \tag{C.8}$$

C.4.2 Case 2 : *i*=*C*-1, *j*=*R*+1

In this situation, the number of contending terminals will decrease by one (*i*=*C*-1) and the number of terminals with reservations will increase by one (*j*=*R*+1) in going from the current

timeslot to the next timeslot. In order for this situation to occur, the current timeslot must be available. In addition, either

1. no *CS* transitions and no *SC* transitions must occur. One of the *C* terminals in the *CON* state must successfully obtain a reservation for the current timeslot;
2. one *CS* transition and one *SC* transition must occur. One of the remaining *C*-1 terminals in the *CON* state must successfully obtain a reservation for the current timeslot.

The one-step transition probability in this case is, therefore, given by

$$\begin{aligned}\pi(i,\, j|C,R,\overline{B}) &= \Pr(noCS, noSC, oneCR) \\ &\quad + \Pr(oneCS, oneSC, oneCR) \\ &= \left(1-\frac{R}{N}\right)\cdot(1-Cg)\cdot(1-Sl_s)\cdot(1-g)\sum_{t=1}^{C}\binom{C}{t}p_s^t(1-p_s)^{C-t} \\ &\quad \times\sum_{u=1}^{\overline{B}}\binom{\overline{B}}{u}p_d^u(1-p_d)^{\overline{B}-u}\cdot t\cdot q(t+u,\overline{m_{coc}}) \\ &\quad + \left(1-\frac{R}{N}\right)\cdot Cg\cdot Sl_s\cdot(1-g)\sum_{t=1}^{C-1}\binom{C-1}{t}p_s^t(1-p_s)^{C-1-t} \\ &\quad \times\sum_{u=1}^{\overline{B}}\binom{\overline{B}}{u}p_d^u(1-p_d)^{\overline{B}-u}\cdot t\cdot q(t+u,\overline{m_{coc}})\end{aligned}$$

$$i = C-1,\ j = R+1 \qquad \textbf{(C.9)}$$

C.4.3 Case 3 : *i*=*C*, *j*=*R*+1

In this situation, the number of contending terminals will remain the same (*i*=*C*) and the number of terminals with reservations will increase by one (*j*=*R*+1) in going from the current timeslot to the next timeslot. In order for this situation to occur, the current timeslot must be available. No *CS* transitions must occur and one *SC* transition must occur. In addition, one of the *C* terminals in the *CON* state must successfully obtain a reservation for the current timeslot. The one-step transition probability in this case is, therefore, given by

$$\begin{aligned}\pi(i,\, j|C,R,\overline{B}) &= \Pr(noCS, oneSC, oneCR) \\ &= \left(1-\frac{R}{N}\right)\cdot(1-Cg)\cdot Sl_s\cdot(1-g)\sum_{t=1}^{C}\binom{C}{t}p_s^t(1-p_s)^{C-t} \\ &\quad \times\sum_{u=1}^{\overline{B}}\binom{\overline{B}}{u}p_d^u(1-p_d)^{\overline{B}-u}\cdot t\cdot q(t+u,\overline{m_{coc}})\end{aligned}$$

$$i = C,\ j = R+1 \qquad \textbf{(C.10)}$$

C.4.4 Case 4 : *i*=*C*-1, *j*=*R*

In this situation, the number of contending terminals will decrease by one (*i*=*C*-1) and the number of terminals with reservations will remain the same (*j*=*R*) in going from the current timeslot to the next timeslot. In order for this situation to occur, the current timeslot can be either reserved or available.

In the case where the timeslot is reserved, one *CS* transition and no *SC* transitions must occur. In addition, the terminal that holds the reservation for the current timeslot must successfully transmit a packet to the base station. The probability of this occurring is given by $(1-g_f)(1-P_{int})$, where P_{int} is the speech packet interference probability, defined previously in (7.10) and g_f is the probability of terminal returning to the *SIL* state.

In the case where the timeslot is available one *CS* transition and no *SC* transitions must occur. In addition, none of the remaining *C*-1 terminals in the *CON* state must successfully obtain a reservation for the current timeslot. The one-step transition probability in this case is, therefore, given by

$$\begin{aligned}\pi(i,j|C,R,\overline{B}) &= \Pr(oneCS,noSC,noRS,noRC) \\ &\quad + \Pr(oneCS,noSC,noCR) \\ &= \frac{R}{N}\cdot Cg\cdot(1-Sl_s)\cdot(1-g_f)(1-P_{int})+\left(1-\frac{R}{N}\right)\cdot Cg\cdot(1-Sl_s) \\ &\quad\times\left(1-(1-g)\sum_{t=1}^{C-1}\binom{C-1}{t}p_s^t(1-p_s)^{C-1-t}\sum_{u=1}^{\overline{B}}\binom{\overline{B}}{u}p_d^u(1-p_d)^{\overline{B}-u}\cdot t\cdot q(t+u,\overline{m_{coc}})\right)\end{aligned}$$

$$i = C-1,\ j = R \qquad \textbf{(C.11)}$$

C.4.5 Case 5 : *i*=*C*, *j*=*R*

In this situation, the number of contending terminals remains the same (*i*=*C*) and the number of terminals with reservations also remains the same (*j*=*R*) in going from the current timeslot to the next timeslot. In order for this situation to occur, the current timeslot can be either reserved or available.

In the case where the timeslot is reserved, either no *CS* transitions and no *SC* transitions must occur, else one *CS* and one *SC* transitions must occur. In addition, the terminal that holds the reservation for the current timeslot must successfully transmit a packet to the base station. The probability of this occurring is given by $(1-g_f)(1-P_{int})$. In the case where the timeslot is available, either:

1. no *CS* transitions and no *SC* transitions must occur. In addition, none of the *C* terminals in the *CON* state must successfully obtain a reservation for the current timeslot;
2. one *CS* and one *SC* transitions must occur. In addition none of the remaining *C*-1 terminals in the *CON* state must successfully obtain a reservation for the current timeslot.

The one-step transition probability in this case is, therefore, given by

$$
\begin{aligned}
\pi(i,\, j|C,R,\overline{B}) &= \Pr(noCS,noSC,noRS,noRC) + \Pr(oneCS,oneSC,noRS,noRC) \\
&\quad + \Pr(noCS,noSC,noCR) \\
&\quad + \Pr(oneCS,oneSC,noCR) \\
&= \frac{R}{N}\cdot\left[(1-Cg)\cdot(1-Sl_s)+Cg\cdot Sl_s\right]\cdot(1-g_f)(1-P_{int}) \\
&\quad + \left(1-\frac{R}{N}\right)\cdot(1-Cg)\cdot(1-Sl_s) \\
&\quad \times\left(1-(1-g)\sum_{t=1}^{C}\binom{C}{t}p_s^t(1-p_s)^{C-t}\sum_{u=1}^{\overline{B}}\binom{\overline{B}}{u}p_d^u(1-p_d)^{\overline{B}-u}\cdot t\cdot q(t+u,\overline{m_{coc}})\right) \\
&\quad + \left(1-\frac{R}{N}\right)\cdot Cg\cdot Sl_s \\
&\quad \times\left(1-(1-g)\sum_{t=1}^{C-1}\binom{C-1}{t}p_s^t(1-p_s)^{C-1-t}\sum_{u=1}^{\overline{B}}\binom{\overline{B}}{u}p_d^u(1-p_d)^{\overline{B}-u}\cdot t\cdot q(t+u,\overline{m_{coc}})\right)
\end{aligned}
$$

$$i = C,\ j = R \qquad \textbf{(C.12)}$$

C.4.6 Case 6 : *i*=*C*+1, *j*=*R*

In this situation, the number of contending terminals will increase by one ($i=C+1$) and the number of terminals with reservations will remain the same ($j=R$) in going from the current timeslot to the next timeslot. In order for this situation to occur, the current timeslot can be either reserved or available.

In the case where the timeslot is reserved, no *CS* transitions and one *SC* transition must occur. In addition, the terminal that holds the reservation for the current timeslot must successfully transmit a packet to the base station. The probability of this occurring is given by $(1-g_f)(1-P_{int})$.

In the case where the timeslot is available no *CS* transitions and one *SC* transition must occur. In addition, none of the *C* terminals in the *CON* state must successfully obtain a reservation for the current timeslot. The one-step transition probability in this case is, therefore, given by

$$\begin{aligned}\pi(i, j|C, R, \overline{B}) &= \Pr(noCS, oneSC, noRS, noRC) \\ &\quad + \Pr(noCS, oneSC, noCR) \\ &= \frac{R}{N}\cdot(1-Cg)\cdot Sl_s\cdot(1-g_f)(1-P_{int}) \\ &\quad + \left(1-\frac{R}{N}\right)\cdot(1-Cg)\cdot Sl_s \\ &\quad \times\left(1-(1-g)\sum_{t=1}^{C}\binom{C}{t}p_s^t(1-p_s)^{C-t}\sum_{u=1}^{\overline{B}}\binom{\overline{B}}{u}p_d^u(1-p_d)^{\overline{B}-u}\cdot t\cdot q(t+u,\overline{m_{coc}})\right)\end{aligned}$$

$$i = C+1,\ j = R \qquad \textbf{(C.13)}$$

C.4.7 Case 7 : *i*=*C*-1, *j*=*R*-1

In this situation, the number of contending terminals will reduce by one (*i*=*C*-1) and the number of terminals with reservations will also reduce by one (*j*=*R*-1) in going from the current timeslot to the next timeslot. In order for this situation to occur, the current timeslot must be reserved. One *CS* transition and no *SC* transitions must occur. In addition, the terminal that holds the reservation for the current timeslot must have no more packets to transmit and, therefore, return to the *SIL* state (with probability g_f). The one-step transition probability in this case is, therefore, given by

$$\begin{aligned}\pi(i, j|C, R, \overline{B}) &= \Pr(oneCS, noSC, oneRS) \\ &= \frac{R}{N}\cdot Cg\cdot(1-Sl_s)\cdot g_f\end{aligned}$$

$$i = C-1,\ j = R-1 \qquad \textbf{(C.14)}$$

C.4.8 Case 8 : *i*=*C*, *j*=*R*-1

In this situation, the number of contending terminals will remain the same (*i*=*C*) and the number of terminals with reservations will reduce by one (*j*=*R*-1) in going from the current timeslot to the next timeslot. In order for this situation to occur, the current timeslot must be reserved. In addition, either

1. no *CS* transitions and no *SC* transitions must occur, else one *CS* transition and one *SC* transition must occur. The terminal that holds the reservation for the current timeslot must have no more packets to transmit and, thus, return to the *SIL* state (with probability g_f);
2. one *CS* transition and no *SC* transitions must occur. The terminal that holds the reservation for the current timeslot must have a transmitted packet corrupted by inter-cell interference and, therefore, return to the contention state to attempt to have the packet retransmitted. The probability of this occurring is given by $(1-g_f)P_{int}$.

The one-step transition probability in this case is therefore given by

$$\begin{aligned}\pi(i, j|C, R, \overline{B}) &= \Pr(noCS, noSC, oneRS) + \Pr(oneCS, oneSC, oneRS) \\ &\quad + \Pr(oneCS, noSC, oneRC) \\ &= \frac{R}{N}\left[(1-Cg)\cdot(1-Sl_s) + Cg\cdot Sl_s\right]\cdot g_f \\ &\quad + \frac{R}{N}\cdot Cg\cdot(1-Sl_s)\cdot(1-g_f)\cdot P_{int}\end{aligned}$$

$$i = C,\ j = R-1 \qquad \textbf{(C.15)}$$

C.4.9 Case 9 : *i*=*C*+1, *j*=*R*-1

In this situation, the number of contending terminals will increase by one (*i*=*C*+1) and the number of terminals with reservations will reduce by one (*j*=*R*-1) in going from the current timeslot to the next timeslot. In order for this situation to occur, the current timeslot must be reserved. In addition, either:

1. no *CS* transitions and one *SC* transition must occur. The terminal that holds the reservation for the current timeslot must have no more packets to transmit and, thus, return to the *SIL* state (with probability g_f);
2. no *CS* or *SC* transitions must occur, else one *CS* and one *SC* transitions must occur. The terminal that holds the reservation for the current timeslot must have a transmitted packet corrupted by inter-cell interference and, therefore, return to the contention state to attempt to have the packet retransmitted. The probability of this occurring is given by $(1-g_f)P_{int}$.

The one-step transition probability in this case is therefore given by

$$\begin{aligned}\pi(i, j|C, R, \overline{B}) &= \Pr(noCS, oneSC, oneRS) \\ &\quad + \Pr(noCS, noSC, oneRC) + \Pr(oneCS, oneSC, oneRC) \\ &= \frac{R}{N}\cdot(1-Cg)\cdot Sl_s\cdot g_f \\ &\quad + \frac{R}{N}\cdot\left[(1-Cg)\cdot(1-Sl_s) + Cg\cdot Sl_s\right]\cdot(1-g_f)P_{int}\end{aligned}$$

$$i = C+1,\ j = R-1 \qquad \textbf{(C.16)}$$

C.4.10 Case 10 : *i*=*C*+2, *j*=*R*-1

In this situation, the number of contending terminals will increase by two (*i*=*C*+2) and the number of terminals with reservations will reduce by one (*j*=*R*-1) in going from the current timeslot to the next timeslot. In order for this situation to occur, the current timeslot must be reserved. No *CS* transitions and one *SC* transition must occur. In addition, the terminal that holds the reservation for the current timeslot must have a transmitted packet corrupted by inter-cell interference and, therefore, return to the contention state to attempt to have the packet

retransmitted. The probability of this occurring is given by $(1-g_f)P_{int}$. The one-step transition probability in this case is, therefore, given by

$$\begin{aligned}\pi(i, j|C, R, \overline{B}) &= \Pr(noCS, oneSC, oneRC) \\ &= \frac{R}{N}\cdot(1-Cg)\cdot Sl_s\cdot(1-g_f)\cdot P_{int}\end{aligned}$$

$$i = C+2,\ j = R-1 \qquad \textbf{(C.17)}$$

C.5 State Probability Distribution

From the one-step state transition probability distribution, $\pi(i, j|C, R, \overline{B})$, it is possible to derive the state probability distribution, $\pi(C, R, B)$, which is the probability of having C speech terminals in the *CON* state, R speech terminals in the RES_i states and B data terminals in the *BKL* state. As was discussed in § 8.2.2, $\pi(C, R, B)$ can be determined from the following relationship

$$\begin{aligned}\pi(C, R, B) &= \pi(C, R|B)\pi(B) \\ &= \pi(C, R|\overline{B}).\end{aligned} \qquad \textbf{(C.18)}$$

assuming that there are always $\overline{B}$ backlogged data terminals, that is $\pi(B = \overline{B}) = 1$. The conditional state probability distribution of {*C*,*R*}, $\pi(C, R|\overline{B})$, given the mean number of backlogged data terminals, $\overline{B}$, can be obtained by solving the following set of simultaneous linear equations [2],

$$\pi(i, j|\overline{B}) = \sum_{R=0}^{N}\sum_{C=0}^{M_s-R}\pi(i, j|C, R, \overline{B})\pi(C, R|\overline{B}), \qquad \textbf{(C.19)}$$

$$\sum_{j=0}^{N}\sum_{i=0}^{M_s-j}\pi(i, j|\overline{B}) = 1. \qquad \textbf{(C.20)}$$

In order to solve these linear equations, standard Gaussian elimination or *LU* decomposition techniques can be employed.

C.6 Inter-Cell Interference Estimation

The analysis presented in the previous sections of this chapter relates to the performance of the central cell only. The analysis does not explicitly take into account the operation of cochannel cells. Instead, the effect that cochannel cells have on the central cell is modelled via the mean inter-cell interference, $\overline{m_{coc}}$, received at the central cell base station per timeslot. This estimate is a key aspect of the overall analysis, as it allows the performance of a multiple cell PRMA system to be determined, through Markov analysis of a single cell. In order for accurate performance estimates of the multiple cell system to be produced, an accurate estimate of $\overline{m_{coc}}$ is required.

Theory is presented in this section for the estimation of $\overline{m_{coc}}$ in a multiple cell speech-data PRMA system with speech packet retransmission and selection diversity. This theory is based closely on that presented in Chapter 6 and 7 for speech only PRMA systems. In particular, the probability of cochannel terminals being in the reservation, contention and backlogged states is determined. It is then possible to estimate the number of cochannel packets attributable to terminals in these respective states. The final estimate of inter-cell interference, $\overline{m_{coc}}$, is the combination of these three sources of interference.

In order to determine the proportion of reserved and contending interferers, a technique similar to that presented in §5.3.2 has been developed. This technique assumes that the system is homogeneous, such that each cell experiences identical performance. Based on this assumption, it is reasonable to expect that, on average, an equal number of reservation, contention and backlog packets would be produced in each cell in a given timeslot. This means that a particular cell would produce the same average number of packets as it would receive from a single cochannel cell. This concept was illustrated previously in Fig. 5.2. Using this approach it is possible to calculate the total mean number of cochannel packets produced in a timeslot as being L times the mean number of packets produced in the central cell, namely

$$\overline{m_{coc}} = L \cdot \sum_{m_{cen}=0}^{M_s+M_d} m_{cen} \Pr(m_{cen}) . \qquad \textbf{(C.21)}$$

The factor of L accounts for the L nearby cochannel cells. The summation on the r.h.s. of (C.21) represents the expectation of m_{cen} (i.e., the mean number of central cell speech and data packets), where $\Pr(m_{cen})$ is the probability of m_{cen} central cell packets being transmitted. $\Pr(m_{cen})$ in (C.21) can be described in terms of the state probability distribution, $\boldsymbol{\pi}(C,R,B)$, according to

$$\Pr(m_{cen}) = \sum_{B=0}^{M_d} \sum_{R=0}^{N} \sum_{C=0}^{M_s-R} \Pr(m_{cen}|C,R,B)\boldsymbol{\pi}(C,R,B) . \qquad \textbf{(C.22)}$$

Assuming that $\boldsymbol{\pi}(C,R,B)$ is given by (C.18), (C.22) can be rewritten as

$$\Pr(m_{cen}) = \sum_{R=0}^{N} \sum_{C=0}^{M_s-R} \Pr(m_{cen}|C,R,\overline{B})\boldsymbol{\pi}(C,R|\overline{B}) , \qquad \textbf{(C.23)}$$

so that (C.21) can be rewritten as

$$\overline{m_{coc}} - \Omega = 0 , \qquad \textbf{(C.24)}$$

where

$$\Omega = L \cdot \sum_{m_{cen}=0}^{M_s+M_d} m_{cen} \sum_{R=0}^{N} \sum_{C=0}^{M_s-R} \Pr(m_{cen}|C,R,\overline{B})\boldsymbol{\pi}(C,R|\overline{B}) . \qquad \textbf{(C.25)}$$

$\Pr(m_{cen}|C,R,\overline{B})$ is the probability of m_{cen} packets being produced in a single timeslot by the M_s central cell speech terminals and M_d central cell data terminals, given that C speech terminals are

in the contention state, R speech terminals are in the reservation state and $\overline{B}$ data terminals are in the backlogged state. $\Pr(m_{cen}|C,R,\overline{B})$ is given by

$$\Pr(m_{cen}|C,R,\overline{B}) = \begin{cases} \frac{R}{N}g_f + \left(1-\frac{R}{N}\right)(1-p_s)^C(1-p_d)^{\overline{B}} & m_{cen}=0 \\ \frac{R}{N}(1-g_f) + \left(1-\frac{R}{N}\right)Cp_s(1-p_s)^{C-1}(1-p_d)^{\overline{B}} & \\ \quad + \left(1-\frac{R}{N}\right)\overline{B}p_d(1-p_d)^{\overline{B}-1}(1-p_s)^C & m_{cen}=1 \\ \left(1-\frac{R}{N}\right)\sum_{i=0}^{m_{cen}}\binom{C}{m_{cen}-i}p_s^{m_{cen}-i}(1-p_s)^{C-m_{cen}+i}\binom{\overline{B}}{i}p_d^i(1-p_d)^{\overline{B}-i} & 1<m_{cen}\le C+\overline{B} \end{cases} \quad \textbf{(C.26)}$$

An iterative procedure is necessary to determine the value of $\overline{m_{coc}}$ which satisfies (C.24). This iterative procedure involves starting with an initial guess and computing step by step approximations of $\overline{m_{coc}}$. In this thesis, the Levenberg-Marquardt method [3] is employed. For particular values of M_s and M_d, the following iterative process is employed to calculate the value of $\overline{m_{coc}}$ which satisfies (C.24):

---

a) The iteration number is set to i=0.

b) An estimate of $\overline{m_{coc}}$, denoted $\overline{m_{coc\,i}}$, is provided. In the absence of any better initial estimate, $\overline{m_{coc\,0}}$, is calculated using

$$\overline{m_{coc\,0}} = L\,l_d\,M_d + \frac{L\cdot SAF\cdot M_s}{N}. \quad \textbf{(C.27)}$$

This estimate is a combination of the estimates of inter-cell interference considered in (5.9) and (6.27) for a data-only S-ALOHA system and a speech-only PRMA system, respectively.

c) The value of Ω_i, given by (C.25), is evaluated. This calculation requires the capture probability be determined using capture probability theory developed in Chapter 4. In addition, it is also necessary to calculate the state probability distribution using the Markov theory presented in § C5.

d) The error term, e_i, is determined according to,

$$e_i = \overline{m_{coc\,i}} - \Omega_i. \quad \textbf{(C.28)}$$

e) If e_i is not within an acceptable error range, i is iterated to $i = i+1$. In addition, $\overline{m_{coc\,i}}$ is iterated to a new value (according to the Levenberg-Marquardt method) and steps *c)* and *d)* are repeated until the equality of (C.24) is satisfied.

f) The value of $\overline{m_{coc\,i}}$ that satisfies (C.24) (denoted by $\overline{m_{coc}}$) can then be used in the calculation of the PRMA performance measures presented in the following section.

C.7 Performance Measures

With knowledge of the distribution $\pi(C,R,B)$, it is possible to study other aspects of the multiple cell PRMA speech-data system such as the total speech packet loss probability, P_{loss}, data packet delay, W, throughput per cell, h, and system utilisation, y. These performance measures were introduced previously in §2.2.4 and §4.6.3. The remainder of this section presents these performance measures in a mathematical form.

The total throughput per cell for a system with M_s speech terminals per cell and M_d data terminals per cell is given by

$$h = \sum_{B=0}^{M_d} \sum_{R=0}^{N} \sum_{C=0}^{M_s-R} h(C,R,B)\pi(C,R,B) . \qquad \textbf{(C.29)}$$

Assuming that $\pi(C,R,B)$ is given by (C.18), (C.29) can be rewritten as

$$h = \sum_{R=0}^{N} \sum_{C=0}^{M_s-R} h(C,R,\overline{B})\pi(C,R|\overline{B}) . \qquad \textbf{(C.30)}$$

where $h(C,R,\overline{B})$ corresponds to the throughput when the system is in state $\{C,R,\overline{B}\}$. $h(C,R,\overline{B})$ for a multiple cell speech-data PRMA system with speech packet retransmission and selection diversity, is given by

$$\begin{aligned} & h(C,R,\overline{B}) \\ &= \frac{R}{N}(1-g_f)q^2(1,\overline{m_{coc}}) \\ &+ \left(1-\frac{R}{N}\right)\sum_{s=0}^{C}\binom{C}{s}p_s^s(1-p_s)^{C-s}\sum_{t=0}^{\overline{B}}\binom{\overline{B}}{t}p_d^t(1-p_d)^{\overline{B}-t}(s+t)\cdot q(s+t,\overline{m_{coc}}) , \end{aligned} \qquad \textbf{(C.31)}$$

where $q^2(1,\overline{m_{coc}})$ is the capture probability for a system with selection diversity (see §7.2). The expressions presented in (C.30) and (C.31) are used to determine the total throughput per cell. This total throughput per cell, is comprised of throughput attributable to speech terminals, h_s, as well as throughput attributable to data terminals, h_d, such that

$$h = h_s + h_d . \qquad \textbf{(C.32)}$$

The speech throughput per cell, h_s, when the system is in state $\{C, R, \overline{B}\}$, is given according to

$$\begin{aligned} & h_s(C,R,\overline{B}) \\ &= \frac{R}{N}(1-g_f)q^2(1,\overline{m_{coc}}) \\ &+\left(1-\frac{R}{N}\right)\sum_{s=0}^{C}\binom{C}{s}p_s^s(1-p_s)^{C-s}\sum_{t=0}^{\overline{B}}\binom{\overline{B}}{t}p_d^t(1-p_d)^{\overline{B}-t}\cdot s\cdot q(s+t,\overline{m_{coc}}), \end{aligned} \quad \textbf{(C.33)}$$

while the data throughput per cell, h_d, when the system is in state $\{C, R, \overline{B}\}$, is given by

$$h_d(C,R,\overline{B}) = \left(1-\frac{R}{N}\right)\sum_{s=0}^{C}\binom{C}{s}p_s^s(1-p_s)^{C-s}\sum_{t=0}^{\overline{B}}\binom{\overline{B}}{t}p_d^t(1-p_d)^{\overline{B}-t}\cdot t\cdot q(s+t,\overline{m_{coc}}). \quad \textbf{(C.34)}$$

The packet dropping probability for a system with speech packet retransmission is similar to the expression presented in (7.26), namely

$$P_{drop} = 1-\frac{N\cdot h_s}{SAF\cdot M_s}, \quad \textbf{(C.35)}$$

where N is the number of timeslots per cell, h_s is the speech throughput per cell, SAF is the speech activity factor and M_s is the number of speech terminals per cell.

References

[1] C. Namislo, "Analysis of mobile radio slotted ALOHA networks," *IEEE J. Selected Areas Commun.*, vol. 2, no. 4, Jul. 1984, pp. 583 - 588.

[2] H. Qi, R. Wyrwas, "Performance analysis of joint voice-data PRMA over random packet error channels," *IEEE Trans. Veh. Technol.*, vol. 45, no. 2, May 1996, pp. 332 - 345.

[3] W. H. Press, B. P. Flannery, S. A. Teukolsky, W. T. Vetterling, *Numerical Recipes, The Art of Scientific Computing.* Cambridge University Press.